Southern California Earthquake Center

2008 Annual Meeting

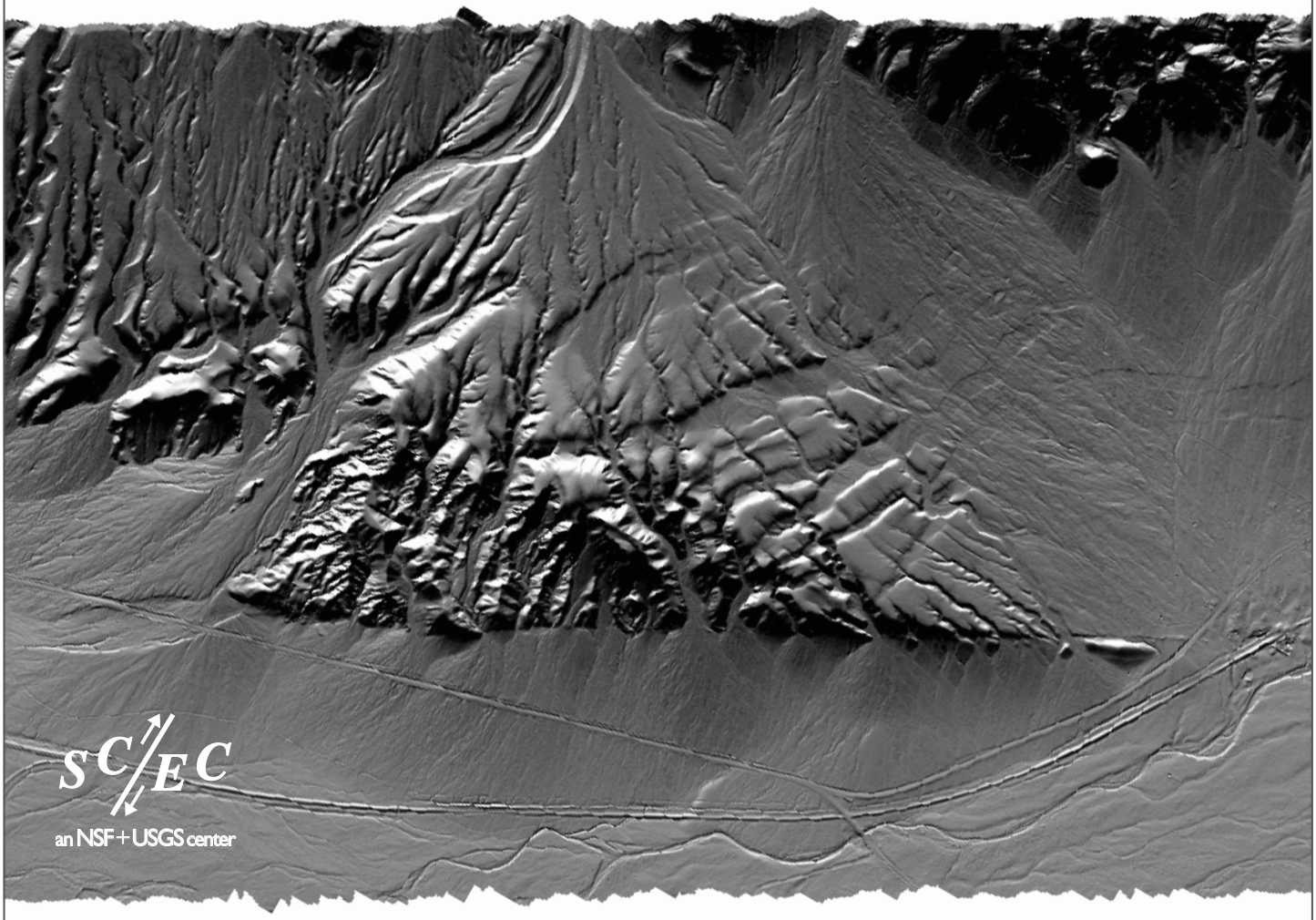

Proceedings and Abstracts, Volume XVIII

September 6-11, 2008

SCEC ORGANIZATION

Center Director, *Tom Jordan*

Deputy Director, *Greg Beroza*

AssocIate Director for Administration, *John McRaney*

Associate Director for Communication, Education, and Outreach, *Mark Benthien*

Associate Director for Information Technology, *Phil Maechling*

Project Planning Coordinator, *Tran Huynh*

Research Contracts and Grants Coordinator, *Karen Young*

Project Specialist, *Shelly Werner*

Education Programs Manager, *Bob de Groot*

Digital Products Manager, *John Marquis*

Research Programmers, *Maria Liukis, David Meyers, Scott Callaghan, Kevin Milner*

Systems Programmer, *John Yu*

SCEC BOARD OF DIRECTORS

Tom Jordan, *Chair, USC*

Lisa Grant-Ludwig, *Vice-Chair, UCI*

Peter Bird, *UCLA*

David Bowman, *CSUF*

Emily Brodsky, *UCSC*

Jim Brune, *UNR*

Ralph Archuleta, *UCSB*

Steve Day, *SDSU*

James Dieterich, *UCR*

Bill Ellsworth, *USGS Menlo*

Yuri Fialko, *UCSD*

Tom Herring, *MIT*

Susan Hough, *USGS Pasadena*

Nadia Lapusta, *CalTech*

Jim Rice, *Harvard*

Paul Segall, *Stanford*

Bruce Shaw, *Columbia*

Rob Wesson, *USGS Golden*

SCEC ADVISORY COUNCIL

Mary Lou Zoback, *Chair, Risk Management Solutions*

Gail Atkinson, *Carlton University*

Lloyd Cluff, *Pacific Gas and Electric*

John Filson, *Scientist Emeritus, U.S. Geological Survey*

Jeffery Freymueller, *University of Alaska*

Patti Guatteri, *Swiss Reinsurance*

Anne Meltzer, *Lehigh University*

Denis Mileti, *California Seismic Safety Commission*

Kate Miller, *University of Texas at El Paso*

Jack Moehle, *Pacific Earthquake Engineering Research Center*

John Rudnicki, *Northwestern University*

SCEC PLANNING COMMITTEE

Chair, *Greg Beroza*

Seismology, *Egill Hauksson, Jamie Steidl*

Tectonic Geodesy, *Jessica Murray, Rowena Lohman*

Earthquake Geology, *Mike Oskin, James Dolan*

Unified Structural Representation, *John Shaw, Jeroen Tromp*

Fault and Rupture Mechanics, *Judith Chester, Ruth Harris*

Crustal Deformation Modeling, *Liz Hearn, Tom Parsons*

Lithospheric Architecture and Dynamics, *Paul Davis, Gene Humphreys*

Earthquake Forecasting and Predictability, *Terry Tullis, Bernard Minster*

Ground Motion Prediction, *Robert Graves, Steve Day*

Seismic Hazard and Risk Analysis, *Paul Somerville, Nicolas Luco*

Southern San Andreas Fault Evaluation, *Ken Hudnut*

Working Group on California Earthquake Probabilities, *Ned Field*

Collaboratory for the tudy of Earthquake Predictability, *Tom Jordan, Danijel Schorlemmer*

Extreme Ground Motion, *Tom Hanks*

Petascale Cyberfacility for Physics-Based Seismic Hazard Analysis, *Phil Maechling*

Table of Contents

SCEC ANNUAL MEETING PROGRAM **1**

Meeting at a Glance 1
Workshop Descriptions and Agendas 3
SCEC Annual Meeting Sessions 12

STATE OF SCEC, 2008 ..... **15**

REPORT OF THE ADVISORY COUNCIL **24**

SCEC COMMUNICATION, EDUCATION, AND OUTREACH **30**

DRAFT 2009 SCIENCE PLAN **41**

I. Introduction 41
II. Guidelines for Proposal Submission 41
III. SCEC Organization 42
IV. Proposal Categories 43
V. Evaluation Process and Criteria 44
VI. Coordination of Research Between SCEC and USGS-EHRP 45
VII. SCEC3 Science Priority Objectives 46
VII-A. Disciplinary Activities 48
1. Seismology 48
2. Tectonic Geodesy 49
3. Earthquake Geology 50
VII-B. Interdisciplinary Focus Areas 51
1. Unified Structural Representation (USR) 51
2. Fault and Rupture Mechanics (FARM) 52
3. Crustal Deformation Modeling (CDM) 52
4. Lithospheric Architecture and Dynamics (LAD) 53
5. Earthquake Forecasting and Predictability (EFP) 54
6. Ground Motion Prediction (GMP) 54
7. Seismic Hazard and Risk Analysis (SHRA) 55
VIII. Special Projects and Initiatives 56
IX. SCEC Communication, Education, and Outreach 60
Appendix: SCEC3 Long-Term Research Goals 61
Basic Research Problems 61
1. Earthquake Source Physics 62
2. Fault System Dynamics 62
3. Earthquake Forecasting and Predictability 63
4. Ground Motion Prediction 64

SCEC ANNUAL MEETING ABSTRACTS **65**

Plenary Presentations 65
Group 1. Poster Abstracts 69
Communication, Education, and Outreach (CEO) 69
Community Modeling Environment (CME); 77
Petascale Cyberfacility for Physics-Based Seismic Hazard Analysis (PetaSHA) ..77
Seismic Hazard and Risk Analysis (SHRA) 81
ShakeOut 90
Ground Motion Prediction (GMP) 95

Extreme Ground Motion (ExGM) 103
Collaboratory for the Study of Earthquake Predictability (CSEP) 109
Working Group on California Earthquake Probabilities (WGCEP) 113
Earthquake Forecasting and Predictability (EFP) 115
Crustal Deformation Modeling (CDM) 122
Lithospheric Architecture and Dynamics (LAD) 133
Group 2. Poster Abstracts 142
Unified Structural Representation (USR) 142
Tectonic Geodesy 147
Earthquake Geology 154
Southern San Andreas Fault Evaluation (SoSAFE) 161
Fault Rupture and Mechanics (FARM) 171
Seismology 197

MEETING PARTICIPANTS 214

GROUP 1 POSTER LAYOUT 216

GROUP 2 POSTER LAYOUT 217

SCEC Annual Meeting Program

Meeting at a Glance

SATURDAY, SEPTEMBER 6, 2008

13:00 – 18:00 Extreme Ground Motion Workshop - Session I (*page 3*)

SUNDAY, SEPTEMBER 7, 2008

08:00 – 12:00 Extreme Ground Motion Workshop - Session II (*page 4)*

08:00 – 12:00 Workshop on Launching an Earthquake Source Inversion Validation Exercise (*page 5-6*)

08:00 – 12:00 The Great Southern California ShakeOut: Living with Earthquakes in California – A Workshop for Science Educators (*page 7*)

08:00 – 15:00 Student Field Trip to the San Jacinto Fault Zone (*page 7*)

13:00 – 17:30 Southern San Andreas Fault Evaluation Workshop (*page 8*)

13:30 – 17:30 Earthquake Engineering and Science Workshop (*page 9*)

16:30 – 18:30 *Poster Session Set-Up*

18:00 *Annual Meeting Ice-Breaker/Welcome Reception*

20:00 – 22:00 SCEC Advisory Council Executive Meeting

20:00 – 22:30 Poster Session I (Group 1 Posters)

MONDAY, SEPTEMBER 8, 2008

08:00 – 12:30 Annual Meeting Session I (*page 12*)

11:00 – 12:30 Science Plan Discussion: GMP/ExGM/SHRA

11:00 – 12:30 Science Plan Discussion: Crustal Deformation Modeling

12:30 *Lunch*

14:00 – 15:30 Poster Session II (Group 1 Posters)

15:30 – 18:30 Annual Meeting Session II (*page 12*)

16:00 – 18:30 Science Plan Discussion: LAD

16:00 – 18:30 Science Plan Discussion: CSEP/EFP/WGCEP

18:30 *Cocktails*

19:15 SCEC *Recognition Banquet*

20:00 – 22:30 Poster Session III (Group 1 Posters)

TUESDAY, SEPTEMBER 9, 2008

07:00 – 08:00	*Poster Turn-Over*
08:00 – 12:00	Annual Meeting Session III (*page 13*)
08:30 – 10:00	Science Plan Discussion: FARM
08:30 – 10:00	Science Plan Discussion: Tectonic Geodesy
10:30 – 12:00	Science Plan Discussion: Geology/SoSAFE
10:30 – 12:00	Science Plan Discussion: CME/PetaSHA
12:00	*Lunch*
13:30 – 15:00	Poster Session IV (Group 2 Posters)
15:00 – 18:30	Annual Meeting Session IV (*page 13*)
16:00 – 17:30	Science Plan Discussion: USR
16:00 – 17:30	Science Plan Discussion: Seismology/SCEDC
17:30 – 18:30	Plenary Science Plan Discussion
18:30	*Cocktails*
19:00	*Dinner*
20:00 – 22:30	Poster Session V (Group 2 Posters)
20:00 – 22:00	SCEC Advisory Council Meeting

WEDNESDAY, SEPTEMBER 10, 2008

07:00 – 08:30	*Remove posters*
08:30 – 11:30	Annual Meeting Session V (*page 14*)
08:30 – 10:00	Panel Debate: Are geologic/geodetic rate discrepancies important for earthquake forecasting?
12:00	*Lunch* (SCEC Board and Planning Committee Only)
12:30 – 14:00	SCEC Board Meeting
12:30 – 14:00	SCEC Planning Committee Meeting
14:00 – 18:00	Salton Trough Seismic Project Workshop I (*page 10*)

THURSDAY, SEPTEMBER 11TH

08:00 – 16:00	Salton Trough Seismic Project Workshop II (*page 11*)

Workshop Descriptions and Agendas

EXTREME GROUND MOTION WORKSHOP
Conveners: Tom Hanks and Norm Abrahamson

The third annual Extreme Ground Motion (ExGM) Workshop will consist of two sessions, the first on Saturday afternoon, September 6, 13:00-18:00, and the second on Sunday morning, September 7, 08:00-12:00. The first session will feature more recent results than those presented at the Extreme Ground Motion special sessions at the Seismological Society of America Annual Meeting in April 2008. We will also lay out the ExGM Endgame as we presently envision it, now that we are three years into the ExGM Program, with just two remaining before the ExGM Final Report is due.

The Sunday morning session will be devoted to precarious-rock research, as performed by scientists funded by ExGM at Yucca Mountain and by scientists funded by SCEC in southern California. The focus will be on turning precarious rocks into real seismic hazard constraints, which requires both the amplitude of toppling ground motions and the age for which the rock has been precarious.

SATURDAY, SEPTEMBER 6, 2008 — *Plaza Ballroom AB*

13:00 – 13:10	Introduction (*T. Hanks and N. Abrahamson*)
1310 – 13:30	Laboratory Studies of Stress-Induced Compaction of the Calico Hills Formation (*D. Lockner and C. Morrow*)
1330 – 13:50	Steps Toward Validation of Physical Limits to Earthquake Ground Motion (*J. Andrews*)
1350 – 14:10	A Physical Model for Widespread Near-Surface and Fault Zone Damage Induced by Earthquakes (*S. Ma*)
14:10 – 14:30	TBA (*B. Duan*)
14:30 – 14:50	TBA (*M. Purvance*)
14:50 – 15:15	Spatial Correlation Between Kinematic Source Parameters Derived From Dynamic Rupture Simulations (*J. Schmedes, R. Archuleta, and D. Lavallee*)
15:15 – 15:30	*Break*
15:30 – 16:10	Gradual Modifications to the Yucca Mountain Landscape over the Past Million Years (*J. Whitney and T. Hanks*)
16:10 – 16:30	Age and Long Term Stability of Rock Outcrops in the Vicinity of Yucca Mountain (*M. Stirling*)
16:30 – 16:50	Exreme Ground Accelerations from Very Shallow Earthquakes Driven by Dynamic Stress (*N. Sleep*)
16:50 – 17:10	Points in Hazard Space (*N. Abrahamson and T. Hanks*)
17:10 – 17:30	The ExGM Endgame (*T. Hanks, N. Abrahamson, and T. Jordan*)
17:30 – 17:50	The ExGM Endgame: Ground Motion Simulations (*R. Archuleta*)
17:50 – 18:00	Comments and Discussion
18:00	*Adjourn*

SUNDAY, SEPTEMBER 7, 2008 — *Plaza Ballroom AB*

08:00 – 08:05	Introduction (*T. Hanks and L. Grant-Ludwig*)
0805 – 08:20	Precarious Rocks as a Subset of Fragile Geologic Structures (T. Hanks)
08:20 – 08:40	Rock Varnish Microlamination Age Dates from Precarious Rocks Near the San Andreas Fault (M. Purvance)
08:40 – 09:00	Geomorphic and Tectonic Setting of the Grass Valley PBR Site in the San Bernardino Mountains (*K. Kendrick*)
09:00 – 09:20	Preliminary Ages of 6 PBRs near the San Andreas Fault from 10Be Concentrations (*D. Rood*)
09:20 – 09:40	Cosmogenic and Soil Age Constraints on PBRs in New Zealand (*M. Stirling*)
09:40 – 10:00	A Comparative Assessment of the Geomorphologic Setting and Geologic Context of Zones of PBR's in Low-Seismicity Regions (*R. Arrowsmith*)
10:00 – 10:20	*Break*
10:20 – 10:40	Statistical Study of PBRs at Lovejoy Buttes, Victorville and Granite Pediment (*J. Brune*)
10:40 – 11:00	Fragilities Derived from Simulations Using Andrews' Calculations (*M. Purvance*)
11:00 – 11:20	Age and Long Term Stability of Rock Outcrops in the Vicinity of Yucca Mountain (*M. Stirling*)
11:20 – 11:50	Birth, Life, and death of PBR's: A Discussion (*R. Arrowsmith, M. Purvance, and D. O'Connell, moderated by L. Grant-Ludwig*)
11:50 – 12:00	Wrap-Up Discussion (*led by L. Grant-Ludwig*)
12:00	*Adjourn*

WORKSHOP ON LAUNCHING AN EARTHQUAKE SOURCE INVERSION VALIDATION EXERCISE

Conveners: Martin Mai, Danijel Schorlemmer, and Morgan Page

Earthquake source inversions image the spatio-temporal rupture evolution, and hence constitute a critical research tool to develop a better understanding of the details of the earthquake source process. However, finite-source rupture models, developed by different research teams for the same earthquake, exhibit surprisingly large intra-event variability. Moreover, a recent, small-scale "source inversion blind test" revealed the difficulties that several inversion methods had, even for a rather simple test case. Despite a number of new developments in source-inversion approaches, the reliability, resolution, and robustness of these inversion strategies has not been rigorously examined and tested.

This workshop serves as a starting point for launching an Earthquake Source Inversion Validation Exercise. We invite researchers working in earthquake source inversion (and inversion theory and application in general), users of source-rupture models (e.g., rupture-dynamic and ground-motion-simulation people), and statistical analysts (testing-center folks and related programmers). The scope of the workshop is (a) to briefly summarize current source-inversion methods; (b) to define the long-term strategy for conducting such a validation exercise; (c) to discuss the logistical and computational framework needed for this exercise; (d) to setup task groups for the different steps of the validation (model building; ground-motion synthesis; statistical analysis of submitted models; computational infrastructure…).

SUNDAY, SEPTEMBER 7, 2008 — *Plaza Ballroom CD*

08:00 – 08:10	Introduction: Scope of the workshop & review of an initial blind-test (*M. Mai*)
08:10 – 08:25	Strategies for uncertainty assessment in source inversions (*M. Page*)
08:25 – 08:40	Importance of covariance components for finite-source inversions (*Y. Yagi*)
08:40 – 08:55	Current status of source inversion methods in Japan (*K. Koketsu*)
08:55 – 09:10	Inverting for dynamic source parameters (*R. Madariaga*)
09:10 – 09:25	Experience from the Dynamic Code Validation Project (*R. Harris*)
09:25 – 09:40	An existing testing center: CSEP (*D. Schorlemmer*)
09:40 – 10:00	*Break*
10:00 – 12:00	**OPEN DISCUSSION:** Planning the source-inversion validation exercise
10:00 – 10:40	**DISCUSSION 1: Science issues / General questions**

- Source inversion: an under-determined problem
- How to best quantify waveform fits?
- How to optimally weight different data sets used in the inversion?
- Effects of source-receiver constellation?
- Effects of different stabilizing/smoothing constraints?

10:40 – 11:20 **DISCUSSION 2: General set-up of the exercise**

- Greens functions: pre-computed or velocity-density models specified?
- Greens functions: Simple media or realistic structures?
- Source geometry: how much information should be provided?
- What "data" (synthetics) are desired? Statics, strong-motion, teleseismics?
- "Clean" synthetics or noise-contaminated?
- How to compare inversion results; what are relevant statistical measures?
- A fully prospective inversion?

11:20 – 12:00 **DISCUSSION 3: Logistics, resource, and management**

- Overall strategy and rough time-frame
- Formats for submission of models/synthetics?
- Authorization of data streams?
- Needed computational/infrastructure resources?
- Proposal for future funding for these efforts?

THE GREAT SOUTHERN CALIFORNIA SHAKEOUT: LIVING WITH EARTHQUAKES IN CALIFORNIA – A WORKSHOP FOR SCIENCE EDUCATORS
Convener: Bob de Groot

SUNDAY, SEPTEMBER 7, 2008 — *Palm Canyon Room AB*
08:00-12:00

A devastating 7.8 earthquake on the southern San Andreas fault will be the backdrop when nearly a million school children in California and major cities from around the globe join California's emergency responders on November 13, 2008 in the largest-ever earthquake preparedness exercises in the state of California. This workshop will address earthquakes in California and connections to topics such as plate tectonics, faults, and earthquake hazards throughout the state. Activities for this workshop will include a plate tectonics activity focused on California's "master" fault, the San Andreas. Participants will learn about how everyone should prepare for an earthquake as well as what they should do during an earthquake. Every participant will receive a CD with earthquake simulations and other resources for earth science education. (*Size limit 25 participants*)

Important Note: While open to the entire SCEC community this workshop is primarily designed for K-12 science educators that work in formal and informal learning environments. Special emphasis will be placed on providing content and activities related to basic earthquake science and preparedness. Additionally, we will address topics such as teaching about earthquakes within the context of the California Science Content Standards and facilitating earthquake education activities in museums and other informal learning environments.

STUDENT FIELD TRIP TO THE SAN JACINTO FAULT ZONE
Trip Leaders: Mike Oskin and Kim Le

SUNDAY, SEPTEMBER 7, 2008 — *Depart from Hilton Hotel Lobby*
08:00-15:00

In southernmost California, the activity of the San Jacinto fault rivals that of the San Andreas fault. This field trip will take students to two field sites along the southernmost San Jacinto fault in the Anza Borrego Desert State Park. Here we will view evidence for fault rupture in alluvial fans that range in age from a few thousand to over thirty thousand years. We will also have the opportunity to compare the field observations to high-resolution topography of the 'B4' survey. During the trip we will also discuss evidence for variability in the rate of slip on the San Jacinto fault, both in space and over time. Time permitting we will also stop to view the Peninsular Ranges mylonite zone - an exposure of the roots of an ancient fault zone near the brittle-ductile transition.

Participants should be prepared for warm weather (hat! sunscreen!) and short (20 minute) hikes across rough desert terrain. We will leave at 8:00 am sharp to take advantage of the cooler morning temperatures.

SOUTHERN SAN ANDREAS FAULT EVALUATION WORKSHOP
Convener: Ken Hudnut

The Southern San Andreas Fault Evaluation (SoSAFE) project has made significant progress in its first two years towards better defining slip rates and earthquake history of southern San Andreas fault system for the last 2000 years. This fifth workshop will again review and highlight the latest scientific progress across the range of SoSAFE investigations. As SoSAFE is now two years into a three-year program, funded primarily by the USGS Multi-Hazards Demonstration Project, we will discuss what remains to be done as the top priorities for the final year of major USGS funding. Do we need or want to prolong the life of SoSAFE beyond three years, and if so, what must be done?

SUNDAY, SEPTEMBER 7, 2008 — *Horizon Ballroom 1*

13:00 – 13:30 Workshop Introduction and Overview of SCEC Activities (*K. Hudnut*) and Opening Remarks from SoSAFE Project Sponsors

13:30 – 14:45 Examples of Current Collaborations (10 minutes each)

- San Andreas – Carrizo (*O. Zielke*)
- San Andreas - Carrizo (*S. Akciz*)
- San Andreas - Northern Big Bend (*K. Scharer*)
- San Andreas - Littlerock (*R. Weldon*)
- San Andreas – Ritter (*P. Sgriccia*)
- San Andreas - San Bernardino (*S. McGill*)

14:45 – 15:00 *Break*

15:00 – 16:15 Examples of Current Collaborations (10 minutes each)

- San Andreas – Biskra 1 (*K. Fletcher*)
- San Andreas – Biskra 2 (*D. Rood*)
- San Andreas - Coachella Valley Section (*P. Williams*)
- San Andreas - Salt Creek (*G. Seitz*)
- Lake Cahuilla chronology (*T. Rockwell*)
- San Jacinto – Hog Lake (*T. Rockwell*)
- San Jacinto – slip rate (*K. Le & M. Oskin*)
- Elsinore, ECSZ, etc. - GeoEarthScope (*D. Phillips*)

16:00 – 17:15 Future Plans and Research Needs of SoSAFE (*chaired by Hudnut*)

(10 minutes each research group's input, with time for discussion)

17:15 – 5:30 Workshop Summary and Closing Remarks from Participants (*chaired by Hudnut*)

EARTHQUAKE ENGINEERING & SCIENCE WORKSHOP
Conveners: Nicolas Luco and Paul Somerville

This ½-day workshop, immediately preceding the SCEC Annual Meeting, offers engineers and scientists an opportunity to focus plans for future collaborative activities related to earthquake engineering and science. The question central to the workshop is: How should SCEC collaborate with the earthquake engineering community? Interested earthquake engineers and scientists are invited to provide recommendations for future research activities through discussions of 1) current collaborative activities supported by SCEC, and 2) relevant activities and needs of the earthquake engineering community. Representatives from the earthquake engineering community (e.g. ASCE 7, ATC, BSSC, CUREE, EERI, LATBSDC, MAE, MCEER, NEES, PEER) and SCEC scientists will provide brief summaries to stimulate discussions. The workshop proceedings and recommendations will be used to plan future SCEC research directions.

SUNDAY, SEPTEMBER 7, 2008 — *Horizon Ballroom 2*

13:30 – 13:35 Workshop Introduction (*N. Luco*)

13:35 – 13:55 Brief Overview of SCEC Activities (*P. Somerville*)

13:55 – 14:55 Examples of Current Collaborations (20 minutes each)

- Tall Buildings Initiative (*Y. Bozorgnia / F. Naeim / J. Stewart; R. Graves*)
- ShakeOut (*R. Graves; S. Krishnan*)
- OpenSHA and OpenRisk (*N. Field; K. Porter*)

14:55 – 15:10 *Break*

15:10 – 17:10 Activities and Needs of Engineering Organizations (≤10 minutes each, plus time for discussion)

- American Society of Civil Engineers 7 and Building Seismic Safety Council (*R. Hamburger*)
- Applied Technology Council (*J. Heintz*)
- Consortium of Universities for Research in Earthquake Engineering (*T. Hutchinson*)
- Earthquake Engineering Research Institute (*T. Anagnos*)
- Los Angeles Tall Buildings Structural Design Council (*F. Naeim*)
- Mid-America Earthquake Center (*A. Elnashai*)
- Network for Earthquake Engineering Simulation (*S. McCabe*)
- Pacific Earthquake Engineering Research Center (*Y. Bozorgnia*)

17:10 – 17:30 Workshop Summary and Closing Remarks from Participants (*N. Luco and P. Somerville*)

SALTON TROUGH SEISMIC PROJECT WORKSHOP
Conveners: John Hole, Joann Stock, and Gary Fuis

NSF (Margins/Earthscope) and the USGS are funding an active-source seismic study of the Salton Trough, including the Mexicali, Imperial, and Coachella Valleys, to take place in January 2010. Please see the web site http://www.geophys.geos.vt.edu/hole/salton for current details. This 1.5 day SCEC workshop is designed to promote synergy between this study and other related research efforts, and to inform relevant land management agencies of the plans and goals of the project. We will discuss the survey plans, other piggyback and complementary studies that have already been proposed, and the general tectonic background of the region. The goal of this workshop is threefold: 1) to update interested researchers and land managers on the current state of plans for this major study; 2) to seek community suggestions for details of instrument placement, timing of shots, etc. in the context of possible piggyback studies; and 3) to encourage discussion of other types of complementary projects in tectonics, geology, seismology, engineering seismology, etc. that may be suitable for proposal submission to SCEC or other funding sources in 2008.

WEDNESDAY, SEPTEMBER 10, 2008 — *Plaza Ballroom AB*

14:00 – 14:10	Intro from SCEC Regarding Objectives of Workshop (*T. Jordan*)
14:10 – 14:25	USGS Multihazards Initiative; Relevance of the Salton Trough Seismic Imaging survey (*L. Jones*)
14:25 – 14:40	Southern San Andreas Fault Evaluation Project (*TBA*)
14:40 – 15:00	Salton Trough Seismic Imaging Survey Goals and Tentative Field Plan (*J. Hole*)
15:00 – 15:15	Q&A
15:15 – 15:30	*Break*
15:30 – 15:45	Gulf of California and Salton Trough Tectonic Overview (*J. Stock*)
15:45 – 16:00	Review of Existing Subsurface Knowledge of Imperial Valley (*G. Fuis*)
16:00 – 16:15	Fault and Basin Structure of the Salton Trough: Insights from the SCEC Community Models (*J. Shaw*)
16:15 – 16:30	Seismicity Patterns, Earthquake Relocations (*E. Hauksson*)
16:30 – 16:45	Active Faulting and Past Earthquakes in the Salton Trough (*TBA*)
16:45 – 17:00	Mexican Research Goals (*A. Gonzalez-Fernandez*)
17:00 – 18:00	Discussion
18:00	Poster viewing

THURSDAY, SEPTEMBER 11, 2008

07:30	*Continental Breakfast*
08:00 – 08:30	Detailed Explanation of Each Survey Line: Design and Scientific Goals (*J. Hole*)
08:30 – 10:15	Short Presentations of Piggyback Projects Tied to the Active Seismic Sources (i.e. projects taking place synchronously with the Salton Trough Seismic Imaging Survey); Discussion of Science Goals -- Workshop Participants
	a) Submitted Proposals
	b) New Ideas or Planned Proposals
10:15 – 10:30	*Break*
10:30 – 12:00	Short Presentations of Complementary Projects (i.e. projects taking place at different times than the Salton Trough Seismic Imaging Survey) -- Workshop Participants
	a) Submitted Proposals
	b) New Ideas or Planned Proposals
	c) Discussion
12:00 – 13:30	Lunch and Poster Viewing
13:30 – 14:45	Suggested Design Changes for the Salton Trough Seismic Imaging Survey Based on Workshop Goals
14:45 – 15:00	Outline of Grant Proposal Deadlines of NSF, SCEC, NEHRP, and Other Funding opportunities (*TBA*)
15:00 – 16:00	Wrap-Up Discussion: How to Make This All Happen
16:00	*Adjourn*

SCEC Annual Meeting Sessions

SUNDAY, SEPTEMBER 7, 2008

16:30 – 18:30	*Poster Session Set-Up*	*Plaza Ballroom*
18:00	*Annual Meeting Ice-Breaker/Welcome Reception*	*Poolside*
20:00 – 22:00	SCEC Advisory Council Executive Meeting	*Boardroom*
20:00 – 22:30	Poster Session I (Group 1 Posters)	*Plaza Ballroom*

MONDAY, SEPTEMBER 8, 2008

	Annual Meeting Session I (*chaired by G. Beroza*)	*Horizon Ballroom*
08:00 – 08:30	Welcome and State of the Center (*T. Jordan*)	*Horizon Ballroom*
08:30 – 08:45	Report from NSF	*Horizon Ballroom*
08:45 – 09:00	Report from USGS	*Horizon Ballroom*
09:00 – 09:15	State of the CEO Program (*M. Benthien*)	*Horizon Ballroom*
09:30 – 10:30	**The ShakeOut Scenario: Getting Our Science Used** (*L. Jones*)	*Horizon Ballroom*
	Outstanding Research Questions Raised by the ShakeOut Scenario (*K. Porter*)	*Horizon Ballroom*
	Using the ShakeOut Scenario: A Practitioner's Perspective (*R. Tognazzini*)	*Horizon Ballroom*
10:30 – 11:00	*Break*	
11:00 – 12:30	Science Plan Discussion: GMP/ExGM/SHRA (*R. Graves, S. Day, T. Hanks, P. Somerville, N. Luco*)	*Horizon Ballroom*
11:00 – 12:30	Science Plan Discussion: Crustal Deformation Modeling (*L. Hearn and T. Parsons*)	*Palm Canyon Room AB*
12:30	*Lunch*	
14:00 – 15:30	Poster Session II (Group 1 Posters)	*Plaza Ballroom*
	Annual Meeting Session II (*chaired by P. Somerville*)	*Horizon Ballroom*
15:30 – 16:00	**Engineering Use of Ground Motions: Challenges and Opportunities** (*J. Baker*)	*Horizon Ballroom*
16:00 – 18:30	Science Plan Discussion: CSEP/EFP/WGCEP (*D. Schorlemmer, T. Jordan, T. Tullis, B. Minster, and N. Field*)	*Horizon Ballroom*
16:00 – 18:30	Science Plan Discussion: LAD (*P. Davis and G. Humphreys*)	*Palm Canyon Room AB*
18:30	*Cocktails*	*Poolside*
19:15	*SCEC Recognition Banquet*	*Horizon Ballroom*
20:00 – 22:30	Poster Session III (Group 1 Posters)	*Plaza Ballroom*

TUESDAY, SEPTEMBER 9, 2008

07:00 – 08:00	*Poster Turn-Over*	*Plaza Ballroom*
	Annual Meeting Session III (*chaired by L. Grant-Ludwig*)	*Horizon Ballroom*
08:00 – 08:30	**The 12 May 2008 MS 8.0 Wenchuan Earthquake, Sichuan, China: Background, Field Investigations and Tectonic Implications** (*J. Liu*)	*Horizon Ballroom*
08:30 – 10:00	Science Plan Discussion: FARM (*J. Chester and R. Harris*)	*Horizon Ballroom*
08:30 – 10:00	Science Plan Discussion: Tectonic Geodesy (*R. Lohman and J. Murray-Moraleda*)	*Palm Canyon Room AB*
10:00 – 10:30	*Break*	
10:30 – 12:00	Science Plan Discussion: Geology/SoSAFE (*M. Oskin, J. Dolan, and K. Hudnut*)	*Horizon Ballroom*
10:30 – 12:00	Science Plan Discussion: CME/PetaSHA (*P. Maechling*)	*Palm Canyon Room AB*
12:00	*Lunch*	
13:30 – 15:00	Poster Session IV (Group 2 Posters)	*Plaza Ballroom*
	Annual Meeting Session IV (*chaired by E. Hauksson*)	*Horizon Ballroom*
15:00 – 15:30	**Seconds Can Make a Difference! Recent Progress in Earthquake Early Warning** (*M. Boese*)	*Horizon Ballroom*
15:30 – 16:00	**C^3 (Correlation of Coda of Correlations): Improving the Reconstruction of Green Functions Between Stations of a Network from Noise Records** (*M. Campillo*)	*Horizon Ballroom*
16:00 – 17:30	Science Plan Discussion: Seismology/SCEDC (*E. Hauksson and J. Steidl*)	*Horizon Ballroom*
16:00 – 17:30	Science Plan Discussion: USR (*J. Shaw and J. Tromp*)	*Palm Canyon Room AB*
17:30 – 18:30	Plenary Science Plan Discussion (*G. Beroza*)	*Horizon Ballroom*
18:30	*Cocktails*	
19:00	*Dinner*	*Poolside*
20:00 – 22:30	Poster Session V (Group 2 Posters)	*Plaza Ballroom*
20:00 – 22:00	SCEC Advisory Council Meeting	*Boardroom*

WEDNESDAY, SEPTEMBER 10, 2008

07:00 – 08:30	*Remove posters*	*Plaza Ballroom*
	Annual Meeting Session V (*chaired by G. Beroza*)	*Horizon Ballroom*
08:30 – 10:00	**Panel Debate: Are geologic/geodetic rate discrepancies important for earthquake forecasting?** (*Moderator: B. Minster; Panelists: R. Bennett, K. Felzer, K. Johnson, and M. Oskin*)	*Horizon Ballroom*
10:00 – 10:30	Advisory Council Report (*M.L. Zoback*)	*Horizon Ballroom*
10:30 – 11:00	Summary Science Plan Discussion (*G. Beroza*)	*Horizon Ballroom*
11:00	Wrap-Up (*T. Jordan*)	*Horizon Ballroom*
12:00	*Lunch* (for SCEC Board and Planning Committee only)	*Tapestry Room*
12:30 – 14:00	SCEC Board Meeting	*Whitewiter Room*
12:30 – 14:00	Planning Committee Meeting	*Palm Canyon Room AB*

State of SCEC, 2008

Thomas H. Jordan
SCEC Director

Welcome to the 2008 Annual Meeting!

This is SCEC's 18th Annual Meeting and the second community-wide gathering under the five-year SCEC3 program. The agenda features some very interesting presentations by keynote speakers, planning sessions for all the major working groups, an outstanding set of science posters, and a variety of IT demonstrations, education & outreach activities, and social gatherings. Five workshops and a student field trip are scheduled on the weekend before the meeting, and a major workshop on the Salton Trough Seismic Project will begin immediately afterwards.

The richness of the week's activities indicates how well the Center is working. SCEC has grown into one of the largest collaborations in geoscience, a fact reflected in the rising participation in our annual collaboration meeting (Figure 1): 453 people have pre-registered this year (compared to 446 last year), and 252 poster abstracts have been submitted. This will be the first annual meeting for 139 of this year's pre-registrants, so we can look forward to seeing many new faces!

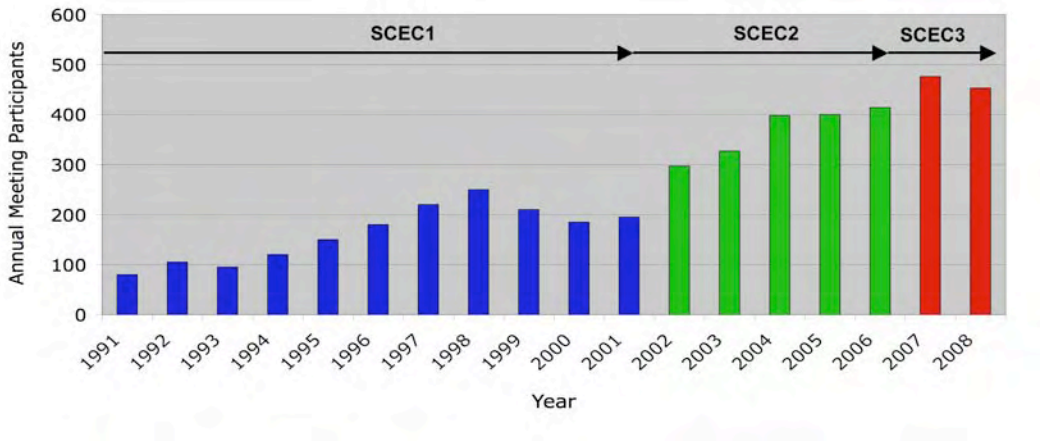

Figure 1. Registrants at SCEC Annual Meetings, 1991-2008. Number for 2008 (453) is pre-registrants.

Goals of the Meeting

The agenda for the Annual Meeting developed by Greg Beroza and the Planning Committee is designed to achieve three goals. The first is to share our individual scientific results and plans with our many SCEC collaborators; for this reason, the agenda includes lots of poster-viewing time and informal sessions around the pool. The second is to mark our progress toward the priority objectives of the SCEC3 Science Plan, which are summarized in the 19 bullet points of Table 1. Each year, we try to assess our achievements in the SCEC Annual Report, and we would like to report

on your scientific contributions, as well as incorporate your ideas for new research into the 2009 SCEC Science Plan.

Obtaining community input to the SCEC planning process is the third major goal of the meeting. A draft of the 2009 Science Plan has been prepared by the Planning Committee and included in this meeting volume. A comprehensive set of working group sessions has been organized to promote detailed discussions of the plan.

We will also be soliciting community input on our priorities for connecting SCEC activities with EarthScope, NEES, the Petascale Computing Initiative, CIG, GEON, and other NSF and USGS programs. A particularly interesting opportunity is the Salton Trough Seismic Project, sponsored by EarthScope and led by John Hole, Joann Stock, and Gary Fuis. This large-scale active seismic experiment, scheduled for 2009-2010, will be the subject of the follow-on workshop, and we encourage your participation.

Table 1. Priority Science Objectives for SCEC3

1. Improve the unified structural representation and employ it to develop system-level models for earth-quake forecasting and ground motion prediction
2. Develop an extended earthquake rupture forecast to drive physics-based SHA
3. Define slip rate and earthquake history of southern San Andreas fault system for last 2000 years
4. Investigate implications of geodetic/geologic rate discrepancies
5. Develop a system-level deformation and stress-evolution model
6. Map seismicity and source parameters in relation to known faults
7. Develop a geodetic network processing system that will detect anomalous strain transients
8. Test of scientific prediction hypotheses against reference models to understand the physical basis of earthquake predictability
9. Determine the origin and evolution of on- and off-fault damage as a function of depth
10. Test hypotheses for dynamic fault weakening
11. Assess predictability of rupture extent and direction on major faults
12. Describe heterogeneities in the stress, strain, geometry, and material properties of fault zones and understand their origin and interactions by modeling ruptures and rupture sequences
13. Predict broadband ground motions for a comprehensive set of large scenario earthquakes
14. Develop kinematic rupture representations consistent with dynamic rupture models
15. Investigate bounds on the upper limit of ground motion
16. Develop high-frequency simulation methods and investigate the upper frequency limit of deterministic ground motion predictions
17. Validate earthquake simulations and verify simulation methodologies
18. Collaborate with earthquake engineers to develop rupture-to-rafters simulation capability for physics-based risk analysis
19. Prepare for post-earthquake response.

Highlights of SCEC Achievements

This has been a banner year for new products in seismic hazard analysis and risk assessment (Figure 2). Last April, the 2007 Working Group on California Earthquake Probabilities (WGCEP

2007), led by Ned Field, released the Uniform California Earthquake Rupture Forecast (UCERF), providing the state with its first comprehensive time-dependent forecast model. The 28-month UCERF study was the product of a very successful partnership among SCEC, the USGS, and the California Geological Survey (CGS), sponsored in part by the California Earthquake Authority (CEA). In its final report, WGCEP (2007) has identified a number of directions for research that could substantially improve time-dependent earthquake forecasting, and their recommendations will be fodder for interesting planning discussions throughout the Annual Meeting.

Another set of studies, conducted by SCEC's PetaSHA collaboration in high-performance computing, delivered simulations of a large scenario earthquake on the southern San Andreas fault. One of these simulations, by Rob Graves and his colleagues, was selected to be the basis for the Great Southern California ShakeOut (Figure 2b). The ShakeOut exercises, scheduled for mid-November, 2008, are being organized by Lucy Jones of the USGS as part of the Multi-Hazard Demonstration Project and will include the largest earthquake drill in U.S. history. The plans for ShakeOut will be a major topic at this Annual Meeting.

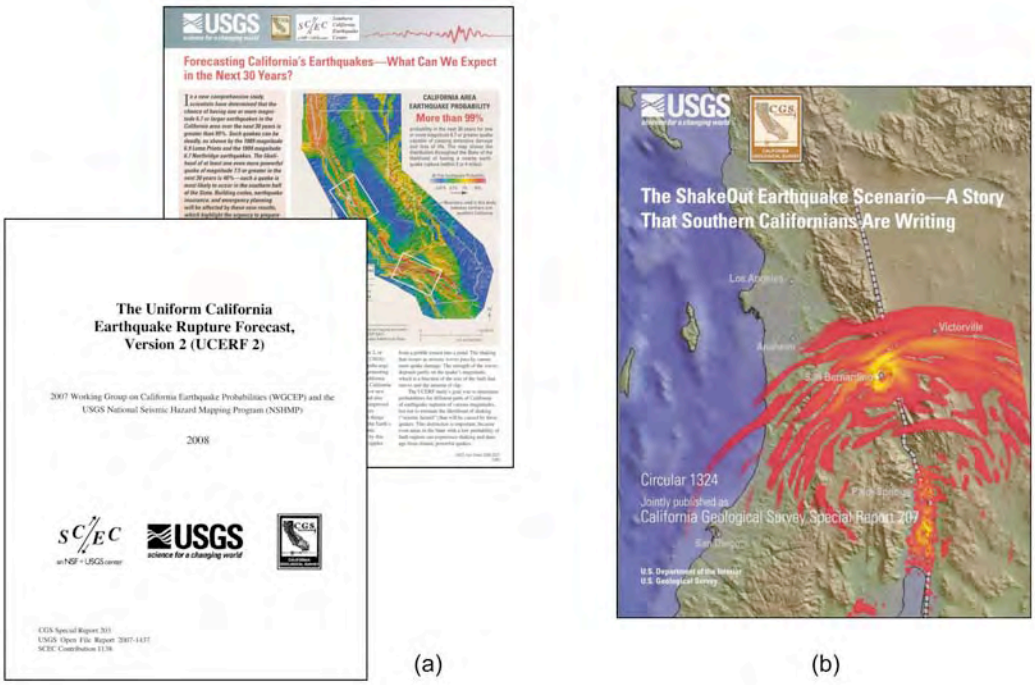

Figure 2. (a) The WGCEP (2007) final report and fact sheet, presenting the Uniform California Earthquake Rupture Forecast (UCERF). (b) USGS Circular 1324, describing the ShakeOut Scenario. The cover shows a snapshot of the M7.8 ShakeOut scenario earthquake on the southern San Andreas fault, simulated by Rob Graves and visualized by Geoff Ely.

Many other projects, large and small, logged significant progress during the past year, and you will be able to view these achievements in the hundreds of posters on display at the meeting. To take one example, the Collaboratory for the Study of Earthquake Predictability (CSEP) became operational in September, 2007, and updated versions of its testing-center software have been released quarterly ever since. As Danijel Schorlemmer will be describe, CSEP is now running earthquake prediction experiments in California, New Zealand, Italy, and, most recently, Japan.

Organization and Leadership

SCEC is an institution-based center, governed by a Board of Directors, who represent its members. The membership currently stands at 16 core institutions and 47 participating institutions (Table 2). SCEC is one of the largest collaborations in geoscience, involving more than 650 scientists and other experts in active SCEC projects. A key measure of SCEC involvement—registrants at our Annual Meetings—is shown for the entire history of the Center in Figure 1.

Table 2. SCEC Institutions (September 1, 2008)

Core Institutions (16)	Participating Institutions (47)
California Institute of Technology Columbia University Harvard University Massachusetts Institute of Technology San Diego State University Stanford University U.S. Geological Survey, Golden U.S. Geological Survey, Menlo Park U.S. Geological Survey, Pasadena University of California, Los Angeles University of California, Riverside University of California, San Diego University of California, Santa Barbara University of California, Santa Cruz University of Nevada, Reno University of Southern California (lead)	Appalachian State University; Arizona State University; Boston University; Brown University; Cal-Poly, Pomona; Cal-State, Long Beach; Cal-State, Fullerton; Cal-State, Northridge; Cal-State, San Bernardino; California Geological Survey; Carnegie Mellon University; Case Western Reserve University; CICESE (Mexico); Disaster Prevention Research Institute, Kyoto University (Japan); ETH (Switzerland); Georgia Tech; Institute of Earth Sciences of Academia Sinica (Taiwan); Earthquake Research Institute, University of Tokyo (Japan); Institute of Geological and Nuclear Sciences (New Zealand); Jet Propulsion Laboratory; Los Alamos National Laboratory; Lawrence Livermore National Laboratory; National Chung Cheng University (Taiwan); National Taiwan University (Taiwan); National Central University (Taiwan); Ohio State University; Oregon State University; Perdue University; Rensselaer Polytechnic University; Texas A&M University; University of Arizona; UC, Berkeley; UC, Davis; UC, Irvine; University of British Columbia (Canada); University of Colorado; University of Massachusetts; University of Minnesota; University of Missouri-Columbia; University of North Carolina; University of Oklahoma; University of Oregon; University of Utah; University of Western Ontario (Canada); University of Wisconsin; URS Corporation; Utah State University; Woods Hole Oceanographic Institution

Board of Directors. Under the SCEC3 by-laws, each core institution appoints one member to the Board of Directors, and two at-large members are elected by the Board from the participating institutions. The Board is chaired by the Center Director, who also serves as the USC representative; the Vice-Chair is Lisa Grant. During the past year, Ralph Archuleta replaced Doug Burbank as the Board member from UCSB. The complete Board of Directors is listed on p. 20 of the meeting volume.

Advisory Council. The Center's external Advisory Council (AC) is charged with developing an overview of SCEC operations and advising the Director and the Board. Since the inception of SCEC in 1991, the AC has played a major role in maintaining the vitality of the organization and helping its leadership chart new directions. A verbatim copy of the AC's 2007 report follows my report in this meeting volume.

We thank Dr. Chris Rojahn, who is rotating off the AC this year, and we welcome Drs. Mary Lou Zoback and John Filson as new AC members. Dr. Zoback, who is Vice President for Earthquake Risk Applications at RMS Inc., succeeds Dr. Sean Solomon as AC chair, and we thank her for her leadership of this important council.

Working Groups. The SCEC organization comprises a number of disciplinary committees, focus groups, and special project teams (Figure 3). These working groups have been the engines of its success. The discussions organized by the working-group leaders at the Annual Meeting have provided critical input to the SCEC planning process.

The Center supports disciplinary science through three standing committees in Seismology, Tectonic Geodesy, and Earthquake Geology (green boxes of Figure 3). They are responsible for disciplinary activities relevant to the SCEC Science Plan, and they make recommendations to the Planning Committee regarding the support of disciplinary research and infrastructure.

SCEC coordinates earthquake system science through five interdisciplinary focus groups (yellow boxes): Unified Structural Representation (USR), Fault & Rupture Mechanics (FARM), Crustal Deformation Modeling (CDM), Lithospheric Architec-ture & Dynamics (LAD), Earthquake Forecasting & Predictabilty (EFP), and Ground Motion Prediction (GMP).

A sixth interdisciplinary focus group on Seismic Hazard & Risk Analysis (SHRA) manages the "implementation interface" as part of SCEC Communication, Education & Outreach (CEO) program (orange box). In particular, SHRA coordinates research partnerships with earthquake engineering organizations in end-to-end simulation and other aspects of risk analysis and mitigation.

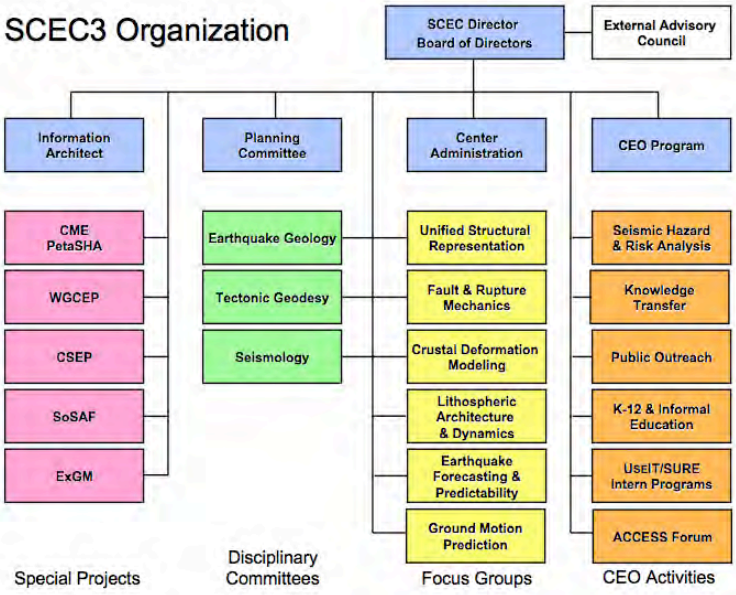

Figure 3. The SCEC3 organization chart, showing the disciplinary committees (green), focus groups (yellow), special projects (pink), CEO activities (orange), management offices (blue), and the external advisory council (white).

Planning Committee. The SCEC Planning Committee (PC) is chaired by the SCEC Deputy Director, Greg Beroza, and comprises the leaders of the SCEC science working groups—disciplinary committees, focus groups, and special project groups (Table 3). The PC has the responsibility for formulating the Center's science plan, conducting proposal reviews, and recommending projects to the Board for SCEC support. The working group leaders and co-leaders are a truly exceptional group of scientists working for the benefit of the SCEC community; please use the opportunity of the Annual Meeting to communicate your thoughts about the SCEC3 Science Plan to them.

Table 3. SCEC3 Working Group Leadership

Disciplinary Committees	
Geology	Mike Oskin*
	James Dolan
Seismology	Egill Hauksson*
	Jamie Steidl
Geodesy	Jessica Murray*
	Rowena Lohman
Focus Groups	
Structural Representation	John Shaw*
	Jeroen Tromp
Fault & Rupture Mechanics	Judi Chester*
	Ruth Harris
Crustal Deformation Modeling	Liz Hearn*
	Tom Parsons
Lithospheric Architecture & Dynamics	Paul Davis*
	Gene Humphreys
Earthquake Forecasting & Predictability	Terry Tullis*
	Bernard Minster
Ground Motions	Robert Graves*
	Steve Day
Seismic Hazard & Risk Analysis	Paul Somerville*
	Nico Luco
Special Project Groups	
CME/PetaSHA Project	Phil Maechling*
WG on Calif. Earthquake Probabilities	Ned Field*
Collaboratory for Study of Equake Predictability	Tom Jordan
	Danijel Schorlemmer*
Southern San Andreas Fault Project	Ken Hudnut*
Extreme Ground Motion	Tom Hanks*

* *Planning Committee members*

Center Budget and Project Funding

The 2008 base funding for the Center was $2,700K from the National Science Foundation and $1,100K from the U.S. Geological Survey. The base funding of $3,800K was augmented with $45K from the Keck Foundation for CSEP, $100K from the GPS royalty funds for GPS activities, $240K from the USGS for SoSAFE, and $255K from PG&E/DOE for the Extreme Ground Motion project. The total funding available was $4,440K.

The base budget approved by the Board of Directors for this year allocated $3,315K for science activities managed by the SCEC Planning Committee; $405K (including $25K for intern programs) for communication, education, and outreach activities, managed by the CEO Associate Director, Mark Benthien; $140K for information technology, managed by Information Architect, Phil Maechling; $280K for administration and $170K for meetings, managed by the Associate Director for Administration, John McRaney; and $130K for the Director's reserve account.

The structuring of the SCEC program for 2008 began with the working-group discussions at our last Annual Meeting in September, 2007. An RFP was issued in October, 2007, and 209 proposals (165 projects, considering collaborations) requesting a total of $6,320K were submitted in

November, 2007. All proposals were independently reviewed by the Director and Deputy Director. Each proposal was also independently reviewed by the leaders and/or co-leaders of three relevant focus groups or disciplinary committees. (Reviewers were required to recuse themselves when they had a conflict of interest.) The Planning Committee met on January 14-15, 2008, and spent two days discussing every proposal. The objective was to formulate a coherent, budget-balanced science program consistent with SCEC's basic mission, short-term objectives, long-term goals, and institutional composition. Proposals were evaluated according to the following criteria:

a. Scientific merit of the proposed research.

b. Competence and performance of the investigators, especially in regard to past SCEC-sponsored research.

c. Priority of the proposed project for short-term SCEC objectives.

d. Promise of the proposed project for contributing to long-term SCEC goals.

e. Commitment of the P.I. and institution to the SCEC mission.

f. Value of the proposed research relative to its cost.

g. The need to achieve a balanced budget while maintaining a reasonable level of scientific continuity given the very limited Center funding.

The recommendations of the PC were reviewed by the SCEC Board of Directors at a meeting on February 3-4, 2008. The Board voted unanimously to accept the PC's recommendations, pending a final review of the program by the Center Director, which was completed on February 26, 2008.

Communication, Education, and Outreach

Through its CEO Program, SCEC offers a wide range of student research experiences, web-based education tools, classroom curricula, museum displays, public information brochures, online newsletters, workshops, and technical publications. Highlights of CEO activities for the past year are reported in the meeting volume by the Associate Director for CEO, Mark Benthien, who will present an oral summary on Monday morning.

SCEC has led the development of the "Earthquake Country Alliance" (ECA), an umbrella organization that includes earthquake scientists and engineers, preparedness experts, response and recovery officials, news media representatives, community leaders, and education specialists. The ECA has become our primary framework for developing partnerships, products, and services for the general public. SCEC has erected and maintained the ECA web portal (*www.earthquakecountry.info*), which provides multimedia information about living in earthquake country, answers to frequently asked questions, and descriptions of other resources and services provided by ECA members. In 2007, ECA organized the *Dare to Prepare* campaign, marking the 150th anniversary of the Ft. Tejon earthquake. It encouraged Southern Californians to "talk about our faults," to understand that "Shift Happens," and to "Secure Your Space" in order to protect yourself, your family, and your property (see *www.daretoprepare.org*).

In the past year, the major focus of the ECA and the SCEC/CEO programs has been the organization of the Great Southern California ShakeOut, a week of special events featuring the largest earthquake drill in U.S. history. At 10 a.m. on November 13, 2008, millions of southern Californians will "Drop, Cover, and Hold On" to practice what to do when a major earthquake happens. ShakeOut is based on a potential 7.8 magnitude earthquake on the southern San Andreas fault. Dr. Lucy Jones of the USGS has led a group of over 300 scientists, engineers, and others to study the likely consequences of this scenario (see Figure 2b). The ShakeOut exercises will be a

dramatic call to action for preparedness (see *www.ShakeOut.org*). All SCEC members are encouraged to participate. On November 12-14, the City of Los Angeles and the Earthquakes and Megacities Initiative will host an International Earthquake Conference, bringing together international experts to discuss policy, planning, and preparedness (see *www.iec.lacity.org*).

Putting Down Roots in Earthquake Country continues to be the principal SCEC vehicle for providing earthquake science, mitigation, and preparedness information to the public. The updated 2007 edition of the handbook is available for download at *www.earthquakecountry.info/roots*, and free copies can be ordered from the Center. In 2008, several *Roots*-related efforts are underway:

- A Utah version of *Putting Down Roots in Earthquake Country*
- *Living on Shaky Ground,* an update to the well-known earthquake booklet for California's north coast, which will include now the *Seven Steps to Earthquake Safety*
- *The Seven Steps to an Earthquake Resilient Business,* an new 16-page supplement developed for businesses by a SCEC-organized committee of experts.
- A major update of the Southern California version of *Roots* to include UCERF probability estimates and ShakeOut scenario results.

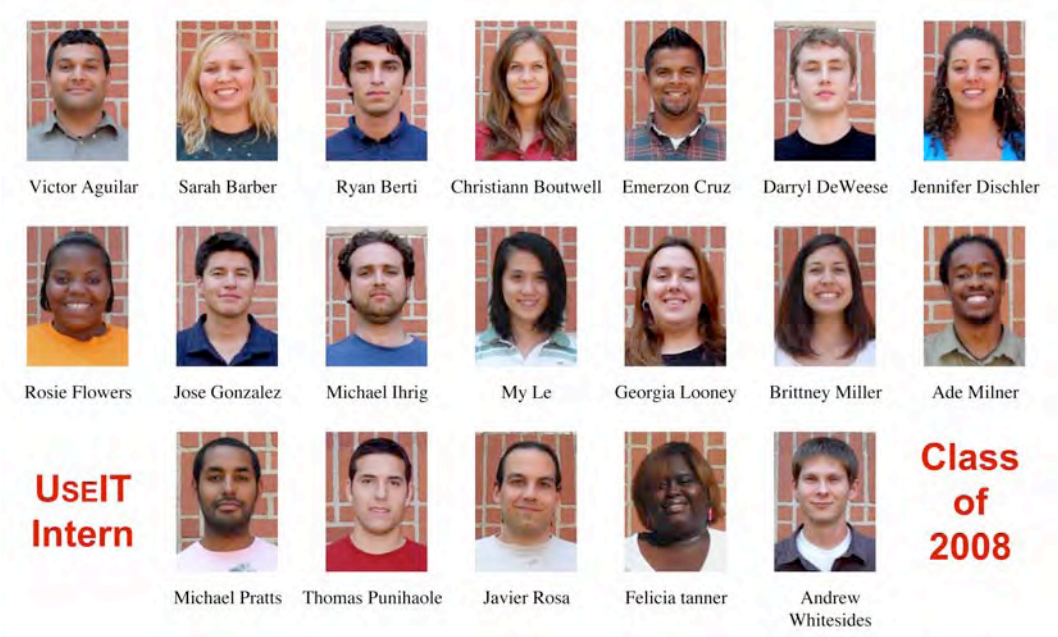

Figure 4. The 19 students from around the country who participated in the 2008 USEIT summer intern program. Many will be attending the Annual Meeting, and they will present posters, demos, and animations, as well as a film about the 2008 USEIT program.

SCEC CEO staff continues to work with museums and other informal education venues to develop content and programs for earthquake education and to distribute SCEC resources, such as *Roots*. In 2008, SCEC organized a group of museums and other locations interested in earthquake education into a network of *Earthquake Education and Public Information Centers* (Earthquake EPICenters).

SCEC is very active in the earth science education community, participating in organizations such as the National Association of Geoscience Teachers, The Coalition for Earth System Education, and

local and national science educator organizations (e.g. NSTA). An example of a current project is a partnership with EarthScope to host a San Andreas fault workshop for park and museum interpreters in Spring 2009.

Last winter, Dr. Robert de Groot took over SCEC's Office for Experiential Learning and Career Development from Sue Perry. The office manages three SCEC intern programs: Summer Undergraduate Research Experiences (SURE), Undergraduate Studies in Earthquake Information Technology (USEIT), and Advancement of Cyberinfrastructure Careers through Earthquake System Science (ACCESS). It also promotes diversity in the scientific workforce and the professional development of early-career scientists. Many of the summer interns will be attending the meeting, and I hope you'll have the opportunity to check out the posters and other presentations of their work.

***

As SCEC Director, I want to express my thanks to all of you for your attendance at the Annual Meeting and your sustained commitment to the collaboration. Please do not hesitate to contact me personally if you have questions or comments about our activities, accomplishments, and plans. Enjoy Palm Springs!

Report of the Advisory Council

Southern California Earthquake Center

September 2007 Meeting

Introduction

The Advisory Council of the Southern California Earthquake Center (SCEC) met during the 2007 SCEC Annual Meeting, held in Palm Springs, California, during 9-12 September 2007. The principal meeting of the council was during the evening of 11 September; an earlier session was held prior to the start of the Annual Meeting on 9 September to outline areas of focus. The council chair summarized the principal council findings and recommendations in an oral report delivered during the closing session of the Annual Meeting on the morning of 12 September.

On 7 September the SCEC Director had circulated to the Advisory Council a report summarizing how SCEC had responded to Advisory Council recommendations from the previous year and presented a number of new issues warranting council attention. Those new issues included an evaluation of the center's Communication, Education, and Outreach (CEO) Program; an evaluation of CEO's Office of Experiential Learning and Career Advancement; feedback on the Collaboratory for the Study of Earthquake Predictability; advice on initiatives in large-scale earthquake simulation; and further advice on issues previously identified by the Advisory Council in the areas of communication, publications, partnerships, and promotion of diversity within the organization.

After a few general remarks below, we discuss the issues raised by the Director in his 7 September mailing, we comment on a number of recurring topics, and we make several recommendations as needed.

Some General Impressions

Because members of the Advisory Council are not also members of SCEC, the Annual Meeting provides an important opportunity for council members to assess annual progress on the center's goals and programs. The 2007 meeting and associated workshops proved again to be impressive demonstrations of the energy and enthusiasm of the SCEC community. The 137 registrants who were attending their first SCEC Annual Meeting (30% of the 451 total registrants) constituted heartening evidence of the center's growing participation and exciting mission.

The Advisory Council again lauds the SCEC membership for the persistently selfless spirit with which everyone involved has worked constructively to develop communal, system-level representations that are advancing the goals of fundamental and applied earthquake science. The structure of the 2007 meeting was well conceived to permit ample discussion of issues, lively interactions at the many poster presentations of new science, and well-chosen overview talks, most featuring early-career scientists who exemplify the new generation of SCEC leaders. The Advisory Council also applauds SCEC's continually developing partnerships with the earthquake engineering community.

It is the view of the Advisory Council that the transition from the second (SCEC2, 2002-2007) to the third (SCEC3, 2007-1012) phase of SCEC has been accomplished smoothly. The new organization appeared to be working constructively and cooperatively toward the accomplishment of the center's newly articulated scientific and programmatic objectives.

Evaluation of the CEO Program

Along with his request of 7 September that the Advisory Council evaluate SCEC's CEO program, the Director posed the following specific questions:

- Are the basic elements of the CEO program – formal and informal education, public outreach, knowledge transfer – in appropriate balance?
- Is the Dare to Prepare campaign, currently SCEC's premier effort in public outreach, appropriately organized through the Earthquake Country Alliance?
- Is the current funding of the CEO program (10% of base budget plus contracted activities) at the appropriate level? What is the role of special projects in the funding of CEO

The Advisory Council knows of no other organization that has accomplished more in the area of communication, education, and outreach, nor done so as effectively and as informed by knowledge from the social and behavioral sciences, than SCEC. Existing CEO activities are laudable across the program, and SCEC should take justifiable pride in its myriad efforts at presenting earthquake issues clearly and compellingly to the public and to decision makers. That said, it is appropriate to consider additional possible CEO tasks and new directions, both in partnership with other organizations and within the program.

Outreach to NGOs. In the area of new partnerships, SCEC should consider devising and implementing specific plans to reach out to those non-government organizations (NGOs) that would be pressed into service after a damaging California earthquake, particularly NGOs likely to provide goods and services to low-income populations not likely to be able to prepare for such a disaster on their own. Coordination with the parallel project sponsored by the Fritz Institute in the San Francisco Bay area (a key contact there is Rich Eisner) on this issue should prove useful in developing this plan.

Targeting CEO opportunities in political systems. One of the general objectives of the SCEC CEO program, and of SCEC in general, is to foster improvements in scientific understanding that result in a seismically safer southern California. Multiple strategies are needed to effect appropriate actions across the diverse sectors of society, e.g., what convinces households to act may not yield actions by local governments or the private sector. It could prove useful for the SCEC CEO program to identify local political action points and craft customized CEO activities to propel local communities or organizations in the direction of enhanced seismic safety. For example, the "Committee of 25" in Palm Springs is made up of influential residents who, if convinced, could easily exercise influence over local political priority setting and subsequent actions for that city's earthquake readiness, e.g., by retrofitting the airport.

Leveraging other hazard planning efforts. SCEC CEO activities are understandably earthquake focused and include laudable outreach efforts to partners throughout the southland and the state. It might be productive to now consider, and selectively pursue, partnerships that leverage SCEC CEO efforts by joining forces with other organizations in the same geographical area that are working on plans to address other hazards, e.g., other natural hazards and acts of terrorism.

Formal review of CEO activities. In the area of new internal directions, it is timely for the SCEC CEO program to initiate a thorough review of its programs. A cost-effective way to accomplish such a review would be through a one-time "visiting committee" or workshop of external CEO professionals expert in hazards issues charged to review CEO program elements and provide critical findings and recommendations.

Use of OES/CSSE survey results. It would be appropriate (particularly given that the SCEC CEO program was instrumental in instigating the survey) to develop a plan to utilize the results of the Office of Emergency Services (OES) California Seismic Safety Commission (CSSC) survey of

household knowledge, mitigation, and preparedness related to earthquake hazards. The survey will produce findings that can be generalized to households in southern California's high-earthquake-risk counties. These findings could point CEO in important new directions.

Communication training for SCEC members. CEO should consider the development of a formal training program for SCEC scientists, through a training manual or short course, in the communication of risk and scientifically based prediction. Such training should include insight from the social sciences regarding the most effective way to craft the content and form of scientifically credible predictions of damaging earthquakes (particularly short-term predictions). SCEC scientists should be prepared in the event that such a prediction emerges from their research.

A CEO research program. The CEO program should consider the development of a modest research program sharply focused on programmatic needs. This program should be crafted to produce new understanding that can enhance the effectiveness of future CEO activities in southern California.

An evaluation of Putting Down Roots. The centerpiece of SCEC CEO activities, *Putting Down Roots in Earthquake Country,* has become the national standard for public hazards education. The document was conceived on the basis of best practices in the social sciences in 1980s and early 1990s, but that knowledge base has since advanced. Moreover, *Roots* has undergone revisions over time, and different organizations now take pride in its ownership. The SCEC CEO program should begin to lay the groundwork for the possible revision of the content of *Roots*, as well as revisions to the strategies used to disseminate it.

Such an evaluation might take the following form: (1) Information learned about the effectiveness of *Roots* in the statewide OES CSSC survey should be used to inform revisions in content and dissemination strategies. (2) A small set of social scientists familiar with the appropriate research record and the results of the statewide survey should be assembled to comment of the substance and form of *Roots* to ensure that it still represents the current state of the art. (3) A private firm should be engaged (and overseen by the appropriate social scientists) to conduct focus groups to determine the most effective way to present the material in the document. (4) The original research that led to *Putting Down Roots in Earthquake Country* had more to say about the effectiveness of such information than what such a document might contain, but the context in which *Roots* is distributed is as important as the substance of the document itself. Existing and previous distributions of *Roots* should be reviewed and evaluated from this "nested communications" model, and the outcomes of such a review should play a central role in future *Roots* distribution plans if the pending statewide survey yields similar conclusions. (5) Finally, the contents of the document should be reviewed to determine if it provides adequate information about household readiness for earthquakes of differing severity and infrastructure damage.

Evaluation of ELCA

SCEC recently established, under the CEO program, an Office of Experiential Learning and Career Advancement (ELCA), staffed by Sue Perry. The responsibilities of this office include supervision of three intern programs and administration of the nascent SCEC Distinguished Speakers Program. The SCEC Director, in his 7 September letter, requested that the Advisory Council provide an evaluation of plans for ELCA activities and organization.

The Advisory Council concurs that the growth of the SCEC intern programs, particularly at member institutions other than the University of Southern California, warrants the appointment of a dedicated administrator. Initial plans for the ELCA office look to be appropriate, but one area deserving of further consideration is communication of the message to students, e.g., through

internships, that there is "life outside academia." The SCEC Distinguished Speakers Program is warmly welcomed by the Advisory Council, which has recommended the initiation of such an outreach effort for several years.

The Advisory Council plans a full evaluation of the ELCA office and its programs in the coming year. That evaluation will be conducted in cooperation with Sue Perry and other SCEC leaders.

Feedback on CSEP

The Collaboratory for the Study of Earthquake Predictability (CSEP), as a SCEC special project in its second year of support from the Keck Foundation, is in a stage of rapid development. SCEC released the first version of CSEP Testing Center software at the Annual Meeting. In his 7 September letter to the Advisory Council, the SCEC Director asked:

- How much effort should SCEC expend on the international aspects of CSEP?
- What should be SCEC's funding strategy after the Keck Foundation grant expires in 2009?
- Is the connection of CSEP to the SEC base program through the Earthquake Forecasting & Predictability (EFP) focus group appropriately configured?
- Should SCEC incorporate younger leadership in the EFP focus area?

It is the Advisory Council view that the approach SCEC is taking to earthquake predictability is appropriately rigorous, a direction likely to engender broad community support. Moreover, SCEC is doing a good job at promoting the capabilities of the collaboratory. The expansion of the program's perspective to geographic settings other than southern California is sensible as means to expand the likelihood of capturing events. The connection to SCEC's base program, although not perceived by all as strong, is appropriately overseen by the EFP focus group.

The future of CSEP will depend, in part, on whether there are interesting outcomes to the collaboratory's activities. Whether all prediction methodologies fail rigorous tests or at least one algorithm shows promise will make a substantial difference in the imperative for long-term support of this endeavor. Another year or two of operation, however, may not be sufficient to decide this question, so it is recommended that SCEC seek support for the continuation of this collaboratory, or the initiation of a successor program, from the U.S. Geological Survey or another appropriate organization. The thoughtful development of evaluation metrics for the program's continuation should be an integral component of seeking such extended support.

Advice on Initiatives in Large-scale Earthquake Simulation

Another special project area within SCEC that is now undergoing rapid growth is large-scale earthquake simulation. At the Annual Meeting SCEC leadership reported that the center had just received notice that a proposal to NSF to support the continued development of such simulations (PetaShake) would be funded at a level of $1.8M for 2 years and that another proposal to NSF at a comparable level, coordinated with the first, was under review. The Director asked the Advisory Council the following questions:

- Is continuing this direction appropriate to SCEC's development of earthquake system science?
- How should these special projects be connected to the SCEC base effort?
- How should SCEC coordinate their development of simulation-based seismic hazard analysis with the engineering community?

It is the view of the Advisory Council that physics-based simulations and coupled hazard assessments as an alternative to standard attenuation relations constitute an integration of knowledge gained in earthquake system science and remain a critical direction for SCEC. The PetaShake efforts in high-performance computing are best linked to the SCEC base effort through testing and validation with actual data. The Advisory Council applauds the Tall Building Initiative as an ideal demonstration project of substantial societal importance and covering a seismic band for which there is considerable confidence in the simulation results. A code validation effort, analogous in part to CSEP, conducted jointly with leaders from the earthquake engineering community, could be critical in establishing user acceptance.

Other Feedback

There are several areas that have warranted recurring feedback from the Advisory Council, and the Director requested additional comments in his 7 September letter. These areas include:

- Tracking progress toward SCEC objectives.
- Providing feedback on special projects.
- Providing advice on new scientific opportunities
- Advising on opportunities for new cross-disciplinary partnerships.
- Evaluating leadership performance.
- Providing recommendations on SCEC publications.
- Advising on mechanisms to promote diversity at all organization levels.

Evaluating SCEC Progress

The Advisory Council was pleased to learn that the SCEC Planning Committee will be addressing, in the near term, the issue of tracking progress toward the achievement of center objectives. We note, as one element of this issue, that our 2006 report recommended that "SCEC should associate the proposals it supports (as well as those received but not supported) with appropriate current objectives and disseminate that information as one measure of the community interest and resource allocation." We affirm that this recommendation remains worthwhile. As requested by SCEC leadership, the Advisory Council will continue to provide advice, as appropriate, on SCEC special projects, via a variety of mechanisms to be explored over the coming year.

New Scientific and Partnership Opportunities

It is the intent of the Advisory Council to continue to provide advice on new scientific opportunities and potential partnerships on an ongoing basis. The Advisory Council regularly provides feedback to SCEC leadership on their performance and encourages SCEC members to voice their views on leadership issues either during the Annual Meeting or privately to Advisory Council members. It is the current sense of the Advisory Council that the senior leadership of SCEC is doing an outstanding job, and that the many individuals now leading committees and focus groups constitute a broadly diverse, extremely able, and committed group.

Publishing SCEC Accomplishments

In its 2006 report, the Advisory Council wrote that "…documentation of the accomplishments of SCEC2 in earthquake system science remains an important goal, both to communicate to Earth scientists the substantial progress that has been made and to provide a benchmark and a resource for work to follow." We wrote further that "Notwithstanding the history of such endeavors by SCEC and the considerable attention of SCEC leadership recently and understandably devoted to planning and fundraising, the organization of a monograph, collection of papers, or other vehicle

to present SCEC2 accomplishments is timely." The Advisory Council still regards this recommendation as having merit.

Promoting Community Diversity

In our 2006 report, the Advisory Council wrote that "SCEC's intern program has been a showcase for the involvement of a broad and diverse spectrum of students and that similar attention to diversity is warranted across all other elements of SCEC programs." We further advised that other SCEC efforts (e.g., the speaker program, media opportunities, summer sabbatical visits by professors at minority institutions and historically black colleges and universities) should be focused on increasing the diversity of participation. We affirm these views, and the Advisory Council commits to continuing to work with SCEC leaders to ensure that the center continues its noteworthy progress in encouraging diversity across all of its programs.

Final Comments

The Advisory Council is pleased to continue to provide assistance to SCEC in its efforts to formulate and accomplish the center's major goals. At any time the council welcomes comments, criticism, and advice from the seismological community, including individuals and groups both inside and outside SCEC membership, on how best to provide that assistance.

The Advisory Council welcomes Mary Lou Zoback as its new chair and looks forward to working with SCEC leadership to help ensure that the products and progress of the center in the SCEC3 era continue to be commensurate with agency and community investment.

SCEC Advisory Council

Sean C. Solomon, Carnegie Institution of Washington (Chair)*

Gail Atkinson, Carleton University

Lloyd S. Cluff, Pacific Gas and Electric Company

Jeffrey T. Freymueller, University of Alaska*

Mariagiovanna Guatteri, Swiss Reinsurance America Corporation*

Dennis Miletti, University of Colorado, Boulder*

Kate C. Miller, University of Texas at El Paso

Jack P. Moehle, Pacific Earthquake Engineering Research Center (PEER)**

Garry C. Rogers, Geological Survey of Canada*

Chris Rojahn, Applied Technology Council

John Rudnicki, Northwestern University*

Ellis M. Stanley, Sr., City of Los Angeles Emergency Preparedness Department

Mary Lou Zoback, RMS Solutions*

---

*Attended at least part of the 2007 Annual Meeting and Advisory Council sessions

** Represented by Yousef Bozorgnia, PEER

SCEC Communication, Education, and Outreach

Mark Benthien
CEO Director for SCEC

Introduction

The SCEC Communication, Education, and Outreach (CEO) program has four long-term goals:

- Coordinate productive interactions among a diverse community of SCEC scientists and with partners in science, engineering, risk management, government, business, and education;
- Increase earthquake knowledge and science literacy at all educational levels, including students and the general public;
- Improve earthquake hazard and risk assessments; and
- Promote earthquake preparedness, mitigation, and planning for response and recovery.

These goals were identified through several workshops involving SCEC scientists and our partner organizations, who were also involved in developing and fulfilling CEO short-term objectives through activities organized within four CEO focus areas: research partnerships coordinated within the SCEC Seismic Hazard & Risk Analysis focus group; Knowledge Transfer activities with practicing professionals, government officials, scientists and engineers; Public Outreach activities and products for the general public, civic and preparedness groups, and the news media; Education programs and resources for students, educators, and learners of all ages, including the Experiential Learning and Career Advancement office which coordinates undergraduate and graduate internships and support for early career scientists. Many activities span more than one CEO Focus area.

A key aspect of SCEC's success are the many partnerships that have been sustained to achieving SCEC's mission, research objectives, and outreach goals. These partners include: other science organizations such as IRIS, EarthScope, and UNAVCO; engineering organizations such as PEER, CUREE, and EERI; Education organizations such as Los Angeles County Unified School District, Southern California County Offices of Education, USC Family of Schools, museums, and the National Association of Geoscience Teachers (NAGT); and Public Service / Risk Management organizations such as California Office of Emergency Services, the California Earthquake Authority, FEMA, and the American Red Cross.

The following are select Public Outreach and Education highlights of activities in the last year.

Public Outreach Activities

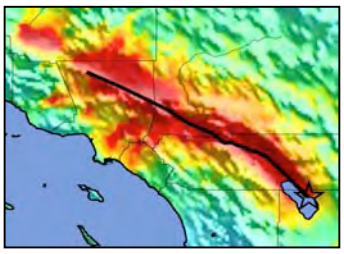

Great Southern California ShakeOut. The major focus of the 2007-2008 CEO program has been co-organizing this week of special events featuring the largest earthquake drill in U.S. history, developed to inspire Southern Californians to get ready for big earthquakes, and to prevent disasters from becoming catastrophes. At 10 a.m. on November 13, 2008, millions of southern Californians will "Drop, Cover, and Hold On" to

practice what to do when a major earthquake happens. Individuals, families, businesses, schools and organizations will join firefighters and other emergency responders (involved in the statewide "Golden Guardian" exercise the same week) in our largest-ever earthquake preparedness activity.

As of August 29, over 2.5 million participants have been registered to participate at www.ShakeOut.org. The goal is for 5 million people total to participate on November 13. Registered participants will receive information on how to plan their drill, connect with other participants, and encourage a dialogue with others about earthquake preparedness. This is the largest public outreach activity for earthquake awareness and preparedness ever attempted (perhaps in the country) and an unprecedented opportunity to educate the public.

ShakeOut is based on a potential 7.8 magnitude earthquake on the southern San Andreas Fault. This type of earthquake occurs in southern California every 150 years on average, and the last was 151 years ago! Dr. Lucy Jones (USGS) has led a group of over 300 scientists, engineers, and others to study the likely consequences of this enormous earthquake in great detail. Many SCEC scientists have been involved including many who produced the ShakeOut Simulation. The final simulation used in analysis of losses was by Rob Graves, and the visualization was by Geoff Ely.

In summary, the ShakeOut Scenario estimates this earthquake will cause some 2,000 deaths, 50,000 injuries, $200 billion in damage and other losses, and severe, long-lasting disruption. The report has regional implications and is a dramatic call to action for preparedness, and is available at www.ShakeOut.org.

In addition to the ShakeOut drill, the City of Los Angeles and the Earthquakes and Megacities Initiative (of which SCEC CEO director Benthien is the Los Angeles liaison) is hosting an International Earthquake Conference November 12-14, bringing together over 45 international experts to discuss policy, planning, and preparedness with U.S. counterparts. Online registration is available, and early registration incentives are available through the end of August. More information can be found at www.iec.lacity.org.

On Friday, November 14, Art Center College of Design will present the "Get Ready Rally" at the new Nokia LA Live in downtown Los Angeles to engage the public in earthquake preparedness. All southern Californians are invited to celebrate the success of the Drill and share their experiences. There will be food, entertainment, and vendors.

Organizers and participants of the ShakeOut include: Southern California Earthquake Center, U.S. Geological Survey, California Office of Emergency Services, City of Los Angeles, Caltech, Art Center College of Design, University of Southern California, State Farm, California Earthquake Authority, the California Seismic Safety Commission, American Red Cross, and business, schools and governments in Riverside, San Bernardino, Orange, Los Angeles, San Diego, Imperial, Kern, Santa Barbara, and Ventura Counties. Also, many other members of the Earthquake Country Alliance.

To be able to reach communities throughout southern California, the ECA is launching "Regional Associate" groups in each county, charged with spreading the word locally to encourage residents to register to participate in the ShakeOut:

- The San Bernardino County is co-chaired by County Supervisor Brad Mitzenfelt and ESRI President Jack Dangermond.
- The Los Angeles Group led by County Fire Chief P. Michael Freeman and LA Area Chamber of Commerce President Gary Toebben.

- Riverside County Associates are led by Congresswoman Mary Bono Mack and County Emergency Manager Peter Lent.
- San Diego County Associates are led by County Emergency Manager Ron Lane, City of Vista Fire Chief Gary Fisher and City of La Mesa Fire Chief David Burk.
- Orange County Associates are led by County Emergency Manager Donna Boston and County Office of Education
- Associate groups for other counties are in formation.

Sponsors of the Great Southern California ShakeOut activities include USGS, National Science Foundation, FEMA, California Office of Emergency Services, Home Depot, City of Los Angeles, State Farm, California Earthquake Authority, Kaiser Foundation Health Plan, Tyco Electronics, Provention Consortium, Dewberry, Degenkolb, Network for Earthquake Engineering Simulation, Institute for Business & Home Safety, ABC7, and others soon to be announced. Organizations wishing to support ShakeOut activities can learn more at www.ShakeOut.org/sponsors.

All SCEC members are encouraged to participate. G to www.ShakeOut.org and register your family, school, business, or organization's participation in the drill. Registered participants will receive information on how to plan their drill, encourage others to participate, and improve their earthquake preparedness. It all begins with registering, which is free and open to everyone.

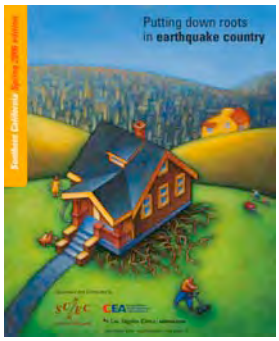

Putting Down Roots in Earthquake Country. In 1995 the Southern California Earthquake Center (SCEC), US Geological Survey (USGS), and a large group of partners led by Lucy Jones (USGS) developed and distributed 2 million copies of a 32-page color handbook on earthquake science, mitigation and preparedness. Funding was primarily from the National Science Foundation and USGS. The booklet was distributed through libraries, preparedness partners, cities, companies, and directly to individuals through SCEC.

For the 10-year anniversary of the Northridge earthquake, a new version was produced by SCEC and the newly-formed Earthquake Country Alliance. The updated handbook features current understanding of when and where earthquakes will occur in Southern California, how the ground will shake as a result, and descriptions of what information will be available online. The preparedness section is now organized according to the "Seven Steps to Earthquake Safety." These steps provide a simple set of guidelines for preparing and protecting people and property.

Since 1994, over 2.2 million copies have been distributed of the new version, with 1.3 million copies distributed via the Los Angeles Times as a "topper"- the booklet was bound on the cover of the Sunday, April 9, 2006 newspaper. Copies of the document have been distributed at home improvement centers (on tables with preparedness products), by the American Red Cross (at neighborhood safety trainings), and by many others. A major revision incorporating new research will be produced in September, 2008. The updated handbook is now at www.earthquakecountry.info/roots as an online version and downloadable PDF, and printed copies can be ordered for free through an online request form.

A notable acheivement in early 2006 was the first-ever Spanish version of Putting Down Roots. A team of Spanish-speaking scientists, emergency managers, and educators worked together to translate the text. 100,000 copies are now being distributed in Southern California. In Spring 2007, a new printing of 600,000 copies (funded by CEA) were distributed through Hoy (LA Times Spanish-language newspaper), the

Los Angeles Mexican Consulate, and other venues, with media promotion on TV and Radio. In September, 2007, another 450,000 copies were be distributed in La Opinion newspaper and through other partners, with an even larger media promotion on Univision.

Putting Down Roots is the principal SCEC framework for providing earthquake science, mitigation, and preparedness information to the public. The "Roots" framework extends beyond the distribution of a printed brochure and the online version. For example, the Birch Aquarium in San Diego developed an earthquake exhibit which featured a "Seven Steps" display, and the Emergency Survival Program (managed by LA County) will be basing it's 2006 campaign around the "Seven Steps." In October 2004 over 15,000 copies were included in the Earth Science Week packets distributed to science teachers and others nationwide.

The new version of Putting Down Roots was designed to allow other regions to adopt its structure and create additional versions. The first is a Greater San Francisco Bay Area version produced by a partnership led by the USGS with SCEC, local and state emergency managers, the Red Cross and many other organizations. The handbook was revised with Bay Area hazards and a new section called "Why Should I Prepare?" was added that includes scenarios for likely damage, casualties, etc., and how life will change during a large earthquake in the region. Over 750,000 copies were printed in September, 2005, with funding from the California Earthquake Authority, USGS, FEMA, Red Cross, OES, CGS, and several others). 500,000 of these copies (with an inserted coupon for furniture straps and other mitigation products) were distributed in the San Francisco Chronicle. To commemorate the Centennial of the 1906 San Francisco earthquake, an additional one million copies were printed and distributed in many Bay Area newspapers, the USGS, and other partners, along with a calendar of activities for the anniversary. In Spring, 2007, 500,000 more copies were printed (with minor updates, including a new "Seven Steps" image). The Bay Area booklet can also be accessed from www.earthquakecountry.info/roots. All printings of the Bay Area version to date have been coordinated through SCEC.

In 2006, the USGS with many Bay Area partners created a new booklet in the Putting Down Roots series, featuring primarily the "Seven Steps" content and produced in two versions- English and Spanish in one booklet, and English, Chinese, Korean, and Vietnamese in another booklet. This new product is titled Protecting Your Family From Earthquakes– The Seven Steps to Earthquake Safety. Developers included the American Red Cross, Asian Pacific Fund, California Earthquake Authority, Governor's Office of Emergency Services, New America Media, Pacific Gas and Electric Company, U.S. Department of Homeland Security Federal Emergency Management Agency, and U.S. Geological Survey. The CEA, FEMA, and others provided funding for 640,000 copies of the English-Spanish version and over 360,000 copies of the English and Asian languages version, with printing coordinated through SCEC. A multi-language media campaign in early 2007 promoted the distribution of the booklets. In September, 2007, 70,000 copies of each booklet were reprinted in order to continue distribution.

For 2008, many Roots-related efforts are underway:

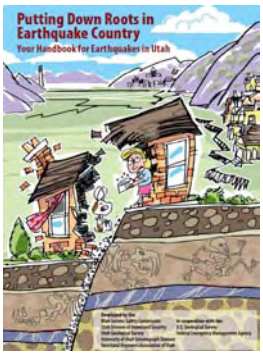

- The first-ever Utah version of Putting Down Roots in Earthquake Country
- Living on Shaky Ground, an update to the well-known earthquake booklet for California's north coast, which will include now the Seven Steps to Earthquake Safety
- The Seven Steps to an Earthquake Resilient Business, an exciting new 16-page supplement for businesses developed by a committee organized by SCEC.
- A major update of the Southern California version of Roots to include UCERF probability estimatesand ShakeOut Scenario results.

Earthquake Country Alliance. To coordinate activities for the 10-year anniversary of the Northridge Earthquake in January 2004 (and beyond), SCEC led the development of the "Earthquake Country Alliance" (ECA) beginning in summer 2003. This group was organized to present common messages, to share or promote existing resources, and to develop new activities and products. The ECA includes earthquake scientists and engineers, preparedness experts, response and recovery officials, news media representatives, community leaders, and education specialists. The mission of the ECA is to:

Earthquake Country **Alliance**
We're all in this together.

- inspire responsibility for community earthquake safety and recovery;
- increase awareness, preparedness, mitigation;
- improve response and recovery planning;
- reduce losses in future earthquakes.

The ECA is now the primary SCEC framework for maintaining partnerships and developing new products and services for the general public.

DARE to prepare

In Summer, 2006, members of the ECA began to organize the Dare to Prepare Campaign, to achieve widespread awareness and preparedness goals to mark the 150th anniversary of the January 9, 1857, Ft. Tejon earthquake on the San Andreas fault. With a strategy of getting southern Californians to "talk about our faults," the campaign acknowledges that "Shift Happens," and if you "Secure Your Space" you can protect yourself, your family, and your property. If you live in earthquake country, secure your space by strapping top-heavy furniture and appliances to walls, adding latches to kitchen cabinets, and securing TVs and other heavy objects that can topple and cause serious injuries. Homes and other buildings should be retrofitted if necessary. These and other actions will greatly reduce your risk of damage or injury, and limit your need for community resources after the next earthquake. On January 9, 2007 a major press briefing was held to kickoff the Dare to Prepare campaign, including local, state, and federal government representatives, SCEC scientists, and ECA partners. A new website (www.daretoprepare.org) was announced, along with other components of the campaign:

- Movers and Shakers: leadership group of prominent Southern California elected officials, business and community leaders, and others;
- Local activities: public events throughout the region (presentations, preparedness fairs, etc.), including demonstrations of Big Shaker, a large portable earthquake simulator;
- Media campaign: television, radio, and print promotion, PSAs, on-air interviews, etc. (Fall)
- Great Southern California Shakeout, a regional public earthquake exercise planned for 2008 (see above)

Earthquake Country Alliance Website. SCEC developed and maintains this web portal (www.earthquakecountry.info.), which provides multimedia information about living in earthquake country, answers to frequently asked questions, and descriptions of other resources and services that ECA members provide. The portal uses technology developed for the E3 project (see above). Each ECA member can suggest links to their organization's resources as answers to questions listed on the site. The site is set up separately from the main SCEC web pages (though has attribution to SCEC) so that all members of the ECA see the site as their own and are willing to provide content. The site features the online version of Putting Down Roots and special information pages that all groups can promote, such as a special page about the "10.5" miniseries and a page about the "Triangle of Life" controversy (see assessments below).

Media Relations. SCEC engages local, regional and national media organizations (print, radio and television) to jointly educate and inform the public about earthquake-related issues. The goal has been to communicate clear, consistent messages to the public–both to educate and inform and to minimize misunderstandings or the perpetuation of myths. In 2008 SCEC coordinated the major release of the Uniform California Earthquake Rupture Forecast, which involved a two-location press conference (with scientists at USC and at USGS in Menlo Park, with streaming video between the locations), a comprehensive website (www.scec.org/ucerf), a new USGS fact sheet, and other resources. SCEC CEO encourages scientists who are interested in conducting interviews with media reporters and writers to take advantage of short courses designed and taught by public information professionals.

Earthquake Country - Los Angeles. This video was produced by Dr. Pat Abbott of SDSU as the second in his "Written in Stone" series. The video tells the story of how the mountains and valleys of the Los Angeles area formed, including the important role of earthquakes. The video features aerial photography, stunning computer animations, and interviews with well-known experts. The video features 3D fault animations produced by SCEC's "LA3D" visualization system. In addition to conducting several focus groups with teachers and preparedness experts where the video was evaluated, SCEC is also developing curricular kits for school and community groups to accompany the video, and has added captions in both English and Spanish. These kits will be duplicated in large quantities with funding from the California Earthquake Authority. The Los Angeles Unified School District has asked SCEC to train teachers how to use these curricular kits, and may include the video in a new sixth-grade Earth science curricula soon to be adopted district wide.

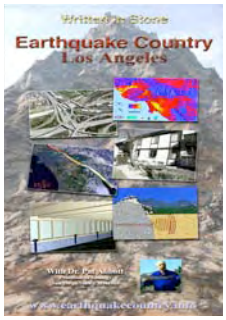

Emergency Survival Program. SCEC serves on the Coordinating Council of the Los Angeles County-led Emergency Surival Program, with emergency managers from all southern California counties, many large cities, the American Red Cross, and Southern California Edison. The primary role of the program is to develop a series of public information materials including monthly Focus Sheets, newsletter articles, and public service announcements related to a yearly theme. In 2006 the

program focused on earthquakes, with seven of the monthly focus sheets based on the "seven steps to earthquake safety" in Putting Down Roots in Earthquake Country. SCEC provided the Spanish version of the seven steps text also, and coordinated the translation of the five other monthly focus sheets for 2006.

Use of SCEC Community Modeling Environment (CME) Products. Many SCEC CME products are being used in public presentations, webpages (scec.org, earthquakecountry.info, etc.), printed publications such as Putting Down Roots in Earthquake Country (English and Spanish), our "Earthquake Country – Los Angeles" DVD ("LA3D" animations) and in other venues to communicate earthquake hazards and encourage preparedness. These products, including the SCEC Terashake simulations, Puente Hills earthquake simulation, and Community Fault Model (CFM), have also had extensive media coverage through press briefings, reporters attending the SCEC Annual Meeting, and television documentaries, and have been used frequently as background imagery in many news stories. Each earthquake simulation is not just a scientific hypothesis, but a visualization of a potential real earthquake that could cause extensive damage and loss of life beyond what has been experienced in southern California previously. SCEC CME visualizations help the public understand how the shaking they may experience will be very intense, and how long it will last. These visualizations were featured extensively in the National Geographic Channel documentary "Killer Quake," which presented SCEC Terashake and Puente Hills animations, along with SCEC VDO fault movies.

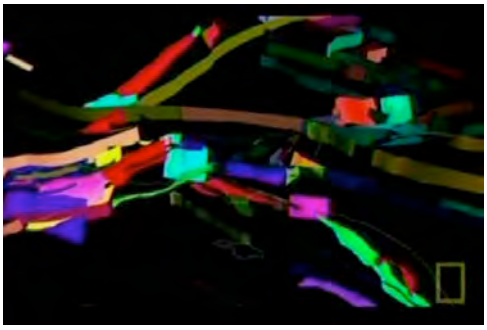

Education Program

SCEC and its expanding network of education partners are committed to fostering increasing earthquake knowledge and science literacy at all grade levels and in a variety of educational environments.

- The SCEC Education Program uses the research literature (science education, learning psychology, sociology, etc) and evaluation methodology to:
- Develop new materials and products (e.g. a lesson plan, an evaluation instrument, a website) where needed.
- Collaborate with partner organizations to enhance existing materials or products to meet the needs for SCEC's Earthquake Program mission.
- Utilize and promote existing materials that coincide with or complement SCEC's earthquake K-12 Education Program mission.
- Provide innovative experiential learning opportunities to undergraduate and graduate students during the summer and year-round.

SCEC education programs include three internship programs, facilitated activities at museum exhibits, earthquake education workshops, public earthquake talks, and activities at conferences such as the National Science Teachers Association. SCEC Education programs and products are implemented in a variety of educational environments- any place, situation, or context where the transmission of knowledge to learners is taking place.

SCEC Experiential Learning and Career Advancement programs

Undergraduate Internships. SCEC has provided internships to over 220 students since 1994. SCEC interns are typically paid a stipend of $5000 over the summer with support from the NSF REU program. SCEC offers two summer internship programs, SCEC/SURE, and SCEC/USEIT. These programs are the principal SCEC framework for undergraduate student participation in SCEC, and have common goals of increasing diversity and retention. In addition to their research projects, participants come together several times during their internship for orientations, field trips, and to present posters at the SCEC Annual meeting. Students apply for both programs at *http://www.scec.org/internships*.

The SCEC Summer Undergraduate Research Experience (SCEC/SURE) has supported students to work one-on-one as student interns with SCEC scientists since 1994. SCEC/SURE has supported students to work on numerous issues related to earthquake science including the history of earthquakes on faults, risk mitigation, seismic velocity modeling, science education, and earthquake engineering.

The SCEC Undergraduate Studies in Earthquake Information Technology (SCEC/USEIT) program, unites undergraduates from across the country in an NSF REU Site at USC. SCEC/ USEIT interns interact in a team-oriented research environment with some of the nation's most distinguished geoscience and computer science researchers. Summer interns interact in a collaborative, team-oriented, interdisciplinary research environment and are mentored by some of the nation's most forward-thinking earthquake and computer scientists. Research activities are structured around "Grand Challenges" in earthquake information technology. Each summer the interns build upon the foundation laid by previous sessions as they design and engineer increasingly sophisticated visualization tools.

ACCESS. Our USEIT and CME experience has identified a "weak link" in CI-related career pathways: the transition from discipline-oriented undergraduate degree programs to problem-oriented graduate studies in earthquake system science. We are addressing this educational linkage problem through a CI-TEAM implementation project entitled the Advancement of Cyberinfrastructure Careers through Earthquake System Science (ACCESS). The objective of the ACCESS project is to provide a diverse group of students with research experiences in earthquake system science that will advance their careers and encourage their creative participation in cyberinfrastructure (CI) development. Its overarching goal is to prepare a diverse, CI-savvy workforce for solving the fundamental problems of system science. Three programmatic elements have been developed to achieve this goal: (1) Undergraduate (ACCESS-U) Internships, support CI-related research in the SCEC Collaboratory by undergraduate students working toward senior theses or other research enhancements of the bachelor's degree. (2) Graduate (ACCESS-G) Internships support up to one year of CI-related research in the SCEC Collaboratory by graduate students working toward a master's thesis. (3) The ACCESS Forum, a new working group managed under the SCEC CEO program to promote CI careers in earthquake system science.

Earthquake Exhibits and Museum Partnerships

Recognizing the key role that museums have in engaging communities not often reached by schools, SCEC facilitates a network of museums and other locations interested in providing earthquake education programming. These organizations also serve as a distribution point for

SCEC resources such as Roots. SCEC has worked with some of these partners for many years, and in summer 2008 they have been organized as Earthquake Education and Public Information Centers (Earthquake EPICenters).

ShakeZone Earthquake Exhibit (Fingerprints Youth Museum, Hemet, CA) Developed originally in 2001, ShakeZone was redesigned in 2006. The current version of the exhibit is based on SCEC's Putting Down Roots in Earthquake Country handbook. Major partners involved in the exhibit redesign included Scripps Institution of Oceanography and Birch Aquarium at Scripps. With funding from the United Way and other donors ShakeZone will be expanded in 2009 to include a section on Earthquake Engineering.

Living on the Edge Exhibit (San Bernardino County Museum, Redlands, CA) This exhibit explains and highlights natural hazards in San Bernardino County (e.g. Fire, Floods, and Earthquakes). SCEC provided resources in the development phase of the project and continues to supply the exhibit with copies of Putting Down Roots in Earthquake Country

Hall of Geological Wonders (San Bernardino County, Redlands, CA) Due to be completed in mid-2009 the Hall is a major expansion of this important cultural attraction in the Inland Empire. One of the main objectives of the Hall is to teach about the region from a geologic perspective. We are devoting a large space to the story of Southern California's landscape, it's evolution and dynamic nature. SCEC has played an ongoing advisory role, provided resources for the development of the earthquake sections of the exhibit, and will have an ongoing role in the implementation of educational programming.

Other Museum Partnerships. SCEC continues to foster new and nurture ongoing relationships with several museums. Some institutions have only requested copies of Roots for distribution in an earthquake exhibit, and others have requested professional development activities for their staff or local educators. Museums have also called upon SCEC to participate in educator open houses or special professional development seminars. Other museum partners includes: Discovery Science Center, Santa Ana; Griffith Observatory, Los Angeles; KidSpace Youth Museum, Pasadena; and several others.

Earthquake Information (California State University (CSULA), Los Angeles, CA) Due to be completed in fall 2008, this exhibit created in partnership with the geology department at CSULA features two computer screens showing recent worldwide and local earthquakes. Located in the lobby of the Physical Science Building this exhibit also displays the seven steps to earthquake safety and components of a basic earthquake disaster supply kit.

Wallace Creek Interpretive Trail. In partnership with The Bureau of Land Management (BLM), SCEC designed an interpretive trail along a particularly spectacular and accessible 2 km long stretch of the San Andreas Fault near Wallace Creek. Wallace Creek is located on the Carrizo Plain, a 3-4 hour drive north from Los Angeles. The trail opened in January 2001. The area is replete with the classic landforms produced by strike-slip faults: shutter ridges, sag ponds, simple offset stream channels, mole tracks and scarps. SCEC created the infrastructure and interpretive materials (durable signage, brochure content, and a website with additional information and directions to the trail). BLM has agreed to maintain the site and print the brochure into the foreseeable future. (*www.scec.org/wallacecreek*)

K-12 Education Partnerships and Activities

Partnerships with Science Education Advocacy Groups and Organizations with Similar Missions. SCEC is an active participant in the broader earth science education community including participation in organizations such as the National Association of Geoscience Teachers, The Coalition for Earth System Education, and local and national science educator organizations (e.g. NSTA). Improvement in the teaching and learning about earthquakes hinges on improvement in earth science education in general. Hence, SCEC wherever possible contributes to the community through participation on outreach committees, co-hosting meetings or workshops, and building long-term partnerships. An example of a current project is a partnership with EarthScope to host a San Andreas fault workshop for park and museum interpreters that will be held in Spring 2009.

Teacher Workshops. SCEC offers teachers 2-3 professional development workshops each year. The workshops provide a connection between developers of earthquake education resources and those who use these resources in the classroom. The workshops include: content and pedagogical instruction; ties to national and state science education standards; and materials teachers can take back to their classrooms Workshops are offered concurrent with SCEC meetings, at National Science Teachers Association annual meetings, and at USC. In 2003 SCEC began a partnership with the SIO Visualization Center to develop teacher workshops. Facilities at the Visualization Center include a wall-sized curved panorama screen (over 10m wide).

Sally Ride Science Festivals. Attended by over 1000 middle school (grades 5–8) age girls at each venue, Sally Ride Science Festivals offer a festive day of activities, lectures, and social activities emphasizing careers in science and engineering. Since 2003 SCEC has presented workshops for adults and students and participated in the Festival's "street fair," a popular venue for hands-on materials and science activities. At the street fair SCEC demonstrates key concepts of earthquake science and provides copies of Putting Down Roots in Earthquake Country. The workshops, presented by female members of the SCEC community share the excitement and the many career opportunities in the Earth sciences.

National Science Teachers Association and California Science Teachers Association. Earthquake concepts are found in national and state standards documents. SCEC participates in national conferences to promote innovative earthquake education in all states. Earthquake related content comprises the bulk of the six grade earth science curriculum in California. SCEC has a dual responsibility to communicate the science and the preparedness and one of the best venues for this effort are the statewide science educator conferences.

USC Science Education Collaborative. Since 2003, SCEC has greatly increased engagement with the inner-city neighborhoods around USC to form various partnerships in order to improve science education and increase earthquake awareness in the local community. One of these partnerships is with USC's Joint Education Project (JEP), which sends USC students into local schools to teach eight one-hour lessons pertaining to what they are learning in their classes. SCEC, in partnership with the USC department of Earth Sciences, now provides educational resources to JEP students in several earth-science courses, and trains the students how to use the resources in their lessons.

SCEC has also partnered with JEP, USC Mission Science, USC Sea Grants and the Jet Propulsion Laboratory (JPL) to create hands-on workshops for teachers at schools in the neighborhoods surrounding USC.

Development of Educational Products

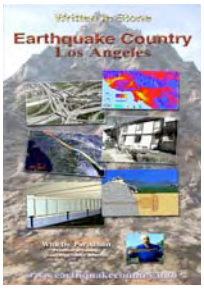

Earthquake Country - Los Angeles Video Kit. The video was produced by Dr. Pat Abbott of SDSU. The video tells the story of how the mountains and valleys of the Los Angeles area formed, including the important role of earthquakes. The video features aerial photography, stunning computer animations, and interviews with well-known experts. The video features 3D fault animations produced by SCEC's "LA3D" visualization system. In addition to conducting several focus groups with teachers and preparedness experts where the video was evaluated, SCEC developed an educator kit for school and community groups. The kit is currently being used in several schools in Los Angeles County, in an earth science education course at Cal Poly Pomona, and is part of educational programming at two museums.

Plate Tectonics Kit. Debuting in fall 2008, this educational product makes plate tectonics activities more accessible for science educators. SCEC developed a user-friendly version of the This Dynamic Earth map used by many in a jigsaw-puzzle activity to learn about plate tectonics, hot spots, and other topics. Feedback from educators indicated that the activity would be used more often if they had maps that had the plate boundaries on the back so that the puzzle could be cut more easily. In addition to designing the new map SCEC has also developed an educator kit.

Use of SCEC Community Modeling Environment (CME) Products in K-12 education. SCEC has included CME animations in its teacher education workshops since 2002 with the initial visualization of the Community Fault Model, and through 2007 with the latest Terashake animations. Our "Earthquake Country – Los Angeles" DVD and Putting Down Roots handbook are used by teachers throughout Southern California, and both feature CME products. A compilation of CFM visualizations have also distributed on a CD, at teacher conferences such as the National Science Teachers Association annual meeting. Also, a supplement module to an earth science textbook (being developed by a publisher) will lead students through analysis of earthquakes using Terashake animations.

Use of SCEC Community Modeling Environment (CME) Products in Higher education. SCEC faculty (and many others) are using CME animations in there undergraduate and graduate courses. Many graduate students have been supported by the CME project and have key in the development of many CFM products. However, the major impact of the CME and related activities however has been in the SCEC Undergraduate Studies in Earthquake Information Technology (USEIT) program, which has developed LA3D and now SCEC-VDO to visualize the SCEC CFM, earthquakes, and other features. This has resulted in a very useful tool but more importantly involved students from computer science, engineering, economics, film, and many other majors in earth science applications of advanced computer science. Several have changed their career paths and are pursuing graduate degrees with SCEC.

Draft 2009 Science Plan

SCEC Planning Committee

September 2008 Meeting

I. Introduction

On February 1, 2002, the Southern California Earthquake Center (SCEC) changed from an entity within the NSF/STC program to a freestanding center, funded by NSF/EAR and the U.S. Geological Survey. SCEC2 was funded for a five-year period, February 2002 to January 2007. SCEC was renewed for the period February 2007 through January 2012, referred to now as SCEC3. This document solicits proposals from individuals and groups to participate in the second year of the SCEC3 research program.

II. Guidelines for Proposal Submission

A. ***Due Date.*** Monday, November 3, 2008, 5:00 pm PST. Late proposals will not be accepted. Note the different deadline for submitting annual progress reports below.

B. ***Delivery Instructions.*** Proposals must be submitted as PDF documents via the SCEC Proposal web site at *http://www.scec.org/proposals*. Submission procedures, including requirements for how to name your PDF files, will be found at this web site.

C. ***Formatting Instructions.***

- ***Cover Page.*** The cover page should be headed with the words "2009 SCEC Proposal" and include the project title, Principal Investigator(s), institutional affiliation, amount of request, and proposal categories (from types listed in Section IV). List in order of priority three science objectives (Section VII) that your proposal addresses, for example A3, A5 and A11. Indicate if the proposal should also be identified with one or more of the SCEC special projects (see Section VIII). Collaborative proposals involving multiple investigators and/or institutions should list all Principal Investigators. Proposals do not need to be formally signed by institutional representatives, and should be for one year, with a start date of February 1, 2009.
- ***Technical Description.*** Describe in up to five pages (including figures) the technical details of the project and how it relates to the short-term objectives outlined in the SCEC Science Objectives (Section VII). References are not included in the five-page limit.
- ***Budget Page.*** Budgets and budget explanations should be constructed using NSF categories. Under guidelines of the SCEC Cooperative Agreements and A-21 regulations, secretarial support and office supplies are not allowable as direct expenses.
- ***Current Support.*** Statements of current support, following NSF guidelines, should be included for each Principal Investigator.
- ***2008 Annual Report.*** Scientists funded by SCEC in 2008 must submit a report of their progress by 5 pm February 28, 2009. 2009 proposals approved by the PC will not be funded until all progress reports are submitted. Reports should be up to five pages of text and figures. Reports should include bibliographic references to any SCEC publication during the past year (including papers submitted and in review), including their SCEC contribution number. Publications are assigned numbers when they are submitted to the SCEC publication database at *http://www.scec.org/signin*.

- ***Labeling the Submitted PDF Proposal.*** PI's must follow the proposal naming convention. Investigators must label their proposals with their last name followed by 2009, e.g., Archuleta2009.pdf. If there is more than one proposal, then the file would be labeled as: Archuleta2009_1.pdf (for the 1st proposal) and Archuleta2009_2.pdf (for the 2nd proposal).

D. ***Principal Investigator Responsibilities.*** PI's are expected to interact with other SCEC scientists on a regular basis (e.g., by attending workshops and working group meetings), and contribute data, analysis results, and/or models to the appropriate SCEC data center (e.g., Southern California Earthquake Data Center—SCEDC), database, or community model (e.g., Community Velocity Model—CVM). Publications resulting entirely or partially from SCEC funding must include a publication number available at *http://www.scec.org/signin*. By submitting a proposal, investigators are agreeing to these conditions.

E. ***Eligibility.*** Proposals can be submitted by eligible Principal Investigators from:

- U.S. Academic institutions
- U.S. Private corporations
- International Institutions (funding will mainly be for travel)

F. ***Collaboration.*** Collaborative proposals with investigators from the USGS are encouraged. USGS employees should submit their requests for support through USGS channels. Collaborative proposals involving multiple investigators and/or institutions are strongly encouraged; these can be submitted with the same text, but with different institutional budgets if more than one institution is involved.

G. ***Budget Guidance.*** Typical SCEC grants funded under this Science Plan in the past have fallen in the range of $10,000 to $35,000. This is not intended to limit SCEC to a fixed award amount, nor to a specified number of awards, rather it is intended to calibrate expectations for proposals written by first-time SCEC investigators.

H. ***Award Procedures.*** All awards will be funded by subcontract from the University of Southern California. The Southern California Earthquake Center is funded by the National Science Foundation and the U.S. Geological Survey.

III. SCEC Organization

A. ***Mission and Science Goal.*** SCEC is an interdisciplinary, regionally focused organization with a mission to:

- Gather data on earthquakes in Southern California and elsewhere
- Integrate information into a comprehensive, physics-based understanding of earthquake phenomena
- Communicate understanding to the world at large as useful knowledge for reducing earthquake risk

SCEC's primary science goal is to develop a comprehensive, physics-based understanding of earthquake phenomena in Southern California through integrative, multidisciplinary studies of plate-boundary tectonics, active fault systems, fault-zone processes, dynamics of fault ruptures, ground motions, and seismic hazard analysis. The long-term science goals are summarized in Appendix A.

B. ***Disciplinary Activities.*** The Center sustains disciplinary science through standing committees in seismology, geodesy, and geology. These committees will be responsible for planning and coordinating disciplinary activities relevant to the SCEC science plan,

and they will make recommendations to the SCEC Planning Committee regarding support of disciplinary research and infrastructure. High-priority disciplinary activities are summarized in Section VII.A.

C. ***Interdisciplinary Focus Areas.*** Interdisciplinary research is organized within five science focus areas. 1) Unified Structural Representation (URS), 2) Fault and Rupture Mechanics (FARM), 3) Crustal Deformation Modeling (CDM), 4) Lithospheric Architecture and Dynamics (LAD), 5) Earthquake Forecasting and Predictability (EFP), 6) Ground Motion Prediction (GMP) and 7) Seismic Hazard and Risk Analysis (SHRA). High-priority activities are listed for each of these interdisciplinary focus areas in Section VII.B.

D. ***Special Projects.*** SCEC supports eleven special projects that will advance designated research frontiers. Several of these initiatives encourage further development of an advanced IT infrastructure for system-level earthquake science in Southern California. High-priority initiatives are listed and described in Section VIII.

E. ***Communication, Education, and Outreach.*** SCEC maintains a strong Communication, Education, and Outreach (CEO) program with four principal goals. 1) coordinate productive interactions among SCEC scientists, and with partners in science, engineering, risk management, government, business, and education; 2) increase earthquake knowledge and science literacy at all educational levels; 3) improve earthquake hazard and risk assessments; and 4) promote earthquake preparedness, mitigation, and planning for response and recovery. Opportunities for participating in the CEO program are described in Section IX. Current activities are described online at *http://www.scec.org/ceo*.

IV. Proposal Categories

A. ***Data Gathering and Products.*** SCEC coordinates an interdisciplinary and multi-institutional study of earthquakes in Southern California, which requires data and derived products pertinent to the region. Proposals in this category should address the collection, archiving and distribution of data, including the production of SCEC community models that are on-line, maintained, and documented resources for making data and data products available to the scientific community.

B. ***Integration and Theory.*** SCEC supports and coordinates interpretive and theoretical investigations on earthquake problems related to the Center's mission. Proposals in this category should be for the integration of data or data products from Category A, or for general or theoretical studies. Proposals in Categories A and B should address one or more of the goals in Section VII, and may include a brief description (<200 words) as to how the proposed research and/or its results might be used in a special initiative (see Section VIII) or in an educational or outreach mode (see Section IX).

C. ***Workshops.*** SCEC participants who wish to host a workshop between February 2009 and February 2010 should submit a proposal for the workshop in response to this RFP. This includes workshops that might be organized around the SCEC annual meeting in September. Workshops in the following topics are particularly relevant:

- Organizing collaborative research efforts for the five-year SCEC program (2007-2012). In particular, interactive workshops that engage more than one focus and/or disciplinary group are strongly encouraged.
- Engaging earthquake engineers and other partner and user groups in SCEC-sponsored research.

- Participating in national initiatives such as EarthScope, the Advanced National Seismic System (ANSS), and the George E. Brown, Jr. Network for Earthquake Engineering Simulation (NEES).

D. ***Communication, Education, and Outreach.*** SCEC has developed a long-range CEO plan and opportunities for participation are listed in Section IX. Investigators who are interested in participating in this program should contact Mark Benthien (213-740-0323; benthien@usc.edu) before submitting a proposal.

E. ***SCEC/SURE Intern Project.*** If your proposal includes undergraduate funding, please note this on the cover page. Each year SCEC coordinates the SCEC Summer Undergraduate Research Experience (SCEC/SURE) program to support one-on-one student research with a SCEC scientist. See *http://www.scec.org/internships* for more information. SCEC will be recruiting mentors in November, 2008, and will request descriptions of potential projects via email. In December, these descriptions will be published on the SCEC Internship web page to allow applicants to identify their preferred projects.

Mentors will be required to provide at least $2500 of the $5000 intern stipend, and SCEC will pay the balance. Mentor contributions can come from any source, including SCEC-funded research projects. Therefore, interested SCEC scientists are encouraged to include at least $2500 for an undergraduate intern in their 2009 SCEC proposals, and then respond to the recruitment emails.

Questions about the SCEC/SURE Intern Project should be referred to Robert de Groot, *degroot@usc.edu*.

F. ***Workshop participation.*** Investigators who wish to only request funding to cover travel to the annual meeting can participate in a streamlined review process with an abbreviated proposal. Investigators who are already funded to study projects that would be of interest to the SCEC community, and investigators new to SCEC who would benefit from exposure to the annual meeting in order to fine-tune future proposals are encouraged to apply.

V. Evaluation Process and Criteria

A. Proposals should be responsive to the RFP. A primary consideration in evaluating proposals will be how directly the proposal addresses the main objectives of SCEC. Important criteria include (not necessarily in order of priority):

- Scientific merit of the proposed research
- Competence and performance of the investigators, especially in regard to past SCEC-sponsored research
- Priority of the proposed project for short-term SCEC objectives as stated in the RFP
- Promise of the proposed project for contributing to long-term SCEC goals as reflected in the SCEC science plan (see Appendix).
- Commitment of the P.I. and institution to the SCEC mission
- Value of the proposed research relative to its cost
- Ability to leverage the cost of the proposed research through other funding sources
- Involvement of students and junior investigators
- Involvement of women and underrepresented groups

- Innovative or "risky" ideas that have a reasonable chance of leading to new insights or advances in earthquake physics and/or seismic hazard analysis.

B. Proposals may be strengthened by describing:

- Collaboration
  - Within a disciplinary or focus group
  - Between disciplinary and/or focus groups
  - In modeling and/or data gathering activities
  - With engineers, government agencies, and others. (See Section IX)
- Leveraging additional resources
  - From other agencies
  - From your institution
  - By expanding collaborations
- Development and delivery of products
  - Community research tools, models, and databases
  - Collaborative research reports
  - Papers in research journals
  - End-user tools and products
  - Workshop proceedings and CDs
  - Fact sheets, maps, posters, public awareness brochures, etc.
  - Educational curricula, resources, tools, etc.
- Educational opportunities
  - Graduate student research assistantships
  - Undergraduate summer and year-round internships (funded by the project)
  - K-12 educator and student activities
    - Presentations to schools near research locations
    - Participation in data collection

C. All research proposals will be evaluated by the appropriate disciplinary committees and focus groups, the Science Planning Committee, and the Center Director. CEO proposals will be evaluated by the CEO Planning Committee and the Center Director.

D. The Science Planning Committee is chaired by the Deputy Director and comprises the chairs of the disciplinary committees, focus groups, and special projects. It is responsible for recommending a balanced science budget to the Center Director.

E. The CEO Planning Committee is chaired by the Associate Director for CEO and comprises experts involved in SCEC and USGS implementation, education, and outreach. It is responsible for recommending a balanced CEO budget to the Center Director.

F. Recommendations of the planning committees will be combined into an annual spending plan and forwarded to the SCEC Board of Directors for approval.

G. Final selection of research projects will be made by the Center Director, in consultation with the Board of Directors.

H. The review process should be completed and applicants notified by the end of February, 2009.

VI. Coordination of Research Between SCEC and USGS-EHRP

A. Earthquake research in Southern California is supported both by SCEC and by the USGS Earthquake Hazards Reduction Program (EHRP). EHRP's mission is to provide the scientific information and knowledge necessary to reduce deaths, injuries, and economic losses from earthquakes. Products of this program include timely notifications of earthquake locations, size, and potential damage, regional and national assessments of

earthquakes hazards, and increased understanding of the cause of earthquakes and their effects. EHRP funds research via its External Research Program, as well as work by USGS staff in its Pasadena, Menlo Park, and Golden offices. The EHRP also supports SCEC directly with $1.1M per year.

B. SCEC and EHRP coordinate research activities through formal means, including USGS membership on the SCEC Board of Directors and a Joint Planning Committee, and through a variety of less formal means. Interested researchers are invited to contact Dr. Sue Hough, EHRP coordinator for Southern California, or other SCEC and EHRP staff to discuss opportunities for coordinated research.

C. The USGS EHRP supports a competitive, peer-reviewed, external program of research grants that enlists the talents and expertise of the academic community, State and local governments, and the private sector. The investigations and activities supported through the external program are coordinated with and complement the internal USGS program efforts. This program is divided into six geographical/topical 'regions', including one specifically aimed at Southern California earthquake research and others aimed at earthquake physics and effects and at probabilistic seismic hazard assessment (PSHA). The Program invites proposals that assist in achieving EHRP goals.

D. The EHRP web page, *http://erp-web.er.usgs.gov/*, describes program priorities, projects currently funded, results from past work, and instructions for submitting proposals. The EHRP external funding cycle is several months offset from SCEC's, with the RFP due out in February and proposals due in early May. Interested PI's are encouraged to contact the USGS regional or topical coordinators for Southern California, Earthquake Physics and Effects, and/or National (PSHA) research, as listed under the "Contact Us" tab.

E. USGS internal earthquake research is summarized by topic at *http://earthquake.usgs.gov/research/topics.php*

VII. SCEC3 Science Priority Objectives

The research objectives outlined below are priorities for SCEC3. They carry the expectation of substantial and measurable success during the coming year. In this context, success includes progress in building or maintaining a sustained effort to reach a long-term goal. How proposed projects address these priorities will be a major consideration in proposal evaluation, and they will set the programmatic milestones for the Center's internal assessments. In addition to the priorities outlined below, the Center will also entertain innovative and/or "risky" ideas that may lead to new insights or major advancements in earthquake physics and/or seismic hazard analysis.

There are four major research areas with the headings A, B, C and D with subheadings given by numbers. The front page of the proposal should specifically identify subheadings that will be addressed by the proposed research.

A. Develop an extended earthquake rupture forecast to drive physics-based SHA

A1. Define slip rates and earthquake history of southern San Andreas fault system for the last 2000 years

A2. Investigate implications of geodetic/geologic rate discrepancies

A3. Develop a system-level deformation and stress-evolution model

A4. Statistical analysis and mapping of seismicity and source parameters with an emphasis on their relation to known faults

A5. Develop a geodetic network processing system that will detect anomalous strain transients

A6. Test scientific prediction hypotheses against reference models to understand the physical basis of earthquake predictability

A7. Determine the origin, evolution and implications of on- and off-fault damage

A8. Test hypotheses for dynamic fault weakening

A9. Assess predictability of rupture extent and direction on major faults

A10. Develop statistical descriptions of heterogeneities (e.g., in stress, strain, geometry and material properties) in fault zones, and understand their origin and implications for seismic hazard by observing and modeling single earthquake ruptures and multiple earthquake cycles.

A11. Constrain absolute stress and understand the nature of interaction between the faulted upper crust, the ductile crust and mantle, and how geologic history helps to resolve the current physical properties of the system.

B. Predict broadband ground motions for a comprehensive set of large scenario earthquakes

B1. Develop kinematic rupture representations consistent with observations and realistic dynamic rupture models of earthquakes.

B2. Investigate bounds on the upper limit of ground motion

B3. Develop high-frequency simulation methods and investigate the upper frequency limit of deterministic ground motion predictions

B4. Validate earthquake simulations and verify simulation methodologies

B5. Improve our understanding of nonlinear effects and develop methodologies to include these effects in broadband ground motion simulations.

B6. Collaborate with earthquake engineers to develop rupture-to-rafters simulation capability for physics-based risk analysis

C. Improve and develop community products (data or descriptions) that can be used in system-level models for the forecasting of seismic hazard. Proposals for such activities should show how they would significantly contribute to one or more of the numbered goals in A or B.

D. Prepare post-earthquake response strategies

Some of the most important earthquake data are gathered during and immediately after a major earthquake. Exposures of fault rupture are erased quickly by human activity, aftershocks decay rapidly within days and weeks, and post-seismic slip decays exponentially. SCEC solicits proposals for a workshop to plan post-earthquake science response. The goals of the workshop would be to: 1) develop a post-earthquake science plan that would be a living document such as a wiki; 2) identify permanent SCEC and other science facilities that are needed to ensure success of the science plan; 3) identify other resources available in the community and innovative ways of using technology for coordination and rapid data processing that will allow for rapid determination of source parameters, maps, and other characteristics of the source and ground motion patterns.; 4) develop plans for use of Peta-scale computing resources in post-earthquake response for

evaluation of crustal stress changes along faults as well as short term prediction of potentially damaging ground motion patterns along 'newly stressed' faults; and 5) develop mechanisms for regular updates of the SCEC post-earthquake response plan.

VII-A. Disciplinary Activities

The Center will sustain disciplinary science through standing committees in seismology, geodesy, and geology. These committees will be responsible for planning and coordinating disciplinary activities relevant to the SCEC science plan, and they will make recommendations to the SCEC Planning Committee regarding the support of disciplinary infrastructure. High-priority disciplinary objectives include the following tasks:

1. Seismology

A. ***Objectives.*** The objectives of the Seismology group are to support the SCEC mission to gather data on earthquakes in Southern California, and use the seismic networks as research tools to integrate the data into physics-based models that improve our understanding of earthquake phenomena. Proposals to enhance the seismic networks as research tools and foster innovations in network deployments, data collection, and data processing are encouraged, especially where they include collaboration with network operators in Southern California and provide community products that support one or more of the numbered goals in A, B, C or D.

Important SCEC resources are the Southern California Earthquake Data Center (SCEDC) whose continued operation is essential to deciphering Southern California earthquakes as well as crustal and fault structure, the network of SCEC funded borehole instruments to record high quality reference ground motions, and the pool of portable instruments that is operated in support of targeted deployments or aftershock response.

B. ***Research Strategies.*** Examples of research strategies that support the objectives above include:

- Enhancement and continued operation of the SCEDC and other existing SCEC facilities. In particular, the near real-time availability of earthquake data from SCEDC and enhanced automated access are important for ongoing SCEC research activities. In support of tomographic, state of stress, earthquake predictability, and other seismicity studies, enhance the availability and usefulness of data products, such as waveforms, catalogs of earthquake parameters, arrival time and polarity information, and signal-to-noise measures as well as moment tensors and first motion mechanisms (A6, A7).
- Enhancements in the real-time processing of network data to improve the estimation of source parameters in relation to known and unknown faults (A3, A4, A10). Other activities could be testing of the performance of new early-warning algorithms, the determination of high precision real-time earthquake locations, or developing finite source algorithms for use in the real-time processing environment (D).
- Experiments that investigate the near-fault crustal properties as well as develop constraints on crustal structure and state of stress are also the goals of other SCEC groups (A7, A10, C). Develop innovative and practical strategies for densification of seismic instrumentation, including borehole instrumentation, along major fault zones in Southern California to measure fault zone properties and capture near-field motions for constraining kinematic and dynamic simulations of earthquakes (B1, B2, B3, B4, B5). Collaborations, for instance with the ANSS and NEES projects, that would augment existing and planned network stations with downhole and surface instrumentation to assess site response, nonlinear effects, and the ground coupling of built structures (B4, B6) are

encouraged. Collaborations with EarthScope and other network operators to develop innovative new methods to search for unusual signals using combined seismic, GPS, and borehole strainmeter data (A5, A6) are also encouraged. Other possible strategies (often started with SCEC seed funds) include the design of future passive and active experiments such as dense array measurements of basin structure and large earthquake properties, OBS deployments, and deep basement borehole studies.

2. Tectonic Geodesy

A. ***Objectives.*** The broad objective of the geodesy group is to foster the availability of the variety of geodetic data collected in Southern California and the integrated use of these observations, in conjunction with other relevant data (e.g., seismic or geologic information), to address the spectrum of deformation processes affecting this region. Topics of interest include, but are not limited to, rapid earthquake response, transient deformation, anthropogenic or nontectonic effects, and the characterization and interpretation of strain accumulation and release, with one goal being the increased use of insights from geodesy in seismic hazard assessment. Proposed work may overlap with one or more focus areas, such as Crustal Deformation Modeling (CDM).

B. ***Research Strategies.*** The following are research strategies aimed at meeting the broad objective:

- Develop reliable means for detecting, assessing, and interpreting transient deformation signals (A5):
  - Apply detection algorithms as part of a planned "blind test" exercise to be initiated in Fall 2008 with the goal of advancing capabilities in this area.
  - Investigate processes underlying detected signals and/or their seismic hazard implications.
- Refine or extend estimates of interseismic crustal motion (A1, A2, A3, C):
  - Identify possible trade-offs in regional slip rate models, conduct quantitative comparison of such models, and/or develop new models.
  - Quantify uncertainties (especially those relating to model uncertainty) in rate estimates.
- Improve and expand geodetic data products in support of a range of applications (A1, A2, A3, A5, B1, D):
  - Reprocess the full southern California GPS data set using consistent, state-of-the art methodology.
  - Advance InSAR processing and data combination strategies.
  - Develop methods for combining data types (e.g., GPS, InSAR, strainmeter, and/or other data) that have differing spatial and temporal apertures, sampling frequencies, and sensitivities. Design of methods for assessing the utility of such combinations for interpreting tectonic or nontectonic signals is encouraged.
  - Improve vertical velocity estimates through, for example, the combined use of multiple data types or improvements in data processing strategies.
  - Conduct a systematic assessment of existing geodetic observations throughout Southern California in order to identify locations for which further data collection is necessary to discriminate among regional deformation models, refine slip rate estimates, conduct future earthquake response and postseismic investigations, or for other applications related to SCEC goals.
  - Increase the usability of high-rate GPS observations by developing community accessible tools for using these data. Such tools can address different goals including immediate response to major earthquakes (for which rapid availability of solutions is a priority) or detailed deformation analysis (for which the highest accuracy solutions are needed). Assessment of the required accuracy for specific problems of interest to SCEC is also encouraged.

Studies should utilize data from the Plate Boundary Observatory wherever possible, and proposals for additional data collection should explicitly motivate how they complement existing coverage.

3. Earthquake Geology

A. ***Objectives.*** The Earthquake Geology group promotes studies of the geologic record of the Southern California natural laboratory that advance SCEC science. Geologic observations can provide important contributions to nearly all SCEC objectives in seismic hazard analysis (A1-A3, A6-A11) and ground motion prediction (B2-B5). Studies are encouraged to test outcomes of earthquake simulations and crustal deformation modeling. Earthquake Geology also fosters data-gathering activities that will contribute demonstrably significant geologic information to (C) community data sets such as the Unified Structural Representation. The primary focus of the Earthquake Geology is on the Late Quaternary record of faulting and ground motion in southern California. Collaborative proposals that cut across disciplinary boundaries are especially competitive.

B. ***Research Strategies.*** Examples of research strategies that support the objectives above include:

- Paleoseismic documentation of earthquake ages and displacement, including a coordinated effort to develop slip rates and earthquake history of southern San Andreas fault system (A1).
- Development of slip rate and slip-per-event data sets, taking advantage of newly collected GeoEarthScope LiDAR data, and with a particular emphasis on documenting patterns of seismic strain release in time and space (A1-A3, A5, A6, A9).
- Development of methods to evaluate multi-site paleoseismic data sets and standardize error analysis (A1, A9).
- Characterization of fault-zone geology, material properties, and their relationship to earthquake rupture processes (A7, A8, A10).
- Quantitative analysis of the role of distributed deformation in accommodating block motions, dissipating elastic strain, and modifying rheology (A2, A3, A7, A10, A11).
- Development of constraints on the magnitude and recurrence of strong ground motions from geomorphic features and secondary ground failures (B2-B5).

C. ***Geochronology Infrastructure.*** The shared geochronology infrastructure supports C-14, optically stimulated luminescence (OSL), and cosmogenic dating for SCEC-sponsored research. The purpose of shared geochronology infrastructure is to allow flexibility in the number and type of dates applied to each SCEC-funded project as investigations proceed. Investigators requesting geochronology support must estimate the number and type of dates needed in their proposal. For C-14 specify if sample preparation will take place at a location other than the designated laboratory. For cosmogenic dating, investigators are required to arrange for sample preparation. These costs must be included in the proposal budget unless preparation has been pre-arranged with one of the laboratories listed. Investigators are strongly encouraged to contact the investigators at the collaborating laboratories prior to proposal submission. Currently, SCEC geochronology has established relationships with the following laboratories:

- C-14: University of California at Irvine (John Southon, jsouthon@uci.edu) and Lawrence Livermore National Laboratory (Tom Guilderson, *tguilderson@llnl.gov*).
- OSL: University of Cincinnati (Lewis Owen, *lewis.owen@uc.edu*) and Utah State University (Tammy Rittenour, *tammy.rittenour@usu.edu*)

- Cosmogenic: Lawrence Livermore National Laboratory (Tom Guilderson, *tguilderson@llnl.gov*).

Investigators at collaborating laboratories are requested to submit a proposal that states the cost per sample analysis and estimates of the minimum and maximum numbers of analyses feasible for the upcoming year. These investigators are also strongly encouraged to request for funds to support travel to the SCEC annual meeting. New proposals from laboratories not listed above will be considered, though preference will be given to strengthening existing collaborations.

Investigators may alternatively request support for geochronology outside of the infrastructure proposal for methods not listed here or if justified on a cost-basis. These outside requests must be included in the individual proposal budget. Please direct questions regarding geochronology infrastructure to the Earthquake Geology group leader, Mike Oskin (*oskin@geology.ucdavis.edu*).

VII-B. Interdisciplinary Focus Areas

Interdisciplinary research will be organized into seven science focus areas: 1) Unified Structural Representation (USR), 2) Fault and Rupture Mechanics (FARM), 3) Crustal Deformation Modeling (CDM), 4) Lithospheric Architecture and Dynamics (LAD), 5) Earthquake Forecasting and Predictability (EFP), 6) Ground Motion Prediction (GMP) and 7) Seismic Hazard and Risk Analysis (SHRA). High-priority objectives are listed below for each of the seven interdisciplinary focus areas below. Collaboration within and across focus areas is strongly encouraged.

1. Unified Structural Representation (USR)

The Structural Representation group develops unified, three-dimensional representations of active faults and earth structure (velocity, density, etc.) for use in fault-system analysis, ground motion prediction, and hazard assessment. This year's efforts will focus on making improvements to existing community models (CVM-H, CFM) that will facilitate their uses in SCEC science, education, and post-earthquake response planning.

A. ***Community Velocity Model.*** Improve the current SCEC CVM-H model, with emphasis on more accurate representations of Vp, Vs, density structure, basin shapes, and attenuation. Generate improved mantle Vp and Vs models, as well as more accurate descriptions of near-surface property structure that can be incorporated into a revised geotechnical layer. Evaluate the existing models with data (e.g., waveforms, gravity) to distinguish alternative representations and quantify model uncertainties. Establish an evaluation procedure and benchmarks for testing how future improvements in the models impact ground motion studies. Special emphasis will be placed on developing and implementing 3D waveform tomographic methods for evaluating and improving the CVM-H.

B. ***Community Fault Model (CFM).*** Improve and evaluate the CFM, placing emphasis on defining the geometry of major faults that are incompletely, or inaccurately, represented in the current model. Evaluate the CFM with data (e.g., seismicity, seismic reflection profiles, geodetic displacement fields) to distinguish alternative fault models. Integrate northern and Southern California models into a statewide fault framework, and update the CFM-R (rectilinear fault model) to reflect improvements in the CFM.

C. ***Unified Structural Representation (USR).*** Develop better IT mechanisms for delivering the USR, particularly the CVM parameters and information about the model's structural components, to the user community for use in generating and/or parameterizing

computational grids and meshes. Generate maps of geologic surfaces compatible with the CFM that may serve as strain markers in crustal deformation modeling and/or property boundaries in future iterations of the USR.

2. Fault and Rupture Mechanics (FARM)

The primary mission of the Fault and Rupture Mechanics focus group in SCEC3 is to develop physics-based models of the nucleation, propagation, and arrest of dynamic earthquake rupture. We specifically solicit proposals that address this mission through field, laboratory, and modeling efforts directed at characterizing and understanding the influence of material properties, geometric irregularities, and heterogeneities in stress and strain over multiple length and time scales (A7-A10, B1, B4), and that will contribute to our understanding of earthquakes in the Southern California fault system.

Proposed studies should aim to:

- Determine the properties of fault cores and damage zones and characterize their variability with depth and along strike, including descriptions of the width and particle composition of actively shearing zones, extent, origin and significance of on- and off-fault damage, and poromechanical behavior (A7-A11).
- Investigate the relative importance of different dynamic weakening and fault healing mechanisms, and the slip and/or time scales over which these mechanisms operate (A7-A10).
- Characterize the probability and possible signatures of preferred earthquake rupture direction (A7-A10, B1, B4).
- Determine the relative contribution of on- and off-fault damage to the total earthquake energy budget, and the absolute levels of local and average stress (A7-A10).
- Develop realistic descriptions of heterogeneity in fault geometry, properties, stresses, and strains, and tractable ways to incorporate heterogeneity in numerical models (A10-11, B1, B4).
- Understand the influence of small-scale processes on larger-scale fault dynamics (A7-11, B1, B4).
- Evaluate the relative importance of fault structure, material properties, and prior seismic and aseismic slip to earthquake dynamics, in particular, to rupture initiation, propagation, and arrest, and the resulting ground motions (A7-A10, B1).
- Better characterize earthquake rupture at the base of the seismogenic zone, and better develop constitutive descriptions of fault behavior at mid- and lower-crustal depths relevant to numerical modeling of fault loading, earthquake mechanisms and fault interactions over single and multiple earthquake cycles using the SCEC USR. Understand implications of slow events and non-volcanic tremors for constitutive properties of faults and overall seismic behavior (A3, A10, A11).

3. Crustal Deformation Modeling (CDM)

The CDM group focuses on deformation occurring within the earthquake cycle, at time scales linking dynamic rupture (minutes) to secular deformation (thousands of years). We are interested in proposals to (1) develop, or facilitate the development of, models of southern California fault systems based on the SCEC USR and (2) develop other models which contribute to the larger goal of understanding stress transfer and the evolving distribution of earthquake probabilities within active fault systems. Items (1) and (2) should contribute to our ultimate goal of developing physics-based seismic hazard assessments (SHA) for southern California faults. We also seek proposals to model postseismic deformation and communicate the results quickly enough to guide GPS site deployment for postseismic deformation monitoring. Collaborative research with other SCEC focus areas is encouraged.

- Develop kinematic or dynamic finite element models of the southern California crust, incorporating SCEC USR products (the CFM, CFM, and/or CBM). C, A3, A11.
- Investigate how assumed rheologies affect modeled stress transfer among Southern California faults. Assess effects of aseismic fault creep (including transient slip events), inelastic upper crust, poroelasticity, and heterogeneous material properties on the seismic cycle and stress transfer. A7, A10 and A11.
- Investigate how to represent multi-scale fault complexity in deformation models, and how to quantify model sensitivity to spatial heterogeneity of structure. Use such models to help geologists discover what to look for, and where to look, to find evidence of how slip and deformation are distributed at fault intersections. A10 and A11.
- Investigate connections between geodetic and geologic slip rates. Investigate factors that might make fault slip rates vary over different time scales. Use GPS and other geodetic data to develop California fault slip rates and compare with the database used by the Working Group on California Earthquake Probabilities 2007 and National Seismic Hazard Map Program 2007 forecast models. Augment the database through joint consideration of geologically- and geodetically-determined slip rates and identify fault slip rates that are dependent on observation period/methods. A1, A2.
- Develop methods to rapidly model postseismic deformation to predict time-dependent deformation as a guide for GPS site deployment, with an emphasis on precomputing and web-based platforms for data and model sharing. D.
- Develop comprehensive earthquake simulators to unify driving and initial-condition stresses and time-dependent stress interactions, with geologic, geodetic, and paleoseismic observations. Understand the statistical parameters of stress heterogeneity on faults and in the crust, and the extent to which such heterogeneity influences simulator results. A3, A6, A10.
- Evaluate sensitivity and use of deformation and triggering models in earthquake forecasting. For example, explore plausible range of seismic release scenarios consistent with deformation observations, or assess how different modeling approaches (or assumptions) affect estimates of hazard-forecast parameters. A6.

4. Lithospheric Architecture and Dynamics (LAD)

The lithospheric architecture and dynamics group (LAD) seeks proposals that will contribute to our understanding of the structure, geologic provenance and physical state of the major Southern California lithospheric units, and how these relate to absolute stress and its evolution (A3, A11). The principal objective of this group is to construct 3D geodynamic models that describe the vertical as well as horizontal tectonics into which the seismogenic crustal deformation model can be embedded. Of particular interest is how flow in the sub-seismogenic zone and the asthenosphere accommodates plate motion and loads faults. The geodynamic models would describe the evolution to the current physical state of the Southern California system. Physics models will be developed that use the paleo-history of the 3D geology to infer prior physical conditions, such as depths of Moho, the seismogenic layer, base of the lithosphere, topography and basin depths, rock type, temperature, water content, rheology and how these relate to mantle flow, velocity, anisotropy and density. The LAD work will interface with the geology group to incorporate fault slip, uplift and subsidence rates, with FARM on rheology and absolute and dynamic stress, with the USR and seismology groups on 3D structure and its provenance, and CDM on current stress and strain rates.

In this context, proposals are sought that contribute to our understanding of geologic inheritance as well as three-dimensional structure and physical properties of the lithosphere. Proposals should indicate how the work relates to stress evolution (A2, A3, A11) as well as the current geological structure (C). The ultimate goal is to obtain an absolute stress/rheology model (important to our understanding of how faults are loaded, the earthquake mechanism, fault friction, seismic efficiency, the heat flow paradox) and the expected evolution of stress and strain transients (A5). The LAD group will be involved in the USGS-NSF Margins/Earthscope Salton Trough Seismic

Project and will interface to the SCUBA offshore-OBS experiment, and will consider proposals that piggyback these experiments and integrate the results into LAD goals.

5. Earthquake Forecasting and Predictability (EFP)

In general we seek proposals that will increase our understanding of how earthquakes might be forecast and whether or not earthquakes are predictable (A6). Proposals of any type that can assist in this goal will be considered, with the provision that they focus on seismicity and deformation data. We are especially interested in proposals that will utilize the new Collaboratory for the Study of Earthquake Predictability (CSEP). In order to increase the number of earthquakes in the data sets, and so decrease the time required to learn about predictability, proposals are welcome that deal with global data sets and/or include international collaborations.

For research strategies that plan to utilize CSEP, see the description of CSEP under Special Projects to learn of its capabilities. Successful investigators proposing to utilize CSEP would be funded via core SCEC funds to adapt their prediction methodologies to the CSEP framework, to transfer codes to the externally accessible CSEP computers, and to be sure they function there as intended (A6). Subsequently, the codes would be moved to the identical externally inaccessible CSEP computers by CSEP staff who will conduct tests against a variety of data as outlined in the CSEP description. In general, methodologies will be considered successful only if they do better than null hypotheses that include both time-independent and time-dependent probabilities. Proposals aimed toward developing useful measurement/testing methodology that could be incorporated in the CSEP evaluations are welcomed, including those that address how to deal with observational errors in data sets.

Proposals are also welcome that assist in attaining the goals of these two Special Projects: WGCEP (the Working Group on California Earthquake Probabilities) and SoSAFE (the Southern San Andreas Evaluation), especially if the proposals focus on understanding some physical basis for connections between earthquakes. Proposals to utilize and/or evaluate the significance of earthquake simulator results are encouraged. Investigation of what is an appropriate magnitude-area relationship, including the maximum depth of slip during large earthquakes, is encouraged. Studies of how to properly characterize the relationship between earthquake frequency and magnitude for use in testing prediction algorithms are also encouraged.

Proposals that can lead to understanding whether or not there exists a physical basis for earthquake predictability (A6) are welcome, even if they are not aimed toward, or are not ready for, tests in CSEP, or are not aimed toward assisting WGCEP or SoSAFE. For example, proposals could include ones that connect to objectives A1, A2, A3, A5, A9, A10 and A11, as well as ones focused on understanding patterns of seismicity in time and space, as long as they are aimed toward understanding the physical basis of some aspect of extended earthquake predictability (A6). Development of methods for testing prediction algorithms that are not yet in use by CSEP is encouraged.

Proposals for workshops are welcome. Specific workshops of interest include one on earthquake simulators and one on setting standards that could be used by CSEP for testing and evaluation, data, and products.

6. Ground Motion Prediction (GMP)

The primary goal of the Ground Motion Prediction focus group is to develop and implement physics-based simulation methodologies that can predict earthquake strong motion waveforms over the frequency range 0-10 Hz. At frequencies less than 1 Hz, the methodologies should deterministically predict the amplitude, phase and waveform of earthquake ground motions using

fully three-dimensional representations of the ground structure, as well as dynamic or dynamically-compatible kinematic representations of fault rupture. At higher frequencies (1-10 Hz), the methodologies should predict the main character of the amplitude, phase and waveform of the motions using a combination of deterministic and stochastic representations of fault rupture and wave propagation.

Research topics within the Ground Motion Prediction program will include developing and/or refining physics-based simulation methodologies, with particular emphasis on high frequency (1-10 Hz) approaches (B3) and the incorporation of non-linear models of soil response (B2, B4, B5). Source characterization plays a vital role in ground motion prediction and research is needed to develop more realistic implementations of dynamic or dynamically-compatible kinematic representations of fault rupture that are used in the simulations (B1, B2). Verification (comparison against theoretical predictions) and validation (comparison against observations) of the simulation methodologies will continue to be an important component of this focus group with the goal being to develop robust and transparent simulation capabilities that incorporate consistent and accurate representations of the earthquake source and three-dimensional velocity structure (B4, C). It is expected that the products of the Ground Motion Prediction group will have direct application to seismic hazard analysis, both in terms of characterizing expected ground motion levels in future earthquakes, and in terms of directly interfacing with earthquake engineers in the analysis of built structures (B6). In addition, activities within the Ground Motion Prediction group will be closely tied to several special projects, with particular emphasis on addressing ground motion issues related to seismic hazard and risk. These special projects include the CEA Project, the Extreme Ground Motion Project, the NGA-H Project, the NSF Implementation Interface Project, and the Tall Buildings Initiative (see SHRA and Section VIII, below).

7. Seismic Hazard and Risk Analysis (SHRA)

The purpose of this activity is to apply SCEC knowledge to the development of useful and useable information and techniques related to earthquake hazard and risk in California. Such information and techniques may include improved representations of seismic hazards, in some cases in terms of new scalar or vector ground motion intensity measures; representations of seismic hazards using ground motion time histories that are also validated for risk analysis applications; rupture-to-rafters simulations that integrate the physics-based generation of ground motion, its propagation through the earth, and its interactions with the built environment; and improved site/facility-specific and portfolio/regional risk analysis (or loss estimation) techniques and tools. Projects that involve interactions between SCEC scientists and members of the community involved in earthquake engineering research and practice are especially encouraged. While supported from the same funds used for other SCEC activities, projects in this activity will often be linked to the Ground Motion Prediction and to special projects. These projects include the CEA Project, the Extreme Ground Motion Project, the NGA-H Project, the NSF LA Tall Buildings Project, and the Tall Buildings Initiative; these projects illustrate the kinds of work that are relevant to SHRA. In the following, the Special Projects are described and related to the various SCEC3 Priority Science Objectives.

The current California Earthquake Authority Project contains activities related to the development of a uniform earthquake forecast for the whole of California (A1, A2), the NGA-H Project discussed below (B1, B3, B4), and rupture-to-rafters simulations involving woodframe buildings (B6). Plans to continue this project in 2008 have not yet been developed.

The Extreme Ground Motion Project supports SCEC research on evaluation and validation of existing rupture dynamics models for ground motion simulation (B1); enhancement of rupture dynamics models to include more physics (B1); the use of these dynamic models, together with

kinematic ground motion modeling, to simulate ground motions (B); and analyses of nonlinear wave propagation and site response (B5), for the purpose of understanding the generation of and potentially identifying bounds on extreme ground motions within the context of the Yucca Mountain Repository (B2). This project will continue in 2009 and beyond.

The planned NGA-H Project will involve the use of broadband strong motion simulation to generate ground motion time histories for use, in conjunction with recorded ground motions, in the development of ground motion attenuation relations for hard rock that are based on improved sampling of magnitude and distance and improved understanding of the relationship between earthquake source and strong ground motion characteristics (B1, B3, B4, B5). Of particular interest is that the NGA-E (empirical) relations are noticeably lower than earlier ground-motion attenuation relations. Are the current SCEC broad-band simulations consistent with the NGA-E findings? Broadband simulation methods are verified (by comparison of simple test case results with other methods) and validated (against recorded strong ground motions) before being used to generate broadband ground motions for use in model development. These simulation activities for verification, validation, and application are done on the SCEC Broadband Simulation Platform, which is currently under development.

The pending NSF LA Tall Buildings Project will involve enhancement of simulations of long period ground motions in the Los Angeles region that have been generated by TeraShake and CyberShake, using refinements in source characterization and seismic velocity models (B1, B4), and evaluation of the impacts of these ground motions on tall buildings (B6). It will also involve the development of methods for evaluating and characterizing the potential of faults to generate buried faulting as well as surface faulting earthquakes (A), and evaluating differences in seismic demands imposed by these two categories of earthquakes (B6).

The current Tall Buildings Initiative involves the simulation of ground motion time histories of large earthquakes in Los Angeles and San Francisco for use by practicing engineers in the design of tall buildings (B), and the development and application of procedures for selecting and scaling ground motion time histories for use in representing design ground motions (B6). As is the case in all of the Special Projects described above, validation of the earthquake simulations (B4) for use in seismic hazard and/or risk analysis is an important step that calls for collaboration between earthquake scientists and engineers.

Proposals for other innovative projects that would further implement SCEC information and techniques in seismic hazard and risk analysis, and ultimately loss mitigation, are encouraged.

VIII. Special Projects and Initiatives

The following are SCEC special projects with which proposals in above categories can be identified.

A. **Networks as Research Tools.** SCEC encourages proposals that enhance the use of seismic and geodetic networks as research tools. The goal of such research is to promote innovations in network deployments and data integration that will provide new information on earthquake phenomena. Projects in this category are meant to be complementary to ANSS, IRIS, Earthscope, and UNAVCO. The Earthquake Early Warning Demonstration Project is an example of such an activity.

B. **Southern San Andreas Fault Evaluation (SoSAFE) project.** The SCEC Southern San Andreas Fault Evaluation (SoSAFE) Project will continue to increase our knowledge of slip rates, paleo-event chronology, and slip distributions of past earthquakes, for the past two thousand years on the southern San Andreas fault system. From Parkfield to

Bombay Beach, and including the San Jacinto fault, the objective is to obtain new data to clarify and refine relative hazard assessments for each potential source of a future 'Big One.' Most work to be funded is expected to involve paleoseismic and geological fault slip rate studies.

The second year of SoSAFE is expected to again be funded at $240K by USGS. Targeted research by each of several selected self-organized multi-investigator teams will be supported to rapidly advance SCEC research towards meeting objective A1. We encourage investigator teams to propose jointly in response to the RFP. Each team will address one significant portion of the fault system, and all teams will agree to collaboratively review one another's progress. We welcome requests for joint infrastructure resources, for example geochronology support. That is, an investigator may ask for dating support (e.g., to date 6 radiocarbon samples). Requests for dating shall be coordinated with Earthquake Geology.

Other SCEC objectives will also be advanced through the research funded by SoSAFE, such as A2, A10, and B1. For example, interaction between SoSAFE and the scenario rupture modeling activity will continue beyond the ShakeOut, as we discuss whether or not additional radiocarbon dating could be used to eliminate the scenario of a "wall-to-wall" rupture (from Parkfield to Bombay Beach). SoSAFE will also work to constrain scenario models by providing the best possible measurements of actual slip distributions from past earthquakes on these same fault segments as input, thereby enabling a more realistic level of scenario modeling. Use of novel methods for estimating slip rates from geodetic data would also potentially be supported within the upcoming year. Slip rate studies will continue to be encouraged, and for these it is understood that support may be awarded to study offset features that may be older than the 2000 yrs. stated in objective A1, perhaps as old as 60,000 yrs. in some cases. It is expected that much support will go towards improved dating (e.g., radiocarbon and OSL) of earthquakes within the past 2000 yrs., however, so that event correlations and coefficient of variation in recurrence intervals may be further refined.

We will also discuss common longer-term research interests and engage in facilitating future collaborations in the broader context of a decade-long series of interdisciplinary, integrated and complementary studies on the southern San Andreas fault system.

C. **Working Group on California Earthquake Probabilities (WGCEP).** The ongoing WGCEP is developing a time-dependent, statewide earthquake-rupture forecast that uses "best available science". This model, called the Uniform California Earthquake Rupture Forecast (UCERF), will have the endorsement of SCEC, USGS, and CGS. The California Earthquake Authority, which holds about two-thirds of all homeowners earthquake insurance policies throughout the state, is interested in using the model to set insurance rates. Development of this model is tightly coordinated with the USGS National Seismic Hazard Mapping Program. For example, the time-independent component of UCERF 2 was used in the 2007 USGS/CGS California hazard map. We are deploying the model in an adaptable, extensible framework where modifications can be made as warranted by scientific developments, the collection of new data, or following the occurrence of significant earthquakes (subject to the review process). Our implementation strategy is to add more advanced capabilities only after achieving more modest goals.

The following are examples of SCEC activities that could make direct contributions to WGCEP goals:

- Extend our UCERF, which gives the magnitude, average rake, and rupture surface of all possible earthquakes throughout the state, to include different viable slip time histories for each of these ruptures (A).
- Develop models that give fault-to-fault rupture probabilities as a function of fault separation, difference in strike, and styles of faulting (A9).
- Refine estimates of observed earthquake rates and their uncertainties, both statewide and as a function of space. This could include associating historic events with known faults (A4 and C).
- Further refinement of fault models including geometries, seismogenic depths, and aseismicity parameters (C).
- Develop self-consistent, Elastic-Rebound-Theory motivated renewal models
- Development of deformation models that give improved slip- and stressing-rates on known faults, as well as off-fault deformation rates elsewhere (A3).
- Further constrain viable magnitude-area relationships, especially with respect to how they are being used in this project (A4). Important here is the question of the down-dip extent of rupture (lower seismogenic depth).
- Resolve interpretation of UCERF2's "Empirical" model (which implies a statewide stress shadow).
- Develop moment-balanced rupture models that predict a long-term rate of earthquakes that is consistent with the historical record (e.g., no discrepancy near magnitude 6.5) (A6). In so doing, also relax segmentation and include fault-to-fault ruptures.
- Develop methodologies for computing time-dependent earthquake probabilities in our model. These methodologies could include approaches that invoke elastic-rebound-theory motivated renewal models, earthquake triggering effects that include aftershock statistics, or physics-based earthquake simulations (A6).
- Develop easily computable hazard or loss metrics that can be used to evaluate and perhaps trim logic-tree branch weights (B6, C).
- Develop a community-standard hazard-to-loss interface (i.e., that can be used by anyone from academics, government officials, and consulting companies) (B6, C).

Further suggestions and details can be found at *http://www.WGCEP.org*, or by speaking with the project leader (Ned Field: field@usgs.gov; (626) 644-6435).

D. **Next Generation Attenuation (NGA) Project.** The NGA Project is lead by PEER with the collaboration of SCEC and USGS to develop response spectral ground motion prediction models. The current focus is on shallow crustal earthquakes in tectonically active regions. The current phase (NGA-E) is nearing completion, and it is anticipated that the next phase (NGA-H) will begin in 2008. The NGA-H Project will involve the use of broadband strong motion simulation to generate ground motion time histories for use, in conjunction with recorded ground motions, in the development of ground motion attenuation relations for hard rock that are based on improved sampling of magnitude and distance, expecially large magnitudes and close distances, and improved understanding of the relationship between earthquake source and strong ground motion characteristics. Broadband simulation methods are verified (by comparison of simple test case results with other methods) and validated (against recorded strong ground motions) before being used to generate broadband ground motions for use in model development. These simulation activities for verification, validation, and application are done on the SCEC Broadband Simulation Platform, which is currently under development. The main SCEC focus groups working on this project are Ground Motion Prediction; Seismic Hazard and Risk Analysis; and PetaSHA – Terashake and Cybershake.

E. **End-to-End ("Rupture-to-Rafters") Simulation.** The purpose of this project is to foster interaction between earthquake scientists and earthquake engineers through the collaborative modeling of the whole process involved in earthquake fault rupture, seismic wave propagation, site response, soil-structure interaction, and building response. Recent sponsors of this project have been NSF (tall buildings) and CEA (woodframe buildings), and new sponsors are being sought. The main SCEC discipline and focus groups working on this project are Geology, especially fault models; Unified Structural Representation; Faulting and the Mechanics of Earthquakes; Ground Motion Prediction; Seismic Hazard and Risk Analysis; and PetaSHA – Terashake and Cybershake.

F. **Collaboratory for the Study of Earthquake Predictability (CSEP).** The goal of CSEP is to develop a virtual, distributed laboratory—a collaboratory—that can support a wide range of scientific prediction experiments in multiple regional or global natural laboratories. This earthquake system science approach seeks to provide answers to the questions: (1) How should scientific prediction experiments be conducted and evaluated? and (2) What is the intrinsic predictability of the earthquake rupture process? Contributions may include: (1) Establishing rigorous procedures in controlled environments (testing centers) for registering prediction procedures, which include the delivery and maintenance of versioned, documented code for making and evaluating predictions including intercomparisons to evaluate prediction skills; (2) Constructing community-endorsed standards for testing and evaluating probability-based and alarm-based predictions; (3) Developing hardware facilities and software support to allow individual researchers and groups to participate in prediction experiments; (4) Providing prediction experiments with access to data sets and monitoring products, authorized by the agencies that produce them, for use in calibrating and testing algorithms; and (5) Conducting workshops to facilitate international collaboratories. A major focus of CSEP is to develop international collaborations between the regional testing centers and to accommodate a wide-ranging set of prediction experiments involving geographically distributed fault systems in different tectonic environments.

G. **National Partnerships through EarthScope.** The NSF Earthscope project provides unique opportunities to learn about the structure and dynamics of North America. SCEC encourages proposals to the NSF Earthscope program that will address the goals of the SCEC Science Plan.

H. **Extreme Ground Motions (EXGM).** Extreme ground motions are the very large amplitudes of earthquake ground motions that can arise at very low probabilities of exceedance, as was the case for the 1998 PSHA for Yucca Mountain. This project investigates the credibility of such ground motions through studies of physical limits to earthquake ground motions, unexceeded ground motions, and frequency of occurrence of very large ground motions or of earthquake source parameters (such as stress drop and faulting displacement) that cause them. Of particular interest to ExGM (and more generally to ground-motion prediction and SHRA) is why crustal earthquake stress drops are so sensibly constant and so much less than the frictional strength of rocks at mid-crustal depths.

   This project is sponsored by DOE. The main SCEC discipline and focus groups that will work on this project are Geology – especially fault zone geology; Faulting and Mechanics of Earthquakes, Ground-Motion Prediction, and Seismic Hazard and Risk Analysis. This project is also discussed above within SHRA.

I. **Petascale Cyberfacility for Physics-Based Seismic Hazard Analysis (PetaSHA).** SCEC's PetaSHA aims to develop and apply physics-based predictive models to improve the practice of seismic hazard analysis. This project will utilize numerical modeling techniques and high performance computing to implement a computation-based approach to SHA. Three scientific initiative areas have been identified for this project to help to guide the scientific research. The PetaSHA initiative areas are: (1) development of techniques to support higher frequencies waveform simulations including deterministic and stochastic approaches; (2) development of dynamic rupture simulations that include additional complexity including nonplanar faults, a variety of friction-based behaviors, and higher inner /outer scale ratios (e.g. (fault plane mesh dimension) / (simulation volume dimension)); and (3) physics-based probabilistic seismic hazard analysis including probabilistic seismic hazard curves using 3D waveform modeling. All of these modeling efforts must be accompanied by verification and validation efforts. Development of new techniques that support the verification and validation of SCEC PetaSHA modeling efforts are encouraged.

   The SCEC PetaSHA modeling efforts address several of the SCEC3 objectives. Development of new verification and validation techniques (B4) are common to each of the PetaSHA initiative areas. Research activities related to the improved understanding and modeling of rupture complexity (A8, B1) support the PetaSHA initiatives. In addition, research into the upper frequency bounds on deterministic ground motion predictions (B2, B3) are SCEC3 science objectives that are important work areas in the PetaSHA Project.

J. **Advancement of Cyberinfrastructure Careers through Earthquake System Science (ACCESS).** ACCESS provides students with research experiences in earthquake system science to advance their careers and creative participation in cyberinfrastructure (CI) development. Three programmatic elements:

   - ***ACCESS-U***: One-term undergraduate internships to support CI-related senior thesis research in the SCEC Collaboratory
   - ***ACCESS-G:*** One-year graduate internships to support CI-related master thesis research in the SCEC Collaboratory
   - ***ACCESS Forum:*** a new CEO working group to promote CI careers in earthquake system science

IX. SCEC Communication, Education, and Outreach

SCEC is a community of over 600 scientists, students, and staff from 56 institutions, in partnership with many other science, engineering, education, and government organizations worldwide. To facilitate applications of the knowledge and scientific products developed by this large community, SCEC maintains a Communication, Education, and Outreach (CEO) program with four long-term goals:

- Coordinate productive interactions among a diverse community of SCEC scientists and with partners in science, engineering, risk management, government, business, and education.
- Increase earthquake knowledge and science literacy at all educational levels, including students and the general public.
- Improve earthquake hazard and risk assessments
- Promote earthquake preparedness, mitigation, and planning for response and recovery.

Short-term objectives are outlined below. Many of these objectives present opportunities for members of the SCEC community to become involved in CEO activities, which are for the most

part coordinated by CEO staff. To support the involvement of as many others as possible, budgets for proposed projects should be on the order of $2,000 to $7,000. Hence proposals that include additional sources of support (cost-sharing, funding from other organizations, etc.) are highly recommended. Smaller activities can be supported directly from the CEO budget and do not need a full proposal. Those interested in submitting a CEO proposal should first contact Mark Benthien, associate SCEC director for CEO, at 213-740-0323 or benthien@usc.edu.

CEO Focus Area Objectives

1. SCEC Community Development and Resources (activities and resources for SCEC scientists and students)

   SC1 Increase diversity of SCEC leadership, scientists, and students

   SC2 Facilitate communication within the SCEC Community

   SC3 Increase utilization of products from individual research projects

2. Education (programs and resources for students, educators, and learners of all ages)

   E1 Develop innovative earth-science education resources

   E2 Interest, involve and retain students in earthquake science

   E3 Offer effective professional development for K-12 educators

3. Public Outreach (activities and products for media reporters and writers, civic groups and the general public)

   P1 Provide useful general earthquake information

   P2 Develop information for the Spanish-speaking community

   P3 Facilitate effective media relations

   P4 Promote SCEC activities

4. Knowledge transfer (activities to engage other scientists and engineers, practicing engineers and geotechnical professionals, risk managers, government officials, utilities, and other users of technical information.

   I1 Communicate SCEC results to the broader scientific community

   I2 Develop useful products and activities for practicing professionals

   I3 Support improved hazard and risk assessment by local government and industry

   I4 Promote effective mitigation techniques and seismic policies

Appendix: SCEC3 Long-Term Research Goals

This section outlines the SCEC science priorities for the five-year period from February 1, 2007, to January 31, 2012. Additional material on the science and management plans for the Center can be found in the SCEC proposal to the NSF and USGS (*http://www.scec.org/aboutscec/documents/*).

Basic Research Problems

SCEC is, first and foremost, a basic research center. We therefore articulate our work plan in terms of four basic science problems: (1) earthquake source physics, (2) fault system dynamics, (3)

earthquake forecasting and predictability, and (4) ground motion prediction. These topics organize the most pressing issues of basic research and, taken together, provide an effective structure for stating the SCEC3 goals and objectives. In each area, we outline the problem, the principle five-year goal, and some specific objectives. We then assess the research activities and the new capabilities needed to attain our objectives.

1. Earthquake Source Physics

Problem Statement. Earthquakes obey the laws of physics, but we don't yet know how. In particular, we understand only poorly the highly nonlinear physics of earthquake nucleation, propagation, and arrest, because we lack knowledge about how energy and matter interact in the extreme conditions of fault failure. A complete description would require the evolution of stress, displacement, and material properties throughout the failure process across all relevant scales, from microns and milliseconds to hundreds of kilometers and many years. A more focused aspect of this problem is the physical basis for connecting the behavior of large ruptures at spatial resolutions of hundreds of meters and fracture energies of megajoules per square meter with laboratory observations of friction at centimeter scales and fracture energies of kilo-joules per square meter. Two further aspects are the problem of stress heterogeneity—the factors that create and maintain it over many earthquake cycles—and the related problem of defining the concept of strength in the context of stress and rheological heterogeneity.

Goal and Objectives. The goal for SCEC3 will be to discover the physics of fault failure and dynamic rupture that will improve predictions of strong ground motions and the understanding of earthquake predictability. This goal is directly aligned with our mission to develop physics-based seismic hazard analysis. Specific objectives include:

A. Conduct laboratory experiments on frictional resistance relevant to high-speed coseismic slip on geometrically complex faults, including the effects of fluids and changes in normal stress, and incorporate the data into theoretical formulations of fault-zone rheology.

B. Develop a full 3D model of fault-zone structure that includes the depth dependence of shear localization and damage zones, hydrologic and poroelastic properties, and the geometric complexities at fault branches, step-overs, and other along-strike and down-dip variations.

C. Combine the laboratory, field-based, and theoretical results into effective friction laws for the numerical simulation of earthquake rupture, test them against seismological data, and extend the simulation methods to include fault complexities such as bends, step-overs, fault branches, and small-scale roughness.

D. Develop statistical descriptions of stress and strength that account for slip heterogeneity during rupture, and investigate dynamic models that can maintain heterogeneity throughout many earthquake cycles.

2. Fault System Dynamics

Problem Statement. In principle, the Southern California fault system can be modeled as a dynamic system with a state vector S and an evolution law $dS/dt = F(S)$. The state vector represents the stress, displacement, and rheology/property fields of the seismogenic layer as well as its boundary conditions. Its evolution equation describes the forward problem of fault dynamics. Many of the most difficult (and interesting) research issues concern two inference or inverse problems: (1) model building—from our knowledge of fault physics, what are the best

representations of S and F?—and (2) data assimilation—how are the parameters of these representations constrained by the data D on the system's present state S0 as well as its history?

The SCEC approach is not to proceed by trying to write down general forms of S and its rate-of-change F. Rather, we use judicious approximations to separate the system evolution into a series of numerical simulations representing the interseismic, preseismic, coseismic, and postseismic behaviors. In particular, the natural time-scale separation between inertial and non-inertial dynamics usually allows us to decouple the long-term evolution of the state vector from its short-term, coseismic behavior. Therefore, in describing many interseismic and postseismic processes, we can treat the fault system quasi-statically, with discontinuous jumps in S at the times of earthquakes. On the other hand, the dynamics of earthquake rupture is clearly important to the basic physics of fault system evolution. In the modeling of stress heterogeneity, for example, the coupling of inertial and non-inertial dynamics must be addressed by integrating across this scale gap.

Goal and Objectives. The principal SCEC3 goal for fault system dynamics is to develop representations of the postseismic and interseismic evolution of stress, strain, and rheology that can predict fault system behaviors within the Southern California Natural Laboratory. The SCEC3 objectives are sixfold:

A. Use the community modeling tools and components developed in SCEC2 to build a 3D dynamic model that is faithful to the existing data on the Southern California fault system, and test the model by collecting new data and by predicting its future behavior.

B. Develop and apply models of coseismic fault slip and seismicity in fault systems to simulate the evolution of stress, deformation, fault slip, and earthquake interactions in Southern California.

C. Gather and synthesize geologic data on the temporal and spatial character and evolution of the Southern California fault system in terms of both seismogenic fault structure and behavior at geologic time scales.

D. Constrain the evolving architecture of the seismogenic zone and its boundary conditions by understanding the architecture and dynamics of the lithosphere involved in the plateboundary deformation.

E. Broaden the understanding of fault systems in general by comparing SCEC results with integrative studies of other fault systems around the world.

F. Apply the fault system models to the problems of earthquake forecasting and predictability.

3. Earthquake Forecasting and Predictability

Problem Statement. The problems considered by SCEC3 in this important area of research will primarily concern the physical basis for earthquake predictability. Forecasting earthquakes in the long term at low probability rates and densities—the most difficult scientific problem in seismic hazard analysis—is closely related to the more controversial problem of high-likelihood predictions on short (hours to weeks) and intermediate (months to years) time scales. Both require a probabilistic characterization in terms of space, time, and magnitude; both depend on the state of the fault system (conditional on its history) at the time of the forecast/prediction; and, to put them on a proper science footing, both need to be based in earthquake physics.

Goal and Objectives. The SCEC3 goal is to improve earthquake forecasts by understanding the physical basis for earthquake predictability. Specific objectives are to:

A. Conduct paleoseismic research on the southern San Andreas and other major faults with emphasis on reconstructing the slip distributions of prehistoric earthquakes, and explore the implications of these data for behavior of the earthquake cycle and time-dependent earthquake forecasting.

B. Investigate stress-mediated fault interactions and earthquake triggering and incorporate the findings into time-dependent forecasts for Southern California.

C. Establish a controlled environment for the rigorous registration and evaluation of earthquake predictability experiments that includes intercomparisons to evaluate prediction skill.

D. Conduct prediction experiments to gain a physical understanding of earthquake predictability on time scales relevant to seismic hazards.

4. Ground Motion Prediction

Problem Statement. Given the gross parameters of an earthquake source, such as its magnitude, location, mechanism, rupture direction, and finite extent along a fault, we seek to predict the ground motions at all regional sites and for all frequencies of interest. The use of 3D velocity models in low-frequency (< 0.5 Hz) ground motion prediction was pioneered in SCEC1 (§II.A), and this type of simulation, based on direct numerical solution of the wave equation, has been taken to new levels in SCEC2 (§II.B.6). The unsolved basic research problems fall into four classes: (a) the ground motion inverse problem at frequencies up to 1 Hz; (b) the stochastic extension of ground motion simulation to high frequencies (1-10 Hz); (c) simulation of ground motions using dynamically consistent sources; and (d) nonlinear wave effects, including nonlinear site response. In addition, there remain scientific and computational challenges in the practical prediction of ground motions near the source and within complex structures such as sedimentary basins, as well as in the characterization of the prediction uncertainties.

Goal and Objectives. The principal SCEC3 goal is to predict the ground motions using realistic earthquake simulations at frequencies up to 10 Hz for all sites in Southern California. The SCEC3 objectives are:

A. Combine high-frequency stochastic methods and low-frequency deterministic methods with realistic rupture models to attain a broadband (0-10 Hz) simulation capability, and verify this capability by testing it against ground motions recorded at a variety of sites for a variety of earthquake types.

B. Use observed ground motions to enhance the Unified Structural Representation (USR) by refining its 3D wavespeed structure and the parameters that account for the attenuation and scattering of broadband seismic energy.

C. Apply the ground-motion simulations to improve SHA attenuation models, to create realistic scenarios for potentially damaging earthquakes in Southern California, and to explain the geologic indicators of maximum shaking intensity and orientation.

D. Investigate the geotechnical aspects of how built structures respond to strong ground motions, including nonlinear coupling effects, and achieve an end-to-end simulation capability for seismic risk analysis.

SCEC Annual Meeting Abstracts

Plenary Presentations

Horizon Ballroom, Hilton Palm Springs Resort

MONDAY, SEPTEMBER 8, 2008 – 09:30

THE SHAKEOUT SCENARIO: GETTING OUR SCIENCE USED

Jones LM

This presentation will explore how earthquake science is being used to improve earthquake safety in southern California through the Great Southern California ShakeOut. The ShakeOut Scenario is a description of the impacts and consequences of a M7.8 earthquake on the Southern San Andreas Fault (USGS OFR2008-1150). The USGS partnered with SCEC, the California Geological Survey and many other organizations to bring 300 scientists and engineers together to formulate a comprehensive description of a plausible San Andreas earthquake. The scenario was released in May 2008.

The ShakeOut Scenario is being used as the science behind the Great Southern California ShakeOut: a week of special events featuring the largest earthquake drill in United States history, organized to inspire Southern Californians to get ready for big earthquakes, and to prevent disasters from becoming catastrophes. The ShakeOut drill will occur in houses, businesses, and public spaces throughout southern California at 10AM on November 13, 2008.With the concrete example of this earthquake, southern California is being shown that what we do now, before a big earthquake, will determine what our lives will be like after. Specific findings of the scenario are being used as exercises both by local governments and corporations and incorporated in a variety of media for use in the ShakeOut. One of the most innovative developments is the "Earthquake Recovery Game", an interactive, online gaming experience, which will educate its gamers in earthquake science and the results of the research while encouraging innovative approaches to social problems in recovery.

MONDAY, SEPTEMBER 8, 2008 – 09:30

OUTSTANDING RESEARCH QUESTIONS RAISED BY THE SHAKEOUT SCENARIO

Porter KA

The USGS and California Geological Survey recently released a major planning scenario document that hypothesizes the occurrence and effects of a MW7.8 earthquake on the southern San Andreas Fault. Major outcomes of the scenario include: fault offsets of up to 13m; peak ground velocities up to 3 m/sec near the fault and exceeding 0.5 m/sec over 10,000 sq km; 1,800 deaths and 50,000 serious injuries; 1,600 fires that destroy the equivalent of 133,000 single-family homes; and economic losses totaling $213 billion, predominantly from fire ($87 billion), shake-related property damage ($46 billion) and business interruption loss from water outages ($53 billion). Despite the scenario's short development time (15 months) and emphasis on realistic rather than probabilistic loss estimation, its contributors applied state-of-the-art science to several study aspects, such as: UCERF 2 estimates of slip rate and past rupture extent; dynamic as well as kinematic rupture modeling; physics-based modeling of wave propagation using both mature and developing community velocity models; advanced structural analysis; and extensive use of GIS. As with any similarly ambitious effort, many research questions were raised, where new insight into

earthquake processes and impacts might yield a greater ability to prepare for such an event and mitigate its negative effects. Questions with potentially 1st-order impacts on scenario impacts include: more detailed knowledge of the relative activity and geometry of various traces of the Southern San Andreas fault system; continued advances to a the community velocity model; a regional, detailed liquefaction model; various enhancements to our model of fire following earthquake; detailed knowledge of the building stock and the likely behavior of the older concrete, steel, and woodframe buildings that contribute so heavily to life-safety risk; a public loss model that employs dynamic structural analysis and other concepts of modern performance-based earthquake engineering; an up-to-date, dynamic model of seismic lifeline damage and interaction; a mechanistic model of human injuries in earthquake-damaged buildings; and a mechanistic model of cost increases in catastrophic earthquakes.

MONDAY, SEPTEMBER 8, 2008 – 09:30

USING THE SHAKEOUT SCENARIO: A PRACTITIONER'S PERSPECTIVE

Tognazzini RA

The purpose of this presentation is to describe how the Los Angeles City Department of Water and Power (LADWP) used the ShakeOut Scenario over the first six months of this year, culminating in a full-scale exercise on July 16 and 17, 2008. The presentation will cover the motivation behind the adoption of the ShakeOut Scenario, the opportunities that it offered, the training that resulted in the full-scale exercise, and the results that were realized in the Nation's largest municipally owned utility. The presentation will also provide information that indicates LADWP's need to improve its infrastructure, emergency management procedures, and emergency response resources to prevent the ShakeOut Scenario from being a catastrophic event for the City of Los Angeles.

Scenario motivations included products from SCEC and its affiliates, mandates from regulatory agencies, a recent major disaster, and several minor emergencies. The opportunity to use an earthquake scenario that exercised all elements of the new emergency response procedures came from the mandatory development of new emergency response plans in 2007, and the need to train to the new plans, starting in 2008. The unstated goal of the full-scale exercise was to conduct the largest and most complex demonstration of emergency management that LADWP has ever undertaken in its 106-year history. The model adopted for this full-scale exercise was a series of orientation and training exercises leading up to the full-scale exercise in July. This model has been adopted by several other utilities in Southern California in preparation for the State's Golden Guardian Exercise in November 2008.

The results were that LADWP experienced an abnormally large number of customer-service outage hours for its Power System, and lost a large amount of its aboveground water storage to fire fighting for the Water System. For this ShakeOut Scenario to avoid becoming a catastrophe, nearly 4,000,000 people in the City of Los Angeles were required to curtail the use of both water and power in unprecedented amounts for long periods.

MONDAY, SEPTEMBER 8, 2008 – 15:30

ENGINEERING USE OF GROUND MOTIONS: CHALLENGES AND OPPORTUNITIES

Baker JW

Ground motions, and measures of ground motion intensity, serve as a link between seismology and engineering for the purpose of earthquake risk assessment and performance-based earthquake engineering. Engineers rely on earth scientists to quantify rates of earthquake activity and associated ground shaking intensity at a site, and increasingly to provide simulated ground motion time histories. As nonlinear dynamic structural analysis becomes increasingly common in

engineering practice, this interface between scientists and engineers will only grow in importance. Unrealized opportunities for benefits at this science/engineering interface still exist, and conversely there is a potential for erroneous conclusions to be drawn if the interface is not properly addressed.

To illustrate challenges and opportunities for engineering use of ground motions, typical uses of ground motions for analysis will be described. These uses include prescriptive checks to satisfy building code requirements, as well as newer procedures to more accurately quantify the probability building failures (often termed "performance-based engineering"). Practical constraints on computing and modeling efforts in these analyses will be highlighted, and implications for selection of recorded ground motions and validation of simulated ground motions will also be discussed. An improved understanding of these engineering analysis approaches and limitations should help earth scientists to increase the impact of their work on the structural engineering profession.

TUESDAY, SEPTEMBER 9, 2008 – 08:00

THE 12 MAY 2008 MS 8.0 WENCHUAN EARTHQUAKE, SICHUAN, CHINA: BACKGROUND, FIELD INVESTIGATIONS AND TECTONIC IMPLICATIONS

Liu J, Zhang Z, Wen L, Sun J, Tapponnier P, Xing X, Hu G, Xu Q, Zeng L, and Ding L

The destructive Ms8.0 Wenchuan earthquake struck the mountainous, western rim of the Sichuan basin in central China on May 12th, 2008. This is the most devastating earthquake in China since the 1976 Tangshan earthquake, with total losses surpassing those of the latter. Strong shaking during the earthquake triggered numerous landslides on the steep slopes, some of which dammed rivers into lakes across the rugged topography of the Longmen Shan, aggravating damage and natural hazard. The tragedy is a sad reminder that seismic vulnerability has risen sharply over the last few decades due to combined economic and population growth and insufficient understanding and awareness of seismic hazard, a situation faced in many other highly seismic parts of the world(e.g., Jackson, 2006). Field mapping, initiated shortly after the event, shows that the earthquake ruptured principally two of the four main, NE-trending thrusts of the Longmen Shan system: the Beichuan and Pengguan thrusts. With a surface rupture at least 225 km-long and maximum slip of 8 – 10 m, it thus ranks as one of the world's largest continental mega-thrust events in the last 150 years. The principal rupture, on the NW-dipping Beichuan fault, displays near equal amounts of NW hanging-wall up–thrust and right-lateral slip. Basin-ward of this rupture, another continuous surface break is observed for about 60 km on the parallel, shallower-NW-dipping Pengguan fault. Slip on this latter fault was a pure thrust, with maximum scarp height of ~ 2.8 m. This is one of the very few reported instances of co-seismic surface rupture on parallel thrusts. The long rupture, large-offsets, and distributed surface breaks that characterize this out-of-sequence event attest to regional, EW-directed, present-day crustal shortening along the NE-SW trending eastern margin of Tibetan plateau. This in turn calls for a re-evaluation of tectonic models anticipating little or no active shortening of the upper crust along that edge of the plateau, and for a re-assessment of seismic hazard along potentially under-rated active faults across the densely-populated western Sichuan basin and mountains.

TUESDAY, SEPTEMBER 9, 2008 – 15:00

SECONDS CAN MAKE A DIFFERENCE! RECENT PROGRESS IN EARTHQUAKE EARLY WARNING

Boese M

Earthquake early warning (EEW) systems are being developed around the world, and a few are already operational. The Mexico City EEW system that warns of earthquakes along the Guerrero

Coast has been in operation for almost two decades. The Japanese EEW system went operational in October 2007. Several European regional EEW systems are at various stages of development under the SAFER project. In the US the CISN is developing and testing three EEW algorithms in cooperation with the USGS/ANSS and SCEC.

The 29 July 2008 Mw5.4 Chino Hills earthquake that was located in less than 50 km distance SE of downtown Los Angeles, once again demonstrated the persistent seismic threat that people in California are exposed to. Further, a recent USGS/CGS/SCEC study states that it is a matter of time only until the next "Big One" will happen and preparative measures need to be developed and implemented as soon as possible. I will describe the possible application of EEW systems, which rapidly detect seismic waves, estimate the earthquake magnitude and associated ground motion, and, if required, issue warnings to potential users before seismic waves arrive. Even if the warning times are in the order of some seconds to about one minute, they can be sufficient to trigger and execute automatic measures to decrease likely damage and numbers of fatalities during strong earthquakes, e.g., by automatically stopping trains and elevators. Depending on the location of the earthquake hypocenter, warning times for large cities such as Los Angeles might range up to about one minute, which is sufficient to implement various mitigation measures to safe lives and reduce the potential impact of the earthquake.

In Oct. 2007, the Japanese Meteorological Agency (JMA) launched the 2nd and arguably the most comprehensive public EEW system in the world. If damaging ground shaking due to a strong earthquake in Japan is expected, the JMA system broadcasts warnings to the public using diverse communication links, including television, radio and e-mail. Some minor problems at the early stage of the system, e.g., the initial underestimation of ground shaking during the Iwate-Miyagi Inland Mw6.9 earthquake in June 2008, caused critical comments by the international press. This user feedback is useful for understanding how to educate the public about the limitations of EEW. The Japanese experience is also encouragement for implementing improvements in communication technologies and EEW algorithm.

TUESDAY, SEPTEMBER 9, 2008 – 15:30

C^3 (CORRELATION OF CODA OF CORRELATIONS): IMPROVING THE RECONSTRUCTION OF GREEN FUNCTIONS BETWEEN STATIONS OF A NETWORK FROM NOISE RECORDS

Campillo M, Froment B, Stehly L, and Weaver RL

Our goal is to extract the Green function between every pairs of receivers of a network by taking advantage of the simultaneous records of the noise by a large number of stations. In the case of an even distribution of noise sources, it has been theoretically demonstrated that the correlation is the exact Green function, including all types of waves. In most cases, the noise is far to be consisting in an even azimuthal distribution of incoming waves. It would be therefore preferable to use multiply scattered waves, which have the adequate equipartition property. Unfortunately we can not separate the direct and scattered waves in the noise records as we can with a simple time window in earthquake records. We use a procedure that allows for removing the effects of the directivity of the noise. We consider two stations A and B for which the Rayleigh waves could not be discerned in the in the correlation of continuous records of ambient noise. We computed all correlations between the station A (resp. B) and all the 150 other stations located at regional distances. Theoretically, these virtual seismograms contain direct waves and coda, although they are clearly contaminated by the influence of the imperfect ambient noise field and most are inadequate for direct analysis. We used these correlation functions as equivalents to seismograms produced by sources acting at the 150 stations locations and recorded in A (resp B). We select time windows in

those virtual seismograms that correspond to coda and compute correlations between them. This meta-correlation is found to exhibit the surface wave part of the Green function that was not visible in the raw correlation of ambient noise. We illustrate the legitimacy of the reconstruction by comparison with raw noise correlations. This procedure can be used to assess seismic velocity between stations, even in presence of a directive and poorly oriented ambient noise. The result shows that, in spite of the small signal to noise ratios often seen in correlations of ambient noise, their late parts are better equipartitioned than was the ambient noise upon which they were based. The codas of correlations contain information on both direct surface waves and also on more complex travel paths. This last point is illustrated by the extraction of 'C5' functions, which, in spite of short times of correlation, still clearly exhibit the direct waves.

Group 1. Poster Abstracts

Plaza Ballroom, Hilton Palm Springs Resort

Communication, Education, and Outreach (CEO)

1-001

TWO PROJECTS FOR EARTHQUAKE EDUCATION AND OUTREACH: CSULA EARTHQUAKE DISPLAY; SCEC PLATE TECTONICS LEARNING KITS *Coss Y Leon D*

During the summer of 2008, I participated in SCEC's internship program Summer Undergraduate Research Experience (SURE) where I worked on education and outreach projects. I was assigned two major projects that were designed to educate the general public on earthquake science and earthquake safety. The first project was the remodeling of the old earthquake display, located in California State University, Los Angeles' Physical Sciences building. The old display consisted of visually unattractive signs, outdated computers, and a seismograph with the rotating drum. The new display now consists of more attractive signs, two computers (each with 28 inch LCD screens that display the latest earthquakes, globally and locally), and information on earthquake preparedness. The second project of the two was a mockup of SCEC's "Plate Tectonics Learning Kit." This kit builds on Purdue University's professor Larry Braille's earlier creation of the plate tectonics kit. The purpose of SCEC's version of the kit is to educate students (primarily middle school students) about plate tectonics and its causes/effects. The kit includes USGS' map This Dynamic Planet along with the plate boundaries on the back so that others may cut the individual plates out of the map. Once the map is cut into its pieces, it could then be used as a puzzle. The kit includes other smaller items that would facilitate the teaching of plate tectonics.

1-002

VISUALIZING AN EARTHQUAKE RUPTURE FORECAST WITH RELATED DATA USING 3D COMPUTER GRAPHICS, AND ASSOCIATED SOFTWARE DEVELOPMENT CHALLENGES ENCOUNTERED. *Aguilar V, Berti R, DeWeese D, Dischler J, Ihrig M, Punihaole T, and Rosa J*

The Uniform California Earthquake Rupture Forecast (UCERF) report was published in 2007. The report aggregated vast amounts of information including past seismic activity, known fault information, and geodesy in order to forecast future earthquakes using a statistical model. There is an obvious need to display this information in an easily digestible way for the general public. In the summer of 2008 the Southern California Earthquake Center Undergraduate Studies in Earthquake Information Technology (SCEC- USEIT) internship participants at the University of

Southern California were given the challenge of presenting the UCERF2 report in an interactive medium using the SCEC-Virtual Display of Objects program. SCEC-VDO is a program developed by participants in the USEIT program for the express purpose of displaying visual information relevant to understanding seismic processes.

The USEIT developers team augmented SCEC-VDO with the ability to display the participation probabilities assigned to various regions around California determined by the UCERF report. These probabilities can be computed within a minute so users can query SCEC-VDO in order to determine the probability that a particular region will participate in a fault rupture above a certain magnitude over a specified period of time. Additionally, many of the fault models and earthquake data used to produce the UCERF2 report are now available within SCEC-VDO and can be displayed simultaneously for analysis. Finally, the code base has been restructured in order to allow for modular development which is more amenable to being used in an open source project.

1-003
ANIMATING, DEPICTING AND EXPLAINING THE FAULTS, EARTHQUAKES, PARTICIPATION PROBABILITIES, AND KEY POINTS OF THE UCERF REPORT THROUGH SCEC-VDO *Milner K, Aguilar V, Dischler J, Cruz-Guandique EA, Le M, and Ihrig M*

The Undergraduate Studies in Earthquake Information Technology (USEIT) program is a team-based summer internship. Each year the interns are given a "Grand Challenge". The 2008 goal of the Virtual Display of Objects (VDO) group was to animate and explain the Uniform California Earthquake Rupture Forecast (UCERF) objects using the Southern California Earthquake Center (SCEC)-VDO software. This software "is an interactive, 4D visualization program created using Java3D and used to visualize earthquakes, faults, maps, and other models and data sets of interest to earth scientists." The group virtually displayed examples of deformation fault models, explanations about the participation probabilities, earthquake catalogs and many other key products of the UCERF Report. The VDO animations explain the alternative deformation models, which show the trade-off of the slip rate between the San Jacinto and San Andreas faults. Another animation depicts the difference between the earthquake rate models, Type-A and Type-B faults, and Type-C zones. The VDO animations also explain in detail the location of the faults in Southern California, display past earthquakes, and clarify the many key products of the UCERF Report to enlighten end-users and the society at large. Extensive research was required to transfer the report into visual animations. The VDO group encountered challenges with the software, most of the tasks required development of plug-in capabilities that were not yet available. The Developer group's goal was to develop new capabilities for displaying UCERF information; both groups collaborated and assigned; both groups collaborated and assigned liaisons to address issues on both ends.

1-004
PIONEERING A DIGITAL ARCHIVE FOR THE IMPORTATION, PRESERVATION, AND ACCESSIBILITY OF SOUTHERN CALIFORNIA EARTHQUAKE CENTER RECORDS *Boutwell C, Cruz-Guandique EA, Gonzalez J, Looney GK, Miller BR, and Pratts M*

As computer-based technology is readily becoming more available and digital material is continuously being created, the need for a digital library emerges. The purpose of the Digital Library created for the Southern California Earthquake Center (SCEC) during the summer of 2008 is to communicate the Uniform California Earthquake Rupture Forecast (UCERF), Version 2 report, as well as to digitally preserve its contents and related materials. SCEC's digital library is supported by the University of Southern California (USC) Libraries system, from which assets and

metadata records are accessible to the public. An asset is a document or item that is to be digitally archived in one or many formats and is described by a metadata record. A metadata record is a brief overview that includes such information as a title, a short description, the author(s) name(s), keywords, etc. The process of creating a metadata record to archive an asset includes careful analysis of the asset's content, the extraction of the asset's key concepts, and the internal and external review necessary to preserve the integrity of the asset itself. The retrieval of pertinent information from an asset is required to prepare an accurate description of the document at hand. Also, a controlled vocabulary used to describe the assets is needed for consistency and precision. Internal review among the archiving individuals, as well as the collaboration with the authors of the assets and other persons familiar with the materials ensure an honest representation of the assets being digitally archived. The assets for which metadata records have been created for SCEC during the summer of 2008 include the UCERF main report, its appendices, tabular datasets, images, the SCEC-VDO software, the SCEC-VDO plug-ins, etc.

1-005
CAPTURING THE INTERN EXPERIENCE *Barber S, Whitesides A, Milner K, Tanner FL, and Flowers R*

The Undergraduate Studies in Earthquake Information Technology (USEIT), an internship program of the Southern California Earthquake Center (SCEC), brings together a variety of undergraduate students from around the nation in order to help communicate earthquake science and risk reduction. Each summer, the USEIT interns work in collaborative teams to tackle a scientific "Grand Challenge". The 2008 Grand Challenge presented was to communicate the value and content of the Uniform California Earthquake Rupture Forecast (UCERF) to end-users and the public at large. The ability to communicate this new information was facilitated by the production of a short educational film illustrating the processes and interactions between each of the intern groups. This seven minute film depicts an in-depth look into how the USEIT interns play a central role in enabling and furthering scientific research and education through group collaboration in a variety of projects, ranging from computer software development to digital archiving to animation. The interns primarily utilized software developed by previous interns called SCEC-VDO (SCEC Virtual Display of Objects), which has the ability to display earthquake-related objects and record animated movies. One of the major challenges faced was the acquisition of the materials necessary to carry out the technical aspects of the film, including camera equipment and editing hardware and software. In addition to this problem, there were also difficulties with time restraints, due to the shortened period of the USEIT program from 10 weeks to 8 weeks. However, the ability to create a project that will promote the USEIT interns and benefit the program was a great opportunity. Not only was this a remarkable learning experience, but also very exciting and rewarding.

1-006
SLUGVIEW: AN EFFICIENT 3-D POINT-CLOUD VISUALIZER *Steffeck MA, and Brodsky EE*

The SlugView application is used by the seismology group at UC Santa Cruz to manipulate and modify point-clouds. SlugView is written in Java and hardware-accelerated by OpenGL to create efficient 3-dimensional images of thousands or millions of points (point-clouds). The point-clouds we use are acquired with a ground-based LiDAR system that scans objects with an accuracy of up to 3mm. Our aim was to develop an application that is efficient, portable across different platforms, and easy to use.

The software rotates, edits, measures, and fits a plane to a point-cloud. Point-clouds are rotated around all three axes by using either the mouse or arrow keys. The user can zoom out to view the cloud at a great distance, or zoom in on an individual point. SlugView provides editing tools to crop away undesired features like trees and bushes. SlugView is able to interface with Matlab. From Matlab, SlugView can export a point-cloud as a matrix of Cartesian coordinates, or import a matrix as a point-cloud. The size of the point-clouds SlugView is able to handle is dependent on the workstation; however, we are currently using point-clouds ranging from a few thousand to nearly 100 million points.

The seismology group would like to distribute the beta version of SlugView 2.0 to anyone interested in having it. It can be downloaded at *www.pmc.ucsc.edu/~msteffec/*. Feedback from our users is welcomed and encouraged.

1-007
SEATREE: AN INTERACTIVE VISUAL ENVIRONMENT FOR EARTHQUAKE SCIENCE *Waterhouse HD, Milner KR, and Becker TW*

The goal of The Solid Earth Teaching and Research Environment (SEATREE) software is to provide a comprehensive and visually engaging tool for both researchers and students alike; it is a program for interdisciplinary solid Earth research collaboration as well as a teaching tool for the classroom. Modules implemented into the SEATREE framework include: HC-Flow Calculator, a mantle flow computational tool for spherical mantle circulation; Larry 2-D Tomography, a toolkit for performing 2-D, global, surface wave phase velocity tomography; and Syn2D, a synthetic 2-D seismic tomography tool.

The newest edition to SEATREE which we present here is the Python based NonLinLoc module, a non-linear earthquake relocation tool. With this new tool students can interactively learn how take-off angles, travel-times, and different velocity models affect the process of earthquake relocation, and more generally how they affect wave propagation. It also allows one to gain an understanding of the structure and patterns of seismicity of an area. By creating a graphical user interface that allows one to toggle the above mentioned parameters, one can visually see the affects on the images produced. Importantly, the SEATREE design philosophy is fully open source and allows looking "under the hood" for all modules. The underlying source code and scripts are provided for lower-level access for more experienced users. For visualization, we use MatLibPlot's sophisticated visualization method within the Python framework. As a research tool, we hope that our implementation of Anthony Lomax' NonLinLoc will help give us a better understanding of earthquake location uncertainty and so lead to an improved knowledge of fault mechanics.

1-008
REPRESENTATION OF PROBABILISTIC SEISMIC RISK MAPS THROUGH GOOGLE EARTH *Ryu H, Luco N, Martinez EM, and Smoczyk GM*

The development of probabilistic seismic risk maps was recently proposed (e.g., see 2006 SCEC Annual Meeting abstract by Luco and Karaca), through combination of ground motion hazard curves from the USGS National Seismic Hazard Mapping Project (*http://earthquake.usgs.gov/research/hazmaps/*) with seismic hazard-compatible building fragility models based, in part, on FEMA's HAZUS-MH earthquake model for loss estimation (*http://www.fema.gov/plan/prevent/hazus/*). The proposed risk maps showed mean annual frequencies (MAFs) of exceeding different structural damage states (none, slight, moderate, extensive, and complete) for each of thirty-six different generic building types (e.g., wood light frame, mid-rise

concrete shear wall, or high-rise steel frame) designed to four different code levels (high-, moderate-, low-, and pre-code).

In this effort, we make three significant improvements: First, we construct the probabilistic seismic risk maps in KML (Keyhole Markup Language) format, which is the file format used to display geographic data in Google Earth and Google Maps. Second, we incorporate new seismic hazard-compatible building fragility models (Ryu et al., 2008) that are derived using multilinear capacity (or "pushover") curves with negative stiffness after an ultimate (capping) point, as an alternative to the curvilinear curves provided in HAZUS. Third, we incorporate the new (2008) hazard curves from the USGS National Seismic Hazard Mapping Project. We display the risk maps in terms of probabilities of exceeding different structural damages states over a 50, 30, or 1-year planning horizon, assuming a Poisson distribution of damage state exceedance in time, with nine contour levels of probabilities from 0% to 100%.

As an interactive way to convey the seismic risk maps to both the general public and seismic engineers, we also construct a website (*http://earthquake.usgs.gov/research/hazmaps/risk/*). Using the website, one can get the pre-computed probabilistic seismic risk map corresponding to a selected combination of building height, construction material (e.g., wood, concrete, or steel), structural system (e.g., shear wall or frame), seismic design level, degree of building damage or loss, and planning horizon. We assist the user in making these selections, and the resulting risk map is automatically viewed in Google Earth. Future improvements to the risk maps and website are planned.

1-009
THE HALL OF GEOLOGICAL WONDERS - SOUTHERN CALIFORNIA'S NEW VENUE FOR EARTHQUAKE SCIENCE EDUCATION *Springer K, Sagebiel J, Scott E, and Valencia R*

The San Bernardino County Museum in Redlands, California, the largest museum in inland California, is currently building a 12,000 square foot three-story expansion called the Hall of Geological Wonders. The main objective is to teach about the region from a geologic perspective. The exhibits are united by a consistent emphasis on geology and geologic processes, as well as on science as an ongoing intellectual pursuit. The Hall of Geological Wonders is designed as a fully integrated educational experience, encouraging visitors to make connections: people to their environment; cultures to their natural heritage; science to life. All exhibits work in tandem with state and national K-12 curriculum standards, to ensure that the Hall provides pertinent, focused, rewarding educational experiences.

We devote significant space in the new Hall to explaining the evolution of southern California's landscape. Visitors will learn about the titanic geologic forces at work beneath their feet - forces that explain the shape of the Earth, its landforms and its sometimes violent nature and will recognize that these same forces have shaped their own region and beyond. The evolution of plate tectonics theory will be placed in the context of scientific discovery via the scientific method. The San Andreas Fault will be interpreted in a manner no other museum ever has attempted. The Hall is designed so that visitors will observe the San Andreas fault zone from our "Earth's Cylinder" – below ground in a re-created excavation of the fault, and above ground in the viewing tower. The viewing tower then segues to an immersive exhibit where the visitors will feel a simulated earthquake in a recreated mountain cabin in our "San Andreas Fault Earthquake Experience". Earthquake preparedness will be the theme of this exhibit. Partnering with SCEC, visitors will be encouraged to participate in the gathering of scientific data (Did You Feel It? and the Earthquake

Catcher Network) as part of the "faux" earthquake experience. Other exhibits will explore the San Andreas Fault, its causes and its effect on California geology, biology and culture. We will also present current research in earthquake science using interviews with a variety of scientists and engineers. The Hall will also be the only static educational venue whereby "The Great Southern California Shakeout" themes and information will remain readily available to the public, long after the exercise is completed.

1-010
EDUCATION FOR EARTHQUAKE DISASTER PREVENTION IN THE TOKYO METROPOLITAN AREA *Oki S, Tsuji H, Koketsu K, and Yazaki Y*

Japan frequently suffers from all types of disasters such as earthquakes, typhoons, floods, volcanic eruptions, and landslides. In the first half of this year, we already had three big quakes and a heavy rainfall, which killed more than 20 people. This is not just for Japan but Asia is the most disaster-afflicted region in the world, accounting for about 90% of all those affected by disasters, and more than 50% of the total fatalities and economic losses.

One of the most essential ways to reduce the damage of natural disasters is to educate general public to let them understand what is going on during earthquakes, typhoons, and so on. This leads individual to make the sound decision on what to do to prevent or reduce the damage. The Ministry of Education, Culture, Sports, Science and Technology (MEXT), therefore, offered for public subscription to choose several model areas to adopt scientific education to the local elementary schools.

ERI, the Earthquake Research Institute, is qualified by MEXT to develop education for earthquake disaster prevention in the Tokyo metropolitan area. The subduction of the Philippine Sea plate beneath this region causes mega-thrust earthquakes such as the 1703 Genroku earthquake (M 8.0) and the 1923 Kanto earthquake (M 7.9) which had 105,000 fatalities. A magnitude 7 or greater earthquake beneath this area is recently evaluated to occur with a probability of 70 % in 30 years. This is of immediate concern for the devastating loss of life and property because the Tokyo urban region now has a population of 42 million and is the center of approximately 40 % of the nation's activities, which may cause great global economic repercussion. To better understand earthquakes in this region, "Special Project for Earthquake Disaster Mitigation in Tokyo Metropolitan Area" has been conducted as a 4-year-project mainly initiated by ERI to develop a high-density network with 400 sites at local elementary schools. We start our education project by using the real seismographs observed at their own schoolyards, emphasizing the reality and causality of earthquake disaster.

1-011
STUDENTS AND TEACHERS FROM HIGH SCHOOLS FOR THE DEAF AROUND THE COUNTRY EXPLORE THE GEOLOGIC HAZARDS OF SOUTHERN CALIFORNIA
Cooke ML, Marshall ST, Dair L, Kendrick KJ, Morton D, Dolan JF, and de Groot R

Earth system students and teachers from 7 high schools around the US came to southern California May 4-10 for a field trip led by Cooke, a deaf geoscientist from the University of Massachusetts, Amherst. All the participating students on the trip conducted experiments on fault systems at their home schools using a deformational sandbox model developed by Cooke. The expedition gave the students a once-in-a-lifetime opportunity to apply knowledge gained from their classroom studies to actual sites in the field.

The theme for the California trip was "Geological Hazards and Society." The students, teachers, and geologists visited areas in the Lone Pine Canyon, Palm Desert, the San Bernardino Mountains,

Los Angeles, and the San Onofre and Laguna Beaches. At each site the students applied the same documenting techniques that professional geologists use when making site observations. They sketched in their notebooks, analyzed topographical maps, made interpretations of the structures, took photographs, and discussed details and patterns of rock formations with fellow participants. Geologists Katherine Kendrick, Doug Morton, Laura Dair, James Dolan and Scott Marshall modeled geologic inquiry and contributed greatly to the trip.

At the end of the week, the students summarized the data they collected during their trip related to their topic assignment, "Living with Landslides," "The San Andreas is Not the Only Fault in Town," or "How Much Shaking Can You Expect?" With the assistance of the geologists, they developed presentations to an assembly at the University High School in Irvine, California. Following the presentations, Dr. Bob DeGroot shared information on earthquake preparedness and on ShakeOut.

The Californian expedition was the third and final expedition led by Dr. Cooke. The first two trips explored faults in Utah and Massachusetts. Cooke included outreach to high school students in her NSF research grant as a way to encourage deaf and hard of hearing students to consider science careers. She wanted give opportunity for deaf students who use American Sign Language (ASL) to apply the same 3-D visual skills they use for communication to visualize geological formations in 3-D. She told the participants that the skills a geologist needs are good observation skills, the ability to think spatially, and, in 3-D, and the ability to imagine pictures in the mind. She has found in observations of deaf students who use ASL that there is a "natural fit between the visual skills geologists use and the skills of deaf learners."

1-012
SHAKEOUT AND PREPAREDNESS OUTREACH *Wilk AC*

This summer as a SURE intern in the SCEC main office, I was involved in the creation of an advertising and outreach campaign for the Great Southern California ShakeOut, as well as promoting earthquake preparedness and fielding public inquiries on both topics. Working with Mark Benthien, Jenny Gruen, Debbie Weiser, John Marquis, and many others, I assisted in the creation of various internet resources for the ShakeOut, including web presences on *www.facebook.com*, *www.myspace.com*, *www.bebo.com*, *www.linkedin.com*, and the official ShakeOut Blog (*http://www.greatsocalshakeout.org*). Through these websites, we were able to reach a new, primarily younger audience about the ShakeOut and the importance of preparedness. With over 5,000 hits to the blog and much more on the other sites created, the public gained insight into how the ShakeOut worked and what went into the planning. Updates on the planning of the ShakeOut in Steering Committee meetings were used in answering questions from the public as well as providing ideas for improving the blog and other web resources.

In addition to this, I also attended numerous public safety events, such as the ShakeOut KickOff at Caltech and a community fair in South El Monte, passing out copies of Putting Down Roots in Earthquake Country as well as registration forms for the ShakeOut. I also sent out thousands more of the Roots handbook through orders coming through the website, in order to prepare as many interested persons as possible.

1-013
WHAT WOULD A MAGNITUDE 7.8 FEEL LIKE? *Leeper RJ, and Perry-Huston LY*

As a member of the USGS's Multi-Hazards Initiative, this summer I developed a tool that will help southern Californians understand what it would be like to experience the M7.8 ShakeOut Scenario

earthquake at different intensities of shaking and distances from the fault. First, I gathered real earthquake footage from around the world. I attempted to ascertain exactly where the earthquake footage was taken in relation to the earthquake source. Then, I matched the footage location as precisely as I could to an intensity level on the USGS ShakeMap for the earthquake. Next, I matched the shaking intensity for the footage location with the intensities of the M7.8 scenario ShakeMap. The ShakeOut Scenario earthquake produces intensity levels IX & X near and far from the fault, and the types of seismic waves that cause these levels of intensity are of different frequency and duration. I wanted to capture all this variation. I obtained a lot of earthquake footage that depicted close-to-the-fault, high-frequency, short-duration shaking that resulted in intensity levels of IX & X, which I matched to near-fault locations in the ShakeOut Scenario. I also obtained earthquake footage that demonstrated low-frequency, long-duration shaking that resulted in intensity levels of I & II, which I matched to far off locations for the Scenario. However, footage taken far from the fault rupture that demonstrated low-frequency, long-duration seismic shaking of intensity levels of IX & X was very difficult to secure. After collecting and interpreting footage, I used Google Earth Pro and iMovie to bring it all together. Assisted Perry-Huston, I created a flyby movie in Google Earth Pro and edited it in iMovie, incorporating and narrating the earthquake footage I had collected from the Internet. This produced an accurate depiction of types of shaking that can be expected at various locations in the M7.8 Scenario earthquake. A future step will be to create an on-line database of the footage that includes earthquake parameters.

Community Modeling Environment (CME); Petascale Cyberfacility for Physics-Based Seismic Hazard Analysis (PetaSHA)

1-019

SUPPORTING SCEC PETASHAKE SIMULATIONS *Cui Y, Zhu J, Chourasia A, Olsen KB, Dalguer LA, Lee K, Davis S, Day SM, Juve G, Maechling PJ, and Jordan TH*

We have performed a set of very-large scale earthquake simulations on the San Andreas Fault on the TeraGrid computing resources, which used more than ten millions of NSF TeraGrid allocations over the past year. The simulations are a collaborative, inter-disciplinary research program coordinated by the Southern California Earthquake Center (SCEC) that makes extensive use of large-scale, physics-based, numerical modeling of earthquake phenomena. This is part of the USGS-led public earthquake preparedness exercise called ShakeOut exercise.

The SCEC AWP-Olsen based ShakeOut simulations were scientifically and computationally challenging for several reasons including: (1) the simulations were performed for a large (600km x 300km x 80km) geographical volume, (2) the simulations were run at high resolution (100m spacing on a regular grid resulting in 14.4 billion mesh points), and (3) in order to simulate the earthquake rupture more realistically, source descriptions based on dynamic rupture simulations (ShakeOut-D) using about ? million subfaults was used as a primary input to the wave propagation simulations. In addition, ShakeOut simulations with kinematic source descriptions (ShakeOut-K) were also carried out for code verification purposes and to compare ground motions computed for various level of complexity.

The simulations were coordinately executed on multiple TeraGrid systems, including the 504 Teraflops Ranger system at Texas Advanced Computing Center (TACC), and Datastar p655 at San Diego Supercomputer Center (SDSC). Additional SDSC Datastar fat nodes p690 and Blue Gene/L were used for pre- and post-processing of these capability simulations. A large part of a hundred terabytes of simulation outputs were registered directly from TACC disks to the SCEC digital library on SAM-QFS at SDSC, managed through SDSC's latest iRODs (integrated Rule-Oriented Data System). We aggressively optimized the iRODs transfer rate up to 135 MB/s, which is many times faster than previously recorded.

Visualization for SCEC ShakeOut-K and ShakeOut-D simulations were performed on site at TACC. Visualizations were created by color mapping the data then overlaying contextual information like freeways, fault lines and topography. Comparative side by side visualization for these two sets of simulations were also created. The visualization movies are available at *http://visservices.sdsc.edu/projects/scec/shakeout*.

1-020

SCEC CME AWP-OLSEN APPLICATION ENHANCEMENTS FOR PETASCALE COMPUTING *Cui Y, Kaiser TH, Zhu J, Lee K, Maechling PJ, Olsen KB, and Jordan TH*

The SCEC CME AWP-Olsen code has been through many optimizations over last few years to meet SCEC research requirements such as running earthquake simulations at 0.5Hz at the TeraShake scale. The recent SCEC ShakeOut exercise is performed at 1Hz, the computational requirement is 16x larger than previous TeraShake simulations. The increased input size, often exceeding one terabyte in size, adds additional challenge to the scalability, memory and fault tolerance of the

initialization. Further code enhancements are highly required to meet the novel challenges that emerge when running at the largest scales.

We ported and optimized the AWP-Olsen code for use on the 504 teraflops TACC's Ranger machine. Special algorithms have been implemented into the code for easy adaptation on different TeraGrid platforms, which proven to be highly effective for use. The optimizations are adjusted at run-time depending on system characteristics. Additional options are also added to selectively decimate the output spatially or/and temporally.

Scaling the reads of initial conditions is a challenging task due to its extraordinary size and highly discontinuous distribution. We have implemented MPI-IO for both source and media initialization. The parallelization and integration of these routines involves first determining the layout of the physical cells that describes physical velocity information and the sources that provide fault information to processors in a manner that can be used by the IO routines. Based on the pre-calculated information, linear abstract data types for both files are created. Each processor can access its local data linearly with the aforementioned customized MPI-IO data types. Temporal source partitioning for the source data has also been introduced to prevent a memory buffer overflow, which may occur when a large amount of source nodes are allocated in a single processor. The initial parallel mesh initialization has already shown a time reduction from previous 15 hours to less than minute. Further tests are under way for different compilers and large data sets.

Furthermore, we implemented an application-initiated check-pointing facility to prepare multiple-day ShakeOut-D mesh initialization on three SDSC BG/L racks. This IBM-based restart library feature is at system-level, where no application-level restart capability is available. This provided an initial insight of the type of fault tolerance feature needed for petascale computing.

1-021
SEARCHING FOR 3D WAVE-PROPAGATION EFFECTS IN SOUTHERN CALIFORNIA *Ely GP*

Ground motions in southern California can be significantly influenced by three-dimensional basin wave-propagation effects. Amplification due to focusing was observed in Santa Monica during the 1994 Northridge event. Simulations of large events on the southern San Andreas within the SCEC Community Velocity Model (CVM) find large amplifications at Whittier Narrows due to basin-guided waves. We have begun a study to search for similar basin effects in southern California, using a series 3D wave-propagation simulations over a suite of potential source scenarios. Selection of scenarios is being guided by the Uniform California Earthquake Rupture Forecast, as well as CyberShake--an effort to estimate probabilistic seismic hazard based on 3D simulations. Simulations will be performed up to 0.5 Hz using the Support Operator Rupture Dynamics (SORD) code and kinematic finite-fault sources, with fault geometry (often non-planar) from the SCEC Community Fault Model. Waves will be propagated through the SCEC-CVM as well as the SCEC-CVMH (Harvard version) with comparisons helping to address uncertainty in the basin effect results. Selected scenarios will recomputed with dynamic rupture sources.

1-022
WEBSIMS: A PYTHON-BASED WEB APPLICATION FOR STORING, EXPLORING AND DISSEMINATING 4D EARTHQUAKE SIMULATION DATA *Ely GP, and Olsen KB*

WebSims aims to provide a tool for cataloging, exploring, comparing and sharing four-dimensional results of large numerical earthquake simulations. Users may extract time histories or two-

dimensional slices via a clickable interface or by specifying precise coordinates. Extractions are plotted to the screen and optionally downloaded to local disk. Time histories may be low-pass filtered, and multiple simulations may be overlayed for comparison. Metadata is sored with each simulation in the form of a Pylab module. A well defined URL scheme for specifying extractions allows the web interface to be bypassed, thus allowing for batch scripting of both plotting and download tasks. This version of WebSims replaces a previous PHP implementation. It is written in Python using the NumPy, SciPy, and Matplotlib modules, which provide a MATLAB-like processing and visualization environment. The web pages are served by a web.py, a simple web application framework similar to Google App Engine. WebSims is open source and freely available, though not supported.

1-023
RUNNING MILLIONS OF SERIAL JOBS ON A CLUSTER USING WORKFLOWS: CYBERSHAKE 2008 *Callaghan S, Maechling PJ, Deelman E, Vahi K, Mehta G, Juve G, Milner KR, Graves RW, Field E, Okaya DA, and Jordan TH*

SCEC researchers use large-scale computational grid-based scientific workflows to perform seismic hazard calculations for the CyberShake project, part of SCEC's PetaSHA project. The scientific goal of CyberShake is to calculate physics-based probabilistic seismic hazard curves for locations in Southern California and combine the curves into a hazard map for the region. For each site of interest, the CyberShake processing includes two large-scale MPI calculations to create strain Green's tensors and a large number of embarrassingly parallel post-processing jobs to calculate intensity measures from possible events. These intensity measures are then processed into a hazard curve.

Our use of scientific workflows, which link the output of one job with the input of the next, enables a greater degree of automation and supports access to the grid tools needed to run and manage this kind of high-throughput calculation. CyberShake has been updated to include the UCERF 2.0 earthquake rupture forecast (ERF), as well as increased rupture variation in hypocenter location and slip distribution. As a result, the number of calculations per site increased by a factor of four, leading to workflows of nearly 1 million jobs. We have recently completed CyberShake seismic hazard curves for 9 sites utilizing large workflows, using the Pegasus Workflow Management System to execute the computations on local and national supercomputing resources. We discuss the advantages of using a grid-based, scientific workflow approach to this type of high-throughput computation. We describe the challenges we encountered and solutions we developed to obtain meaningful scientific results.

1-024
SCEC RESEARCH USING HIGH PERFORMANCE COMPUTING BY THE SCEC/CME COLLABORATION *Maechling PJ, Jordan TH, Archuleta RJ, Beroza GC, Bielak J, Chen P, Cui Y, Day SM, Deelman E, Graves RW, Minster JB, Olsen KB, and the SCEC/CME Collaboration*

The SCEC Community Modeling Environment (SCEC/CME) collaboration performs basic scientific research using high performance computing with the goal of developing a predictive understanding of earthquake processes and seismic hazards. SCEC/CME research is currently funded through two NSF awards, the NSF-EAR PetaSHA-2 project, and the NSF-OCI PetaShake projects. These two projects have complementary goals with PetaSHA-2 focusing on basic seismic hazard research and PetaShake focusing on increasing the scale and resolution of SCEC computational codes to use petascale supercomputers. SCEC/CME research areas including dynamic rupture modeling, wave propagation modeling, probabilistic seismic hazard analysis, and

full 3D tomography. SCEC/CME computational capabilities are organized around the development and application of robust, re-usable, well-validated simulation systems we call computational platforms.SCEC/CME research activities this year included the following. OpenSHA was used to calculate PSHA hazard curves and hazard maps using the new UCERF2.0 ERF and new 2008 attenuation relationships. Three SCEC/CME modeling groups ran 1Hz ShakeOut simulations using different codes and computer systems and carefully compared the results. The DynaShake Platform was used to calculate several dynamic rupture-based source descriptions equivalent in magnitude and final surface slip to the ShakeOut 1.2 kinematic source description. A SCEC/CME modeler produced 10Hz seismograms for the ShakeOut 1.2 scenario rupture by combining 1Hz deterministic seismograms with 10Hz stochastic seismograms. SCEC/CME modelers ran an ensemble of seven ShakeOut-D simulations to investigate the variability of ground motions produced by dynamic rupture-based source descriptions. The CyberShake Platform was used to calculate 10 new probabilistic seismic hazard analysis (PSHA) hazard curves using full 3D waveform modeling and the new UCERF2.0 ERF. Large-scale SCEC/CME high performance codes were run on NSF TeraGrid sites including simulations that use the full PSC Big Ben supercomputer (4096 cores) and simulations that ran on more than 10K cores at TACC Ranger. OpenSHA was ported onto an NSF supercomputers. The SCEC/CME group used scientific workflow tools to run more than 1.5 million jobs at NCSA for the CyberShake project. Visualizations produced by a SCEC/CME researcher of the 10Hz ShakeOut 1.2 scenario simulation data were used by USGS in ShakeOut publications and public outreach efforts.

Seismic Hazard and Risk Analysis (SHRA)

1-025

PRELIMINARY REPORT ON THE 29 JULY 2008 MW5.4 CHINO HILLS, EASTERN LOS ANGELES BASIN, CALIFORNIA, EARTHQUAKE SEQUENCE *Giveon M, Hauksson E, Hutton K, Kanamori H, Wei S, Hough SE, Felzer K, Given D, Sevilgen V, and Yong A*

The 29 July 2008 Mw5.4 Chino Hills earthquake was the largest event to occur within the greater Los Angeles metropolitan region since the 1994 Northridge earthquake. The earthquake was widely felt in a metropolitan region with a population of over 10 million people, and was recorded by hundreds of broadband and strong motion instruments. Preliminary analysis reveals that this event fits into a two decade long sequence of events in the northern Los Angeles basin.

The initial real-time SCSN moment tensor solution was determined using an automated analysis of waveforms from six stations. The moment tensor was also determined using the "cut-and-paste" technique, where we analyzed the broadband waveforms of regional seismograms from 22 stations with epicentral distances between 100 to 200 km and maximum azimuth gap of 32°. Both techniques yielded the same mechanism of oblique composite of thrust and left-lateral slip on an east-northeast or alternatively on a north-northwest striking plane. We relocated the mainshock and aftershocks, using a 3D velocity model and HypoDD. The relocations revealed three off-fault clusters and minimal clustering of aftershocks around either mainshock nodal plane. The first motion focal mechanisms of the two M>3 aftershocks exhibited strike-slip motion on the northwest or northeast striking nodal planes.

The 2008 Chino Hills earthquake sequence occurred in the depth range of 13 to 16 km, with low aftershock productivity, a large difference between ML and Mw, and a high mainshock stress drop revealing the state of stress at depth, near the brittle-ductile transition zone. Portions of the Whittier and Chino faults were likely brought closer to Coulomb failure by the mainshock. Felt ground motions appear to correlate with expected basin effects. All these attributes shed more light on the seismotectonic setting, ground motions, and state of stress of this region.

1-026

NONSTATIONARITIES IN THE CALIFORNIA CATALOG *Page MT, Alderson D, Doyle J, and Michael AJ*

We search for several types of nonstationarity in the ANSS California catalog. First, we search for one type of spatial nonstationarity, variation in maximum magnitude. In areas that have high seismicity rates and low maximum magnitudes there are some constraints on the maximum magnitude; we show that furthermore there is resolvable spatial variation in the maximum magnitude.

We also investigate seismicity near faults in the SCEC Community Fault Model. We search for anomalously large events that might be signs of a characteristic earthquakes distribution. We find a null result – seismicity near major fault zones in Southern California is well-modeled by a Gutenberg-Richter distribution, with no evidence of characteristic earthquakes is observed up to approximately magnitude 7.

Finally, we search for temporal magnitude nonstationarity in the California catalog. We investigate the magnitude autocorrelation function, which in the case of a stationary parent distribution should exhibit no significant deviations from zero. As expected, we find positive magnitude correlations at short time lags, which are likely the result of short-term aftershock incompleteness.

However, the degree of aftershock incompleteness is larger than expected. We find that the time interval for aftershock incompleteness given by Helmstetter et al. (2005) is too conservative for the largest events by a factor of approximately 10.

1-027
THE CAMARILLO FOLD BELT, SOUTHERN CALIFORNIA: AN ORDER OF MAGNITUDE YOUNGER THAN PREVIOUSLY THOUGHT *DeVecchio DE, Keller EA, Owen LA, and Fuchs M*

Deformation in the Camarillo Fold Belt (CFB) is an order of magnitude younger than previously thought and has rates of vertical uplift comparable to other studied fold belts in southern California. We integrate fifteen (15) new Optically Stimulated Luminescence dates (OSL), geologic mapping, GIS-based topographic analyses, and compile subsurface data to elucidated the relative timing of deformation on active faults, develop a chronology of deformed surfaces, and shed light on the landscape evolution in this part of the western Transverse Ranges. Our geochronology investigation of Q4 and Q5 sediments, previously mapped as Saugus Formation and thought to be no younger than 200 ka, indicates strata are as young as 23 ka and likely do not exceed 150 ka, in the CFB. Vertical uplift rates are estimated to be between 1 mm/yr. and 1.6 mm/yr. A maximum earthquake magnitude for the Simi fault is estimated to be Mw = 6.4.

Deformation of Q4 and Q5 occurs along segmented east-tending reverse faults that accommodate Pleistocene transpressional shortening. Fault segment boundaries are characterized by transverse tear faults and distinct changes in the structural geometry, magnitude, and timing of deformation. Geologic relations indicate that most of the active faults dip-steeply (~75°) and are characterized by Miocene normal displacement. GIS-based topographic analysis of hangingwall anticlines and subsurface data indicates a systematic westward decrease in erosion and structural relief across fault segment boundaries, indicating the onset of deformation in the CFB is migrating to the west. Additionally, transverse faults serve or have served as structural barriers to lateral growth of faults and folds in the study area and locally may act to limit the maximum earthquake rupture length and moment magnitude.

Younger deformed Quaternary units are manifested by an extensive erosion surface (Q3p) and aggradational event (Q2), which both correlate well to changes in late Quaternary global climate. Beveling of the Q3p pediment surface occurred between ~26-18 ka and is coeval with Oxygen Isotope Stage 2, while >20m of Q2 valley fill began accumulating at the Pleistocene-Holocene transition (~12 ka) and continued until ca. 4ka. Data from the San Gabriel Mts. and preliminary data from the Ojai Valley (Heermance personal comm.) suggests these landscape evolution events are regionally extensive and may be valuable geomorphic markers in southern California tectonic studies.

1-028
STATISTICAL FEATURES OF SHORT- AND LONG-PERIOD NEAR-SOURCE GROUND *Yamada M, Olsen AH, and Heaton TH*

Large earthquakes are infrequent, but when one does occur, it affects a large area. The frequency of large earthquakes should not be the sole consideration in engineering studies, rather the probability of a strong ground motion at a particular site must additionally include the large area affected by a large earthquake. This study collects recorded ground motions in the near-source region of earthquakes (sites less than 10 km from the surface projection of the rupture) with magnitudes greater than 6.0. We show that the marginal distribution of peak ground acceleration (PGA) is log-normally distributed, and the marginal distribution of the logarithm of peak ground

displacement (PGD) is approximately uniform on the range of recorded PGD. Since PGA saturates with magnitude, each large earthquake has approximately the same distribution of PGA. For a single earthquake, the distribution of PGD is approximately log-normal. The mean of the logarithm of PGD, however, increases linearly with magnitude, resulting in the approximately uniform marginal distribution for the entire data set. For example, near source ground displacements between 10 cm and 20 cm are approximately as equally likely as those between 100 cm and 200 cm. This study uses earthquake scaling arguments to provide a theoretical basis for the observed distribution of PGD. We expect that future records of near-source ground motions in large earthquakes will change the observed marginal distribution of PGD, but future records will not change the distribution of PGA.

1-029
SEMI-PROBABILISTIC VERSUS PROBABILISTIC IMPLEMENTATION OF NONLINEAR SITE FACTORS IN GROUND MOTION HAZARD ANALYSIS *Goulet CA, and Stewart JP*

It is common for ground motions to be estimated using a combination of probabilistic and deterministic procedures. Probabilistic seismic hazard analyses (PSHA) are performed to estimate intensity measures (IMs) for reference site conditions (usually rock). This is followed by a deterministic modification of the rock IMs to account for site effects, typically using site factors from the literature or seismic codes. We demonstrate for two California sites and three site conditions that the deterministic application of nonlinear site factors underestimates ground motions evaluated probabilistically for return periods of engineering interest. Reasons for this misfit include different standard deviation terms for rock and soil sites, different controlling earthquakes, and overestimation of the nonlinear component of the site response in the deterministic procedure. This problem is solved using site-specific PSHA with appropriate consideration of nonlinear site response, within the hazard integral.

1-030
CORRELATIONS BETWEEN AFTERSHOCKS PRODUCTIVITY AND REGIONAL CONDITIONS: OBSERVATIONAL TEST OF DAMAGE MODEL PREDICTIONS *Yang W, and Ben-Zion Y*

Aftershock sequences are commonly observed but their properties vary from region to region. Ben-Zion and Lyakhovsky (2006) developed a solution for aftershocks decay in a damage rheology model. The solution indicates that the productivity of aftershocks decreases with increasing value of a non-dimensional material parameter R given by the ratio of timescale for brittle deformation to timescale for viscous relaxation. The parameter R is inversely proportional to the degree of seismic coupling and is expected to increase primarily with increasing temperature, and also with increasing thickness of sedimentary cover. To test these predictions we use aftershock sequences from several southern California regions. We first analyze properties of individual aftershock sequences generated by the 1992 Landers and 1987 Superstition Hills earthquakes. The results show that the ratio of aftershock productivities in these sequences spanning 4 orders of event magnitudes is similar to the ratio of the average heat flow in the two regions. To perform stronger statistical tests we systematically analyze the average properties of stacked aftershock sequences in five regions. In each region we consider events with magnitudes between 4.0 and 6.0 to be mainshocks. For each mainshock, we consider events to be aftershocks if they occur in the subsequent 50 days, within a circular region that scales with the magnitude of the mainshock, and in the magnitude range between that of the mainshock and 2 units lower. This procedure produces 28-196 aftershock sequences in each of the five regions. We stack the aftershock sequences in each region and analyze the properties of the stacked data. The results indicate that the productivities of

the stacked sequences are inversely correlated with the heat flow and thickness of sedimentary cover, in agreement with the damage model predictions. Using the observed ratios of aftershock productivities along with simple expressions based on the damage model, we estimate the relative values of the material parameter R and seismic coupling coefficient in the different regions. The employed methodology for estimating the seismic coupling of fault systems can be useful for seismic hazard studies.

1-031
ELASTIC MODULI AND SEISMIC VELOCITIES IN A CHAUVIGNY LIMESTONE
Goebel T, Stanchits SA, and Shapiro S

Limestone as one of the most important reservoir rocks is subject to very different states of stress. This can be due to tectonic or stratigraphic reasons but also caused by anthropogenic influence. A big difference between geological processes and anthropogenic influence in settings and results is understandable. Human impacts on pre-existing stress fields happen in small time intervals. Changes of pressure can be abrupt and range from very small to extremely high values. Examples are found in reservoir exploitation, geothermal projects and CO2 induction in the subsurface. The examination (in terms of elastic Moduli, seismic velocities and deformation) of limestone's behaviour with pressure changes can be essential to interpret seismic data and explain rock development under changing conditions.

1-032
PHYSICS BASED PROBABILISTIC SEISMIC HAZARD CALCULATIONS FOR SOUTHERN CALIFORNIA *Graves RW, Callaghan S, Deelman E, Field E, Gupta N, Jordan TH, Juve G, Kesselman C, Maechling PJ, Mehta G, Okaya DA, and Vahi K*

Deterministic source and wave propagation effects such as rupture directivity and basin response can have a significant impact on near-fault ground motion levels, particularly at longer shaking periods. CyberShake, as part of the Southern California Earthquake Center's (SCEC) Community Modeling Environment, is developing a methodology that explicitly incorporates these effects within seismic hazard calculations through the use of physics-based 3D ground motion simulations. To calculate a waveform-based probabilistic hazard curve for a site of interest, we begin with Uniform California Earthquake Rupture Forecast, Version 2 (UCERF2) and identify all ruptures (excluding background seismicity) within 200 km of the site of interest. We convert the UCERF2 rupture definition into multiple rupture variations with differing hypocenter location and slip distribution, which results in about 400,000 rupture variations per site. Strain Green Tensors are calculated for the site of interest using the SCEC Community Velocity Model, Version 4 (CVM4), and then, using reciprocity, we calculate synthetic seismograms for each rupture variation. Peak intensity measures (e.g., spectral acceleration) are then extracted from these synthetics and combined with the original rupture probabilities to produce probabilistic seismic hazard curves for the site. Thus far, we have produced hazard curves for spectral acceleration at a suite of periods ranging from 3 to 10 seconds at about 20 sites in the Los Angeles region, with the ultimate goal being the production of full hazard maps. Our results indicate that the combination of rupture directivity and basin response effects can lead to an increase in the hazard level for some sites, relative to that given by a conventional Ground Motion Prediction Equation (GMPE). Additionally, and perhaps more importantly, we find that the physics-based hazard results are much more sensitive to the assumed magnitude-area relations and magnitude uncertainty estimates used in the definition of the ruptures than is found in the traditional GMPE approach. This reinforces the need for continued development of a better understanding of earthquake source characterization and the constitutive relations that govern the earthquake rupture process.

1-033
DISTRIBUTED COMPUTING AND MEMS ACCELEROMETERS: THE QUAKE CATCHER NETWORK *Cochran ES, Lawrence JF, Christensen C, and Jakka RS*

Recent advances in distributed computing provide exciting opportunities for seismic data collection. We are in the early stages of implementing a high density, low cost strong-motion network for rapid response and early warning by placing accelerometers in schools, homes, and offices. The Quake Catcher Network (QCN) employs existing networked laptops and desktops to form a dense, distributed computing seismic network. Costs for this network are minimal because the QCN uses 1) strong motion sensors (accelerometers) already internal to many laptops and 2) low-cost universal serial bus (USB) accelerometers for use with desktops. The Berkeley Open Infrastructure for Network Computing (BOINC!) provides a free, proven paradigm for involving the public in large-scale computational research projects. In the first six months of limited release of the QCN software, we successfully received triggers and waveforms from laptops near the M 4.7 April 25, 2008 earthquake in Reno, Nevada and the M 5.4 July 29, 2008 earthquake in Chino, California.

Engaging the public to participate in seismic data collection is not only an integral part of the project, but an added value to the QCN. The software will provide the client-user with a screen-saver displaying seismic data recorded on their laptop, recently detected earthquakes, and general information about earthquakes and the geosciences. Furthermore, this project will install USB sensors in K-12 classrooms as an educational tool for teaching science. Through a variety of interactive experiments students will learn about earthquakes and the hazards earthquakes pose.

1-034
COMPLETENESSWEB: AN ONLINE RESOURCE FOR SEISMIC NETWORK COMPLETENESS DATA *Schorlemmer D, and Euchner F*

Reliable estimates of the spatio-temporal evolution of detection completeness of seismic networks and the catalogs compiled by these networks are an essential prerequisite for almost any study in earthquake statistics. We present a new online resource for completeness data computed using the probability-based magnitude of completeness (PMC) method. Raw completeness data, datasets in plotting-friendly format, and maps of completeness magnitude and detection probabilities are available through a RESTful web service that is easy to consume from the command line. The raw data sets contain detection probabilities for a set of magnitude levels, and completeness magnitudes for different probability levels. They are encoded in an XML-based format. Spatial maps of these values are provided in publication-ready quality. The web service is accompanied by a web site providing a detailed method description, and codes and data sets which allow for reproducing the presented results, see completeness.usc.edu. Currently, completeness data of the Southern California Seismic Network for the years 2001-2007 are provided. Data of the Northern California Seismic Network, the Italian National Seismic Network, the Friuli Network (Italy), the Swiss Digital Seismic Network, and the Network of the Japanese Meteorological Agency are in preparation by different groups of researchers.

1-035
CREATING GLOBAL-SCALE SEISMIC HAZARD MAPS WITH OPENSHA AND PARALLEL COMPUTING *Milner KR, Meyers DP, Field E, Callaghan S, Ogale M, Juve G, Maechling PJ, and Jordan TH*

Using parallel computing resources at high performance computing (HPC) centers across the country, including USC HPCC, the National Center for Supercomputer Applications (NCSA), and

Purdue University, SCEC researchers and computer scientists were able to create probabilistic seismic hazard maps at very high resolution using Open Seismic Hazard Analysis (OpenSHA). OpenSHA is an open-source seismic hazard framework developed as a joint project between the Southern California Earthquake Center and the United States Geological Survey. While OpenSHA currently implements Earthquake Rupture Forecasts and attenuation relationships only for California, we were able to demonstrate that OpenSHA can scale-up computationally to the scale required to produce global hazard maps. We demonstrated this by discretizing California at a very fine level, resulting in over 1.6 million hazard curves, and calculating a very high-resolution PSHA hazard map for California. The number of curves in our very high resolution California PSHA maps is comparable to the number of curves required to produce a global hazard maps at 10 km spacing. Demonstrating this type of scalability is an essential step towards meeting the needs of the Global Earthquake Model (GEM) program's goal of generating uniform, worldwide seismic hazard maps.

It took almost 18,000 CPU hours to generate all 1.6 million curves, which we completed in 51 wall clock hours on 400 CPU cores (including overhead). The curves were calculated using the Working Group on California Earthquake Probabilities' 2007 Uniform California Earthquake Rupture Forecast (UCERF), an extremely computationally complex forecast that requires much more computation time than forecasts for other parts of the world. This suggests that a Global run could be computed in less CPU time using simpler models. One major achievement was making the hazard map creation workflow as portable and automatic as possible. In fact, it is just as easy to run the workflow at the University of Southern California's HPC cluster as it is on many of the clusters that are part of the National Science Foundation's TeraGrid grid infrastructure. The 1.6 million curve workflow was run on the National Center for Supercomputing Applications (NCSA)'s Abe cluster.

1-036
SEISMIC LOSS ESTIMATION BASED ON END-TO-END SIMULATION *Muto M, Krishnan S, Beck JL, and Mitrani-Reiser J*

Recently, there has been increasing interest in simulating all aspects of the seismic risk problem, from the source mechanism to the propagation of seismic waves to nonlinear time-history analysis of structural response and finally to building damage and repair costs. This study presents a framework for performing truly “end-to-end” simulation. A recent region-wide study of tall steel-frame building response to a M7.9 scenario earthquake on the southern portion of the San Andreas Fault is extended to consider economic losses. In that study a source mechanism model and a velocity model, in conjunction with a finite-element model of Southern California, were used to calculate ground motions at 636 sites throughout the San Fernando and Los Angeles basins. At each site, time history analyses of a nonlinear deteriorating structural model of an 18-story steel moment-resisting frame building were performed, using both a pre-Northridge earthquake design (with welds at the moment-resisting connections that are susceptible to fracture) and a modern code (UBC 1997) design. This work uses the simulation results to estimate losses by applying the MDLA (Matlab Damage and Loss Analysis) toolbox, developed to implement the PEER loss-estimation methodology. The toolbox includes damage prediction and repair cost estimation for structural and non-structural components and allows for the computation of the mean and variance of building repair costs conditional on engineering demand parameters (i.e. inter-story drift ratios and peak floor accelerations). Here, it is modified to treat steel-frame high-rises, including aspects such as mechanical, electrical and plumbing systems, traction elevators, and the possibility of irreparable structural damage. Contour plots of conditional mean losses are generated for the San Fernando and the Los Angeles basins for the pre-Northridge and modern

code designed buildings,allowing for comparison of the economic effects of the updated code for the scenario event. In principle, by simulating multiple seismic events,consistent with the probabilistic seismic hazard for a building site, the same basic approach could be used to quantify the uncertain losses from future earthquakes.

1-041
THE CALTECH VIRTUAL SHAKER *Krishnan S*

The Caltech Virtual Shaker is a web interface *http://virtualshaker.caltech.edu* to facilitate the sharing and exchange of end-to-end simulation research between various groups, and the transfer of end-to-end simulation technology to various stake-holders. The unique features of this interface are a building model database, a ground-motion database, and a the facility to remotely analyze structural models on the new Civil Engineering high-performance computing cluster (HPCC) at Caltech, GARUDA, dedicated for research into end-to-end simulations. Facilitating end-to-end simulations is a priority science objective for the Southern California Earthquake Center, and the portal will be an effective tool to help achieve this objective.

The web interface will consist of the following modules:

1. Ground motion database: Simulated ground motion waveforms from various scenarios will be archived in this database and will be available for remote analysis of structural models through the E-Analysis facility for use by structural engineers in evaluating the seismic performance of new construction.

2. Structural model database: One of the difficulties facing the structural engineering research community is the lack of detailed design information on existing building models. This database will collate and archive models of existing buildings as well as newly designed buildings accessible to the entire community to conduct structural engineering studies. The E-Analysis facility described below will provide the incentive for contributing structural models to this database. Models of buildings that get submitted for remote analysis using the high-performance computing cluster at Caltech will automatically be added to the database and will become publicly available for researchers to access. The database will thus be populated without the need for extensive solicitation.

3. E-analysis facility: This module will facilitate the remote analysis of structural models on the dedicated high-performance computing cluster for end-to-end simulations at Caltech. Registered users will be able to submit structural models for analysis under earthquake ground motion submitted by them or taken from the ground motion database. The analyses will be queued and carried out when enough processors become available. Upon completion, an email will be sent to the user with information on how to download the results. This facility will be made available to practicing engineers as well.

1-042
IS STRUCTURAL IRREGULARITY ALL THAT BAD? *Bjornsson AB, and Krishnan S*

In the computational simulation of a magnitude 7.9 San Andreas fault earthquake (similar to the 1857 Fort Tejon earthquake), two present-day 18-story steel moment-frame building models collapse at many locations under severe long-period, long-duration ground shaking in the San Fernando and Los Angeles basins. The collapse mechanisms at all these locations were quite similar and localized in a few stories in the bottom-third of the structure. This observation suggests the possibility of local retrofitting by the introduction of braces in a few selected stories, thus

preserving the architectural integrity of the structure to a large extent. However, such localized intervention may render the structure irregular (mass or stiffness irregularity, where there is a sudden jump or drop in stiffness or mass from one story to the next) which is been considered undesirable in current building codes. In this study, we investigate whether this widely-held view holds true universally, or whether there are some forms of irregularity that may actually be helpful in preventing tall building collapse under severe ground motion. Using the analogy of wave propagation in a shear beam, we develop various retrofitting schemes, and investigate them using state-of-the-art computational tools in structural engineering. We find that the most beneficial retrofitting scheme consists of introducing braces to only four stories in the bottom-third of the buildings, reducing the number of collapses under the simulated 1857 ground motions by 25%.

1-043
3-D MODELING OF BRACED STEEL STRUCTURES AND APPLICATIONS TO END-TO-END SIMULATIONS *Krishnan S*

A modified elastofiber (MEF) element for modeling braces and buckling-sensitive slender columns has been developed. It is a 5-segment version of the elastofiber element, developed recently for efficiently modeling nonlinearity in steel frame structures. It consists of three fiber segments, two at the member ends and one at mid-span, with two elastic segments sandwiched in between. The fiber segments are divided into 20 fibers in the cross-section that run the length of the segment. The fibers exhibit nonlinear axial stress-strain behavior. Member-end yielding and mid-span buckling, with fracture or rupture of fibers leading to complete severing of the brace, can be accurately modeled. The element has been integrated into the nonlinear analysis framework for the 3-D analysis of steel buildings, FRAME3D. It is validated with the help of data from three pseudo-dynamic experimental studies, two of them on struts, and one on a full-scale 6-story braced frame structure subjected to the 1978 Miyagi-Ken-Oki earthquake record.

In 2005 I collaborated with Professors Jeroen Tromp of Caltech, Chen Ji of the University California, Santa Barbara, and Dimitri Komatitsch of the University of Pau, to simulate a magnitude 7.9 earthquake on the San Andreas fault, with rupture initiating at Parkfield in central California and propagating southward a distance of about 290km. We computed the 3-component ground motions at 636 sites located on an uniform 3.5~km grid in southern California, and analyzed the response of two 18-story steel moment frame building models, one that of an existing building designed using the 1982 Uniform Building Code (UBC) which experienced fracture in the full-penetration welds of many beam-column connections during the Northridge earthquake, and the other that of the same building but redesigned according to the more modern 1997 UBC. The existing building is being redesigned using a lateral force-resisting system consisting of steel braced frames (instead of moment frames), and its region-wide response under the 1857-like San Andreas fault earthquake ground motions is being studied. The redesigned braced frame building is being modeled using FRAME3D with the braces modeled using the newly developed MEF element. Damage maps will be produced. The performance of the braced frame building will be compared against that of the moment frame version with particular emphasis on the nature of the collapse mechanisms in the two systems.

1-044
MEASURES OF GROUND MOTION TO PREDICT BUILDING RESPONSE *Olsen AH, and Heaton TH*

Spectral acceleration is a measure of ground motion commonly used to predict seismic building response. However, there may be other ground motion measures that better predict building response for different types of lateral force-resisting systems and for different severities of building

response. We consider pseudo-spectral acceleration (PSA), peak ground displacement (PGD), and peak ground velocity (PGV) as measures of long-period ground motions to predict the response of tall, steel moment-resisting frames (MRFs). The building responses of interest are: simulated collapse; total structural loss; and peak inter-story drift ratio, given that the building is not a total structural loss. We study steel MRFs of 6- or 20-stories, with either a stiffer, higher strength design or a more flexible, lower strength design. The welded moment-resisting connections have either sound or brittle welds. We perform a non-linear time history analysis of finite element models of each building in 75,000 simulated ground motions. A combination of PGD and PGV best predict collapse of steel MRFs. Depending on the building design, PSA or a combination of PGD and PGV best predict whether the building is a total structural loss. PSA alone best predicts the peak inter-story drift ratio, assuming the building is not a total structural loss.

ShakeOut

1-037

DELIVERING THE SHAKEOUT SCENARIO TO GOLDEN GUARDIAN *Perry SC, and Holbrook CC*

The ShakeOut Scenario earthquake study was developed to meet the needs of end users, particularly emergency management at Federal, State, and local levels, and the customization has continued after initial publication. The Scenario was released in May, 2008, to a key planning conference for November's Golden Guardian Exercise series. According to long-standing observers, this year's Golden Guardian event is the biggest and most ambitious of their experience. The scientific foundation has attracted a large number of participants and there are already requests to continue using the Scenario in 2009 exercises. Successful exercises cover a limited range of capabilities, in order to test performance in measurable ways, and to train staff without overwhelming them. Any one exercise would fail if it attempted to capture all of the complexity of impacts from a magnitude 7.8 earthquake. Instead, exercise planners have used the Scenario like a magnifying glass to identify risk and capabilities most critical to their own jurisdictions. Presentations by project scientists and a 16-page narrative provided an initial overview of the Scenario. However, many planners were daunted in attempts to extract details from the project's 300-page report, 12 supplemental studies, and 10 appendices, or in attempts to cast the reality into straightforward "events" to drive successful exercises. Thus we developed an evolving collection of documents that included an overview of how the earthquake would affect a specific jurisdiction such as a county or military base; a distillation of Scenario damages and consequences pertinent to that jurisdiction; and bullet lists of capabilities and situations to consider when planning exercises under this Scenario. Moreover, some planners needed realistic extrapolations beyond posited damages; others sought reality checks to uphold the science; yet others needed results in additional formats. Through all this, it was essential to maintain flexibility, allowing planners to adjust findings where appropriate (e.g., locations of smaller hazmat incidents), while indicating which aspects of the Scenario could not be tweaked (e.g., the physics of aftershock simulations). Thus we fielded questions, consulted in and out of meetings, and created a planners-only web site. The results of these efforts have been exercises that use a richer, more detailed set of scientific findings; and for future scenarios, an improved understanding of user needs.

1-038

HOPE FOR THE BEST, PREPARE FOR THE WORST: RESPONSE OF TALL STEEL BUILDINGS TO THE M7.8 SHAKEOUT SCENARIO EARTHQUAKE *Muto M, and Krishnan S*

Currently, there is a significant campaign being undertaken in southern California to increase public awareness and readiness for the next large earthquake along the San Andreas Fault, culminating in a large-scale earthquake response exercise. The USGS ShakeOut scenario is a key element to understanding the likely effects of such an event. A source model for a M7.8 scenario earthquake has been created (Hudnut et al. 2007), and used in conjunction with a velocity model for southern California to generate simulated ground motions for the event throughout the region (Graves et al. 2008). We were charged by the USGS to provide one plausible realization of the effects of the scenario event on tall steel moment-frame buildings. We have used the simulated ground motions with three-dimensional non-linear finite element models of three buildings (in two orthogonal orientations and two different connection fragility conditions, for a total of twelve cases) in the 20-story class to simulate structural responses at 784 analysis sites spaced at approximately 4 km throughout the San Fernando Valley, the San Gabriel Valley and the Los Angeles Basin. Based on the simulation results and available information on the number and

distribution of steel buildings, we have recommended that the ShakeOut drill be planned with a damage scenario comprising of 5% of the estimated 150 steel moment frame structures in the 10-30 story range collapsing (8 collapses), 10% of the structures red-tagged (16 red-tagged buildings), 15% of the structures with damage serious enough to cause loss of life (24 buildings with fatalities), and 20% of the structures with visible damage requiring building closure (32 buildings with visible damage and possible injuries).

Hudnut, K.W., L.M. Jones, and B.T. Aagaard (2007), "The Southern California ShakeOut Scenario, Part 1: Earth Science Specification of a Big One," Annual Meeting of the Seismological Society of America. Abstract reference number 07-501.

Graves, R., B. Aagaard, K. Hudnut, L. Star, J. Stewart, and T. Jordan (2008), "Broadband Ground Motion Simulations for a Mw 7.8 Southern San Andreas Earthquake," manuscript in preparation.

1-039

MULTI-HAZARD DEMONSTRATION PROJECT: SEISMICALLY INDUCED LANDSLIDE HAZARD ANALYSIS AND POTENTIAL DAMAGE TO LIFELINE CROSSINGS FOR THE MW 7.8 SOUTHERN SAN ANDREAS EARTHQUAKE SCENARIO *Wilson RI, McCrink TP, Treiman JA, and Silva MA*

As part of the scenario Mw 7.8 earthquake on the San Andreas Fault (Multi-Hazard Demonstration Project), the California Geological Survey (CGS) analyzed potential seismically induced landslides in four transportation and utility lifeline corridors for Southern California: Cajon Pass, San Gorgonio Pass, Highway 14 near Palmdale, and Interstate 5 near Pyramid Lake. Although site-specific geotechnical data were limited in all areas, CGS's familiarity with the geologic and topographic conditions in similar Southern California settings provided background for analysis. Our assessment consisted of: 1) compiling landslide inventories within the focus areas, 2) performing pseudo-static slope stability and deformation (Newmark displacement) analyses on the interpreted "worst case" locations of landslides and landslide prone areas, and 3) estimating the style and magnitude of ground failure and its resulting damage to lifelines in the focus areas. Results from analyses indicate that slope failures will be common in three of the four lifeline corridor areas due to the prevalence of steep slope conditions, weak geologic formations, and extremely high ground shaking levels. For some existing landslides Newmark displacement values were calculated to be well over one-meter, which increases the potential for those landslides to change behavior from a sliding block to a flow-type failure. Such failures could inflict considerable damage to lifelines because of their increased internal disruption and long run-out distances. It is estimated that damage caused by landslides, especially in the Cajon Pass and San Gorgonio Pass areas, could take weeks or months to repair assuming full access and resources are available.

1-040

DIGITAL MAP LAYERS OF LIQUEFACTION AND LANDSLIDE SUSCEPTIBILITY FOR THE SOUTHERN CALIFORNIA REGION IMPACTED BY THE SHAKEOUT SCENARIO EARTHQUAKE *Ponti DJ, and Tinsley JC*

In order to evaluate regional liquefaction and landslide hazards caused by the ShakeOut scenario earthquake, it was necessary to build a consistent set of digital map layers of ground failure susceptibility for the entire 8-county study area. These layers consist of: (1) a 5-category liquefaction susceptibility map; (2) two landslide susceptibility maps (for saturated and dry conditions) that use 10 m slope-angle data specially derived for this study; and (3) an autumn time-period depth-to-water-table map. These data can be readily imported into HAZUS-MH MR3 and

are an important step in the development of a complete and consistent set of updatable data layers for evaluating geologic hazards in southern California at regional and sub-regional scales.

Susceptibility maps classify surficial geologic materials based on the likelihood that the materials will undergo liquefaction and ground failure in an earthquake. We used geologic maps from 43 sources that represent the best regional geologic mapping available and supplemented these maps locally with airphoto interpretation. Because digital large- to medium-scale maps do not cover the entire 8-county study area, we started with the 1:250,000-scale materials map of Wills and Clahan (2006) and supplanted these data with higher resolution maps in the urbanized areas where ground failure would most likely affect the built environment. For liquefaction, the map units were assigned to five susceptibility classes, following the system presented by Youd and Perkins (1978). For landslides, the units were binned into 3 classes and then intersected with slope data to produce a 10-category assignment modified from Wilson and Keefer (1985). The map of the water table was constructed using measurements at over 37,000 localities and binned into 10 depth classes. In practice, the process of translating geologic map units into corresponding susceptibility classes is difficult because many geologic map units do not adequately reflect the depositional environments and material properties that are critical to inferring susceptibility. Where classification was ambiguous, we tended to classify conservatively so as not to underestimate any potential hazard. Following classification, any differences that may have been present across map boundaries were reconciled using expert judgment in order eliminate any major map boundary discontinuities.

1-045
SHAKEOUT SIMULATIONS: VERIFICATION AND COMPARISONS *Bielak J, Graves RW, Olsen KB, Taborda R, Ramirez-Guzman L, Day SM, Ely GP, Jordan TH, Maechling PJ, Urbanic J, Juve G, and Roten D*

For the past three years we have presented results of several large-scale earthquake simulations run by different research groups, but our verifications have been limited to qualitative comparisons. This work presents a preliminary verification of three simulation sets for the ShakeOut earthquake scenario, version 1.1, an Mw 7.8 earthquake on a portion of the San Andreas fault in southern California. Two of the simulation sets use a finite difference approach while the third one uses finite elements. The verification is done in a quantitative manner by means of the goodness-of-fit criteria proposed by Anderson (2004) and the misfit criteria proposed by Kirstekova et al. (2006). The results indicate good agreement between the three implementations and the metrics of the comparisons for ten selected locations throughout the region signal that the agreement can be regarded as excellent according to the scale defined by Anderson. All three groups used a common discrete representation of SCEC's Community Velocity Model (CVM, version 4). Discrepancies observed among the different synthetics are associated to intrinsic differences between the numerical methods used and their implementation by each simulation group. We conclude that the three schemes are consistent, reliable, and sufficiently accurate for future large-scale simulations.

1-046
SHAKEOUT-D: GROUND MOTION ESTIMATES USING AN ENSEMBLE OF LARGE EARTHQUAKES ON THE SOUTHERN SAN ANDREAS FAULT WITH SPONTANEOUS RUPTURE PROPAGATION *Olsen KB, Day SM, Dalguer LA, Cui Y, Zhu J, Mayhew JE, Maechling PJ, Jordan TH, Chourasia A, and Okaya DA*

We simulate ground motion in southern California from an ensemble of 7 spontaneous rupture models of large (Mw7.8) northwest-propagating earthquakes on the southern San Andreas fault (ShakeOut-D). Median rock-site 3 sec spectral accelerations follow the Next Generation

Attenuation (NGA) empirical relations very closely (i.e., within roughly their epistemic uncertainty) over the distance range 2-200 km, and intra-event standard deviations are very close to the empirical values over the distance range 0 and 50 km. The simulations predict entrainment by basin structure of a strong directivity pulse, with long-period spectral accelerations in Los Angeles and Ventura basins significantly larger than those predicted by the empirical relations. The ShakeOut-D ground motion predictions differ in some important respects from a recent kinematically parameterized simulation of a geometrically similar scenario: (1) the kinematic rock-site predictions depart significantly from the common distance-attenuation trend of the NGA and ShakeOut-D results, and (2) ShakeOut-D predictions of long-period spectral acceleration within the basins of the greater Los Angeles area, including those with concentrations of high-rise buildings, are lower by factors of 2-3 than the corresponding kinematic predictions. The latter result agrees with the results from a previous comparison of kinematically and dynamically parameterized simulations of Mw7.7 San Andreas scenarios (TeraShake). As in the previous study, we attribute the difference to reduced forward directivity due to the less coherent wavefield excited by the spontaneous-rupture sources.

1-047

IMPLICATIONS OF THE SHAKEOUT SOURCE DESCRIPTION FOR RUPTURE COMPLEXITY AND NEAR-SOURCE GROUND MOTION *Dalguer LA, Day SM, Olsen KB, Cruz-Atienza VM, Cui Y, Zhu J, Gritz A, Okaya DA, and Maechling PJ*

With the goal to evaluate the implications of the source description of the SoSAFE ShakeOut scenario for the rupture and ground motion, we developed a diversity of large-scale dynamic models in the Southern San Andreas fault. Four classes of models are considered: Each of the first three classes incorporates stochastic irregularities in the stress drop compatible with seismological observations, combined with some degree of constraint on the long-wavelength component of slip: (i) Models that have stress drop preconditioned such that Mw and final surface slip approximate the corresponding moment and slip-profile (or background slip) distribution along the strike of the fault specified for ShakeOut by Hudnut et al. (2008). (ii) Models preconditioned so as to the depth-averaged slip matches the slip-profile specified by Hudnut et al. and such that they match Mw as well (iii). Models that match the ShakeOut Mw only. The constraints were imposed using a slip-matching technique that iteratively performs kinematic and dynamic rupture simulations to find stress drop distribution that yields the prescribed ShakeOut static slip characteristics. We also investigated a fourth class of model based on simple asperities following the rules proposed by Dalguer at al., 2008, BSSA, and matching only the fault dimensions of ShakeOut (notice that by simply using this rule, the Mw also approximates the ShakeOut Mw). The class (i) and class (ii) models each have two well-defined patches of high stress drop at the extremes of the fault, corresponding to the a priori slip constraints from the ShakeOut scenario. All the fault models are planar faults, and each dynamic model is the first step of a two-step procedure to calculate ground motion for the ShakeOut scenario (see the poster of Olsen et al). Here we examine the rupture complexity and the qualitative ground motion characteristics of these models, referring to the poster of Olsen et al. for quantitative details of the ground motion estimates. All the models generate the strongest ground motion next to the fault, driven mainly by deep patches of high stress drop. Qualitatively, we note that the class (iii) and (iv) models are apparently more efficient in exciting the San Gabriel and Los Angeles basin areas than are the slip-constrained class (i) and (ii) models, probably because the slip distribution imposed on the latter models is not optimal for exciting the guided-wave channel between San Andreas fault and Los Angeles basin.

1-048

SOCIAL AND ECONOMIC LOSSES EXPECTED FROM A LARGE EARTHQUAKE ON THE SOUTHERN SAN ANDREAS FAULT: A COMPARISON OF ESTIMATES BASED ON DYNAMICALLY-DERIVED VERSUS KINEMATICALLY-DERIVED SHAKEOUT SCENARIOS *Mayhew JE, and Olsen KB*

Olsen et al. (this volume) simulated ground motion in southern California from an ensemble of 7 spontaneous rupture models of large (Mw7.8) northwest-propagating earthquakes on the southern San Andreas fault (ShakeOut-D). Due to the less coherent wavefield excited by the spontaneous-rupture sources, ShakeOut-D predictions of long-period spectral acceleration within the basins of the greater Los Angeles area were lower by factors of 2-3 than the corresponding kinematic predictions (ShakeOut-K). Here, we estimate the differences in social and economic losses for ShakeOut-D and ShakeOut-K using HAZUS-MH. We generated the Shake maps required for calculations in HAZUS-MH with the assumption that PGA and spectral acceleration values are proportional to the PGV values calculated from ShakeOut-D and ShakeOut-K. This proportionality was gained by ratios between attenuation relationships of PGVs versus PGAs and spectral accelerations at the given distances from the fault and site specific Vs30 values (Boore and Atkinson, 2008, based on three Vs30 values: 300, 760, and 1300 m/sec). Our results are strikingly different for the ShakeOut-D and ShakeOut-K scenarios. For example, we find that the direct economic loss predictions from building and lifeline damage for ShakeOut-K (~$132.4 billion) are significantly higher than those predicted from ShakeOut-D (~$18.7 billion). Only 3,787 buildings (~3% of total inventory) incur complete irreparable damage from ShakeOut-D as compared to 46,125 (~18%) from ShakeOut-K. ShakeOut-D predictions indicate that 32,913 homes will be without electricity after 7 days and 838,876 homes without potable water, while the numbers for ShakeOut-K are 650,655 and 4,529,232, respectively. ShakeOut-D predicts 34 - 131 fatalities dependent on the time of day, as compared to 883 – 3,545 for ShakeOut-K. In summary, due to differences in ground motion levels, the expected social and economic losses due to a Mw 7.8 northwest-propagating earthquake on the southern San Andreas fault for our dynamically-derived sources (ShakeOut-D) are significantly smaller than those estimated for the kinematically-derived source (ShakeOut-K). Thus, while the HAZUS estimates are associated with a large uncertainty, the details of the source description appears to be a key ingredient to obtain the most reliable estimate of the social and economic impact in southern California from the next large earthquake on the San Andreas fault.

Ground Motion Prediction (GMP)

1-049

BROADBAND GROUND MOTION SIMULATION OF THE 07/29/08 MW 5.4 CHINO HILLS EARTHQUAKE *Graves RW*

The July 29, 2008 Mw 5.4 Chino Hills earthquake was an oblique-slip event occurring at a depth of about 14 km. The SCSN moment tensor solution gives the best fitting double couple solution as: strike=291, dip=59, rake=142 and Mo=1.53e+24 dyne-cm. In the epicentral region, observed PGA and PGV values were around 0.4 g and 37 cm/s, respectively. I simulate the broadband (0-20 Hz) waveforms for this event using the methodology of Graves and Pitarka (2004). At low frequencies ($f < 1$ Hz) the computation is purely deterministic and uses a 3D anealsitic FD simulation code with the SCEC CVM4. At high frequencies ($f > 1$ Hz), the computation uses a semi-stochastic representation of source and wave propagation effects. For the FD model, I used a grid spacing of 125 m and a minimum shear velocity of 620 m/s. To account for the lower near surface shear velocities, a frequency dependent amplification function is applied to simulations on a site-by-site basis. These amplification functions are based on the site-specific values of Vs30 (Wills et al., 2000). The simulation covers a 125 km by 250 km region of Southern California and broadband three-component waveforms are calculated on a 1 km mesh over this region, resulting in about 32,000 sites.

Using a simple point source model with the 3D SCEC CVM4 velocity structure produces a reasonable fit to the recorded motions for frequencies less than 1 Hz, and matches the general characteristics of the broadband motions. At a number of basin sites, the simulation reproduces later arriving pulses that are seen in the data, and which are presumably due to basin generated phases. The point source simulation predicts stronger motions to the north and east of the epicenter than are seen in the recorded data.

The fault area for this Mw 5.4 event is probably on the order of about 20 – 25 km2 (roughly 5 km by 5 km). In the epicentral region, and for frequencies around 1 Hz, the point source approximation is probably not fully justified. Given a 5 km by 5 km finite-fault with strike=291 and dip=59, I consider another possible scenario where the rupture begins at the deep eastern end of the fault and then ruptures updip toward the southwest. The finite-fault simulation produces a slight westward shift of the peak motions compared to the point source result, which is more consistent with the observed pattern.

1-050

EARTHQUAKE GROUND MOTIONS RECORDED AT THE FACTOR BUILDING AT UCLA *Hauksson SE, and Kohler MD*

We have analyzed ground motions recorded in the steel, moment-frame Factor building at UCLA from nearby earthquakes. After the 1994 Northridge earthquake, accelerometers were installed on every floor either at the mid-sections or corners of the building. We have used two methods for analyzing the recorded building motions. First, we created 2D animations of the building shaking as observed from four unique points of view. We have uploaded the highest-quality animations for public view on the website factor.gps.caltech.edu. The animations show time-varying horizontal displacements as recorded at each sensor in the building. They are played back at true-time speed and amplified to provide visible building shaking. Second, we have analyzed the rocking of the building for several of the strongest earthquakes. Two accelerometers each in the basement and subbasement detect vertical motions. We computed rocking as the difference between vertical motions on the east and west walls, and between motions on the north and south walls. Rocking

motions can potentially occur during strong ground shaking as the result of the soil being much softer than the building foundation. The vertical motion is characterized by spectral peaks at 0.71 Hz, 0.82 Hz, 1.1 Hz, and higher. These are larger than the first few modes of horizontal vibrations. Computing the spectral ratios between the top floor and basement for evidence of soil-structure interactions is a topic for further research. We also analyze the peak rocking motion as a function of earthquake distance and magnitude.

1-051
"RUPTURE-TO-RAFTERS" SYNTHETIC GROUND MOTIONS AND THE ROLE OF NONLINEAR SITE RESPONSE PREDICTIONS *Asimaki D, and Li W*

Overarching goal of our research is to develop quantitative criteria that will allow efficient integration of site response models in broadband ground motion simulations. For this purpose, we combine downhole array observations and broadband ground motion synthetics and study the prediction sensitivity of ground surface motion and nonlinear structural performance due to the bias and uncertainty in nonlinear site response simulation. This work focuses on three downhole arrays in Southern California installed at medium to soft soil sites, where we have evaluated broadband synthetics based on the regional geology and fault systems for finite-source dynamic rupture scenarios of weak, medium and large magnitude events (M = 3.5~7.5), on a surface station grid of epicentral distances 2km~75km. For each site, we conduct elastic and nonlinear analyses using multiple soil models, and first estimate the modeling ground motion variability by means of the COV (coefficient of variation) of site amplification. For each model, we then assess the parametric uncertainty of ground motion predictions by systematically randomizing selected input parameters. Based on our results, we develop a frequency index, which, combined with the ground motion intensity, is used as a quantitative measure to describe the site and ground motion combinations where the nonlinear models show large prediction COV, namely where incremental nonlinear analyses significantly deviate from empirical methodologies. We finally illustrate the role of nonlinear soil response simulation in physics-based seismic hazard predictions by subjecting a series of inelastic SDOF (single-degree-of-freedom) to the ensemble of ground motion predictions obtained via the alternative site response methodologies. The bias and uncertainty in the structural response predictions is also evaluated as a function of the frequency-intensity criteria proposed in this work, to quantify the propagation of site response modeling variability to the assessment of structural performance measures in rupture-to-rafters simulations. Our results show that large sensitivity in the selection of site response methodology yields high bias and uncertainty in the assessment of the inelastic displacement ratio for nonlinear structural response predictions, indicating the efficiency of the proposed criteria for the optimal selection of site response model.

1-052
COMPARISON OF MEASURED VS30 VALUES AGAINST VS30 PREDICTIONS BASED ON TOPOGRAPHIC SLOPE *Pancha A, Louie JN, Yong A, Thompson M, and Dhar M*

Independently, geology and topographic slope have been used as predictors of shallow shear wave velocity (Vs30 or the average shear-wave velocity in the upper 30 meters) for seismic hazard assessment. In the former approach, dominant grain size within site-response units have been observed to correlate to variations in shallow Vs30 (e.g., Borcherdt 1970; Tinsley & Fumal, 1985; Fumal & Tinsley, 1985; Wills et al., 2000; Wills & Clahan, 2006). In the latter approach, topographic slope has been introduced as a correlative to Vs30, which can be easily computed from readily available DEMs to provide first-order maps of site conditions (Allen & Wald, 2007; Wald & Allen, 2007). These maps predict shallow shear-wave velocity on the basis of Vs30 and slope correlations. We compare results from 509 sites having observed Vs30 measurements acquired through the refraction microtremor surface-wave dispersion analysis method, against the predicted Vs30 from

Wald & Allen (2007). Our measurements were taken at 509 sites in California and Nevada. Most of the southern California measurements (188 sites) were taken along the San Gabriel River (Thelen et al., 2006) and were used by Wald & Allen (2007) in their regressions. An additional 96 sites were measured as a part of smaller studies in other parts of California. In Nevada, 109 sites were measured in the Reno basin affected by fluvial, alluvial, lacustrine, and tectonically-driven processes. On the basis of our Reno observations, the low correlation between Vs30 and slope we interpret to be influenced by the complexity of landscape evolution and less by topographic slope alone. Measurements in southern Nevada (116 sites) were influenced by the caliche development that dominates local soil development. Here, higher velocities are observed where topographic slope is lowest, contrary to the Wald & Allen (2007) model. Our analysis finds that 67% of our Vs30 measurements (338 of 509) lie outside ±20% of the predicted values based on topographic slope. The RMS topographic prediction error is 161 m/s, or 45% of the measured Vs30. These results suggest that the Wald & Allen (2007) first-order approach based on slope is not able to reliably predict measured Vs30 values in regions of complex geology. Our results also highlight the inherent variability of shallow shear-wave velocity in complex environments and the need for more detailed Vs30 measurements to determine more refined predictive methods for microzonation.

1-053
CALCULATING THE SOURCE SENSITIVITY OF BASIN GUIDED WAVES BY TIME-REVERSED SIMULATIONS *Day SM, Roten D, and Olsen KB*

Simulations of earthquake rupture on the southern San Andreas fault (e.g., TeraShake; ShakeOut) reveal large amplifications associated with channeling of seismic energy along contiguous sedimentary basins. Geometrically similar excitation patterns can be recognized repeatedly in different SAF simulations (e.g., Love wave-like energy with predominant period around 4 seconds, channeled southwestwardly from the San Gabriel basin into Los Angeles basin), yet the amplitudes with which these distinct wavefield patterns are excited differ, depending upon source details (slip distribution, direction and velocity of rupture).

To improve understanding of the excitation of the high-amplitude patterns, we propose a numerical method for determining the sensitivity of a given wavefield pattern (i.e., one identified in a simulation, such as the above-cited sedimentary channeling effect identified in the ShakeOut simulations) to perturbations of the source kinematics. We first define a functional (phi(u), where u is the wavefield perturbation) that isolates the wavefield feature of interest and is proportional to its level of excitation. We then calculate the pullback of that functional onto the source by means of a single time-reversed (i.e., adjoint) simulation. The resulting functional (G*phi) now acts on the space of sources (slip functions) rather than wavefields, so given any source perturbation, we can calculate the resulting feature excitation without actually doing any forward wavefield simulations. In practice, the kernel of the pulled-back functional G*phi itself gives much insight into the feature-excitation sensitivity, and the time-reversal simulation itself helps ellucidate the wave propagation process leading to the wavefield feature in question.

We applied this method to analyze the source sensitivity of the San Gabriel/Los Angeles channeled wave seen in ShakeOut simulations, finding: (i) Excitation is relatively insensitive to slip on the southernmost ~60 km long segment of the SAF (between Bombay Beach and Indio). (ii) Excitation is highly sensitive to slip on the ~100 km long SAF segment between Indio and San Bernardino, but only when the rupture is toward the NW, and especially when rupture velocity is near the maximum S wavespeed. (iii) Excitation is very insensitive to slip on the SAF north of San

Bernardino, regardless of rupture direction. We successfully verified these interpretations through direct (forward time) simulations of ground motion.

1-054
DYNAMIC RUPTURES FROM SIMULATIONS OF LONG-TERM SLIP HISTORIES: A FEASIBILITY STUDY *Mai PM, Song S, Hillers G, Pitarka A, Dalguer LA, and Ampuero J*

One of the key questions in seismic-hazard driven research on ground-motion prediction and earthquake source dynamics is how to generate rupture models that are consistent with observed source complexity. Ideally, we would like to be able to generate hundreds of physically self-consistent source models for ground motion calculation whose occurrence in space and time reflects the basic observations of earthquake scaling and earthquake statistics, and whose rupture characteristic show the spatio-temporal heterogeneity of past earthquakes. To this end, we examine how 3D-simulations of long-term slip histories on 2D-faults with spatial variation in rate-and-state parameters can be used to construct input models for spontaneous dynamic rupture calculations.

Starting from an existing catalog of model-quakes with more than 1,500 events in the magnitude range 4.7 <= Mw <= 7.3, obtained from simulating long-term slip histories governed by rate-and-state-friction (RS) with spatially variable RS-parameters (Hillers et al., 2006, 2007), we construct dynamic models using a simple slip-weakening framework. We investigate several approaches to derive dynamic input parameters (i.e. strength excess and slip-weakening distance) that promote sustained dynamic ruptures. For a total of ~170 models, we perform dynamic rupture calculations, and then investigate the nucleation and early propagation behavior, evaluate the sustained-rupture stage (rupture speed and its variations) and the rupture arrest (abrupt termination versus smooth rupture cessation). We also examine the local slip-velocity functions to detect subtle differences in rupture speed, peak-slip velocity and general shape of the slip-function which affect the seismic radiation and the resulting near-field ground motions.

1-055
EXPLORING SPATIAL COHERENCE IN KINEMATIC AND DYNAMIC EARTHQUAKE RUPTURE MODELS *Song S, Pitarka A, and Somerville P*

Understanding coherence that may be embedded in kinematic motions of earthquake rupture is an essential element not only in understanding earthquake source characteristics, but in developing effective source modeling tools for strong ground motion prediction. We investigated spatial coherence between earthquake source parameters by analyzing both kinematic and dynamic rupture models. The coherence is considered not only at the same point (zero offset), but in neighboring areas (nonzero offset), by adopting the coherence analysis method of 2D spatial data, which is commonly used in Geostatistics. Our results show that earthquake slip has a significant level of correlation with temporal source parameters such as rupture velocity, peak slip rate, and slip duration (or rise time) in both kinematic and dynamic rupture models. This coherence pattern shows interesting decay patterns as the nonzero offset distance increases. Many interesting features of earthquake source characteristics, such as directional effects of earthquake rupture, can be captured by spatial coherence analysis, in particular, in 2D spatial coherence analysis. For instance, the correlation maximum can be located away from the zero offset, i.e., large slip may generate faster rupture velocity ahead of the current rupture front rather than at its current location, which may be an important characteristic of rupture directivity effects. Our simple kinematic inversion tests show that spatial coherence may be used in examining the robustness of kinematic source inversion methods by keeping track of how the inversion distorts or preserves the coherence originally embedded in kinematic motions of earthquake rupture. This type of coherence analysis

may provide the potential for improved understanding of earthquake source characteristics, and how they control the intensity and variability of near-field strong ground motions.

1-056
A TIME-REVERSED RECIPROCAL METHOD FOR DETECTING WELD FRACTURES IN CIVIL STRUCTURES *Kohler MD, and Heaton TH*

The 1994 Northridge earthquake highlighted a common type of structural failure, fractured welds in beam-column connections, that is difficult to identify either visually or through localized ultrasonic testing. The prevalence of fractured welds in mid-rise and high-rise structures shows how new computational tools are needed to identify their occurrence after a large earthquake for the health of the structure and the safety of the occupants. We present the theory for a new, high-frequency numerical method of detecting a failure event in engineered structures that uses the property of wave propagation reciprocity and time-reversed reciprocal Green's functions. The focus is on a specific type of structural failure event: brittle-fractured welds of beam-column connections. In this study, we postulate that if we can compile a numerical database of pre-event, source-receiver Green's functions for multiple locations of potential damage in a structure, we should be able to use that database to identify the location and time of occurrence of a subsequent, real failure event in the structure. Once a fracture source emits a wavefield that is recorded at a distributed set of accelerometers in the structure, time-reversed waves can be obtained by stacking the displacements convolved with the database of time-reversed impulse-source Green's functions. The pre-event impulse sources can be, for example, hammer blows applied to the welded connections, ideally during construction when they are still accessible. Computation of the spatial derivatives of the Green's functions is needed to obtain the exact displacement response for a fracture source. However, we show that the impulse source Green's function can be used instead, in the far-field approximation. The correct location and time of a subsequent fracture source can be inferred from the set of Green's functions that results in a stack exhibiting the best focus in the form of the tightest delta function.

1-057
ESTIMATION OF SCALED SEISMIC ENERGY AND APPARENT STRESS USING THE SEISMIC CODA AND EMPIRICAL GREEN'S FUNCTION CORRECTIONS *Baltay AS, Prieto GA, and Beroza GC*

Measurements of seismic energy from scattered coda waves indicate that apparent stress increases with increasing seismic moment, a consequential result for several reasons. For one, it may constrain possible forms of fault weakening with increasing slip. Moreover, if larger earthquakes more efficiently generate energy than their smaller counterparts, strong ground motion from large events would be more intense than anticipated from the extrapolation of smaller events. The relatively sparse strong motion data set does not seem to support this conclusion, leading us to reexamine seismic energy estimates and thus apparent stress. Our approach to the estimation is two-fold. The first technique, an empirical Green's function method, creates spectral ratios of co-located events, so that path and site terms need not be removed. The second method follows Mayeda et al. [2003] in making coda wave corrected spectra accounting for both path and site terms. This method is of particular interest as events occurring over a broad region can be compared. Using the two energy estimation methods, we compare results from a large data set in California spanning several networks. We find no strong departure from constant scaled energy in our data, which spans a range of Mw 3.0 – 7.1, implying earthquake self-similarity. Our analysis reveals several events in Southern California that have anomalous apparent stress, both low and high. Understanding the origin of high and low apparent stress events is important for strong ground motion prediction.

1-058
GROUND MOTION SIMULATIONS OF SCENARIO EARTHQUAKE RUPTURES OF THE HAYWARD FAULT *Aagaard B, Graves RW, Larsen S, Ma S, Rodgers A, Brocher T, Graymer RW, Harris RA, Lienkaemper J, Ponce DA, Schwartz D, Simpson R, Spudich P, Dreger D, Petersson A, and Boatwright J*

We compute ground motions in the San Francisco Bay area for a suite of 35 magnitude 6.7-7.2 scenario earthquake ruptures involving the Hayward fault. The suite of scenarios encompasses variability in rupture length, hypocenter, distribution of slip, rupture speed, and rise time. The five rupture lengths include the Hayward fault and portions thereof, as well as combined rupture of the Hayward and Rodgers Creek faults and the Hayward and Calaveras faults. For most rupture lengths, we consider three hypocenters, yielding north-to-south rupture, bilateral rupture, and south-to-north rupture. We also consider multiple random realizations of the slip distribution, accounting for creeping patches (Funning et al., 2007) either through simple assumptions about how creep reduces coseismic slip or a slip-predictable approach. The kinematic rupture models include local variations in rupture speed and use a ray-tracing algorithm to propagate the rupture front. Although we are not attempting to simulate the 1868 Hayward fault earthquake in detail, a few of the scenarios are designed to have source parameters that might be similar to this event.

This collaborative effort involves four modeling groups, using different wave propagation codes and domains of various sizes and resolutions, computing long-period (T > 1-2 s) or broadband (T > 0.1 s) synthetic ground motions for overlapping subsets of the suite of scenarios. The simulations incorporate the 3-D geologic structure as described by the USGS 3-D Geologic Model (Jachens et al., 2006; Watt et al., 2007) and USGS Bay Area Velocity Model (Brocher et al., 2007). The simulations illustrate the dramatic increase in intensity of shaking for a magnitude 7.0 bilateral rupture of the entire Hayward fault compared with a magnitude 6.8 bilateral rupture of the southern two-thirds of the fault; the area subjected to shaking stronger than MMI VII increases from about 10% to more than 40% of the San Francisco Bay urban area. For a given rupture length, the synthetic ground motions exhibit the strongest sensitivity to the distribution of slip and proximity to sedimentary basins. The hypocenter also exerts a strong influence on the amplitude of the shaking due to rupture directivity. The synthetic waveforms exhibit a weaker sensitivity to the rupture speed and are relatively insensitive to the rise time.

1-059
FIELD-TESTING PRECARIOUSLY BALANCED ROCKS IN THE VICINITY OF SAN BERNARDINO, CALIFORNIA: SEISMIC HAZARD RAMIFICATIONS *Anooshehpoor R, Purvance MD, and Brune JN*

A number of faults exist in the immediate vicinity of San Bernardino which contribute substantially to the seismic hazard. These include the San Andreas, San Jacinto, Cleghorn, and Cucamonga faults among others. Groups of precariously balanced rocks (PBRs) exist in close proximity to many of these fault zones. In the absence of extensive near-source strong motion recordings over sufficiently long periods of time, we utilize these PBRs to constrain the ground motion amplitudes which have not been exceeded during the PBR residence times. Field tests have recently been conducted on seven PBRs near Lake Arrowhead, two PBRs near Silverwood Lake, and two PBRs south of Beaumont. These field tests consist of accurate determination of the PBR shapes using photogrammetry along with quasi-static tilting tests of a subgroup of these PBRs to determine accurate restoring force versus tilt curves. This information is vital for accurate PBR fragility determination. As outlined in Rood et al. (2008), recent Be-10 cosmogenic age dates are consistent with the PBRs having been exhumed no more recently than 16-23 ka which are broadly consistent with VML minimum surface exposure ages on granite corestones in Southern California. These age

estimates strongly suggest that the PBRs have experienced strong ground motions from many earthquakes in the region and provide very important seismic hazard constraints. The PBRs are compared with simplified seismic hazard estimates based on ground motions from the largest earthquakes contributing to hazard at each site; both older ground motion prediction equations (GMPEs) and the recently developed Next Generation of Attenuation (NGA) GMPEs are utilized. These data, combined with data from previous PBR field testing initiatives, will be utilized in the future to constrain synthetic PetaSHA ground motion catalogues.

1-060
ROCK DAMAGE DURING STRONG SEISMIC GROUND MOTIONS *Sleep NH, and Hagin PN*

The shallow subsurface (upper 10s of meters) behaves nonlinearly and anelastically during strong ground motions. This nonlinear behavior causes attenuation of through-going seismic waves. We estimate the total diminution of energy strong seismic waves using the difference in P-S delays from small repeating earthquakes before and after strong shaking. We relate the change in low-amplitude S-wave velocity to damage during strong shaking that increases porosity. Two effects suggest that rate and state friction formalism is applicable. (1) The S-wave velocity then slowly increases with the logarithm of post-seismic time. (2) Strong seismic motion triggers slick-slip small seismic events in the shallow subsurface (Fischer et al, 2008 BSSA). The rock fails locally at pre-stressed places on cracks. Failure on numerous cracks over numerous strong earthquakes maintains heterogeneous pre-stress. We distinguish quantities from rate and state friction. (1) The ratio of dynamic shear stress to normal traction that would pulverize the rock if sustained. This quantity is measured in the laboratory as the starting coefficient of friction of intact rock. The Linker and Dieterich (1992) relationship adequately represents its dependence on normal traction. Well-bore failure provides a convenient method of calibration. (2) Given the presence of pre-stress, there is a somewhat lower dynamic stress that if sustained through a vibration cycle would attenuate the energy supplied by the seismic wave. It represents the practical limit above which augmentation of the amplitude of the incoming wave does not significantly augment shaking at the surface. The maximum stress in Coulomb-based Masing rules has similar implications. The limiting sustained acceleration for extreme ground motions is less than 1.5 g and does not depend strongly on rock type. We apply percolation-theory relationships between S-wave velocity and porosity change provide an energy balance associated with changes in low-amplitude S-wave velocity. We then use this relationship to estimate the work done to open pore space and damage rock during strong ground motion. Work to open pore space against lithostatic pressure is a major cause of nonlinear attenuation in intact rock at depth. This situation differs from that of mature laboratory gouge where dilatant work against normal traction is only ~1/17 of the macroscopic frictional work. Micromechanically after strong shaking has ceased, failure leaves residual stress and strains in its wake. These stresses do work against confining pressure and surface free energy when they extend crack tips. Failure during strong seismic shaking involves inelastic strains comparable to the elastic strains. The work to open pore space is thus a significant fraction of the anelastic work. In contrast, the strains on real contacts in gouge and on sliding faults greatly exceed the elastic strains. Only a small fraction of the anelastic work scaling to the ratio of real grain strength to grain shear modulus is available to do work. Furthermore, kinematic dilatancy (rolling square blocks and broken things not fitting back together where inelastic shear and dilatant strains are comparable) is important at small strains, but cannot have a net effect at large inelastic strains in gouge. Energy balance indicates that failure under repeated dynamic strains that just exceed the elastic limit is applicable to pulverized rocks near major fault zones.

1-061

DISTRIBUTION OF PRECARIOUS ROCK TOPPLING ACCELERATIONS WITH DISTANCE FROM THE SAN ANDREAS FAULT: LOVEJOY BUTTES AND GRANITE PEDIMENT *Brune JN*

For precariously balanced rocks (PBRs) in the Mojave, the toppling acceleration (TAs) of the most easily toppled rocks decreases with distance from the San Andreas fault, about 0.4 g at 15 km to about 0.25 g at 30 km. The approximate frequency of occurrence of rocks of different alphas (about 30% less than TAs in g's, assuming a waveform for an earthquake on the San Andreas fault) as a function of distance is estimated at Lovejoy Buttes (about 15-17 km) and Granite Pediment (hundreds of km). At Lovejoy Buttes there are no rocks with alphas of 0.2 or 0.1, whereas at Granite Pediment there are a number. Preliminary conclusions are:

(1) At Granite Pediment, far from known active faults, hundreds of km from the San Andreas fault, there is no indication of a strong dependence of numbers of rocks as a function of fragility.

(2) For alphas of 0.5 (toppling accelerations of about 0.65 g) the areal density of rocks is about 380/km2 at Granite Pediment, and about 230/km2 at Lovejoy Buttes, 15-17 km from the San Andreas Fault. The relatively small difference can be easily explained by the difference in characteristic joint in spacing, rather than ground accelerations from earthquakes.

(3) If we normalize the number of rocks to 100 at both sites, for the least fragile rocks, alphas of 0.5, then at Lovejoy Buttes there are obviously less rocks with alphas of .3 (21 vs. 77), and none with of 0.2 and 0.1 (vs. 42 and 7 at Granite Pediment, respectively), a clear indication that these more fragile rocks have been toppled by earthquakes on the nearby San Andreas fault. There are not a great deal more rocks with alphas of 0.5 than rocks with alphas of 0.4 at any sites.

(4) For alphas of 0.3, 0.4 and 0.5, when compared to Lovejoy Buttes, which has been shaken by dozens of M~8 earthquakes, there are no indications of very much larger numbers of such rocks (multiplicative factors of over 1000 suggested by some) at any site east of Lovejoy Buttes.

(5) Considering the above, there is no indication that the rocks at Lovejoy Buttes with alphas of 0.3 or 0.4 (toppling accelerations of 0.4 g and 0.5 g) are only remnants of a much larger population, most of which have hypothetically been knocked down by previous earthquakes.

Extreme Ground Motion (ExGM)

1-062

A COMPARATIVE ASSESSMENT OF THE GEOMORPHOLOGIC SETTING AND GEOLOGIC CONTEXT OF ZONES OF PRECARIOUSLY BALANCED ROCKS IN LOW-SEISMICITY REGIONS *Haddad DE, and Arrowsmith JR*

The utility of precariously balanced rocks as negative indicators of previous strong ground motion has proven to be promising in seismically active regions of Southern California and Nevada. Understanding the geomorphic context and processes that control the production and preservation of precariously balanced rocks is essential to any analysis of precarious rock zone. This study compares the geomorphic and geologic context of four precarious rock zones (Granite Dells, Chiricahua National Monument, Texas Canyon, and Granite Pediment) in low-seismicity regions of Arizona and Southern California. The Granite Dells locality is a ~20 km2 Proterozoic granite field that is ~5 km from the Prescott Valley graben faults (<0.2 mm/yr of Quaternary slip). The Chiricahua National Monument is composed of Cenozoic rhyolitic tuff with spectacular hoodoo geomorphology. The studied ~500 km2 of the Chiricahua National Monument is ~8 km from the Chiricahua fault zone (<0.2 mm/yr of Quaternary slip). The Texas Canyon locality is a ~132 km2 Mesozoic granite field that is ~23 km from the Little Rincon Mountains fault (<0.2 mm/yr of Quaternary slip). The Granite Pediment locality is a ~12 km2 Mesozoic granite pediment located ~96 km from the eastern section of the Garlock fault (>5 mm/yr of Quaternary slip).

Reconnaissance geologic characterization of these sites and their context included assembling a digital elevation and geologic database for Arizona, Southern California, and southern Nevada. The geologic data were queried for granitic bodies and Quaternary deposits. Morphometric analyses of the elevation data included computing slope, local relief, and total relief for each site using computational windows of varying dimensions. The analyses indicated that computational windows of 10,000 m2 and 10,000π m2 are suitable to assess the slope and relief distributions, respectively.

Our results enabled the development of a preliminary conceptual model that suggests the incision of major drainages into systematically jointed and compositionally homogeneous bedrock is an important driving mechanism for the production of precariously balanced rocks. The response of the landscape to this incision is evidenced by pockets of high slope and local relief that coincide with locations of precariously balanced rocks. These results motivate detailed geomorphic mapping of each locality to refine our conceptual model of the production and preservation of precariously balanced rocks.

1-063

AN INITIAL STUDY OF PRECARIOUSLY-BALANCED ROCKS AT THE GRASS VALLEY SITE, AND THEIR RELEVANCE TO QUATERNARY FAULTS IN AND NEAR THE SAN BERNARDINO MOUNTAINS, CA *Schlom TM, Grant Ludwig LB, Kendrick KJ, Brune JN, Purvance MD, Rood DH, and Anooshehpoor R*

Precariously balanced rocks (PBRs) are known natural "seismoscopes" (Brune, 1996) common to currently arid and semi-arid regions, including those of southern California. Typically found in granitic areas, these narrow-based or tall and thin PBRs sit in unstable positions on wider-based pedestals when the surrounding soil is removed by erosion. These rocks can be shaken down when ground motion amplitudes exceed certain values, and thus provide constraints on ground motion from previous earthquakes in a given area. By indicating the strength of past ground motions, PBRs can also provide significant data for seismic hazard analysis (Brune, 2002).

One group of PBRs in southern California—known as the Grass Valley site—sits in close proximity to major regional faults, making it an important location for studying ground motions. At least eight major faults are within this structurally complex area of the Transverse Ranges, including those of the North Frontal Thrust System of the San Bernardino Mountains, the San Andreas, and the southwest segment of the Eastern California shear zone. Some of these faults have been interpreted to have ruptured during the Holocene and have high (> 1mm/yr) reported slip rates. The southern Cleghorn, a sinistral strike-slip fault that traverses the Grass Valley PBR site has a reported Holocene slip rate of 3 mm/yr (Meisling, 1984) that has recently been questioned (Bryant, QFFDB, 2003). Numerous PBRs are present within 1 km of the Cleghorn fault in the Grass Valley drainage. Samples of two pedestals and a PBR from the Grass Valley site yielded preliminary Be-10 exposure ages of 23-28 ka for two pedestal rocks and 50 ka for one PBR (see Rood et al., 2008 SCEC abstract). The late Pleistocene exposure ages suggest that the rocks have been precariously balanced during the Holocene and have not been toppled by an earthquake on the southern Cleghorn fault. Therefore, we infer that the southern Cleghorn fault has not been active during the Holocene.

1-064
SENSITIVITY OF GROUND MOTION AT YUCCA MOUNTAIN TO UNCERTAINTIES IN FAULT GEOMETRY AND FAULT ZONE STRUCTURE *Duan B, and Day SM*

To explore how uncertainties in fault geometry and fault zone structure may affect physical limits on ground motion at Yucca Mountain, we conduct dynamic, deterministic 2D finite element calculations. We start from the model with maximum slip (nearly complete stress drop) on Solitario Canyon fault studied by Andrews et al. (2007), in which the 60° west-dipping fault is embedded in a tilted and layered geologic structure offset by normal faults with fluctuating topography. The velocity waveforms at the underground repository site that we obtained from this reference model are very close to those obtained by Andrews et al. (2007), with difference in velocity peaks within 10-15% (probably due to small difference in setup of the initial stress). Based on this reference model, we also find that different treatments of pore-pressure (i.e., time-dependent or non-time-dependent) can have significant effects on velocity peaks when off-fault material behaves elasto-plastically. In this case, we obtain a vertical velocity peak of ~ 3 m/s with time-dependent pore-pressure, compared with ~ 4 m/s with non-time-dependent pore-pressure at the site.

Inclusion of a low-velocity fault zone with a width of 50 m on each side of the fault, within which the seismic velocities are reduced by 20% compared with the corresponding layer's country rock, has no obvious effects on velocity peaks at the site in either elastic and elastoplastic off-fault response calculations, though the introduction of the low-velocity zone appears to introduce more high frequency motion. A change of 10° of the fault dip from 60° at shallow depth (< 1 km) to 50° at greater depth results in a larger fault slip and higher velocity peaks at the site, particularly in the elastic off-fault response calculation, mainly because the shallower dip increases the down-dip fault dimension. The numerical methodology accommodates the introduction of further complexities in the fault-plane and rock-mass constitutive models and in the fault geometry, and also enables future simulations in 3D.

1-065
NONLINEAR RESPONSES OF HIGH-RISE BUILDINGS IN SEATTLE FOR SIMULATED GROUND MOTIONS FROM GIANT CASCADIA SUBDUCTION EARTHQUAKES (MW 9.2) *Yang J, and Heaton TH*

With the exception of the 2003 Tokachi-oki earthquake, strong ground recordings from large subduction earthquakes (Mw >8.0) are meager. Furthermore there are no strong motion recordings

of giant earthquakes. However, there is a growing set of high-quality broadband teleseismic recordings of large and giant earthquakes. In this poster, we use recordings from the 2003 Tokachi-oki (Mw 8.3) earthquake as empirical Green's functions to simulate the rock and soil ground motions from the scenario M w 9.2 subduction earthquake expected on Cascadia subduction zone in the frequency band of interest to flexible and large-scale buildings (0.1 to 1 Hz). The effect of amplification by the Seattle basin is considered as a Green function which is derived from deconvolving the teleseismic waves recorded at rock sites from soil sites at SHIP02 experiment. These strong ground motions are used to simulate the fully nonlinear seismic responses of 20-story and 6-story steel moment-frame buildings designed according to both the U.S. 1994 UBC and also Japanese building code published in 1987. We consider several realizations of the hypothetical subduction earthquake; the down-dip limit of rupture is of paticular importance to the simulated ground motions in Seattle. If slip is assumed to be limited to offshore regions, then the building simulations indicate that the building responses are mostly in the linear rang. However, our simulation shows that buildings with brittle welds would collapse for rupture models where rupture extends beneath the Olympic Mountains.. The ground motions have very long durations (more than 4 minutes), and our building simulations should be considered as a minimum estimate since we have used a very simple model of degradation of the structure.

1-068

DYNAMIC RUPTURE THROUGH A BRANCHED FAULT CONFIGURATION WITH OFF-FAULT INELASTIC RESPONSE *Templeton EL, Bhat HS, Dmowska R, and Rice JR*

We analyze the propagation of shear cracks along branched fault paths with off-fault elastic-plastic deformation. Numerical and experimental investigations have focused on both the role of off-fault material behavior and that of geometrical complexities during earthquake rupture. Recent studies of earthquake dynamics have allowed for off-fault inelastic deformation [Andrews, 2005,2007; Shi and Ben-Zion, 2006; Templeton and Rice, 2008; Viesca et al., 2008; Duan, 2008]. These studies use pressure-dependent yield criteria such as Mohr-Coulomb or Drucker-Prager (DP), which are simple models for describing the onset of plastic deformation in granular or cracked materials. We use the dynamic finite element method to extend previous branching studies to include effects of inelastic off-fault response during dynamic slip-weakening earthquake rupture with an elastic DP plastic off-fault material description.

We outline current understanding of the dynamics of rupture along branched fault systems, as supported by field and laboratory comparisons with modeling, and then address rupture through faults bordered by damage zones which have inelastic response during dynamic rupture. Previous numerical studies by others in our group [Poliakov et al., 2002; Kame et al., 2003; Bhat et al., 2004,2007; Fliss et al., 2005] based on boundary integral equation implementations of slip-weakening rupture showed how the choice of rupture path at a branching junction is determined by the orientation of maximum compressive stress, branch angle, and rupture velocity at the junction. We show how off-fault inelastic deformation contributes to the dynamic path selection process.

In particular, we address the possibility of rupture through a fault branch along the Solitario Canyon Fault (SCF) bordering Yucca Mountain. An issue is whether the next seismic rupture along SCF could also induce rupture along a nearby fault such as the Windy Wash Fault or the Boomerang Fault. Analyses using branch configurations suggested by cross-sectional views [Brocher et al., 2998; Potter et al., 1999,2004] with a vertical tectonic pre-stress suggest that branching is unlikely for these configurations when inelastic deformation is allowed in the bulk except in cases of extreme stress drops or super shear rupture velocities. We also address the

energy partitioning during rupture, and find that the plastic strain energy dissipated in the bulk can be several times the slip-weakening fracture energy.

1-069
SPATIAL CORRELATION BETWEEN KINEMATIC SOURCE PARAMETERS DERIVED FROM DYNAMIC RUPTURE SIMULATIONS *Schmedes J, Archuleta RJ, and Lavallee D*

For a kinematic model to accurately predict ground motion, it is necessary not only to know the spatial distribution of the source parameters but also to know the correlation among the parameters. Because there are limitations from inversions of seismic data, we determine the spatial correlations from physically based dynamic ruptures.

We computed and analyzed 150 dynamic subshear rupture models to get a quantitative understanding of the correlation and amplitude distributions of parameters describing the earthquake source, such as stress drop, rupture velocity, and rise time. The dynamic ruptures are based on a slip weakening friction law and different approaches to create random heterogeneous initial stress and strength distributions on the fault. While there is much to be learned by looking at differences among all the models, we focus on features that are common among all models, that is, features that show the least dependence on the choice of the initial model. Using the 150 dynamic ruptures, we are able to construct probability density functions (PDF's) for the amplitude distributions of the source parameters as well as for the spatial correlation between the source parameters.

We find: (1) slip amplitude does not show systematic correlations with rupture velocity, and it is positively correlated with rise time; (2) peak slip rate shows strong correlation with rupture velocity and rise time; (3) the PDF of rupture velocity has a well defined maximum between 80%-90% of the shear wave velocity. The value of this maximum probability density increases with distance from the hypocenter, while the width of the PDF decreases, i.e., the rupture velocity tends toward a more constant value. A similar dependence is found for the PDF of the rise times, which has a width that decreases with increasing distance from the nucleation zone; moreover, the mean value of the rise time shifts to a smaller value.

Our findings will be used to refine the rupture model currently used in the SCEC broadband simulation platform.

1-070
IS TIME/SLIP/VELOCITY WEAKENING NECESSARY IN DYNAMIC RUPTURE SIMULATIONS? APPLICATION OF A DISCRETE ELEMENT METHOD TO MODEL YUCCA MOUNTAIN GROUND MOTIONS *Purvance MD*

Using geotechnical and fault offset data, Andrews et al. (2008 - AEA08) developed dynamic rupture models to constrain the physical limits on ground motions at Yucca Mountain. The AEA08 model uses a traction-at-split-node finite difference and includes realistic material properties, topography, and initial stresses. To independently verify the AEA08 ground motions, this work builds a distinct element (DEM) dynamic rupture model for Yucca Mountain. The bulk material is discretized by a triangular lattice consisting of linear springs connecting nodes (32 m spacing, 0.25 Poisson ratio). This Lagrangian approach tracks nodal positions and velocities using the Velocity Verlet algorithm (accurate to 4th order in position, 2nd order in velocity). The fault sides interact through a soft contact law where normal stresses develop from overlap between a node on one side of the fault and the opposite fault member. Shear stress increments are obtained by calculating the

relative shear displacement of each fault node. The fault nodes are tested for contact with the opposite fault member at each time step. This DEM model does not suffer from numerical instability when discontinuities occur (e.g., instantaneous friction changes, fault separation, etc.). Thus arbitrary friction laws and fault surface roughness' can be incorporated.

A smooth fault is used to emulate AEA08; the DEM model incorporates the AEA08 material properties and surface topography. The initial stress state is obtained by displacing the nodal positions and cycling the damped model to quiescence. Initial investigations used linear time weakening friction following AEA08. The DEM model produces ground motions for the maximum slip event at the repository location which are very similar to AEA08 motions. An instantaneous friction law which drops from static to dynamic value in one time step very slightly increases the rupture velocity and yields nearly identical ground motions. Fault separation occurs locally near the free surface for very short time periods. AEA08 results for the "smooth" supershear and subshear 2.7 m slip cases compare favorably with the DEM ground motions with and without time weakening. These results indicate that beyond modulating the rupture velocity, frictional weakening is not a necessary component of dynamic rupture simulations utilizing DEM. These results strongly suggest that the physical significance of the so-called critical slip weakening distance must be scrutinized.

1-071
OBSERVED RELATIONS AMONG FAULT STRENGTH LOSS, STRESS DROP, SLIP VELOCITY, AND NEAR-FAULT PARTICLE VELOCITY DURING DYNAMIC RUPTURE PROPAGATION, AND THEIR IMPLICATIONS FOR LIMITS ON GROUND MOTION *Beeler N, Kilgore BD, Boettcher M, McGarr A, Fletcher J, Evans J, and Baker S*

Extreme ground motions implied by the PSHA at Yucca Mountain at low exceedance probability require earthquake stress drop to approach the in situ shear stress. Lab rupture propagation experiments and seismic studies are not generally consistent with this requirement; static stress drops are <20% of fault strength and apparent stress is typically 25% of the stress drop. Thus, seismic efficiency is low at <0.06 [McGarr, 1994; 1999]. Nevertheless, the mechanisms that produce natural low seismic efficiency cannot be assumed ubiquitous in the crust. The existence of extreme motions can't be dismissed entirely without advances in understanding of the earthquake source.

From direct measurements made during large bi-axial friction experiments we report relations among stress drop, strength loss, fault slip rate, rupture propagation rate, and near-fault particle velocity over a range of loading stresses. Shear stress, fault slip, particle velocity and acceleration were recorded during dynamic rupture propagation at multiple locations along strike and at small fault-normal distances. Stress drop increases weakly with normal stress. Average slip rate depends linearly on the static stress drop with a nonzero intercept. The constant of proportionality is the reciprocal of the product of fault stiffness and rupture duration. The minimum fracture energy can be inferred directly from the intercept. The ratio of apparent stress to static stress drop is ~27%, consistent with overshoot and significant on-fault fracture energy and with typical seismic observations. Rupture propagation rates reach approximately 85% of the shear wave speed. Peak slip velocity depends linearly on the dynamic strength loss with non-zero intercept. The constant of proportionality is approximately twice the ratio of the shear wave speed to the shear modulus as suggested by Brune [1970]. The non-zero intercept, again, likely is due to fracture energy. We conclude that average and near-fault peak velocities are limited by both in-source dissipation processes and the strength loss. The limits implied by these observations do not allow for extreme motions in normal faulting environments such as Yucca Mtn. However, these estimates are likely

to be unrealistically low. The experiments have weakly pressure dependent strength loss and large fracture energy which extrapolate to very low slip rate and particle velocity at crustal conditions.

1-072

THE SCEC/USGS 3D RUPTURE DYNAMICS CODE COMPARISON EXERCISE *Harris RA, Barall M, Archuleta RJ, Aagaard B, Ampuero J, Andrews DJ, Cruz-Atienza VM, Dalguer LA, Day SM, Duan B, Dunham EM, Ely GP, Kaneko Y, Kase Y, Lapusta N, Liu Y, Ma S, Oglesby DD, Olsen KB, Pitarka A, Song S, and Templeton EL*

Computer simulations of earthquake source rupture physics started three decades ago, with a few researchers developing and using their own methods to solve problems of mostly theoretical interest. In contrast, in current times numerous spontaneous rupture computer codes are now being developed and used by researchers around the world, and the results are starting to be used in earthquake hazard assessment, for both seismological and engineering applications. Since most of the problems simulated using these numerical approaches have no analytic solutions, it is essential to compare, verify, and validate the various versions of this research tool. To this end, a collaborative project of the Southern California Earthquake Center, that has received some funding from the DOE Extreme Ground Motion project, has been underway. We started with the basic problem of earthquake nucleation and spontaneous rupture propagation on a vertical strike-slip fault in a homogeneous material and subsequently moved on to problems with slightly more heterogeneous stresses and with differing material properties on opposite sides of the fault. Our next exercises are 1) the case of rupture on a dipping fault, which is relevant to the Yucca Mountain fault-rupture scenarios, and 2) the case of rate-weakening friction, rather than the slip-weakening friction used in most of our previous exercises. With SCEC and DOE support, we have a website that enables easier comparisons of the results among the modelers, and also supplies information about the benchmarks and codes. Our overall objective is a complete understanding of the simulation methods and their ability to faithfully implement our assumptions about earthquake rupture physics and calculate the resulting ground motion.

Collaboratory for the Study of Earthquake Predictability (CSEP)

1-073

THE COLLABORATORY FOR THE STUDY OF EARTHQUAKE PREDICTABILITY (CSEP) TESTING CENTER ROADMAP *Liukis M, Schorlemmer D, Yu J, Maechling PJ, Zechar JD, Jordan TH, Euchner F, and the CSEP Working Group*

SCEC began development of the Collaboratory for the Study of Earthquake Predictability (CSEP) in January of 2006 with funding provided by the W. M. Keck Foundation. Since that time, a large group of scientists and software engineers have translated the concepts of CSEP into an operational testing center. The initial implementation of the W. M. Keck Foundation Testing Center at SCEC for the California natural laboratory became operational on September 1, 2007 and was further improved, optimized, and extended over the past year. The design and implementation of the SCEC Testing Center have been guided by four design goals that were originally identified as objectives for the RELM testing center which are: (1) Controlled Environment, (2) Transparency, (3) Comparability, and (4) Reproducibility. By meeting these goals, the CSEP Testing Center can provide clear descriptions of how all registered earthquake forecasts are produced and how each of the forecasts are evaluated. As of September 2008, there are four testing centers established around the globe. SCEC Testing Center hosts forecasts models for California and Western Pacific testing regions. There are nineteen 5-year forecast models, two 1-year models, seven 3-month forecast models, and three daily forecasts under evaluation, all of which are seismicity-based forecast models. We describe how the currently operational CSEP Testing Center at SCEC has been constructed to meet the design goals, the status of the Testing Center and our experiences operating the center since its inception.

1-074

EXPANDING AND STARTING CSEP TESTING REGIONS *Schorlemmer D, Zechar JD, and Jordan TH*

For the purposes of the Collaboratory for the Study of Earthquake Predictability (CSEP), a testing region consists of two elements: a precisely defined geographic region in which earthquake models are tested and the test specifications. Delineating a natural laboratory requires precise characterization of available data, particularly regional earthquake catalogs. This includes information about data generation processes, measurement uncertainties, and derived properties such as catalog completeness. CSEP employs working groups for data, test, and model standards to develop guidelines for testing region developments. We present the details of the California testing region and describe the ongoing efforts to establish comparable testing regions in New Zealand, Italy, the Western Pacific region, and Japan. The unique challenges of global testing are also addressed.

1-075

PROSPECTIVE TESTING OF EARTHQUAKE FORECAST MODELS IN EUROPE *Woessner J, Wiemer S, Schorlemmer D, Euchner F, and Marzocchi W*

Earthquake forecasting and prediction related research has been plagued by controversy in the last few decades. As a consequence, the focus has changed to more formal assessment of earthquake predictability using well-defined quantitative hypothesis-testing algorithms in the framework of the international Collaboratory for the Study of Earthquake Predictability (CSEP, *http://www.cseptesting.org*). Funded by national agencies and ongoing European Union (EU) projects, seismologists are currently building a European node of this global infrastructure

(eu.cseptesting.org). It will consist of one central testing center installation hosted by ETH Zurich and a number of testing regions. Testing regions are and will be defined based on the quality of seismic data, the availability of forecast models, and the commitment of network operators to provide earthquake catalog data timely and quality-controlled.

Italy is the first region to become a testing region after a detailed catalog completeness study was performed. Based on this study, a preliminary testing region and data collection area, as well as the source of earthquake data have been defined. Under these definitions, a range of models are calibrated for comparative prospective testing including different flavors of the Epidemic Type Aftershock Sequence (ETAS) model and a modification of the Short-Term Earthquake Probabilities (STEP-Italy) model. The roadmap for an operational start of the testing center will be defined at a workshop on the Italian testing region (27 and 28 October 2008), with the target date for the start of prospective testing set as March 1, 2009. This presentation summarizes the proposition for the Italian testing region, the extensions to further testing regions and future plans for testing earthquake forecast models in Europe and beyond.

1-076
THE COLLABORATORY FOR THE STUDY OF EARTHQUAKE PREDICTABILITY: ESTABLISHING A TESTING CENTER IN JAPAN *Tsuruoka H, Hirata N, Schorlemmer D, Euchner F, and Jordan TH*

The Collaboratory for the Study of Earthquake Predictability (CSEP) is promoting earthquake predictability research by rigorous testing of earthquake forecast hypotheses. CSEP developed standardized procedures for registering earthquake forecast models, conducting tests, and disseminating results. The underlying Testing Center software system was developed and deployed to several institutions to host CSEP Testing Centers. Besides California, Testing Centers are installed in New Zealand and Europe to host prediction experiments for their regions. Here, we present the international effort to establish a CSEP node in Japan. A prototype Testing Center is installed the Earthquake Research Institute of the University of Tokyo and started operation. We introduce the earthquake catalog characterization used for the definition of the Japanese testing region, the first set of models to be tested, and the setup of the Testing Center software. This Testing Center constitutes an open collaboration to researchers contributing earthquake forecast models for the testing region of Japan.

1-077
FIRST RESULTS OF THE REGIONAL EARTHQUAKE LIKELIHOOD MODELS EXPERIMENT *Zechar JD, Schorlemmer D, Werner MJ, Jordan TH, and the RELM Working Group*

Successfully predicting the future behavior of a system is a poignant indication that the system is well-understood. Certainly many details of the earthquake system remain obscure, but several hypotheses related to earthquake occurrence and seismic hazard have been proffered, and predicting earthquake behavior is a worthy goal and demanded by society. Along these lines, one of the primary objectives of the Regional Earthquake Likelihood Models (RELM) working group was to formalize earthquake occurrence hypotheses in the form of prospective earthquake rate forecasts in California. RELM members, working in small research groups, developed more than a dozen 5-year forecasts; they also outlined a performance evaluation method and provided a conceptual description of a Testing Center in which to perform predictability experiments. Subsequently, researchers working within the Collaboratory for the Study of Earthquake Predictability (CSEP) have begun implementing Testing Centers in different locations worldwide, and the RELM predictability experiment--a truly prospective earthquake prediction effort--is

underway within the U.S. branch of CSEP. The experiment, designed to compare time-invariant 5-year earthquake rate forecasts, is now approximately halfway to its completion. We present, for the first time, preliminary results of this unique experiment. While these results are preliminary--the forecasts were meant for an application of five years--we find interesting results: most of the models are consistent with the observation and one model is identified as forecasting the spatial distribution of earthquakes best.

1-078
TIME-DEPENDENT FLUCTUATIONS OF THE EARTHQUAKE MAGNITUDE DISTRIBUTION: STATISTICAL ESTIMATION AND PREDICTIVE POWER *Olsen S, and Zaliapin I*

This study reports new results on statistical analysis of time-dependent earthquake magnitude distribution and connection between fluctuations in the magnitude distribution and large regional earthquakes. Specifically, we consider the following two problems: 1) How to effectively describe and detect local deviations of the magnitude distribution from the long-term Gutenberg-Richter (GR) approximation? 2) What is the connection between those deviations and the occurrence of large regional earthquakes? We develop a statistical estimation framework for the b-value (slope of the GR approximation to the observed magnitude distribution) and for the ratio a(t) between intensities of earthquake occurrence in two non-overlapping magnitude intervals. The time-dependent dynamics of these relevant parameters of the magnitude distribution is analyzed using sequential Bayesian estimation (filtering) based on homogeneous Markov chain models. The main advantage of this approach over the traditional window-based estimation is its "soft" parameterization, which allows one to obtain reliable and stable results with realistically small samples available for analysis. The developed methods are applied to the observed seismicity of California, Nevada, and Japan on different temporal and spatial scales. We report an oscillatory dynamics of the estimated GR parameters and find that the detected oscillations are positively correlated with the occurrence of large regional earthquakes. The reported results have important implications for further development of earthquake prediction and seismic hazard assessment methods and contribute to the SCEC science program in the framework of the Collaboratory for the Study of Earthquake Predictability.

1-079
A PROBABILISTIC COMPLETENESS STUDY IN JAPAN *Schorlemmer D, Hirata N, Euchner F, Ishigaki Y, and Tsuruoka H*

The Japan Meteorological Agency (JMA) operates a seismic network and additionally gathers real-time seismic data from many other seismic networks in Japan, among them the Hi-net of the National Research Institute for Earth Science and Disaster Prevention (NIED) and many local and regional networks operated by universities. In total, this aggregated network comprises more than 1000 stations distributed over the many islands of Japan. Locally this network is able to detect earthquakes with magnitudes of less than M=0, however, estimates about recording completeness were only given for seismically active regions. Here, we present the first application of the probability-based magnitude of completeness (PMC) method to the JMA network. We show detection probabilities for any given magnitude and completeness magnitudes for selected probability levels for the entire area of Japan. The results show the strong performance of the JMA network and that the network can provide the data of required quality for CSEP (Collaboratory for the Study of Earthquake Predictability) testing.

1-080

EARTHQUAKE PREDICTABILITY TEST OF THE LOAD/UNLOAD RESPONSE RATIO METHOD *Zeng Y, and Shen Z*

In this paper, we extend our test of the Composite Load/Unload Response Ratio (CLURR) method for intermediate-term earthquake forecast to large historical events in China. Our previous test in the western US has found significant precursor anomalies for almost all of the M>6 earthquakes in California since 1979. The method is modified from the Load/Unload Response Ratio (LURR) method proposed by Yin and others (1995) for long and intermediate term earthquake forecasts. The basic assumption and algorithm of LURR are that large earthquakes occur in response to critical loading stress surrounding the seismogenic fault, whose state of criticality could be detected through anomalous response monitoring of regional seismicity to the Coulomb stress changes on faults induced by earth tides. We have developed an open source code for the LURR evaluation using Agnew's (1996) method to compute tidal induced Coulomb stresses on the fault and applied both the stress "state" and "rate" as criteria for differentiating the loading and unloading events based on those Coulomb stress changes. A range of frictional coefficients is used to calculate the Coulomb stress change and the averages based on the root mean squares of those LURR functions are then used to form the composite LURR function. We test against large Chinese earthquakes that have occurred in the last 30 years, including the M7.3 Haicheng earthquake in 1975 and M7.6 Tangshan earthquake in 1976. We have found good success for most events except the most recent M7.9 Sichuan earthquake on May 12, 2008.

Working Group on California Earthquake Probabilities (WGCEP)

1-082
IS THERE BASIS FOR PREFERRING CHARACTERISTIC EARTHQUAKES OVER A GUTENBERG-RICHTER DISTRIBUTION IN PROBABILISTIC EARTHQUAKE FORECASTING? *Parsons T, and Geist EL*

The idea that faults rupture in repeated, characteristic earthquakes is central to most probabilistic earthquake forecasts. The concept is elegant in its simplicity, and if the same event has repeated itself multiple times in the past, we might anticipate the next. In practice however, assembling a fault-segmented characteristic earthquake rupture model can grow into a complex task laden with unquantified uncertainty. We weigh the evidence that supports characteristic earthquakes against a potentially simpler model made from extrapolation of a Gutenberg-Richter magnitude-frequency law to individual fault zones. We find that the Gutenberg-Richter model satisfies key data constraints used for earthquake forecasting equally well as a characteristic model. Therefore, judicious use of instrumental and historical earthquake catalogs enables large-earthquake-rate calculations with quantifiable uncertainty that should get at least equal weighting in probabilistic forecasting.

1-083
NEOKINEMA MODELS BASED ON COMMUNITY DATASETS *Bird P*

I merge the SCEC, WGCEP, PBO, & WSM community datasets in deformation models for the western US. In California I use: (1) fault traces, dips, and slip senses from WGCEP Fault Models 2.1 or 2.2; (2) fault offset rates and uncertainties obtained by Bird [2007, Geosphere, 3(6)] from offsets in the USGS Paleosites Database; (3) a 2006 California joint GPS solution for interseismic benchmark velocities by Shen, King, Wang, & Agnew; and (4) stress-direction indicators from World Stress Map. In other western United States I use: (5) my collection of fault traces and offset rates as documented in Bird [2007]; and (6) selected GPS velocities from PBO. All are fit by weighted least-squares in kinematic F-E NeoKinema. As described previously, this program (a) interpolates stress directions to determine their uncertainties, (b) attempts to minimize off-fault strain-rates and align them with stress, and (c) iteratively corrects geodetic velocities from short-term to long-term using local dislocation-in-halfspace corrections.

It is already clear that all datasets can be fit at a common level of 1.7 standard errors (RMS or N2 norm). If "acceptable" fit is defined as N2 < 2 for all datasets, there is a range of acceptable models, defining a range of long-term fault slip rates and (anelastic) continuum strain-rates.

In preferred model GCN2008060, the mean long-term slip rates for trains of the San Andreas fault are (SE to NW): Coachella 15 mm/a, San Gorgonio Pass-Garnet Hill 6, San Bernardino South 12, San Bernardino North 19, Mojave South 16, Mojave North 17, Big Bend 15, Carrizo 25, Cholame 26, Parkfield 31, Creeping 29, Santa Cruz Mt. 23, Peninsula 18, North Coast 16, & Offshore 9 mm/a. Up to Cajon Pass, these all agree with 2007 WGCEP [2008], but my Mojave N & S and Big Bend rates are much slower, my Carrizo & Cholame rates are marginally slower, and my North Coast & Offshore rates are much slower.

These differences are due to greater amounts of permanent (anelastic) straining off the mapped fault traces in NeoKinema, relative to the elastic-microplate models of 2007 WGCEP [2008]. I have not been able to lower the RMS continuum strain rate in these models below 5E-16/s (=1.6%/Ma). Such distributed straining results from gaps and geometric incompatibilities in the fault network

and from geologic/geodetic discrepancies. This straining probably also occurs on faults (which are not part of WGCEP Fault Models), and it probably also produces earthquakes.

1-084

MULTI-FAULT RUPTURE AND EARTHQUAKE RATE IN SOUTHERN CALIFORNIA

Black NM, and Jackson DD

Past earthquakes have combined numerous faults in a single event and ruptured unmapped faults. However, fault length is often used to estimate future rupture length and maximum magnitude. How can we use the current fault maps to infer future rupture length? In previous work we have shown there are several simple rules that will allow fault-to-fault rupture, and will increase the length of mapped faults. Separate faults can be treated as a single fault line if 1) the mapped surface traces of separate faults are within 10 km, and 2) the faults overlap, or the extrapolation of the non-overlapping fault traces intersect within a 30-degree angle. If more than one fault-pair opportunity is available, preference can be given to fault pairs that have the same sense of slip, or to more likely combinations of strike-slip to reverse/normal faults (etc.).

What are the implications of a rupture breaking beyond mapped faults or combining separately mapped fault lines? 1) Large magnitude events may be under estimated and 2) the frequency of smaller events may be over estimated. To demonstrate the above points I have combined the mapped lengths of neighboring California faults that are separated by less than 10 km. I use the combined length to calculate the maximum magnitude and the cumulative earthquake rate. Then, I calculate the cumulative earthquake rate using the traditional method of summing the moment rates of the individual faults. I plot the 'combined' rate and compare this to the 'individual summed' rate. I find that combining fault lengths increases the maximum magnitude, which allows for moment to be released in infrequent large magnitude events (+7). Therefore, when compared to the 'summed' rate for the individual fault lines, the 'combined' fault length rate decreases the number of magnitude 5-7 earthquakes.

Earthquake Forecasting and Predictability (EFP)

1-085
MEDIUM-TERM EARTHQUAKE FORECASTING WITH NUMERICAL EARTHQUAKE SIMULATORS *Van Aalsburg JD, Rundle PB, Morein G, Rundle JB, Turcotte DL, Grant Ludwig LB, Donnellan A, and Tiampo KF*

Topologically realistic earthquake simulations are now possible using numerical codes such as Virtual California (VC). Currently, VC is written in modern object-oriented C++ code, and runs under MPI-II protocols on parallel HPC machines such as the NASA Columbia supercomputer. In VC, an earthquake fault system is modeled by a large number of Boundary Elements interacting by means of linear elasticity. A friction law is prescribed for each boundary element, and the faults are driven at a stressing rate that is consistent with their observed long-term average offset rate. We note that the parameters that enter into the model are set using the long term average properties of the fault system -- earthquake and plate rate variability are not used at this stage of the simulation. We have carried out simulations for earthquakes on models of California's fault system for simulation runs over time intervals from tens of thousands of years to millions of years. Using these simulations, we have now developed techniques to assimilate observed earthquake variability into the simulations. Our technique is based on mining the simulation data to identify time intervals that look most like the recent past history of earthquakes on the California fault system. We then use these optimal time intervals to "look into the future" and forecast the likely locations of future major earthquakes. Here we describe this method and develop fault-based probabilities that are comparable with recent results from the Working Group on California Earthquake Probabilities.

1-086
A VIRTUAL CALIFORNIA EARTHQUAKE SIMULATION TEST *Yikilmaz MB, Turcotte DL, Yakovlev G, Rundle JB, and Kellogg LH*

Virtual California (VC) is a geometrically realistic numerical model which is specifically designed to simulate earthquake occurrences along the San Andreas and adjacent faults. It is a stochastic, cellular automata (CA) simulation of an earthquake backslip model. The term backslip specifies that the loading of each fault segment occurs due to the accumulation of a slip deficit at the prescribed slip rate of the segment. Recurrence intervals are also specified. VC includes the major strike-slip faults in California and is composed of more than 650 vertical fault segments, each having a width of ~ 10 km and a depth of 15 km. The fault segments are treated as dislocations and interact with each other elastically, utilizing dislocation theory. In this paper we present the initial results of a simple fault geometry model from a recently updated VC code. The model consists of a linear and vertical fault divided into two equal segments each having 23, 10 x 10 km, elements. The interaction of the two segments is studied by gradually making one segment stronger by prescribing higher recurrence intervals for this segment. In all cases a limit cycle is obtained. We observe that the number of periods in the system increases with increasing recurrence interval.

1-087
MULTISCALE EARTHQUAKE SIMULATOR FOR PARKFIELD, CALIFORNIA, USING RATE AND STATE FRICTION AND FAST MULTIPOLES *Tullis TE, and Beeler N*

We have developed a multiscale grid and corresponding distribution of constitutive parameters to simulate earthquake sequences over a wide range of scales at Parkfield, CA. The geometry of grid elements and the distribution of constitutive parameters have been designed based on the distribution of microseismicity at Parkfield, including earthquakes ranging from magnitude 1 to magnitude 6. The intent of this work is to understand the interplay between earthquakes of a wide

range of magnitudes, in particular what conditions allow small earthquakes to grow into larger ones and whether accelerating seismicity at a smaller scale presages larger events. Because we employ a realistic geometry, use rate and state friction, and use a quasi-static approach to the behavior during rapid slip, we hope that the behavior of the simulated sequence of events will be as similar to that of real earthquakes as possible. Because a detailed time-space history of microseismicity and larger events at Parkfield exists, it will be possible to make comparisons between the properties of the simulated history of events and those of the actual events. The smallest elements in the multiscale grid are 7 m in dimension, values small enough to represent a continuum with laboratory values of Dc and the other constitutive parameters. The multiscale grid is used so that only the areas having experienced earthquakes are represented by the smallest elements. The largest elements are used in areas where microearthquakes do not occur, and these are 200 m in dimension. A total model area 47 km along the San Andreas by 15 km deep that is based on the observed distribution of 4966 microearthquakes has 1,464,433 elements. Running this entire model for sufficient time steps, even with the Fast Multipole approach, is probably beyond the range of existing computers. Consequently we are starting with subsets of the total area having a range of sizes and numbers of actual earthquakes, to gain experience with the behavior of the simulations. Note that although the distribution of constitutive parameters and of the smallest elements may restrict the simulated earthquakes in the model to be spatially similar to actual earthquakes at Parkfield, the time histories of the simulated earthquakes will occur spontaneously. The space-time distribution of simulated seismicity is the output of the simulation that we plan to analyze to see if detectable patterns of activity premonitory to larger events can be detected.

1-088

COMPARISON OF A MULTI-CYCLE EARTHQUAKE SIMULATOR WITH A DYNAMIC FINITE ELEMENT METHOD FOR A HETEROGENEOUS PLANAR FAULT

Stevens JA, Dieterich JH, Oglesby DD, and Richards-Dinger KB

RSQSim is an earthquake simulator that produces fast simulations of numerous earthquake ruptures, up to 10^6 events in a simulation, in complex fault systems under the effects of rate- and state-dependent friction. As part of an effort to validate the quasi-dynamic rupture propagation aspects of RSQSim, we compare rupture propagation on a variable-strength planar fault in RSQSim to that on a similar fault in DYNA3D (a fully dynamic finite element mode employing slip-weakening friction). Validation of the final slip and stress change distributions are important to ensure that subsequent events in RSQSim will inherit the proper stress fields. In addition, if the time evolution of ruptures in RSQSim is realistic, they may be useful as kinematic sources for ground motion calculations.

By using fairly consistent values of physical variables in both codes, previous comparisons for ruptures with uniform fault properties found that both methods produced very similar results. Our asperity model consists of multiple rectangular zones of increased normal stress of varying size and amplitude. In both modeling methods the heterogeneities produce complex ruptures - as the rupture front encounters a barrier, it tends to wrap itself around the barrier and create a burst of energy once it propagates across the barrier. Both codes allow rupture propagation over significant zones of negative stress drop in these asperity regions. Rupture durations, average rupture propagation speeds and overall slip pattern are quite similar with both methods. However, ruptures with the fully dynamic method (DYNA3D) propagate more rapidly through the barriers, and generate less high-frequency variations of slip than ruptures with the quasi-dynamic method (RSQSim). Regardless, the qualitative agreement of these two very different methods is remarkably good and may improve more with further tuning of quasi-dynamic computational parameters.

1-089
A FIVE-YEAR FORECAST OF EARTHQUAKE LARGER THAN 5 IN CALIFORNIA BASED ON SMOOTHED SEISMICITY *Wang Q, Jackson DD, and Kagan YY*

A forecast method based on smoothed seismicity was presented by Kagan and Jackson (1994) and has been widely used since then. It is based on earthquake occurrences, and it assumes the earthquake rate density is constant in time and the rate density is proportional to a smoothed version of past seismicity. Kagan and Jackson (2007) have presented a five-year forecast of southern California earthquake with magnitude larger than 5. At present, we extend the forecast region from southern California to all of California using the new California earthquake catalog. This catalog covers all known earthquakes larger than 4.7 in California from 1800 to 2007. All earthquake magnitudes are converted to moment magnitude in this catalog. Earthquakes less then magnitude 6.5 are treated as point sources. Some earthquakes larger than 6.5 are replaced by ensembles of smaller events with equivalent total moment, distributed along the rupture surface. This forecast model differs from others like it because it includes historical as well as instrumented earthquakes, and because larger events are represented by multiple point sources.

1-090
SHORT- AND LONG-TERM EARTHQUAKE FORECASTS FOR CALIFORNIA AND NEVADA *Kagan YY, and Jackson DD*

We present estimates of future earthquake rate density (probability per unit area, time, and magnitude) on a 0.1 degree grid for a region including most of California and Nevada. Our long-term forecast is inherently independent of time and it is suitable for testing over a five-year period as part of the experiment conducted by the Collaboratory for Study of Earthquake Predictability (CSEP). In the short-term forecast the earthquake rate decreases following each past earthquake by an Omori-type temporal decay. The short-term forecast is meant to be updated daily and tested against similar models by CSEP. The full forecast includes a fraction of our long-term forecast plus contributions from the short-term forecast. Both forecasts estimate rate density using a radially symmetric spatial smoothing kernel decreasing approximately as in the reciprocal of the square of epicentral distance, weighted according to the magnitude of each past earthquake. Both forecasts are based on cataloged earthquakes only, with no dependence on mapped faults or geodetic strain rates. We made two versions of both the long- and short-term forecasts, based on the ANSS and PDE catalogs, respectively. The two versions are quite consistent, and for testing purposes we prefer those based on the ANSS catalog as it is complete to a lower magnitude threshold and has more precise locations. Both forecasts apply to shallow earthquakes only (depth 25 km or less) and they assume a modified Gutenberg-Richter magnitude distribution extending to a lower threshold of 4.0.

1-091
EARTHQUAKE PATTERNS IN DIVERSE TECTONIC ZONES OF THE GLOBE *Kagan YY, Bird P, and Jackson DD*

We extend existing branching models for earthquake occurrence by allowing their parameters to vary by tectonic zone. We partition Earth's surface into five zones: Trenches (including subduction zones, oceanic convergent boundaries, and earthquakes in the outer rise or overriding plate), Fast spreading ridges and oceanic transforms, Slow spreading ridges and transforms, Active continents, and Plate interiors (everything else). Our purpose is to specialize the models to give them the greatest possible predictive power for use in earthquake forecasts. We expected the parameters of the branching models to be different in the various tectonic zones, because earlier studies [Bird & Kagan, 2004] found that magnitude limits and other parameters differed by plate boundary class.

We compiled subsets of the CMT and PDE catalogs corresponding to each tectonic zone, and optimized the parameters for each using a maximum likelihood procedure. We also analyzed branching models for California and Nevada using regional catalogs.

Our estimates of parameters that can be compared to those of other models (e.g., proportion of triggered earthquakes, exponent describing temporal decay) were consistent with published results. Contrary to our expectation, we found no dramatic differences in the branching parameters across tectonic zones. We did find some modest differences that were robust under changes in catalog and lower magnitude threshold: Subduction zones have the highest earthquake rates, the highest upper magnitude limit, and the highest proportion of triggered events. Fast spreading ridges have the smallest upper magnitude limit and the lowest proportion of triggered events. The statistical significance of these variations cannot be assessed until methods are developed for estimating confidence limits.

Some results depend on decisions adopted in the analysis. The proportion of triggered events decreases as the lower magnitude threshold is increased, possibly because our procedure for assigning independence probability favors larger earthquakes, or because a catalog with fewer events allows fewer triggering instances to be recognized. In some tests we censored earthquakes occurring near and just after a previous event, to account for the fact that most such earthquakes will be missing from the catalog. Fortunately the branching model parameters were hardly affected, suggesting that the inability to measure immediate aftershocks does not cause a serious bias.

1-092
LONG-RANGE EARTHQUAKE FORECASTING ALLOWING FOR AFTERSHOCKS
Rhoades DA

An earthquake occurrence model aimed at forecasting mainshocks can be adjusted to allow for the occurrence of aftershocks conforming to well-known empirical relations describing their temporal decay, magnitude distribution and spatial extent. Modifications are proposed to the EEPAS (Every Earthquake a Precursor According to Scale) long-range forecasting model to allow for the occurrence of aftershocks of predicted events. Using earthquake catalogues of California and the Kanto region, central Japan, versions of the modified and original EEPAS model are fitted to an early period and independently tested on a later period of each catalogue. For the testing period, the increase in the log likelihood per earthquake of the modified models over their original counterparts is about 0.1 on average. This gives preliminary confirmation of the efficacy of the modifications. Versions of the modified model will be submitted to regional testing centres of the Collaboratory for the Study of Earthquake Predictability for further independent performance testing in real time.

1-093
ESTIMATION OF ETAS MODELS FOR EARTHQUAKE OCCURRENCES *Chu A, Wong K, Schoenberg FP, Wang Q, Kagan YY, Jackson DD, Bird P, and Werner MJ*

Branching models such as Epidemic-Type Aftershock Sequence models have become widely used to describe earthquake occurrence data. There is, however, a lack of consensus on the particular form for the spatial distribution of triggered events. We review various forms proposed by Ogata (1998), as well as alternatives based on the analysis of relative spatial locations of earthquakes in Southern California. A discussion is given of the fitting of such models separately to data from various tectonic zones, such as those identified in Bird (2003), in order to summarize and compare the main empirical features of aftershock behavior in these zones. We also describe issues of bias in

the estimation of ETAS models, which are conventionally estimated by maximum likelihood. Under suitable conditions such a procedure produces estimates that have desirable asymptotic properties such as unbiasedness, consistency, and efficiency. In practice, however, earthquake catalogs are typically limited only to earthquakes above some lower threshold magnitude, and the fact that many smaller events are not observed can lead to substantial biases in the estimation of ETAS parameters.

1-094

WHY BASS, NOT ETAS *Turcotte DL, Van Aalsburg JD, Abaimov SG, and Rundle JB*

What is the ETAS model? It is a stochastic model for the generation of aftershock sequences. It is based on the concept of parent and daughter earthquakes. The number of daughter earthquakes that a parent earthquake generates is determined randomly from a productivity relation. The magnitude and time of occurrence of each daughter earthquake is determined randomly from the Gutenberg-Richter and Omori laws. Each first generation daughter earthquake becomes a parent for second generation daughters, and so forth until the sequence dies out. What is the BASS model? The BASS model is the self-similar limit of the ETAS model. Instead of the productivity relation, the modified form of Bath's law is used. The two arbitrary parameters in the productivity relation are replaced by the b-value in the GR law and the magnitude difference Delta m* between the parent earthquake and the largest expected daughter earthquake. Why is the BASS model preferred to the ETAS model? Because the BASS model is in better agreement with observations than the ETAS model. Specifically: (1) The BASS model generates Bath's law statistics since they are an input; (2) The BASS model generates inverse GR statistics for foreshock generation. The distribution of magnitudes of foreshocks is independent of the mainshock magnitude. The ETAS model has an exponential dependence of foreshock magnitude on the mainshock magnitude which is not in agreement with observations. Why do ETAS model proponents reject the BASS model? Because the BASS model is inherently unstable generating infinite numbers of aftershocks. However, this instability is easily removed by making the physically reasonable hypothesis that the excess magnitudes of daughter earthquakes over the parent earthquake cannot exceed a specified difference.

1-095

EXTENDING THE CISN EARTHQUAKE EARLY WARNING (EEW) WEB SITE INTO THE CISN EEW TESTING CENTER USING CSEP TESTING CENTER CONCEPTS AND SOFTWARE *Zeleznik MP, Maechling PJ, Liukis M, Callaghan S, Boese M, Hauksson E, Cua G, Solanki K, Allen RM, Neuhauser D, Hellweg M, Fischer M, Heaton TH, and Jordan TH*

As a part of the California Integrated Seismic Network (CISN) earthquake early warning (EEW) algorithm development, funded through USGS NEHRP, we have developed the CISN EEW web site to collect the results of multiple EEW algorithms and to display these results in a comparative manner (*http://www.scec.org/eew*). During the last year, the CISN EEW algorithm development group defined a set of EEW algorithm evaluation tests (termed performance summaries). These compare EEW algorithm reports (generated by the real-time or near real-time EEW algorithms) against seismicity data in the ANSS catalog and observed ground motion information available through the SCEC Data Center (SCECDC) and the Northern California Earthquake Data Center (NCEDC). To automatically generate the performance summaries, a software development group at SCEC has integrated elements of the SCEC Collaboratory for the Study of Earthquake Predictability (CSEP) Testing Center into the CISN EEW web site. This has helped establish a CISN EEW Testing Center with capabilities similar to the CSEP Testing Center. After the integration of the CSEP software, the CISN EEW testing center now automatically creates EEW performance summaries and posts them on the CISN EEW web site each day.By leveraging the capabilities of

the CSEP Testing Center, the CISN EEW Testing Center has been able to implement several of the testing concepts originally developed on CSEP. These concepts include the following: (a) earthquake, or ground motion, forecasts are reported in standardized data formats, (b) commonly-agreed upon performance evaluation reports are used for all algorithms, (c) observed data is retrieved from "authorized" data sources and the same observed data is used to evaluate all algorithms, (d) only forecasts and observed data for a specific testing region are considered, and (e) the testing center saves information indicating how results were produced. In this poster, we present an overview of the CISN EEW Testing Center including the scientific design goals for the system, and a description of the system's current capabilities. We describe the performance summaries specified by the CISN EEW algorithm development group, and how the current CISN EEW Testing Center produces those summaries using the automated testing capabilities from the CSEP software framework.

1-096
STATIONARY STATISTICS AND ERGODICITY: IMPLICATIONS FOR EARTHQUAKE FORECASTING *Tiampo KF, Klein W, Li H, Mignan A, Toya Y, Rundle JB, and Chen CC*

In recent years, several different forecasting methods based upon the quantification of patterns in seismicity data, but relying on different approaches, have been proposed with varying degrees of success (Keilis-Borok, 1982; Bowman et al., 1998; Tiampo et al., 2002). However, the physical basis of these methods is not always well understood. This lack of understanding presents a significant barrier to the determination of the accuracy of these methods, the best route to improving their forecasting capability, and the possible limits to their accuracy as imposed by the physics. Recently the equilibrium property of ergodicity was identified in an earthquake fault system (Tiampo, et al., 2007). Ergodicity in this context not only requires that the system is stationary for these networks at the applicable spatial and temporal scales, but implies that they are in a state of metastable equilibrium in which the ensemble averages can be substituted for temporal averages when studying their behavior in space and time. Here we show that this property can be used to identify those regions of parameter space which are stationary using a particular measure of ergodic behavior, the TM metric (Thirumalai et al., 1989). We apply this measure to one particular seismicity-based forecasting tool, the PI index (Tiampo et al., 2002), in order to test the hypothesis that the identification of ergodic regions can be used to improve and optimize forecasts that rely on historic seismicity catalogs and to synthetic catalogs in order to better understand the physical process that affects this accuracy. We show that these ergodic regions, defined by magnitude and time, provide more reliable forecasts of future events in both natural and synthetic catalogs. Ergodicity can be used to identify those spatiotemporal regions for which the statistics of these fault systems are stationary and suggests that earthquake forecasting methodologies based upon the linearized analyses of seismic catalog data require that certain equilibrium properties, such as stationarity, are necessary to produce accurate results.

1-100
USING SEISMICITY TO IDENTIFY CHANGES IN THE LOCAL STRESS FIELD DUE TO THE LANDERS 1992 EARTHQUAKE *Latimer CD, and Tiampo KF*

It has long been recognized that large earthquakes affect and are affected by the stress in the crust in the region which they occur. The regional stress orientation is measured and used with earthquake modeling, particularly those involving stress changes (King et al., 1994). The change in the local stress field due to an earthquake is not so easily determined, but carries the same importance in understanding the mechanics of earthquakes. Work has started with the goal of determining the local stress field around the Landers 1992 Californian earthquake. To create our

reference model, we use the Pattern Informatics (PI) method (Tiampo et al., 2002) which identifies areas of increase and decrease in the seismicity rate for days to months after the earthquake event. Of particular increase are the areas of seismic quiescence, which are related to "stress shadows" often calculated using Coulomb stress changes (Stein, 1992; Stein, 1999; Tiampo et al., 2006). We will use slip models of the Landers earthquake to calculate the Coulomb stress changes (Lin and Stein, 2004; Toda et al., 2005), and manipulate the constitutive parameters in order to recreate a stress field comparable to that of the reference model. These parameters include the calculation depth, the coefficient of friction, and most importantly the principal stress orientations. Currently, we assume a uniform stress field, but further studies will introduce the complication of heterogeneities which might improve the scale and detail of the resulting models. Determining the stress field can improve earthquake modeling, and thus advance our understanding of the principal mechanics involved with them.

1-101
QUANTIFYING LONG AND SHORT-RANGE EARTHQUAKE TRIGGERING AS A FUNCTION OF DYNAMIC STRAIN *van der Elst NJ, and Brodsky EE*

Remote earthquake triggering by dynamic strain from seismic waves is a regularly observed feature of earthquake interactions. However, the effectiveness of dynamic strains at triggering earthquakes has not been well quantified. Do dynamically triggered earthquakes make up a large proportion of earthquakes as a whole? Here we quantify the rate at which dynamic strains trigger earthquakes at long distances, using the ANSS and JMA earthquake catalogs, and compare pre-and post-trigger interevent time statistics. We find that the intensity of dynamic triggering scales continuously as a function of peak dynamic strain, estimated from the seismic wave amplitude. We compare these rates to aftershock triggering rates very near a mainshock, and find that dynamic triggering can account for the majority of local aftershocks. Dynamic triggering also appears to be ubiquitous -- not confined to geothermal and magmatic provinces. Some regions however, like California, are more prone to triggering than others, like Japan. This result points the way to a new methodology for earthquake forecasting based on the amplitude of the observed seismic waves.

1-102
EVIDENCE FOR MOGI DOUGHNUT BEHAVIOR IN SEISMICITY PRECEDING SMALL EARTHQUAKES IN SOUTHERN CALIFORNIA *Shearer PM, and Lin G*

We examine the average space-time behavior of seismicity preceding M 2–5 earthquakes in southern California from 1981 to 2007 using a high-resolution catalog and identify regions of enhanced activity in a 1-day period preceding larger earthquakes at distances comparable to their predicted source radii. The difference in precursory behavior between large and small earthquakes is subtle but statistically significant when averaged over many earthquakes, and has similarities to the "Mogi doughnut" seismicity pattern observed to occur prior to some M 6 and larger earthquakes. These results indicate that many standard earthquake triggering models do not account for all of the processes involved in earthquake occurrence.

Crustal Deformation Modeling (CDM)

1-097

DETAILED SEISMIC AND TECTONIC MOMENT RATE DISTRIBUTION IN CALIFORNIA AND THE GREAT BASIN *Kreemer C, Torres R, Zaliapin I, Pancha A, and Anderson JG*

Regional earthquake occurrence rate and seismic moment rate estimates are an integral part of any physics-based seismic hazard assessment. Ultimately, one would want to be able to connect the moment rate from the observed seismicity to its long-term predictions based on geodetic and geological information. Previous statistical research, theoretical and numerical, has found that geodetic and geological information can improve significantly the catalog-based estimations of the moment rate and earthquake occurrence models. In this study we compared a most detailed geodesy- and geology-based expected moment release with the observed one on different temporal and spatial scales in California and the Great Basin. We have analyzed GPS data from all continuous sites in California and the Great Basin and combined the resulting horizontal velocities with those from published campaign-style studies. A high-resolution continuous strain rate tensor model is derived from an interpolation of those geodetic velocities. Additional constraints on the style, rate, and localization of strain are incorporated from Quaternary faults used in the 2002 Seismic Hazard Map. The strain rate model is characterized by having both the highest strain rates narrowly concentrated along major faults as well as lower strain rates heterogeneously distributed over the remaining plate boundary. Strain rates are converted to long-term, or tectonic, moment rate estimates for sub-regions of varying size. This tectonic moment rate is then compared with the observed earthquake occurrence rate and seismic moment release. The comparison with the observed moment rate clearly demonstrates a well-documented moment deficiency that arises due to the combination of the heavy-tailed distribution of seismic moment and the typically short time-span of catalogs. Our results expand the previously established spatio-temporal bounds of the statistical modeling framework for the seismic moment release from hundreds of years and thousands of kilometers down to years and tens of kilometers.

1-098

EFFECTS OF 3-D VARIATIONS IN FAULT GEOMETRY AND ELASTIC STRUCTURE ON GEODETIC VELOCITIES, VENTURA BASIN REGION, CALIFORNIA *Lu J, Gable CW, Williams CA, and Hager BH*

Geodetic observations of interseismic elastic strain accumulation and coseismic strain release are sensitive to the heterogeneous rheology of the lithosphere. Even though models assuming simple rheology might fit observed geodetic velocities well, conclusions about fault behavior could be biased if lateral and vertical variations of the lithosphere's mechanical properties are not accounted for. We are developing 3-D Crustal Deformation Models (CDM) of southern California using the Finite Element Method (FEM), accounting for realistic fault geometries provided by the SCEC Community Fault Model (CFM) and 3-D variable elastic properties provided by the SCEC Community Velocity Models (CVM). We are using the mesh generation package LaGriT to create the meshes. To perform the modeling itself, we are using PyLith. The model we present here encompasses the region around the Ventura Basin, including the San Cayetano, Oak Ridge and Santa Susana faults.

We perform three different calculations of coseismic displacements of the Ventura Basin model: 1) analytic models using the rectangular dislocation based (CFM-R) fault geometry assuming homogeneous elastic properties; 2) FEM models using our meshing of the T-surf based CFM assuming homogeneous elastic properties; 3) FEM models using our meshing of the CFM including

elastic structure from the latest CVM-H. We also explore different boundary conditions by assuming a) fixed, b) free and c) displacements computed from analytical models. By comparing model results, we find that both realistic fault geometry and inhomogeneous elastic structure have significant effects on the surface displacements. The effects of differing fault geometry can reach surprisingly far from the faults in certain places; the CFM-R fault model does not always provide a good representation of the CFM. The effects of the inhomogeneous elastic structure on surface displacements are substantial in a much broader region and the inhomogeneous model shows more concentrated deformation across the basin. Incorporating the variations of elastic properties and fault geometry, coseismic displacements can differ on the order of 30~40% in the near field, and the azimuth can differ by as much as 90 degrees. We conclude that ignoring realistic variations in fault geometry by using rectangular dislocations and ignoring 3-D elastic structure can lead to large errors in calculations of coseismic and interseismic displacements.

1-099
DIGITAL FAULT MODEL VISUALIZATION AND INTERACTION *Yikilmaz MB, Van Aalsburg JD, Kreylos O, Kellogg LH, and Rundle JB*

Digitial Fault Models (DFM) play a vital role in the study of earthquake dynamics, fault-earthquake interactions, and seismicity. DFMs serve as input for finite-element method (FEM) or other earthquake simulations such as Virtual California. Generally, digital fault models are generated by importing a digitized and georeferenced (2D) fault map and/or a hillshade image of the study area into a geographical information system (GIS) application, where individual fault lines are traced by the user. Data assimilation and creation of a DFM, or updating an existing DFM based on new observations, is a tedious and time-consuming process. In order to facilitate the creation process, we are developing an immersive virtual reality (VR) application to visualize and edit fault models. This program is designed to run in immersive environments such as a CAVE (walk-in VR environment), but also works in a wide range of other environments, including desktop systems and GeoWalls. It is being developed at the UC Davis W.M. Keck Center for Active Visualization in the Earth Sciences (KeckCAVES, *http://www.keckcaves.org*). Our program allows users to create new models or modify existing ones; for instance by repositioning individual fault-segments, by changing the dip angle, or by modifying (or assigning) the value of a property associated with a particular fault segment (i.e. slip rate). With the addition of high resolution Digital Elevation Models (DEM) , georeferenced active tectonic fault maps and earthquake hypocenters, the user can accurately add new segments to an existing model or create a fault model entirely from scratch. Interactively created or modified models can be written to XML files at any time; from there the data may easily be converted into various formats required by the analysis software or simulation. We believe that the ease of interaction provided by VR technology is ideally suited to the problem of creating and editing digital fault models. Our software provides the user with an intuitive environment for visualizing and editing fault model data. This translates not only into less time spent creating fault models, but also enables the researcher to easily generate and maintain any number of models for use in ensemble analysis.

1-103
STRESS UNCERTAINTIES OF THE SAN ANDREAS FAULT SYSTEM *Smith-Konter BR, Solis T, and Sandwell DT*

Major ruptures along the San Andreas Fault System (SAFS) are driven by stress accumulation in the upper locked portion of the crust. Stress rate and the accumulated stress on a fault over several earthquake cycles depends largely on fault slip rate, locking depth, fault rheology, and the rupture history of a fault over the past few thousand years. Uncertainties in paleoseismic slip history, combined with ongoing discrepancies in geologic/geodetic slip rates and variable locking depths

throughout the earthquake cycle can introduce moderate uncertainties in stress rate and in present-day stress accumulation calculations. For example, a number of recent geodetic studies have challenged geologic slip rates along the SAFS, varying by as much as 25% of the total slip budget; geodetically determined locking depths, while within the bounds of seismicity, typically have uncertainties that range from 0.5-5.0 km. Furthermore, uncertainties in paleoseismic chronologies can span several decades, with slip uncertainties on the order of a few meters.

To assess the importance of both paleoseismic estimates and basic stress model components, we use a 3-D semi-analytic time-dependent deformation model of the SAFS and perform a sensitivity analysis of Coulomb stress rate and present-day accumulated stress with respect to the six primary parameters of our model: slip rate, locking depth, mantle viscosity, elastic plate thickness, coefficient of friction, and slip history. In each case, we use our current best fitting geodetic model as a starting point and calculate a stress derivative with respect to a parameter over the estimated range of uncertainty and parameter tradeoffs. Our results suggest that a 20% change in system-wide slip rates will yield a change in stress rate by only 0.5-1.0 MPa/100yrs, whereas a 50% decrease in locking depth can increase stress rates by as much as 5 MPa/100yrs. We also examine stress accumulation changes based on a suite of plausible historical faulting scenarios; for example, when 70% of estimated paleoseismic slip is modeled, we calculate a ~0.5-2.0 MPa increase in stress accumulation spanning several segments of the SAFS. These example stress sensitivity analyses emphasize the importance of both geologic and geodetic data contributions, and their associated uncertainties, for identifying critical missing data that may help further quantify stress evolution and seismic hazards of the SAFS.

1-104

AFTERSHOCK DISTRIBUTION AS A CONSTRAINT FOR THE 2004 PARKFIELD EARTHQUAKE COSEISMIC SLIP MODEL *Bennington N, Thurber CH, and Feigl K*

We present preliminary results for a coseismic slip model for the 2004 Parkfield earthquake where geodetic observations from the event were used to obtain the slip model with the constraint that edges of the slip patches align with aftershocks. This constraint is based on the hypothesis that coseismic slip on a patch may increase the stress on an adjacent patch where no slip has occurred. This could in turn cause aftershocks to occur at the edges of coseismic slip patches. Adapting the method of Gallardo and Meju [2004, 2007], our technique uses the cross gradient (the cross product of the gradients of slip and aftershock density) as a weighted penalty function to encourage the edges of the slip model to align with the aftershock distribution. The aftershock distribution and slip model are considered structurally identical when the cross gradient value in each cell is minimized. The gradient values associated with the aftershocks are non-zero only within and along the edges of the aftershock clusters, and they are largest at the edges of the clusters. Thus, minimization of the cross-gradient constraint should produce a preferred solution where the edges of coseismic slip patches are encouraged to align with the aftershocks clusters. More over, the coseismic slip model is allowed to change freely in locations devoid of aftershocks. Cross validation is used to select optimal weights for smoothing and the cross gradient penalty with the optimal weights chosen as those which minimize the average residual.

Our initial results show coseismic slip to be very compact with the majority of slip extending from 4 to 6 km depth. This is in contrast to previously published coseismic slip models for the event, which show the majority of slip extending over a broader depth range (~4 to 10 km depth). While the distribution of slip for this model differs greatly from that of previously published results, the predicted surface displacements fit the observed data quite well with a chi-square value of 405. The same geodetic data were used to obtain a coseismic slip model that excluded the aftershock

distribution constraint. The resulting coseismic slip model has a similar distribution to previously published slip models with a chi-square value of 371.

1-105
FRICTION PARAMETERS INFERRED FROM NUCLEATION OF AFTERSLIP FOLLOWING THE 2003 TOKACHI-OKI EARTHQUAKE *Fukuda J, Johnson KM, Larson KM, and Miyazaki S*

We use high-rate GPS measurements of postseismic deformation in the first five hours following the 2003 Tokachi-oki earthquake located off-shore of Hokkaido, Japan to estimate frictional parameters of the afterslip zone on the subduction interface. The data show little motion immediately after the earthquake with sudden acceleration at about 1.2 hours after the mainshock. We interpret the delayed acceleration as nucleation of afterslip. We model the GPS time series using a spring-slider system obeying a rate-state friction law. An inversion method is developed to estimate the posterior probability distributions of critical slip distance, D_c, a*sigma, and (a-b)*sigma, where a and b are friction parameters and sigma is effective normal stress. The estimated values of D_c, a*sigma, and (a-b)*sigma are 1.1*10^(-3) m, 0.32 MPa, and 0.217 MPa, respectively. Estimated D_c is 10 to 10^3 times larger than laboratory values. Estimated (a-b)*sigma is consistent with previous estimates from afterslip models.

1-106
THE 2008 WELLS EARTHQUAKE, NEVADA FROM ENVISAT ASAR DATA *Nee P, and Funning GJ*

An earthquake of magnitude 6.0 struck Wells, Nevada on February 21st, 2008 at 6:16AM PST. The epicenter was located approximately 10 km northeast of the city of Wells with a depth of 6.7 km according to the Nevada Seismological Laboratory. Over 20 buildings were reported severely damaged, over 700 buildings lightly damaged and more than three people were injured (NEIC). It was Nevada's most destructive earthquake since the magnitude 7.1 earthquake in December, 1954 near Dixie Valley.

The Wells earthquake epicenter is covered by four Envisat ASAR tracks with multiple coseismic pairs of images on each. One descending pair from track 127 (baseline 210 m, spanning 140 days) and one ascending pair from track 220 (27 m, 140 days) were used in our analysis. Interferograms were processed using ROI_PAC and a digital elevation model from the Shuttle Radar Topography Mission. Our data show a four-fringe deformation signal in both pairs, which implies approximately 12 cm of peak downward displacement of the ground. We subsample our data using a quadtree decomposition and run inverse elastic dislocation models using the 'okinv' code in order to find a best-fitting set of fault parameters. We obtain a satisfactory fit to data with both nodal planes; however we prefer the model with a SE-dipping fault (strike 31, dip 33, rake -97, depth 3.2-9.8 km, Mw 6.0), which has a smaller misfit to data and agrees with aftershock locations, which also favor a SE dip (*http://www.seismo.unr.edu/feature/2008/Preliminary_relocations1.pdf*). This preliminary model has dip of 33 degrees which is shallower than that obtained by seismic waveform inversion (e.g. global CMT, UC Berkeley).

1-107
PYLITH: A FINITE-ELEMENT CODE FOR MODELING QUASI-STATIC AND

DYNAMIC CRUSTAL DEFORMATION *Aagaard B, Williams CA, and Knepley MG*

We have developed open-source finite-element software for 2-D and 3-D dynamic and quasi-static modeling of crustal deformation. This software, PyLith (current release is version 1.3), combines the quasi-static viscoelastic modeling functionality of PyLith 0.8 and its predecessors (LithoMop and Tecton) and the wave propagation modeling functionality of EqSim. The target applications contain spatial scales ranging from tens of meters to hundreds of kilometers with temporal scales for dynamic modeling ranging from milliseconds to minutes and temporal scales for quasi-static modeling ranging from minutes to hundreds of years. PyLith is part of the NSF funded Computational Infrastructure for Geodynamics (CIG) and runs on a wide variety of platforms (laptops, workstations, and Beowulf clusters). It uses a suite of general, parallel, graph data structures called Sieve for storing and manipulating finite-element meshes. This permits use of a variety of 2-D and 3-D cell types including triangles, quadrilaterals, hexahedra, and tetrahedra. Current features include kinematic fault ruptures, Dirichlet (displacement or velocity), Neumann (traction), and absorbing boundary conditions, linear elastic, generalized Maxwell, and Maxwell linear viscoelastic materials, gravitational body forces, and automatic time step selection for quasi-static problems. Future releases will add dynamic fault interface conditions (employing fault constitutive models), additional viscoelastic and viscoplastic materials, and automated calculation of suites of Green's functions. We also plan to extend PyLith to allow coupling multiple simultaneous simulations. For example, this could include (1) coupling an interseismic deformation simulation to a spontaneous earthquake rupture simulation (each using subsets of the software), (2) coupling a spontaneous earthquake rupture simulation to a global wave propagation simulation, or (3) coupling a short-term crustal deformation simulation to a mantle convection simulation and an orogenesis and basin formation simulation.

1-108

CO-SEISMIC DISPLACEMENT FROM THE MW7.9 SICHUAN EARTHQUAKE DERIVED FROM ALOS RADAR INTERFEROMETRY *Tong X, Sandwell DT, and Mellors R*

On May 12th 2008, a Mw 7.9 earthquake struck Wenchuan county, Sichuan Province in China. The causalities include approximately 70,000 dead and 374,000 injured. The rupture accompanying the events extended over 270 km toward the northeast, and is a result of the convergent tectonic movement associated with Longmen Shan fault.

We assemble ALOS PALSAR data including 6 tracks, totally 36 frames, to map the co-seismic displacement with a full coverage of 400 km by 400 km of the fault zone. We use SIOSAR to process the dataset, including pre-processing, SAR image focusing, matching the slave scenes to the master scenes, phase calculating, and topographic correcting. The code has been revised to apply more precise orbit information to remove the phase discontinuity of adjacent frames along a single track. More, the topographic phase has been shifted according to cross correlation to improve the phase correction. So far, we have processed 4 tracks and the interferogram of track 473 is consistent with those of the other groups. However, we found a trending error in the phase of the track 471. In the future, two more tracks will be analyzed to get the complete displacement field. Either pixel offset measurements or ScanSAR mode interferometry is required to acquire the 3 dimensional displacement field. GPS displacement measurements, especially in the large ground motion area, will support the analysis on co-seismic and post-seismic deformation. Models of post-seismic deformation, driven by the co-seismic stress perturbation, will provide important estimation of seismic hazards from future earthquakes and aftershocks.

1-109
CREEP EPISODES ON THE SUPERSTITION HILLS FAULT: A SILENT M5.0 EVENT OCTOBER 3-6, 2006 *Wei M, Sandwell DT, and Fialko Y*

During October of 2006, the 20-km long Superstition Hills fault in Salton Trough, Southern California, slipped aseismically producing maximum offset of 27 mm as recorded by a creep meter. We investigate this creep event as well as the spatial and temporal variations in slip history since 1992 using ERS-1, ERS-2, and Envisat Satellites data. During this 15-year period, quasi-steady creep is punctuated by at least three events. The first two events are associated with the 1992 Landers and 1999 Hector Mine earthquakes suggesting the creep events were dynamically triggered. In contrast, there is no obvious triggering mechanism for the October 2006 event. Field measurements of fault offset after the 1999 and 2006 events are in good agreement with the InSAR data suggesting the creep is highly localized. A dislocation model of the 2006 creep event shows that the slip is concentrated in the upper 500 m with a maximum depth of 2-3 km. The moment released during this event is equivalent to a Mw5.1 earthquake; it is surprising that such a significant event produced no detectable aftershocks and was not recorded by the continuous GPS stations in the area. Modeling of the long-term creep (1992 to 2000) using stacked ERS interferograms also shows a maximum creep depth of 2-3 km with slip concentrated in the upper 500 m. This is shallower that the basement depth of 3-5 km suggesting that the creep depth is unrelated to sediment thickness.

1-110
MULTI-SCALE BLOCK MODELING OF THE PACIFIC-NORTH AMERICA PLATE BOUNDARY ZONE *Meade BJ, and Loveless JP*

To understand geodetic constraints on both regional tectonics and seismic hazard we present results from a block model for southern California that is consistent with the kinematics of the western United States (including Pacific-North America-Juan de Fuca plate motions). At the synoptic scale of southern California, we use the rectilinear Community Fault Model and at the scale of the Los Angeles basin we model the Puente Hills thrust system, and Parkfield segment of the San Andreas fault using triangulated fault surfaces as defined in the Community Fault Model. By embedding locally high-resolution fault geometry within a regionally consistent model we can simultaneously analyze regions of complex faulting and estimate plate motions at larger scales. The block modeling technique accounts for the effects of local block rotations, elastic strain accumulation, and a parameterization of deformation that can be effectively represented as internal block strain. Estimates of internal block strain allow us to determine; 1) whether or not we have failed to include structures that accommodate significant deformation, 2) are there particular regions of internal blocks strain that are correlated with macroscopic parameters such as heat flow or rock type?, and 3) the fraction of deformation (in terms of geometric moment) accommodated on structures explicitly represented in our model. We use ~1500 GPS stations to estimate kinematically consistent fault slip rates in southern California and estimate spatially variable slip on the the individual sections of the Puente Hills thrust. This analysis allows for an assessment of how similar the present day pattern of deformation is to geologic estimates.

1-111
THREE-DIMENSIONAL MODELS OF ELASTO-STATIC DEFORMATION IN HETEROGENEOUS MEDIA: APPLICATION TO THE EAST CALIFORNIA SHEAR ZONE *Barbot S, Fialko Y, and Sandwell DT*

The static displacements accompanying the 1992 Mw 7.3 Landers and the 1999 Mw 7.1 Hector Mine earthquakes in the East California Shear Zone (ECSZ) exhibit localized strain along the trace of nearby active faults, as revealed by anomalous line-of-sight (LOS) displacements in radar

interferograms (InSAR). We investigate the potential of compliant zones (CZ), areas with reduced elastic moduli compared to ambient rock, to explain the radar observations. We derive an iterative procedure that evaluates the three-dimensional deformation due to the presence of faults in an arbitrary heterogeneous half space, with vertical as well as lateral variations in elastic properties. The latter are modeled with equivalent body forces and equivalent surface traction in a homogenized elastic medium. Displacement field in the computational volume is obtained in the Fourier domain using semi-analytic Greens' functions. We find that CZs in the ECSZ along the Rodman, the Calico and the Pinto Mountain faults can explain simultaneously InSAR data for the Landers and the Hector Mine earthquakes. InSAR data require a 60% reduction in effective rigidity in the Pinto Mountain CZ accompanied by a 7% increase in Poisson's ratio compared to ambient crust. Large wavelength of LOS displacements around the Pinto Mountain fault is best modeled with a CZ extending to at least 9km depth. Best fit for the Rodman and the Calico CZs, north of Galway Dry Lake, is obtained for a 4.5km deep CZ, with a 60% reduction in shear modulus and 0% and 20% increase in Poisson's ratio for the Calico and the Rodman CZ, respectively. We find that required effective rigidity reduction in the Calico CZ, south of Galway Dry Lake is less dramatic than in the northern segment, demonstrating possible along-strike variations of effective elastic moduli within a long CZ. Best model thickness for the Mojave desert CZ varies between 0.8 and 1.5km. These observations suggest pervasive and widespread damage around active crustal faults.

1-112
MODELING SENSITIVITY OF GPS NETWORKS TO GROUND DEFORMATION IN SOUTHERN CALIFORNIA *Williams NR, and Lohman RB*

We generated strain and error models from Global Positioning System (GPS) data for the Southern California (SoCal) Fault System and quantified the impact of potential new campaign observations. We explored varying levels of spatial smoothing to determine shear strain and dilation, and performed Monte Carlo tests to determine the expected variance on these values. Extending the temporal span of GPS observations for individual stations will decrease model errors and result in better estimates on strain or other model parameters. This improvement factor can determine which GPS stations in SoCal would most benefit the geophysical modeling of Southern California faults if resurveyed. We conducted similar tests on determining slip rate and errors of some of the major SoCal faults. We converted these results to files viewable in Google Earth and made them available on a public website for easy distribution and visualization. Future work may include a comparison to updated models from Crustal Motion Map version 4 to determine the accuracy of estimated error improvements.

1-113
NEW GEODETIC DATA FOR CRUSTAL DEFORMATION IN THE SAN BERNARDINO MOUNTAINS *Velasquez CM, and McGill SF*

Global Positioning System (GPS) data in the vicinity of the San Bernardino Mountains are minimally existent. At 16 survey sites GPS data were gathered for a time span of twenty-four hours or more. At remotely located survey sites data were gathered for two to five continuous days. Differences in rates at the various benchmarks will be used to infer the amount of elastic strain that is accumulating due to faults in the vicinity. The measurements that have been collected are currently being processed at the University of Arizona by Rick Bennett and Joshua Spinler. When combined with prior data collected in 2005, the new data will provide the first GPS velocity vectors for many parts of the San Bernardino Mountains.

In addition to collecting new GPS data, one-dimensional elastic modeling of data from SCEC's Crustal Motion Model version 3 (CMM3) was conducted along a transect through the San

Bernardino Mountains from San Clemente Island to southwestern Nevada. Published Holocene to late Pleistocene slip rates (Peterson et al., 1996) for faults within the transect do not fit the GPS velocity data from CMM3. The CMM3 data are best fit by rates in the Eastern California shear zone (ESCZ) that are higher than rates estimated over geologic time scales, and by rates for the San Andreas and San Jacinto faults that are lower than published geologic rates. Locking depths of13-18 km were used in the modeling (Peterson et al., 1996). Slip rates that fit the CMM data well are as follows: the Eastern California shear zone, 20 mm/yr; San Andreas fault, 11 mm/yr; San Jacinto fault, 6mm/yr; the Elsinore fault, 5 mm/yr; the NIFZ, 2 mm/yr, and the Palos Verde fault, 3 mm/yr. The discrepancy between geologically and geodetically estimated slip rates for the San Andreas and San Jacinto faults and for the ESCZ could be a result of variations in strain accumulation rates at different stages of the earthquake cycle (for a viscoelastic medium). The low rate of geodetically measured strain accumulation on the San Andreas fault could be because it is in the late stage of the earthquake cycle. The high rate of strain accumulation modeled in the ECSZ could be a result of recent activity--the Landers and Hector Mine earthquakes. An alternative hypothesis could simply be that the San Andreas fault is no longer the primary fault in the vicinity, but movement has been shifted to the ECSZ within the last few decades.

1-114
B4-AUGMENTED IDENTIFICATIONS OF SAN ANDREAS FAULT SURFACE FEATURES: SPATIAL STRUCTURE OF THE PLATE BOUNDARY BETWEEN BOMBAY BEACH AND DESERT HOT SPRINGS *Lynch DK, and Hudnut KW*

We present preliminary results of a hyper-accurate (± few m) inventory of SAF features between Bombay Beach and Desert Hot Springs based on overhead imagery. The ultimate goal is to identify fault features that can be used to determine offset distance and slip rates. Many fault structures have been previously reported and about two dozen new ones have been found in this study. Using approximately 80 fault components we defined a map view piecewise continuous trace of features (and interpolations when no structure could be discerned) that we are calling the provisional plate boundary (PPB). The resulting PPB trace closely matches the faults reported by Clark (1984) and those in the qfaults data base. We analyzed the PPB and present evidence of spatial structure on scales of a few hundred meters.

1-115
SMALL-SCALE UPPER MANTLE CONVECTION AND CRUSTAL DYNAMICS IN SOUTHERN CALIFORNIA *Fay NP, Bennett RA, Spinler JC, and Humphreys ED*

We present numerical modeling of the forces acting on the base of the crust caused by small-scale convection of the upper mantle in southern California. Three-dimensional upper mantle shear wave velocity structure is mapped to three-dimensional density structure that is used to load a finite element model of instantaneous upper mantle flow with respect to a rigid crust, providing an estimate of the tractions acting on the base of the crust. Upwelling beneath the southern Walker Lane Belt and Salton Trough region and downwelling beneath the southern Great Valley and eastern and western Transverse Ranges dominate the upper mantle flow and resulting crustal tractions. Divergent horizontal and upward directed vertical tractions create a tensional to transtensional crustal stress state in the Walker Lane Belt and Salton Trough, consistent with transtensional tectonics in these areas. Convergent horizontal and downward directed vertical tractions in the Transverse Ranges cause approximately N–S crustal compression, consistent with active shortening and transpressional deformation near the ''Big Bend'' of the San Andreas fault. Model predictions of crustal dilatation and the forces acting on the Mojave block compare favorably with observations suggesting that small-scale upper mantle convection provides an important contribution to the sum of forces driving transpressional crustal deformation in southern

California. Accordingly, the obliquity of the San Andreas fault with respect to plate motions may be considered a consequence, rather than a cause, of contractional deformation in the Transverse Ranges, itself driven by downwelling in the upper mantle superimposed on shear deformation caused by relative Pacific–North American plate motion.

1-116
MODELING OF MULTIPLE EARTHQUAKE CYCLES IN SOUTHERN CALIFORNIA USING THE COMMUNITY FAULT MODEL *Williams CA, Gable CW, Hager BH, and Meade BJ*

To understand the complicated fault interactions in southern California, one useful approach is to create simulations that examine a long history of interseismic and coseismic slip on a large number of faults. Each of these faults will have different slip rates and average earthquake recurrence times, providing different time-varying contributions to the predicted surface deformation field as well as the overall stress field. When viscoelastic behavior is considered, it is necessary to 'spin up' such models so that near steady-state behavior is achieved. As a first step in providing such simulations we have computed several simulations using a subset of the faults in the Community Fault Model (CFM).

We use the analytical block model of Meade and Hager (JGR, 2005) to compute a consistent set of block rotation poles for a subset of the blocks defined in their model. Although these rotation poles were computed using a simplified rectangular fault geometry, our finite element simulations use the full geometry defined by the CFM. Our present model consists of 11 blocks, which are bounded by 55 of the faults from the CFM. The model is purely kinematic, and is driven by a combination of coseismic slip above the 15 km locking depth and velocity boundary conditions consistent with the computed rotation poles applied along the lateral boundaries of the mesh.

We examine several different rheological models, including homogeneous elastic, heterogeneous elastic (using the Community Velocity Model), Maxwell viscoelastic, and generalized Maxwell viscoelastic (two Maxwell models in parallel). We use published recurrence times for the main faults, and use a simple empirical rule to assign recurrence times for the additional faults. The simulations are run for a sufficient period of time to allow each fault to experience several coseismic events. Since the faults of the CFM do not form closed blocks, we also examine the effects of allowing stress and strain dissipation using viscoelastic behavior in the upper crust.

1-117
TECTONIC UPLIFT RATES FROM NEW IN-SITU COSMOGENIC AGES ON TERRACE SURFACES IN THE OJAI VALLEY, W. TRANSVERSE RANGES, CALIFORNIA *Heermance RV*

Fluvial terraces provide distinctive geomorphic markers useful for constraining the timing and amount of uplift, incision, and deformation within tectonically active regions. Furthermore, strath terraces represent times of lateral erosion, which occurs under specific hydraulic conditions that can be related to either tectonics or climate. New cosmogenic ages from fluvial terraces within the Ojai valley of the Western Transverse Ranges indicate major strath erosion between 15,000-10,000 years before present (y.b.p), and an earlier period of strath formation circa 30,000-25,000 y.b.p. The height of these abandoned floodplains above the active Ventura riverbed, combined with the new ages, yield incision rates of at least 1-3 mm/year since at least 15,000 y.b.p. Surprisingly, these rates imply that the valley bottom is uplifting at rates similar to those observed in the mountain range adjacent to the valley. Comparison of terrace ages with paleoclimate indicators from ODP drill core 893a in the nearby Santa Barbara Channel suggest that the Ojai terraces formed just after a climatic

shift from dry (~50 mm rainfall/year) to wet (~100 mm rainfall/year) at ~14,000 y.b.p. This climate shift caused an increase in sediment load and discharge during a time of rapidly rising sea level (base level). Although aggradation might be expected during this time of rising base level, the very weak bedrock within the Ojai Valley was preferentially eroded instead of aggradation of the more-resistant, coarse-grained fluvial river sediment, creating the broad alluvial strath-terraces of the Ojai Valley. A change to a drier climate during the Holocene caused incision and abandonment of these terrace straths. The new geochronologic data presented here suggest that much of the Ojai landscape developed only over a few thousand years, and that rapid uplift has combined with climate shifts to control landscape evolution.

1-118
SIMULATING HETEROGENEOUS ROCK PROPERTIES IN CRUSTAL DEFORMATION MODELS: PRELIMINARY RESULTS *Marshall ST, Cooke ML, and Owen SE*

Using a two-step Boundary Element Method approach, we simulate geologic and interseismic deformation along multiple interacting non-parallel faults in the Los Angeles and Ventura regions of southern California. Models with homogeneous rock properties match well geologic slip rate data. Interseismic model results, in general, reproduce GPS velocities well, but mismatch GPS velocities at several sites within the Los Angeles and Ventura sedimentary basins. We suggest that much of the model-GPS misfit is produced by two main factors: many large geodetic gradients are likely non-tectonic in nature, and the model is unable to simulate the mechanics of spatially-variable rock properties such as those that are likely to occur between uplifted basement rocks (high stiffness) in the mountains and subsiding sedimentary basins (low stiffness) in the valleys. To better constrain the effects of heterogeneous rock properties on resultant deformation patterns and fault slip rates, we develop a methodology for simulating compliant (less stiff) regions within an otherwise homogeneous model. To simulate a region of less stiff rock (e.g. a sedimentary basin), we populate the specified region with randomly-oriented cracks, which accumulate slip and interact based on the applied tectonic boundary conditions. To validate this technique, we create an unfaulted rectangular-shaped compliant zone in a two-dimensional Finite Element Method model and compare results to our Boundary Element Method model simulation.

1-119
FAULT SLIP RATE ESTIMATES FOR SOUTHERN CALIFORNIA USING VISCOELASTIC PLATE-BLOCK MODELS *Chuang Y, and Johnson KM*

Estimates of fault slip rates using geodetic data are model dependent. For example, it has been demonstrated that models that assume an elastic earth with creeping faults extending to infinite depth may yield different slip rate estimates than a model with faults in an elastic plate overlying a viscous substrate. The most comprehensive fault slip rate estimates using GPS data for southern California are derived from elastic block models. In these models, tectonic blocks bounded by faults are assumed to move as undeformed bodies over the long-term. During the interseismic period, elastic strain accumulation due to locking of faults is modeled as a perturbation to this long-term block motion and steady fault slip with back-slip on locked portions of faults using dislocations in an elastic half-space. However, using this model, slip rate estimates for the Garlock Fault, Mojave segment of the San Andreas Fault, and the San Bernadino bend in the San Andreas Fault are all significantly lower than estimates from geologic data.

We are examining the possibility that the discrepancy between slip rates estimated using geologic and geodetic data can be attributed to assumptions in the forward model and inversion scheme. We examine a suite of models with either spatially uniform or variable interseismic creep on faults

and either low or high asthenosphere viscosities to examine the effect of model assumptions on slip rate estimates. In particular, we are developing a new block models for southern California in which faults are modeled in an elastic lithosphere overlying a viscoelastic asthenosphere. The 3D viscoelastic block model is an extension of 3D elastic block models previously developed. Our 3D viscoelastic cycle model also uses the concept of a "steady-state" deformation field in the absence of fault locking, similar to elastic block models. The interseismic velocity field is obtained by modifying the steady-state velocity field with contributions from interseismic fault locking and periodic earthquakes on faults.

Preliminary results suggest that models with low asthenosphere viscosity infer low slip rates on the above-mentioned faults, consistent with the results of elastic block models. Decreasing the asthenosphere viscosity raises the estimated fault slip rates. We show that the model slip rates approach the high geologic slip rates on the Mojave segment and San Bernadino segment with asthenosphere viscosities less than 10^19 Pa s.

1-120
METHODS FOR ESTIMATING FAULT SLIP RATES USING GEODETIC AND GEOLOGIC DATA *Johnson KM, and Fukuda J*

Significant discrepancies between slip rates estimated using geodetic data and slip rates estimated from geologic data are surfacing in the literature. Perhaps the most recognized is the discrepancy between geologic and geodetic estimates of fault slip rate on the Altyn Tagh fault in northwestern Tibet where inversions of geodetic data infer a slip rate of 4-10 mm/yr and geologic estimates range from 8-34 mm/yr. Inversions of GPS data in southern California illustrate not only discrepancies between geodetic and geologic estimates of fault slip rates, but also discrepancies between different models of geodetic data. Inversions using elastic half-space block models by Becker et al. [2004] and Meade and Hager [2005] infer fault slip rates in the Mojave desert region of southern California that are a factor of two or more lower than geologic estimates on the Garlock fault and the San Andreas and San Bernadino segments of the San Andreas fault. In contrast, a joint inversion of GPS, geologic, and focal mechanism data by McCaffrey [2005] results in slip rate estimates on these fault segments that are consistent with the geologic estimates.

It is not yet clear the extent to which the noted discrepancies between geodetic and geologic estimates of fault slip rates are real differences due to sampling of time-varying slip rates at different times, or errors in the calculation of geodetic or geologic rates. One possibility for the discrepancies is that the model used to estimate slip rate from geodetic data is wrong or that the inversion method is insufficient.

We outline a method for modeling long-term and interseismic deformation of elastic lithospheric blocks moving over a viscoelastic asthenosphere. We present a fully probabilistic scheme for inverting geologic and geodetic data for model parameters including fault slip rates, earthquake recurrence times, lithosphere thickness, and asthenosphere viscosity. The forward model and inverse method are designed to address the limitations of previous methods and to allow for the integration of multiple data sets, such as geodetic and geologic data, into a unified probabilistic estimation of the uncertainties in our knowledge of long-term block motions and fault slip rates.

Lithospheric Architecture and Dynamics (LAD)

1-121

INTERNATIONAL COLLABORATION IMAGES THE NORTH ANATOLIAN FAULT SYSTEM IN MARMARA SEA, TURKEY: SUBSIDED LOWSTAND DELTAS, ONLAPPING BASIN FILL, THRUST-FOLD TRANSVERSE RIDGES, TRANSTENSION, AND DISTRIBUTED ACTIVE FAULTING *TAMAM Scientific Party**

We collected high-resolution multichannel seismic reflection (MCS) data to image the North Anatolian Fault (NAF) and basin sediments in the Marmara Sea. The North strand of the NAF, passing closest to Istanbul, is considered to carry most of the current and late Holocene plate motion, based on GPS data, historic seismicity and onshore trenching. Three >1200 m-deep bathymetric basins and the 800 m-deep Kumburgaz basin are arrayed along the northern NAF. Our results may support long-standing yet still controversial suggestions that the NW-SE releasing segment of the northern NAF is non-vertical with a normal component of slip, and that this ongoing process is responsible for the basin. However, additional advanced data processing (migration) is planned to better image the fault geometry. Extension or transtension, however, are by no means universal within Marmara Sea. We image transverse (NE-SW) ridges between the basins to be thrust-related anticlines. We also imaged large-scale deep-seated landslide complexes on the basin flanks that are important contributors to basin fill.

Our chirp data image several strands of the southern fault system, 50 km south of the northern NAF, to offset strata above the Last Glacial Maximum unconformity. A WNW-striking segment of the intervening Imrali fault system is associated with normal-separation, 300 m-high sea floor scarps, and numerous young secondary faults in its hanging-wall. There, stacked low-stand shelf edge deltas, whose tops were formed near sea level or lake level, are now >400 deep. Sea level and climate cycles control delivery of sediment to the deep basins, resulting in a repeating pattern of onlapping fill on the progressively-tilting basin flanks. We will attempt to relate the onlapping fill events to the succession of low-stand deltas by tracing horizons via regional strike profiles.

MCS profiles with simple migrations indicate that the E-W segment of the NAF through Kumburgaz basin adjacent to western Istanbul is associated with shortening structures. The deep part of a N-dipping transpressional fault there would be closer to western Istanbul than would a south-dipping transtensional NAF.

*Selin D. Akhun, A. Evren Buyukasik, Melis Cevatoglu, Günay Çifçi, Süleyman Coskun, Emin Demirbag, John Diebold, Derman Dondurur, Savas Gurcay, Caner Imren, H. Mert Kucuk, Hülya Kurt, Pinar G. Özer, Emre Perinçek, Leonardo Seeber, Donna Shillington, Christopher C. Sorlien, Michael Steckler, and Duygu Timur

1-122

SOUTHERN CALIFORNIA MODELING OF GEODYNAMICS IN 3D (SMOG3D): TOWARD QUANTIFYING THE STATE OF TECTONIC STRESS IN THE SOUTHERN CALIFORNIA CRUST *Fay NP, Becker TW, and Humphreys ED*

We present results from numerical modeling of three-dimensional geodynamics of the southern California lithosphere. Our primary objective is to quantify how faults are loaded and, more generally, the state of stress in the southern California crust. We evaluate how buoyancy and rheology control this stress state, and aim to better understand the relationships to active deformation and earthquakes, horizontal coupling between tectonic plates, and the vertical coupling between the lithosphere and upper mantle. We use a 3D finite element approach

incorporating visco-elastic-plastic rheology to model the viscous and frictional behavior of the crust and mantle lithosphere. Density heterogeneities within the crust and upper mantle (surface topography, Moho topography, and mantle seismic/density anomalies) produce a state of deviatoric horizontal tension in the Transverse Ranges with principal stresses of ~5-20 MPa. These stresses must be balanced by compression caused by crustal block motions related to plate interaction. We also present results of modeling the southern California lithosphere under shear (representing relative Pacific Plate motion) with embedded faults of the San Andreas system. We find that if all the faults of the San Andreas system are of similar long-term shear strength, deviatoric tension is produced in the central and eastern Transverse Ranges. Models with the San Andreas weaker than other major faults (e.g., 10 MPa San Andreas, 30 MPa San Jacinto, depth-averaged shear strength) produce compression in the Transverse Ranges suggesting the San Andreas may be weaker than other faults in the system. Further work will include incorporating lateral variations in lithospheric viscosity and self-consistent determination of the effects of buoyancy variations on lithospheric viscous flow.

1-123
THE MECHANICS OF CONTINENTAL TRANSFORMS: IMPLICATIONS FOR THE TECTONICS OF CALIFORNIA *Platt JP, Becker TW, and Kaus BJ*

Displacement on intracontinental transforms is commonly distributed over a zone several hundred km wide, and may incorporate large regions of transtensional and transpressional strain, but no consensus exists on what controls the distribution and style of this deformation. We model the transform boundary as a weak shear zone of finite length that exerts shear stress on the deformable continental lithosphere on either side. Strain rate decreases away from the shear zone on a scale related to its length. Force balance in this system requires gradients in shear-strain rate normal to the shear zone to be balanced by gradients in stretching rates parallel to the zone. The shear-zone parallel gradients create zones of lithospheric thickening and thinning distributed anti-symmetrically about the shear zone. Simple analytical estimates, two-dimensional (2D) spectral models, and 2D/3D numerical models give consistent indications of the spatial scales and magnitudes of the zones of uplift and subsidence. Using reasonable parameter values, the models yield geologically relevant rates. Strain-rate components inferred from the GPS-determined 2-D velocity field, and analysis of seismicity using Kostrov's method, taken together with the geological data on the distribution of active faults, uplift, and subsidence, suggest that the distribution and rates of active deformation in California are consistent with our predictions. This validates the assumptions of the continuum approach, and provides a tool for predicting and explaining the tectonics of California and of other intracontinental transform systems.

1-124
EFFECTS OF LATERAL VISCOSITY VARIATIONS ON THE DYNAMICS OF

WESTERN NORTH AMERICA *Ghosh A, Becker TW, and Humphreys ED*

We investigate the effects of lateral viscosity variations (LVVs) and long-range force transmission on the dynamics of the deforming North American lithosphere, with focus on the western region close to the plate boundary. We address the question how the basal shear tractions as generated by mantle convection affect the stress field in North America on top of the inherited gravitational potential energy variations. Our goal is to find a model that self-consistently explains both kinematic surface constraints and internal deformation indicators. For the latter, our efforts are partially motivated by the finding of Humphreys & Coblentz (2007) that an inversion for plate forcing requires cratonic drag and mantle tractions, but at a reduced amplitude from the

predictions of an earlier model without LVVs by Becker & O'Connell (2001). Traction amplitude variations can be induced by LVVs, and a major source of such variations underneath North America is the presence of old continental lithosphere with underlying cratonic keels. Those keels are inferred to be high viscosity and reach deep into the mantle, up to a depth of ~300 km. The presence of the thick high viscosity keel, along with weak plate boundaries, likely creates large LVVs, which will potentially have long-range effects on the deformation of the North American plate. We quantify these effects by computing the basal tractions globally using a high resolution finite element mantle convection code, CitcomS, that can take into account several orders of lateral viscosity variations. The flow in the model is driven by density anomalies, as imaged by seismic tomography. Since the relative viscosities of the stiff keel and the weak plate boundaries are poorly constrained, a number of models with varying viscosities are tested. The stress fields associated with these predicted tractions are then compared with stress observations such as the World Stress Map and strain-rates from the Global Strain Rate Map. The ultimate goal is to construct a global, spherical geodynamic model that is adapted to the North American plate. This background model can provide information on how long-distance forcing affects regional tectonics, such as in southern California. This will in turn provide a deeper understanding of how faults in this region are loaded and how strain is localized on the plate boundary.

1-125
CONSTRAINING THE EVOLVING ARCHITECTURE OF THE PLATE BOUNDARY ZONE THROUGH 3D SEISMIC VELOCITY AND ANISOTROPY MAPPING *Kosarian M, Davis PM, Clayton RW, and Tanimoto T*

The two main data sources for seismic anisotropy in Southern California, SKS splitting data and surface wave data, show inconsistent patterns. The primary goal of this project is to understand the source of this discrepancy and to obtain a seismic structure that satisfies both sets of data. The key must be in the depth variations in anisotropy, as the two types of data have different depth sensitivities. We formulated a scheme to invert surface waves and obtained S-wave velocity anisotropy maps. We present results of crust and mantle anisotropy derived from measurements of core–refracted phases (SKS and SKKS) recorded at stations in Southern California. We calculated splitting parameters using a single layer anisotropy model. We have made new shear wave splitting measurements for 126 seismic stations with best data (50 earthquakes out of 190 earthquakes) for the period of 1990-2008. On average, fast directions are east-west with about 1 second delay. For the surface wave anisotropy model we computed predicted SKS splitting times from the mantle-lithosphere. We find that predicted splitting times are much less than SKS splitting times. The surface wave fast axes directions are also different in that our results are mostly parallel to the relative plate motion direction. Larger variations closer to the major faults also seem to be a new observation. Anisotropic structure derived from surface waves clearly cannot explain SKS splitting data. We suggest that the SKS waves are sensitive to the deeper parts of the upper mantle.

1-126
ANELASTIC EARTH STRUCTURE FROM THE AMBIENT SEISMIC FIELD *Prieto GA, Beroza GC, and Lawrence JF*

Cross correlation of the ambient seismic field is now routinely used to measure seismic wave travel times; however, relatively little attention has been paid to other information that could be extracted from these signals. In this paper we demonstrate the relationship between the spatial coherency of the ambient field and the elastodynamic Green's function in both time and frequency domains. Through measurement of the frequency domain coherency as a function of distance, we sequentially recover phase velocities and attenuation coefficients. From these measurements we generate 1D shear wave velocity and attenuation models for southern California. The ambient field

measurements of attenuation and the exceptional path coverage that results from the many inter-station measurements, allow us to extend Q estimates to higher frequencies than has previously been possible using earthquake data. Measurements from paths that cross major sedimentary basins show both slower wave speeds and lower quality factors than other paths, as expected. Our results indicate that there is a wealth of information available in the spatial coherency of the ambient seismic field.

1-128
UPPER MANTLE P VELOCITY STRUCTURE BENEATH SOUTHERN CALIFORNIA FROM TELESEISMIC TOMOGRAPHY USING LOCAL AND REGIONAL ARRAYS
Schmandt B, and Humphreys ED

Strong seismic heterogeneity in the upper mantle beneath Southern California has been revealed by several tomographic studies. Previous models require complex seismic structure on a variety of length-scales, and include high amplitude velocity anomalies at depths ranging from near Moho to greater than 200 km. Resolution of such structures is limited by the depth distribution of crossing rays, and modeling of finite frequency and ray bending effects on travel times. We use broadband data from USArray, permanent regional networks, and temporary deployments spanning 1997 through 2008 to create a new model of upper mantle P velocity. Our tomographic imaging method uses ray-theoretical travel time sensitivity kernels, and we are currently working on iterative 3-D ray tracing to mitigate ray bending effects. In the future we plan to model S velocity and incorporate new 3-D crustal velocity models in our analysis.

1-129
BASAL CRUSTAL ANISOTROPY BENEATH THE SAN GABRIEL MOUNTAINS AND ADJACENT INNER BORDERLAND: A FOSSIL REGIONAL DETACHMENT? *Zandt G, Porter RC, and Ozacar AA*

Receiver functions calculated for long-operating seismic stations in southern California located in the San Gabriel Mountains (MWC, CHF) and adjacent Inner Borderland (RPV) exhibit converted phases from the mid- to lower-crust and Moho with large variations in amplitude and polarity reversals on both the radial and transverse components. These data characteristics are similar to those observed at station PKD located in the Salinian terrane near Parkfield, central California. The large amplitudes and small move-out of the phases, and the broad similarity of data patterns on widely separated stations support an origin primarily from a sub-horizontal layer of hexagonal anisotropy with a dipping symmetry axis, rather than planar dipping interfaces. However, in some cases, localized dip or offsets on the interfaces may contribute to complexity in the data (Yan and Clayton, 2007).

Neighborhood algorithm searches for depth and dip of interfaces, and trend and plunge of anisotropy symmetry axis have been completed for station PKD and are in progress for the other stations. At PKD, the best fitting models require a 6-km-thick, high Vp/Vs layer at the base of the crust with slow axis hexagonal anisotropy > 15% and a slow axis orientation consistent with ENE dipping (~35 degree) rock fabric. A very similar anisotropy model is recovered from the preliminary MWC data inversion and is anticipated for the other stations with similar data characteristics.

The orientation of the anisotropy is consistent with a fossilized fabric created from top-to-the-west sense of shear that existed along the length of coastal California during past subduction. Under MWC the top of the anisotropic layer is at ~20 km, the approximate depth of the San Gabriel Bright Spot (SGBS) observed in LARSE I reflection data ~20 km to the east, and modeled by a 500-m-thick,

low-velocity layer. Ryberg and Fuis (1998) interpreted it as a possible "master" decollement for active thrust faults in the area. A possible explanation for this apparent age contradiction is that the SGBS is a young feature that was localized at the top of an older and thicker regional detachment layer.

1-130
MARINE SEISMIC STUDY OF THE PACIFIC-NORTH AMERICAN PLATE BOUNDARY *Kohler MD, and Weeraratne D*

To study the Pacific-North America plate boundary in southern California, a diffuse, transpressional, 500+ km wide interplate zone of deformation, we present plans to deploy 24 ocean bottom seismometers (OBS) in a passive seismic experiment offshore. This experiment will complement the simultaneous recording of excellent land based instruments provided by arrays such as the California Integrated Seismic Network (CISN) and the recent occupation of USArray and improve our understanding of the physical properties and deformation style of the Pacific plate contributing to plate boundary dynamics. The marine seismic experiment, to be deployed in July 2010 for a 12 month period, will extend westward across the borderlands, cover the Arguello and Patton microplates, and include relatively undisturbed ~9 My Pacific seafloor at its western most extent. Data and results from this work will be integrated with crustal and lithospheric studies in the SCEC program to improve our understanding of the plate boundary considering both North American and Pacific plate dynamics and deformation. Three-dimensional variations in upper mantle seismic velocity, seismic anisotropy, and improved local earthquake location by surface wave, body wave, and shear wave splitting analysis will be used to identify variations in lithospheric plate thickness, faulting, plate fracture, rotational dynamics, and mantle flow patterns at mantle depths for comparison with surface observables and styles of deformation on the North American crust and lithosphere. Seismic anisotropy will also be utilized to differentiate between recent models for asthenospheric flow in western north America. Extended seismic coverage by OBS's offshore is also expected to produce a more accurate offshore hypocenter catalog that can be used to identify spatial relationships between background seismic activity with mapped offshore faults.

1-131
MODELING SOUTHERN CALIFORNIA CRUSTAL ANISOTROPY USING TELESEISMIC RECEIVER FUNCTIONS *Culp DB, Sheehan AF, Schulte-Pelkum V, and Shearer PM*

The detection and modeling of seismic anisotropy is a powerful tool for mapping 3-dimensional crustal fabrics in a variety of tectonic settings. Crustal deformation can lead to fabric development in the middle and deep crust, which may result to zones of seismic anisotropy, detectable by a variety of methods. Recent improvements in teleseismic converted wave (receiver function) techniques can be used to provide insight into kilometer-scale crustal structures under Southern California. While there have been numerous studies of receiver functions in Southern California in the past, few have emphasized features in the midcrust or anisotropic signatures from the converted waves. The current research builds upon our previous work with crustal anisotropy and converted waves in the Himalaya and New Zealand, with new applications to the broadband seismic stations of the Southern California Seismic Network. Focusing on the highest quality long-term stations in the greater Los Angeles area, which are most likely to have a good distribution of teleseismic events with backazimuth, we have begun to model crustal features, including depth to Moho, midcrustal arrivals, and possible anisotropic structures. Anisotropic features can be modeled using the observed backazimuthal variations in the radial and transverse receiver functions. Strong patterns with back-azimuth have been recognized at a number of stations, which

we will model in terms of underlying structure. Our ultimate plan is to trace the structures modeled at the long-term seismic stations to those from dense shorter-term deployments in order to create a map of midcrustal interfaces beneath the Los Angeles region. These analyses will help determine the extent that detachment surfaces found in 1D reflection/refraction profiles in the Los Angeles region continue laterally, and will provide information complementary to ongoing seismicity, structure, and deformation modeling studies of the region.

1-132
SUBSURFACE STRUCTURE BENEATH SAN FERNANDO VALLEY, SOUTHERN CALIFORNIA, BASED ON SEISMIC, POTENTIAL-FIELD, AND WELL DATA
Langenheim VE, Okaya DA, Wright TL, Fuis GS, Thygesen K, and Yeats RS

We provide new perspectives on the subsurface geology of San Fernando Valley, home of two of the most recent damaging earthquakes in southern California, from analysis of multichannel seismic profiles acquired by the petroleum industry, interpretation of potential-field data, and the LARSE (Los Angeles Regional Seismic Experiment) II deep-crustal profiles. The combined geological and geophysical datasets permit a new 3-D analysis of this basin, with structure contour maps of various Quaternary to Miocene horizons providing insight into the bounding structures of this valley.

Seismic reflection data are primarily located in the north central and southwestern parts of the valley and provide depths to four Quaternary to Miocene horizons, showing in greater detail the Northridge Hills anticline and the Mission Hills syncline as well as additional smaller folds throughout the valley. These data also reveal a down-to-the-north fault beneath the Northridge Hills thrust fault that corresponds to thinning of the Neogene section and narrowing of the Northridge Hills anticline and a north-dipping unconformity at the base of the Plio-Pleistocene Saugus Formation. Beneath the base of the late Miocene Modelo formation are largely non-reflective rocks of the Topanga and older formations. Crystalline basement is only imaged on one profile in the SE part of the valley, revealing a down-to-the-north fault that does not offset the top of the Modelo. Gravity data show that this fault strikes NW and bounds a concealed basement high, which influenced the Miocene Tarzana fan. LARSE refraction data image basement.

Gravity and seismic-refraction data indicate that the basin underlying San Fernando Valley is asymmetric, with the north part of the basin reaching depths of 5-8 km. LARSE II data show that the basin fill in the north part of the valley has higher velocity than that south of the Mission Hills fault. Magnetic data suggest a major boundary at or near the Verdugo fault, the SE margin of the basin, and show a change in the dip sense of the fault along strike. The western margin of the basin as defined by gravity data is linear and strikes about N45E. The NE-trending gravity gradient follows part of the 1971 San Fernando aftershock distribution called the Chatsworth trend and the aftershocks of the 1994 Northridge earthquake. These data may suggest that the 1971 San Fernando and 1994 Northridge earthquakes may have reactivated portions of Miocene normal faults.

1-133
NON-VERTICAL DIPS OF THE SOUTHERN SAN ANDREAS FAULT AND THEIR RELATIONSHIPS TO MANTLE VELOCITIES, CRUSTAL TECTONICS, AND EARTHQUAKE HAZARD *Scheirer D, Fuis GS, Langenheim VE, and Kohler MD*

The San Andreas Fault (SAF) in southern California is in most places non-vertical, based on seismic-imaging, potential-field, earthquake-aftershock, and selected microseismicity studies of the crust. The dip of the SAF changes from SW (55-75 degrees) near the Big Bend to NE (10-70 degrees) southeastward of the eastern San Gabriel Mountains, forming a crude propeller shape. The

uncertainty of most of the dip observations is about 5-10 degrees. To examine the geometry of the fault surface, we have developed a three-dimensional model of a dipping SAF, extending from Parkfield in central California to the SAF's southern termination at the Salton Sea. Knowledge about the dip of the SAF is important for estimating shaking potential of scenario major earthquakes and for calculating geodetic deformation.

In sections across the SAF, P-wave tomographic images of the mantle beneath southern California (Kohler et al., 2003) suggests that the plate boundary extends into the mantle and is continuous with the SAF in the crust. The dip of the plate boundary appears to steepen in the mantle. Seismicity sections across the locked part of the SAF, from Indio towards the northwest, reveal different seismicity regimes on either side of our model SAF surface, but do not reveal the fault itself. These differences include changes in the maximum depth of the seismogenic zone and in the abundance of seismicity over the past ~20 years. The different seismicity regimes may reflect changes in physical properties and/or stress state of the crust on either side of the SAF at seismogenic depths. Mantle velocities southwest of this projected plate boundary, within the Pacific Plate, are relatively high and constitute the well documented upper-mantle high-velocity body of the Transverse Ranges. This relationship is similar, in some ways, to that between the Alpine fault of New Zealand and its underlying mantle, and suggests that in both California and New Zealand, Pacific lithospheric mantle is downwelling along the plate boundary (Fuis et al., 2007).

1-134
GEOLOGY AND TECTONICS OF THE CHOCOLATE MOUNTAINS *Powell RE, and Fleck RJ*

The Chocolate Mountains (CM), situated along the NE margin of the southern Salton Trough, lie NE of the post-5-Ma San Andreas (SA) fault and SW of the southeastward projection of the early and middle Miocene Clemens Well (CW)-Fenner-San Francisquito-SA strand of the SA system. The CM are the western part of a highly extended terrain in SE CA and SW AZ that evolved during the late Oligocene-middle Miocene and is bounded to the NE by the CW-SA fault.

The principal structural feature in the CM is a complexly faulted, NW-trending array of en echelon antiforms that runs the length of the range and continues into AZ. Orocopia Schist in the core of the antiforms is structurally overlain by Proterozoic rocks (augen/pelitic/layered gneiss; anorthosite-syenite) and Mz mylonite, orthogneiss, and plutonic rocks (TR Mt Lowe, J mafic and intermediate rocks) at the ductile CM thrust.

All these units are intruded by a late Oligocene composite batholith comprising plutons of gabbro-diorite, granodiorite, and grante. Dacitic to rhyolitic hypabyssal, volcanic, and pyroclastic rocks cap the batholith, and are coeval with it. Younger Miocene volcanic rocks also are present.

Structure in the CM manifests late Oligocene-middle Miocene extensional tectonism that culminated in exhumation of Orocopia Schist by tectonic denudation. Tectonism was accompanied by sedimentation and by magma-generation forming the batholith and its volcanic cap. Brittle extensional faulting has largely reactivated and cut out the ductile CM thrust and has created a stack of fault plates in the basement rocks above the thrust and in a superjacent steeply west-tilted section of syntectonic Oligocene-Miocene redbeds, megabreccia, and volcanic and volcaniclastic rocks. Along the NE flank of the CM, the extensional fault stack was dropped to the NE along a normal fault representing final phase of extension.

Field relations and dating the widespread Cz igneous rocks allows us to bracket intervals of extensional deformation between the late Oligocene and middle Miocene. In the context of an ongoing or intermittent extensional regime between about 28 and 13 Ma, our 40Ar-39Ar dates and many published K-Ar dates indicate intervals of extensional faulting ca 28-24 Ma, 24 to 20 Ma, and 19 to 13 Ma. The latter interval is coeval with displacement on the CW-SA strand of the early SA system, suggesting that diminishing strike-slip displacement on that fault is accommodated southeastward on CM normal faults.

1-135

DOES THE WEST SALTON DETACHMENT EXTEND THROUGH SAN GORGONIO PASS, SOUTHERN CALIFORNIA? *Matti JC, and Langenheim VE*

We use geologic and geophysical data to speculate on continuation of the West Salton Detachment (WSD)—a key element of the early San Andreas Fault system—northwestward beyond its last known occurrence along the east side of the Santa Rosa Mts. We propose that the WSD originally extended from the NW head of Coachella Valley west into San Gorgonio Pass (SGP), where the detachment probably forms the base of the late Cenozoic marine and terrestrial sedimentary sequence south of the Banning strand of the San Gabriel Fault. The WSD probably continues west beyond SGP, with extensional translation decreasing until the detachment intersects the Banning Fault near Calimesa. There, we propose that the WSD bounds a subsurface sedimentary package north of the San Timoteo badlands and south of the Banning Fault that a gravity low suggests is 2 km thick, and that purportedly contains marine sediment penetrated in boreholes. When ~44 km of right-slip is restored on the Banning Fault (Matti and Morton, 1993), the gravity low restores opposite a similar low in the northwestern Coachella Valley. The juxtaposed gravity lows thus mark a late Cenozoic depocenter that formed at the northwestern head of the nascent Salton Trough during evolution of the San Gabriel and San Andreas Faults (10 Ma to 1.2 Ma).

This reconstruction has several implications: (1) the WSD was active while the late Cenozoic sedimentary sequence in SGP accumulated in its hangingwall at 7 Ma (marine Imperial Fm) and probably as early as 8-9 Ma (Hathaway Fm); (2) At that time the San Jacinto Mts (SJM) began to rise in the WSD footwall, shedding sediment and landslide breccia into the SGP basin. Simultaneously, Transverse Ranges sources shed sediment southwest, south, and southeast into the SGP basin and the adjoining San Timoteo basin; (3) Prior to disruption by right-slip on the Banning Fault, the WSD probably extended around the NW head of the nascent Salton Trough, where the detachment would have separated crystalline rock of SGP from hangingwall deposits of the Salton Trough (Coachella Fanglomerate, Imperial and Painted Hill fms). The enigmatic Whitewater Fault in the SE San Bernardino Mts may be the WSD. (4) Because extensional translation on the WSD diminished westward through SGP, it is doubtful that >3 km of topographic relief on the WSD footwall in the SJM resulted only from footwall uplift during the period 8-9 Ma to 1.2 Ma. Quaternary uplift must account for an unknown component of this relief.

1-136

CONTROLLED-SOURCE SEISMIC IMAGING OF RIFT PROCESSES AND EARTHQUAKE HAZARDS IN THE SALTON TROUGH *Hole JA, Stock JM, and Fuis GS*

The NSF MARGINS program, the NSF EarthScope program, and the U.S. Geological Survey have funded a large seismic refraction and reflection survey of the Salton Trough in southern California and northern Mexico, including the Coachella, Imperial, and Mexicali Valleys. The goals of the project include both rifting processes at the northern end of the Gulf of California extensional province and earthquake hazards at the southern end of the San Andreas fault system. In the central Salton Trough, the 20-22 km thick rifted crust is apparently composed entirely of new crust

added by magmatism from below and sedimentation from above. The seismic survey will image the effects of rapid sedimentation upon extension and magmatism during continental rifting. The vertical and lateral partitioning of strain will be investigated in this oblique rift. The southernmost San Andreas Fault is considered at high risk of producing a large damaging earthquake, yet structure of the fault and adjacent basins are not currently well constrained. The seismic survey will image the structure of the San Andreas and Imperial Faults, structure of sedimentary basins in the Salton Trough, and three-dimensional seismic velocity of the crust and uppermost mantle. Fieldwork is tentatively scheduled for January 2010. The purpose of this poster and a workshop to be held immediately after the 2008 SCEC meeting is to communicate plans for the seismic project and encourage synergy with piggyback and complementary studies.

Group 2. Poster Abstracts

Plaza Ballroom, Hilton Palm Springs Resort

Unified Structural Representation (USR)

2-001

SCEC COMMUNITY VELOCITY MODEL (CVM-H 5.5) *Plesch A, Shaw JH, Hauksson E, and Tanimoto T*

We present a new version of the SCEC Community Velocity Model (CVM-H version 5.5) that incorporates several enhancements to better facilitate its use in strong ground motion prediction and seismic hazards assessment. These improvements include updates to the background models, basin structures, geotechnical layer, and the code that delivers the CVM-H. The extent of the model was expanded to an area between longitudes 120d52'20"W and 113d19'16"W and latitudes 30d56'49"N and 36d37'17"N to accommodate larger numerical experiments.

Improvements to the basin structures include new Vp, Vs, and density parameterizations within the Santa Maria and Ventura basins that are based on direct velocity measurements from petroleum well logs and seismic reflection data. These new basin structures were used as input for the development new P and S wave tomographic velocity models, and a new upper mantle teleseismic and surface wave model. The CVM-H thus consists of the revised basin representations embedded in self-consistent regional crust and upper mantle models. In addition, we also enhanced the geotechnical layer (GTL) representation. The GTL in the major sedimentary basins remains unchanged, following the approach of the SCEC CVM 4.0 (Magistrale et al., 2000). In bedrock sites, however, we implemented a new GTL based on the depth-velocity relations of Boore & Joyner (1997). In this implementation, we used the empirical velocity gradient from Boore & Joyner (1997) to scale upwards from the base of the GTL (top of basement). This bedrock GTL implementation results in gradual velocity gradients and variable velocities at the surface.

In addition, we provide a series of enhancements to the C-code that delivers the CVM-H. This code specifies Vp, Vs, and density values at arbitrary points (x,y,z) defined by the user by locating the nearest neighbor grid point in the appropriate CVM-H voxet. The new model version consists of high (250m) and medium (1000m) resolutions voxets, or regular grids, defining both Vp and Vs structure (density is derived using a scaling relationship from Vp). To support the needs of SCEC scientists who employ the code to help parameterize their computational grids, we enhanced the code to deliver several additional functions. First, the code now provides the location, in addition to the value, of the nearest neighbor grid point. This allows users to identify the locations where the values were initially parameterized in the CVM-H, ensuring data integrity and supporting the use of a variety of interpolation schemes that can be tailored to the users application. A sample implementation of an interpolation routine which handles material boundaries correctly is provided. Second, the code now provides the depths (distances) from the arbitrary points to the surfaces used to construct the CVM-H, namely the surface topography/bathymetry, the top of crystalline basement, and the Moho. This information is of particular value when using the CVM-H to guide the construction of computational meshes.

2-002
TESTING COMMUNITY VELOCITY MODELS FOR SOUTHERN CALIFORNIA USING THE AMBIENT SEISMIC FIELD *Ma S, Prieto GA, and Beroza GC*

We correlate the vertical component of ambient seismic noise data recorded on 56 broadband stations with dense coverage in the greater Los Angeles area, to determine station-to-station Green's functions. These Green's functions provide an important test of community velocity models (SCEC CVM 4.0 and CVM-H 5.2) used for strong ground motion prediction for future scenario earthquakes in southern California. Comparisons of the ambient-noise Green's functions for nearly 300 paths, with those calculated by the finite-element method in the community velocity models reveal a strong waveform similarity for the dominant surface waves between 0.1 and 0.2 Hz. We find a mean correlation coefficient between the ambient-noise and finite-element Green's functions of 0.62 for the CVM 4.0 and 0.49 for the CVM-H 5.2, indicating stronger waveform similarity for CVM 4.0. We also find that for 77% of the paths, the surface waves in the finite-element Greens' functions for CVM 4.0 arrive early, suggesting that the CVM 4.0 has velocities in the upper 10 km that are too fast along these paths. The same bias is evident for CVM-H 5.2, but is substantially smaller, with only 61% of the paths too fast. For 67% of the paths CVM 4.0 has velocities faster than CVM-H 5.2. The time lags we obtain between the ambient-noise and finite-element Green's functions provide key information for improving future community velocity models.

2-003
RESOLVING 3D FAULT GEOMETRY AT DEPTH ALONG ACTIVE STRIKE-SLIP FAULTS: SIMPLE OR COMPLEX? *Nicholson C, Hauksson E, Plesch A, and Shearer PM*

A primary concern for SCEC in terms of understanding earthquake rupture and seismic hazard is resolving active 3D fault geometry at seismogenic depths. This is particularly important for properly extrapolating near-surface observations to depth where principal ruptures occur. This collaborative project is using recently developed seismicity and focal mechanism catalogs to identify the geometry and sense of slip of active fault segments at depth, and to help evaluate the SCEC Community Fault Model (CFM). This comparison forms the basis for identifying and developing improved fault representations for CFM, as well as identifying possible systematic biases in hypocentral location or fault models. In several places, aligned hypocenters are systematically offset from CFM 3D fault surfaces. This offset could be the result of: a) incorrect extrapolation of mapped surface fault traces to depth; b) earthquake mislocation owing to velocity models or location procedures used; or possibly c) existence of previously unidentified active subparallel fault strands. Along the Elsinore fault, active fault segments exhibit dips that vary along strike from about 80°SW to near-vertical to 70°NE. However, in CFM this fault is presumed to be vertical. Similar changes in dip along strike are found for the adjacent Agua Tibia-Earthquake Valley fault. Where the Elsinore fault is multi-stranded, fault segments separated by only a few kilometers can either remain subparallel throughout the seismogenic zone, or merge at depth to form y-shaped structures and intervening half-grabens, as appears to be the case beneath Lake Elsinore. Farther north, where the fault zone splays to form the Whittier and Chino faults, the seismicity exhibits a more complex 3D fault structure that includes intersecting high- and low-angle faults, as reflected in the recent 2008 Chino Hills earthquake sequence. At issue is whether these complex fault geometries defined by the microearthquakes are necessarily representative of the primary, through-going strike-slip fault that will likely produce the major slip and seismic moment release, or whether these structures illuminated by the seismicity only represent adjacent secondary faults. This issue is particularly important along the San Andreas fault, where various sections are largely aseismic and where models of the fault geometry at depth--being either

relatively simple (vertical and planar) or more complex (non-vertical and non-planar)--have been proposed.

2-004
TERA3D: A TERA-SCALE FULL-3D WAVEFORM TOMOGRAPHY (F3DT) IN SOUTHERN CALIFORNIA *Chen P, Allam AA, and Jordan TH*

We are automating our full-3D waveform tomography (F3DT) and seismic source inversion algorithm based on the scattering-integral (SI) method and applying the automated algorithm to iteratively improve the 3D SCEC Community Velocity Model Version 4.0 (CVM4) in Southern California. In F3DT, the starting model as well as the derived model perturbation is 3D in space and the sensitivity kernels are calculated using the full physics of 3D wave propagation. The SI implementation of F3DT is based on explicitly constructing and storing the sensitivity kernels for individual misfit measurements. Compared with other F3DT implementations, the primary advantages of the SI method are its high computational efficiency and the ease to incorporate 3D Earth structural models into real-time seismic source parameter inversions. In a previous study, we have successfully applied the SI method to improve the 3D seismic velocity structure model (SCEC CVM3) and seismic source models in the Los Angeles region. In this presentation we will report our recent progresses on automating the complete F3DT workflow, including an automated phase-picking algorithm, and extending our analysis to a much larger region in Southern California.

2-007
STRONG SOUTHERN CALIFORNIA CRUSTAL HETEROGENEITY REVEALED BY ADJOINT TOMOGRAPHY *Tape CH, Liu Q, Maggi A, and Tromp J*

Adjoint tomography utilizes 3D simulations of seismic wave propagation in conjunction with a tomographic technique based on adjoint methods. We begin with an initial 3D model of shear and compressional wavespeeds for southern California provided by the Southern California Earthquake Center (SCEC; model CVM-H), extending to a depth of 60~km. We use the spectral-element method to simulate 140 good-quality local earthquakes, each recorded by as many as 160 stations. We compute misfits between observed and synthetic seismograms by using a new automated time-window selection algorithm that picks any time window within which the data and 3D synthetics are reasonably similar (e.g., P, S, Love, and Rayleigh waves). Within each time window we measure a frequency-dependent traveltime anomaly. For each record with a measurement, we compute an adjoint source that is used to create an adjoint wavefield. The interaction between the adjoint wavefield and the regular wavefield forms the gradient of the misfit function for one event. These gradients are combined using a source subspace projection method to compute a model update.

We are presently on the seventh iteration of a southern California crust and upper mantle model. Thus far we have applied changes in excess of +/- 20 percent from the initial 3D model. With each iteration, the changes in wavespeeds have improved the data fit, and we are able to include additional seismograms whose fits to the data for previous model iterations were too poor for selection. In general, the tomographic results compare well with surface geology, the most striking features being the low wavespeeds of the southern San Joaquin basin, the high wavespeeds and depth extent of the Santa Monica Mountains, the low wavespeeds in the Coast Ranges, the low wavespeeds in the eastern Mojave shear zone, and the sharp contrast at the eastern front of the Sierra Nevada due to volcanism in the Coso Junction area. Having applied relatively large-scale, large-amplitude changes, we can now exploit more of the shorter-period measurements to resolve and reveal km-scale features in the southern California crust.

2-008

LARGE EARTHQUAKES, AFTERSHOCKS, AND BACKGROUND SEISMICITY: ANALYSIS OF INTERSEISMIC AND COSEISMIC SPATIAL SEISMICITY PATTERNS IN SOUTHERN CALIFORNIA *Hauksson E*

We associate waveform-relocated background seismicity and aftershocks with the 3D shapes of late Quaternary fault zones in southern California. Major earthquakes that can slip more than several meters, aftershocks, and near-fault background seismicity mostly rupture different surfaces within these fault zones. Major earthquakes rupture along the mapped traces of the late Quaternary faults, called the principal slip zones (PSZs). Aftershocks occur in the immediate vicinity of the PSZs, within ±2 km wide fault zones. In contrast, the near-fault background seismicity is accommodated on a secondary heterogeneous network of small slip surfaces and forms spatially decaying distributions extending out to distances of ±10 km away from the PSZs. We call the regions where the enhanced rate of background seismicity occurs, the seismic damage zones. One possible explanation for the presence of the seismic damage zones and associated seismicity is that they develop as faults accommodate bends and geometrical irregularities in the PSZs. The seismic damage zones mature and reach their finite width early in the history of a fault, during the first few kilometers of cumulative offset. Alternatively, the similarity in width of seismic damage zones suggests that most fault zones are of almost equal strength, although the amount of cumulative offset varies widely. It may also depend on the strength of the fault zone, the time since the last major earthquake as well as other parameters. In addition, the seismic productivity appears to be influenced by the crustal structure and heat flow, with less active seismic damage zones in area of low heat flow and thick crust.

2-009

DETAILED P- AND S-WAVE VELOCITY MODELS ALONG THE LARSE II TRANSECT, SOUTHERN CALIFORNIA *Murphy JM, Fuis GS, Ryberg T, Lutter WJ, Catchings RD, and Goldman MR*

Structural details of the crust determined from P-wave velocity models can be improved with S-wave velocity models, and S-wave velocities are needed for model-based predictions of strong ground motion in southern California. We picked P- and S-wave travel times for refracted phases from explosive-source shots gathers of the Los Angeles Region Seismic Experiment, Phase II (LARSE II), and we developed refraction velocity models from these picks using two different inversion algorithms. Vp/Vs ratios were calculated from the resulting P- and S-wave models where both models are constrained by ray coverage. The two P-wave velocity models are compared to each other and to results from forward modeling. Generally, the P-wave inverse and forward models agree well for velocities lower than 5.0 km/s but only broadly agree with each other for velocities above 5.0 km/s. Similarly, the S-wave inverse models agree well with each other for velocities lower than 2.5 km/s but only broadly agree for velocities higher than 2.5 km/s. The most prominent structures in our S-wave models are two north-dipping low-velocity zones in the Central Transverse Ranges that we interpret as faults. These low-velocity zones differ somewhat between the two inversion models, but the Vp/Vs models (one model for each technique) show these features to be remarkably similar. Interestingly, both Vp/Vs models have several features that are not visible in either the P- or S-wave models alone. Two of these features (relatively high Vp/Vs ratios) occur in the vicinity of wells that bottom in "granitic" rocks and we interpret these high Vp/Vs ratios to indicate that the granitic rocks are highly fractured or even brecciated. Finally, to evaluate the Southern California Earthquake Center (SCEC) Community Velocity Model (CVM), which predicts Vs based on the Vp model, we compare data from our Vp and Vp/Vs models to empirical formulas that relate P- to S-wave velocities (see Brocher, 2005). These empirical curves provide an adequate average relationship between Vp and Vs, but our

model Vs varies as much as ±20% for Vp > 5.0 km/s and as much as ±35% for Vp < 5.0 km/s. This large variation in the predicted S-wave velocity demonstrates the value of determining Vs independently from Vp.

Tectonic Geodesy

2-014

GEOEARTHSCOPE: NEWLY ACQUIRED AERIAL AND SATELLITE IMAGERY AND GEOCHRONOLOGY *Phillips DA, Jackson ME, and Meertens CM*

UNAVCO has acquired aerial and satellite imagery and geochronology as part of GeoEarthScope, a component of the EarthScope Facility project funded by the National Science Foundation. All GeoEarthScope airborne LiDAR data acquisitions are now complete and cover a total area of more than 5000 square kilometers. Of particular interest to the SCEC community, we have collected high resolution airborne LiDAR imagery of major fault systems in southern and eastern California including the Garlock fault, the Elsinore fault, and numerous other active faults and structures in the Mojave, Panamint valley, Owens valley and elsewhere. These LiDAR data were collected in Spring 2008 and preliminary processed imagery will be shown. These new LiDAR data complement the previously acquired B4 and GeoEarthScope NoCal LiDAR datasets. In addition to airborne LiDAR imagery, we have acquired a significant volume of InSAR imagery covering southern California and other targets within the EarthScope footprint from several satellites, including ERS-1/2, ENVISAT and RADARSAT. ENVISAT satellite tasking for GeoEarthScope will continue through and conclude on September 30, 2008. Besides imagery data, twelve geochronology labs have been funded to provide analysis services including 14C, OSL, Cosmogenic, (U-TH)/He, Fission Track, 40Ar/39Ar and U-Pb dating techniques.

2-019

IMPROVING PRESENT-DAY LOADING RATE ESTIMATES FOR THE SOUTHERNMOST SAN ANDREAS FAULT USING THE JOSHUA TREE AND SAN BERNARDINO GPS NETWORKS *Spinler JC, Bennett RA, Anderson ML, Hreinsdottir S, and McGill SF*

We present the first results from a new dense network of Global Positioning System (GPS) stations located in the eastern Transverse Ranges Province (ETR), a transition zone between the southern San Andreas fault (SSAF) and eastern California shear zone (ECSZ). The Joshua Tree Integrative Geodetic Network (JOIGN) is composed of 23 campaign stations, which have been observed each May, September, and February from September 2005 to September 2007. We also analyzed data from 37 nearby continuous stations from the PBO NUCLEUS-SCIGN and PBO GPS networks (1994-2007), and an additional 7 campaign sites located in the San Bernardino Mountains. We used the GPS-determined site velocity estimates and elastic block models to constrain loading rates for model faults for four fault-block scenarios. For each model, we estimated relative block motions accounting for elastic strain on locked faults using a weighted least squares algorithm that annihilates common mode rotation and translation attributable to reference frame errors. We tested models variously representing the Pinto Mountain and Blue Cut faults of the ETR, a hypothetical new NNW striking fault (the "Landers-Mojave earthquake line") that cuts obliquely across the ETR and Mojave Desert faults, and models including various combinations of these end-member fault-block models. All models produce fault loading rate estimates for the SSAF that reduce the discrepancy between previous geodetic loading rate models and the majority of estimates for intermediate- and short-term fault slip rates based on tectonic geomorphology and paleoseismology. We attribute the improved match between long- and short-term loading/slip-rate estimates to a more realistic parameterization of the fault system in the ETR, which allows geodetic estimates for SSAF slip to vary along strike from 21.0-21.5 ± 0.1 mm/yr in the Coachella Valley to 3.2-5.6 ± 0.1 mm/yr near San Bernardino, depending on the model. However, our slip rate estimates are markedly different from the overall temporal-average slip rate of 30 mm/yr based on

160 km offset of ~5 Ma monzogranite rocks (Frizzell et al. 1986). In contrast, our rate estimates for the ECSZ appear to disagree with the geologic record on all time-scales.

2-020
THE PACIFIC–NORTH AMERICA PLATE VELOCITY ALONG THE SAN ANDREAS FAULT IN CALIFORNIA *Argus DF, and Gordon RG*

Using geodetic observations from four space techniques (GPS, VLBI, SLR, and DORIS), we find the Pacific–North America plate velocity along the straight and narrow segment of the San Andreas fault (at 36°N 120.6°W) to be 50.3 ±0.9 mm/yr toward N38.4°W ±1.0°, which is 4.6 mm/yr faster and 2.6° clockwise of the NUVEL–1A [DeMets et al. 1990, 1994] velocity used in the comparison between western U.S. fault slip rates and the Pacific–North America plate velocity in Uniform California Earthquake Rupture Forecast 2 [Fields et al. 2008, Wisely et al. 2008]. We find the North America–Pacific plate angular velocity to be 50.3°N 75.0W, 0.776 °/Myr.

Along the spreading center in the Gulf of California at 23.5°N 108.5°E, we find the Pacific-North America velocity to be 52.4 ±0.9 mm/yr toward N54.5°W ±1.0°. This azimuth parallels the loosely constrained direction of Pacific–North America plate motion deduced from transform azimuths and earthquake slip vectors in the Gulf. The rate is 4 mm/yr faster than the mean spreading rate since 0.8 Ma (anomaly 1o) and 8 mm/yr faster than the mean spreading rate since 3.1 Ma (anomaly 2A) [DeMets et al. 1995; spreading rates corrected for outward displacement of 2 km are: 48.5 mm/yr (1o, 0.78 Ma), 48.2 (Jarmillo, 1.03 Ma), 46.0 (2, 1.86 Ma), 44.4 (2Ay, 2.58 Ma), and 44.5 mm/yr (2Ao, 3.58 Ma). This is because seafloor spreading in the Gulf of California records motion relative to the North American plate of Baja California, which Plattner et al. [2007] find from GPS to be moving southeast relative to the Pacific plate at 4 to 6 mm/yr.

2-021
INSAR AND TIME SERIES INVESTIGATIONS IN CASCADIA *Steinberg L, and Lohman RB*

There is not a deep understanding of the mechanisms and processes of silent earthquakes. Further study of these events can help in the assessment of the hazards of subduction zones. Our focus is in the Cascadia region, using interferometric synthetic aperture radar (InSAR) processing and time series analysis to complement existing GPS and seismic data in this area. We used SAR data from ERS-1 and ALOS satellites to process and test InSAR and time series methods in this area. We created interferograms from ALOS data using ROI_PAC and made observations of poor correlation in vegetated mountainous regions, patch-like patterns in farming areas, missing landforms in our DEM, and a linear pattern of interferometric baselines across time due to satellite steering by JAXA. Since the release of the ALOS satellite in 2006, only 6 to 8 scenes have been acquired for any given frame in Cascadia. Given that at least 15 SAR images are required for time series analysis, we could not perform those methods on ALOS data. We performed time series methods on ERS data, using the StaMPS and SBAS methods. Both methods showed similar correlation and processing problems in vegetated mountainous regions, and strong signals in flat and city areas. Future improvements to InSAR methods working to minimize decorrelation effects in mountainous and vegetated regions will help further study in this area.

2-022
THE SLIP HISTORY OF SLOW SLIP EVENTS ALONG THE CASCADIA SUBDUCTION ZONE FROM 1998 TO 2008 *Gao H, and Schmidt DA*

We estimate the slip distribution and propagation path of prominent slow slip events (SSEs) along the Cascadia subduction zone from 1998 to 2008. We process continuous GPS data from the PBO, PANGA and WCDA networks from January 1998 to June 2008 using GAMIT/GLOBK processing package. We discretize the Juan de Fuca-North American plate interface into triangular subfaults and interpret transient surface motions as slip on the interface. The slip distribution of 16 SSEs is estimated using the Extended Network Inversion Filter (ENIF). Of these events, 13 events are centered around the Puget Sound area, 2 events are resolved around the Columbia River and 1 event is located in southern Oregon. Other smaller events beneath Northern Vancouver Island, Oregon and Northern California are not well resolved because of the limited station coverage. For the major events analyzed in this work, the horizontal displacements observed at benchmarks range from 2-6 mm and the maximum cumulative down-dip slip is estimated to be 2-6 cm for each event. The propagation direction of SSEs is variable from one event to the next, indicating that the propagation direction of SSEs is not systematic. Therefore, slab geometry or fault properties likely do not dictate the propagation direction. The estimated moment magnitude of SSEs is between 6.1-6.7 and the average stress drop of 0.06-0.1 MPa is nearly two orders of magnitude smaller than that for the normal earthquakes (1-10 MPa). The stacked maximum cumulative slip for these 16 events from 1998 to 2008 is ~ 25 cm, which is centered beneath the northern edge of the sedimentary Olympic embayment between the 25-45 km depth contours on the slab interface. This is where the subducting slab has a more gradual dip compared to the north and south, and the interface bends along-strike. We hypothesize that the geometry of the slab plays an important role for focusing transient strain release at this location along the subduction zone.

2-023
CHARACTERIZING NOISE LEVELS ON THE PLATE BOUNDARY OBSERVATORY BOREHOLE SEISMOMETERS AND STRAINMETERS *Barbour AJ, and Agnew DC*

We are analyzing the spectral and temporal characteristics of data from the seismic band (0.001 to 10 Hz) recorded on the borehole strainmeters and seismometers installed by the Plate Boundary Observatory (PBO). Our aim is to characterize these data as well as possible in order to determine what can be detected using these sensors, and also to develop guidelines which can be used to search for unusual behavior, such as episodic tremor. We use sine multitaper spectral estimation (with prewhitening) to determine the power spectral density, since this provides estimates with low variance and bias, without any loss of data. We summarize the spectrum by performing local regressions in log-log space; this reduces the data volume by factors of 1000 or more, with little loss of information. A preliminary analysis shows that some stations have had persistent operational problems (e.g. B004 during early 2006), though others show consistently good behavior (e.g. B012 during early 2006). The noise levels for seismometers within tens of kilometers show similar temporal changes but (apparently) different absolute levels; comparing records of teleseisms shows that there are significant differences in relative gain (compared to the official values provided by PBO). The seismic noise also shows a clear diurnal signal which may be correlated with coastal proximity; at frequencies lower than the microseism band the spectrum appears to be dominated by instrumental noise. The borehole strainmeters show noise levels that are also dominated by instrumental noise (probably digitizer noise) at frequencies above the microseism band. At lower frequencies (0.001 to 0.1 Hz) the noise level increases with decreasing frequency at levels higher than is seen on long-base instruments at the surface. Future plans include: (1) analyzing as many stations as possible, including stations in the Anza network, for the purposes of network characterization; (2) removal of times with instrumental artifacts (and large earthquakes) to

provide a clearer picture of how the instruments respond to true geophysical signals, such as episodic tremor and slip; and (3) comparison of the detection levels of borehole and longbase strainmeters, borehole seismometers, and (when available) co-located surface-mounted broadband seismometers.

2-024
PBO NUCLEUS: THE HOME STRETCH *Blume F, Boyce E, Miller MM, Eriksson SC, and Borsa A*

Tectonic and earthquake research in the US has experienced a quiet revolution over the last decade precipitated by the recognition that slow-motion faulting events can both trigger and be triggered by regular earthquakes. Transient motion has now been found in essentially all tectonic environments, and the detection and analysis of such events is the first-order science target of the EarthScope Project. Because of this and a host of other fundamental tectonics questions that can be answered only with long-duration geodetic time series, the incipient 1400-station EarthScope Plate Boundary Observatory (PBO) network has been designed to leverage 445 existing continuous GPS stations whose measurements extend back over a decade. The irreplaceable recording history of these stations will accelerate EarthScope scientific return by providing the highest possible resolution. This resolution will be used to detect and understand transients, to determine the three-dimensional velocity field (particularly vertical motion), and to improve measurement precision by understanding the complex noise sources inherent in GPS. The PBO Nucleus project supports the operation, maintenance and hardware upgrades of a subset of the six western U.S. geodetic networks until they are subsumed by PBO. Uninterrupted data flow from these stations will effectively double the time-series length of PBO over the expected life of EarthScope, and has created, for the first time, a single GPS-based geodetic network in the US. The other existing sites remain in operation under support from non-NSF sources (e.g. the USGS), and EarthScope continues to benefit from their continued operation On the grounds of relevance to EarthScope science goals, geographic distribution and data quality, 209 of the 432 existing stations were selected as the nucleus upon which to build PBO. Conversion of these stations to a PBO-compatible mode of operation was begun under previous funding, and as a result data now flow directly to PBO archives and processing centers while maintenance, operations, and meta-data requirements are continue to be upgraded to PBO standards. At the end of this project all 209 stations will be fully incorporated into PBO, meeting all standards for new PBO construction including data communications and land use permits. Funds for operation of these stations have been included in planned budgets for PBO after the construction phase ends and PBO begins an operational phase in 2008.

2-025
HETEROGENEOUS RUPTURE OF 2008 WENCHUAN, CHINA EARTHQUAKE CONSTRAINED BY JOINTED INVERTING SEISMIC AND INSAR DATA *Ji C, Lu Z, Hudnut KW, Liu J, and Shao G*

We study the rupture process of the 2008 Wenchuan earthquake using both seismic and INSAR data and explore an unprecedented complex rupture process. The rupture of this event occurred simultaneously on two parallel faults which intersect each other and extend unilaterally to over 250 km. The entire rupture exended over 100 sec. We observed the strong dynamic interaction between the two faults. The rupture initiated at the low angle Pengguan fault at a depth around 11 km below the intersection of Pengguan and high angle Beichuan faults and then triggered the Beichuan fault 10 s later. The rupture continued on Pengguan fault for another 30 sec with slip gradually changing from pure thrust to oblique motion and then ceased 90 km northeast of the epicenter. The rupture on Beichuan fault had similar change in slip direction but extend a much

longer distance and reached the maximum slip of 8.5 m about 130 km northeast of the epicenter. It was presumably the cause of huge damage at nearby Beichuan city. Northeast of Beichuan city, the rupture on Beichuan fault significantly reduced, accompanying with the rupture of a large blind thrust on Pengguan fault. The later apparently triggered the strike-slip motion on the last segement of Beichuan fault at 180 km northeast of the epicenter at about 75 sec.

2-026
MODELING AND DETECTION OF SEISMIC SWARMS TRIGGERED BY ASEISMIC TRANSIENTS *Llenos AL, McGuire JJ, and Ogata Y*

The rate of earthquake occurrence varies by many orders of magnitude in a given region due to variations in the stress state of the crust. Of particular interest are variations in seismicity rate triggered by transient aseismic processes such as fluid flow, fault creep or magma intrusion. While these processes have been shown to trigger earthquakes, implementing an inversion algorithm that can map seismicity variations into estimates of stress rate variations has been challenging. Essentially aftershock sequences can obscure changes in the background seismicity rate resulting from aseismic processes. Two common approaches for estimating the time dependence of the underlying driving mechanisms are the stochastic Epidemic Type Aftershock Sequence model (ETAS) (Ogata, 1988) and a physical approach based on the rate-and state-model of fault friction (Dieterich, 1994). The models have different strengths that could be combined to allow more quantitative studies of earthquake triggering. To accomplish this, we identify the parameters that relate to one another in the two models and examine their dependence on stressing rate. A particular conflict arises because the rate-state model predicts that aftershock productivity scales with stressing rate while the ETAS model assumes that it is time independent. To resolve this issue, we estimate triggering parameters for 4 earthquake swarms associated with geodetically observed deformation transients in various tectonic environments. Our results suggest that stressing rate transients increase the background seismicity rate without affecting aftershock productivity.

We can then specify a combined model for seismicity rate variations that can be used in a data assimilation algorithm to invert seismicity catalogs for variations in aseismic stressing rates. For a given earthquake catalog, we produce maximum likelihood estimates of the ETAS parameters and use an extended Kalman filter to estimate the evolution of underlying state variables (background stress rate, aseismic stress rate, and \gamma of the rate-state model). We have tested our algorithm on the 2005 Obsidian Buttes earthquake swarm, which was triggered by geodetically-observed shallow aseismic creep (Lohman and McGuire, 2007). Our algorithm successfully detects the swarm and produces an estimate of the aseismic stressing rate transient that triggered it. Our method therefore has the potential to be a highly sensitive detector of transient deformation.

2-027
COMBINING GPS AND METEOROLOGICAL DATA TO MITIGATE ATMOSPHERIC PHASE IN INTERFEROGRAMS: THE SAN GABRIEL VALLEY, CALIFORNIA *Funning GJ, Houlié N, and Burgmann R*

GPS and InSAR data both independently sample the troposphere state at the time of observation. Given the recent proliferation of continuous GPS sites, the use of this redundant information to characterise and remove tropospheric signals from InSAR data is becoming increasingly viable. This capability is critical if transient deformation signals are to be identified with confidence.

Here we focus on data from southern California, where a dense continuous GPS network and a diverse set of tectonic and nontectonic deformation sources make for an excellent test site. We focus on an uplift transient that occurred in the San Gabriel valley, approximately 30 km NE of Los

Angeles, in early 2005. Up to 6 cm of vertical deformation affecting seven GPS sites, centered on the site LONG, can be seen in both GPS and InSAR data. This has been interpreted as a hydrogeological response of an aquifer to high rainfall in the spring of 2005 by other authors (e.g. N. King et al., 2007, JGR). We assess here the effects and potential data improvements that arise from the integration of meteorological data into our GPS processing, and hence the proportion of the InSAR signal that has a tropospheric origin.

We find that the inclusion of meteorological data in GPS data processing corrects for a persistent vertical bias in GPS station coordinates and improves the repeatability of tropospheric delay estimates. In addition, we find that the observed InSAR signal in the

San Gabriel Valley spanning the period of uplift in 2005 cannot be solely interpreted as a hydrological uplift but includes significant contributions from tropospheric delay. This tropospheric phase contribution could result in an overestimate of peak aquifer uplift by as much as 30% if left unaccounted for.

2-028
MITIGATION OF TROPOSPHERIC EFFECTS ON SITE VELOCITIES OF THE BAY AREA REGIONAL DEFORMATION NETWORK (BARD) *Houlié N, Funning GJ, Friday J, Gardner J, Burgmann R, and Romanowicz B*

The BARD network is a permanent GPS network comprising 40 GPS sites, installed since 1994 in northern California (Romanowicz et al., 1994). Originally started as a collaborative effort of different Bay Area institutions, since the establishment of the Plate Boundary Observatory, it is now focused on real-time data acquisition from stations operated by UC Berkeley, with plans for expansion in collaboration with USGS/Menlo Park. The BARD network streams data to the Berkeley Seismological Laboratory in real-time (sampling rates of 1s and 15s, depending on the site). All sites transmit data using Frame Relay technology which improves reliability in case of earthquake occurrence. Data are archived at the Northern California Earthquake Data Center (NCEDC, *http://www.ncedc.org*) and are freely available (Neuhauser et al., 2001). The BARD network is currently able to provide high precision (error < 1mm/yr) velocities over most of northern California.

In the vicinity of San Francisco Bay, however, heterogeneous tropospheric effects can scatter site coordinates significantly (amplitudes ~5 mm) during a single day of measurements. Such effects can be seen when comparing sites from either side of the Bay, or between the Bay and the Great Valley, further inland. With seven sites located less than 15 km from the Hayward fault, the BARD network is well suited for constraining the slip amplitude (currently ~5 mm/yr of creep) along the fault's length; however in order to detect small changes in creep rate, such as slip transients, such tropospheric effects need to be mitigated. We will show recent developments, completed over the past year, designed to improve the estimation of troposphere delay over the BARD network by incorporating additional constraints from ground- and air-based meteorological measurements into our processing.

2-029
INSTANTANEOUS DEFORMATION FROM CONTINUOUS GPS: CONTRIBUTIONS FROM QUASI-PERIODIC LOADS *Bennett RA*

Continuous GPS (CGPS) coordinate time-series are known to experience repeating deformation signals with seasonal and other periods. It is unlikely that these signals represent perfect sinusoids with temporally constant amplitude. A complete understanding of these "quasi-periodic" motions

may be critical to our ability to use CGPS time-series to investigate a wide class of potential non-periodic time-dependent crustal deformation processes. Toward this end, I have developed an analysis method to investigate temporal variations in the amplitudes of sinusoidal signals. I demonstrate the method using simulated coordinate time-series to numerically explore the potential consequences of neglecting decadal variation in amplitude of annual motions on the residual-error spectra of CGPS measurements, as well as potential bias in estimates for secular site velocity. I show that secular velocity bias can be appreciable for shorter time-series, and that residual-error time-series of longer duration may contain significant power in a broad band centred on semi-annual frequency if temporal variation in the amplitude of annual motions is not accounted for in the model used to reduce the observations to residuals. It may be difficult to differentiate the bandpass filtered signature of mismodelled loading signals from power-law noise using residual-error spectra for shorter time-series. I provide an example application to a ~9-yr coordinate time-series for a CGPS station located in southern California at Carbon Creek Control Structure (CCCS), which is known to experience large amplitude seasonal motions associated with the Santa Ana aquifer system.

2-030

NEAR REAL-TIME PROCESSING OF RESULTS FROM THE 2008 IMPERIAL VALLEY, CALIFORNIA, GPS SURVEY *Crowell BW, Bock Y, Sandwell DT, Fialko Y, and Lohman RB*

In February of 2008, we surveyed with Global Positioning System (GPS) 38 geodetic monuments established by Imperial College, London and 14 National Geodetic Survey (NGS) sites using the rapid-static mode of surveying at a sampling rate of 1-Hz. We also installed and surveyed 10 new monuments spanning the Imperial Fault trace along irrigation culverts. As base stations, 4 1-Hz real-time stations in the California Real Time Network (CRTN) were used. Previous GPS surveys of this dense array of monuments occurred in 1993, 1999 and 2000 [Genrich et al., 1997; Lyons et al., 2002]. Data streamed over Bluetooth from Ashtech Z-XII3 receivers and was collected using Geodetics, Inc. RTD Rover software installed on a Verizon XV6700 smartphone and processed in real-time by connecting to SOPAC for ephemeris information. Raw data was also saved on the phone's memory card as well as on the SOPAC servers for use in post-processing with Geodetics, Inc. RTD software (*http://www.geodetics.com*) [de Jonge et al., 2000]. Inclusion of site metadata into the RINEX files and the conversion of raw files to RINEX files were performed using PGM Server, which also archived the campaign and provides the associated RINEX and SINEX files (*http://sopac.ucsd.edu/projects/impvall2008.html*). Crustal motion was computed for the periods ranging from 1993 to 2008 and from 2000 to 2008 using both pre-processed and post-processed positions. When North American plate motion is removed, the average velocity residual between the pre-processed and post-processed positions is 1.62 mm/yr and 3.09 mm/yr for the periods ranging from 1993 to 2008 and from 2000 to 2008 respectively. This results in roughly a 2 cm difference between the pre-processed and post-processed positions, and part of the difference can be accounted for by the 2007.0 epoch being used for the pre-processed positions and the epoch of the survey was used for the post-processed positions. The azimuths and magnitudes of the velocity vectors for the periods ranging from 1993 to 2008 and from 2000 to 2008 are fairly consistent, indicating that both shallow and deep creep on the Imperial fault is essentially steady-state on a time scale of several years.

Earthquake Geology

2-031

STRUCTURE OF THE IMBRICATE THRUST SYSTEM THAT SOURCED THE 2008 M7.9 WENCHUAN EARTHQUAKE *Hubbard JA, Shaw JH, and Klinger Y*

The 2008 M7.9 Wenchuan earthquake ruptured an imbricate thrust fault system in the frontal part of the Longmen Shan range, which forms the eastern boundary of the Tibetan plateau.

We use industry seismic reflection data combined with surface geologic maps and relocated aftershocks to define the geometry of the thrust faults that ruptured in the earthquake. We identify a segmented pattern to the fault system, with slip in the southern region partitioned between the steeply-dipping Beichuan fault and the shallower Pengguan fault, which likely merge at depth forming an imbricated thrust stack. Based on the mapped surface rupture (Xu et al., 2008), the steeply dipping Beichuan thrust exhibits a combination of dip and strike slip displacements, whereas the more shallowly dipping Pengguan fault has primarily dip slip motions. In contrast, slip is limited to the Beichuan fault in the northern part of the rupture. The transition in rupture patterns occurs in the vicinity of a major lateral geometric segment boundary in the Beichuan fault. Thus, the Wenchuan earthquake clearly demonstrates the ability of thrust fault earthquakes to involve multiple thrust splays and rupture across significant lateral segment boundaries, which has major implications for how maximum earthquake magnitudes should be assessed for active thrust fault systems in southern California.

Prior to the earthquake, this mountain range showed very low geodetic and geologic shortening rates, leading to the suggestion of lower crustal inflation rather than brittle crustal shortening as the main mechanism creating and maintaining its significant topographic relief. In addition to constraining the three dimensional geometries of the faults in this range front, we also show that the relief in the eastern margin of the Longmen Shan can be explained by crustal shortening alone, without calling on lower crustal flow. The Wenchuan earthquake demonstrates the role of active crustal shortening in developing and supporting the range, and illustrates the potential for large and very destructive earthquakes on similar active thrust faults that have been observed in other populated regions of the world.

2-032

NEW LATE PLEISTOCENE AND HOLOCENE SLIP RATES ON THE SOUTHERN SEGMENT OF THE COMPTON BLIND-THRUST FAULT, LAKEWOOD, CALIFORNIA *Dooling PR, Leon LA, Dolan JF, Shaw JH, Pratt TL, and Martinez AU*

Newly collected borehole data from the southern segment of the Compton fault provide both Late Pleistocene and Holocene slip rates. Preliminary analysis of sediments extracted from our study site in the city of Lakewood, California (~35 km SE of downtown Los Angeles and 2 km West of the San Gabriel River), reveal an upward-narrowing zone of folding to within a few meters of the surface. Shaw and Suppe (1996) originally identified the Compton thrust through their observation on petroleum-industry seismic reflection data of a fault-bend fold associated with the thrust ramp. High-resolution seismic data were acquired in October 2007 to better image deformation associated with the Compton fault in young strata within the uppermost 200 m, above the shallowest industry data. During Summer 2008 we excavated seven boreholes to depths of 30- to 45 m along a 1.4-km-long, north-south transect across the backlimb active axial surface of the fault-bend fold above the ramp of the Compton Thrust. These boreholes, along with five boreholes excavated in 2007, reveal layers of fine- to coarse-grained sand and gravel interbedded with fine-grained silt and clay and organic-rich units. Radiocarbon dates from detrital charcoal and bulk-soil samples give ages

ranging from ~2.3 ka to ~32 ka. Analysis of the borehole data yields slip rates for the Compton ramp averaged over two different time intervals: a 32 ka rate of 1.7 +0.2/-0.1 mm/yr, and a 10±2 ka rate of 1.9±0.5 mm/yr. These southern Compton segment slip rates are somewhat faster than the 1.2 +0.5/-0.3 mm/yr rate measured by Leon et al. (in review, 2008) along the northern segment. Ongoing analysis of the Lakewood borehole should provide a paleoseismologic record of individual earthquakes, as well as a greater understanding of the behavior of the segmented Compton blind-thrust fault.

2-033

A SHALLOW BOREHOLE STUDY OF PULVERIZED GRANITE ALONG THE SAN ANDREAS FAULT, LITTLE ROCK, CA, PART A: CHEMISTRY *Wechsler N, Allen EE, Rockwell TK, Chester JS, Girty GH, and Ben-Zion Y*

Pulverized rocks are becoming increasingly recognized as a common structural unit of large faults (Dor et al., 2006; Stillings, 2007), although their properties and mechanism of damage remain poorly understood. We present preliminary results from a shallow drill into pulverized granites adjacent to the San-Andreas fault. The site, Little Rock Creek, has extensive outcrops of granites with varying degrees of damage, at distances of up to a few hundreds of meters from the fault's active strand. We used an auger drill-rig to recover a continuous core of damaged rocks to a depth of 42 meters. The core is composed mainly of pulverized granitic rocks, with chemical alterations comprising a significant part of the core samples in the lower portion of the core. The borehole crossed several high clay content zones which likely correspond to secondary fault cores. In this ongoing study, we present preliminary detailed chemical analysis of the core using XRF and light microscopy. We are also investigating the timing relations between fracturing, weathering and re-mineralization. A principal goal of our work is to eliminate the signal from surface weathering and to isolate the mechanism(s) that causes the rocks to shatter. We conclude that there is no significant weathering trend with depth, and that the existing alterations are a primary function of the rock types.

2-034

A SHALLOW BOREHOLE STUDY OF PULVERIZED GRANITE ALONG THE SAN ANDREAS FAULT, LITTLE ROCK, CA, PART B: PARTICLE SIZE DISTRIBUTION *Allen EE, Wechsler N, Chester JS, Rockwell TK, Girty GH, and Ben-Zion Y*

We present preliminary results from a shallow core through damaged granitoids adjacent to the San Andreas fault near Little Rock Creek. The site has extensive outcrops of granitic rocks with varying degrees of damage, at distances of up to a few hundreds of meters from the fault's primary active strand. We used an auger drill-rig to recover a continuous core of damaged rock to a depth of 42 meters. The core is composed mainly of pulverized granite and granodiorite, with chemical alterations comprising a significant part of the core samples in the lower portion of the core in the more mafic rock types. The borehole crossed several high clay content zones which likely correspond to secondary fault cores. Preliminary results of particle size distribution (PSD) measured using a laser particle analyzer and standard sieving and pipette methods indicate that medium to coarse silt and fine sand are the dominant particle sizes for these pulverized granitic rocks. Very little clay size particles were observed in both surface and depth samples. We observed a shift in the PSD towards finer sizes with depth, in agreement with the Anderson et al. (1980) results. There was also a difference in PSD between different lithologies. We present a comparison between the laser particle analyzer and the sieve+pipette method. Based on those results, we conclude that there is no significant weathering trend with depth, and that the existing alterations are a primary function of the rock type.

2-035
HIGH GEOLOGIC SLIP RATES SINCE EARLY PLEISTOCENE INITIATION OF THE SAN JACINTO AND SAN FELIPE FAULT ZONES IN THE SAN ANDREAS FAULT SYSTEM: SOUTHERN CALIFORNIA, USA *Janecke SU*

The San Jacinto fault system is crucial for understanding dynamics and seismic hazards in southern California, yet its age of initiation and long-term average slip-rate are controversial and little is known about its structural evolution. We synthesize four studies in the Salton Trough that provide evidence for initiation of structural segments of the San Jacinto fault zone at or slightly before the 1.07-Ma base of the Jaramillo subchron and creation of new fault segments after ~ 0.6 Ma. Strands of the San Jacinto and adjacent San Felipe fault zones began to cut, fold, and deactivate the older West Salton detachment fault ~1.3-1.1 Ma. The San Felipe, Coyote Creek and Clark faults all show evidence of major structural adjustments after about 0.6 to 0.5 Ma.

The Clark and Buck-Ridge-Santa Rosa faults accumulated about 14.4 km of right separation in its lifetime near Clark Lake and at least 5.6 ± 0.4 km in the last 0.5 to 0.6 Ma in its San Felipe Hills segment. The Coyote Ridge segment of the Coyote Creek fault has a displacement of ~3.5 ± 1.3 km since before about 0.8 to 0.9 Ma, whereas the Borrego Mountain and Borrego Badlands segments have only 1-2 km of right slip since ~0.6 Ma. The San Felipe fault accumulated between 4 and 13.5 km (~6.5 km preferred) of right slip in the last 1.1 to 1.3 Ma at Yaqui and Pinyon ridges. Combining these five estimates of displacement with ages of fault initiation indicate a lifetime geologic slip rate of 17.8 +2.6/-2.3 mm/yr across the San Jacinto fault zone (sum of Clark, Buck Ridge and Coyote Creek faults) and about ~5.4 +6.9/-2.3 mm/yr across the San Felipe fault zone at Yaqui and Pinyon ridges. This suggests that the San Jacinto and San Felipe fault zones accommodated slightly more plate motion than the southern San Andreas fault since their inception roughly 1-1.3 Ma.

The Coyote Creek fault zone is narrower and more continuous than adjacent faults yet it is slightly younger, has < 1/4 the total displacement, and slipped at a much slower rate than the Clark fault. The San Felipe fault zone displaces late Pleistocene deposits, has ~ 6.5 km of displacement, and has a slip rate comparable to that of major adjacent faults. Its lifetime slip rate exceeds those of the central and southern Elsinore and the Coyote Creek faults. The San Felipe fault zone may have slowed in the recent past or may be experiencing a lull in activity. Our structural and stratigraphic data do not support steady state assumptions of slip rate.

2-036
REVISED DATES OF 5 LARGE EARTHQUAKES AT THE BIDART FAN SITE ALONG THE CARRIZO SECTION OF THE SAN ANDREAS FAULT, CALIFORNIA, SINCE A.D. 1310±30 *Akciz SO, Grant Ludwig LB, and Arrowsmith JR*

Precise knowledge of the age and magnitude of past earthquakes is essential for characterizing models of earthquake recurrence and key to forecasting future earthquakes. We present 28 new radiocarbon analyses that refine the chronology of the last five earthquakes at the Bidart Fan site along the Carrizo section of the San Andreas Fault. We first present redrafted versions of Grant's (1993) original trench logs and include a table containing a systematic evaluation of the quantity and the quality of paleoearthquake evidences. Note that this makes the complete logs available to a broader audience, given that Grant and Sieh (1994) only published critical portions of the logs for brevity. The new data show that the penultimate earthquake in the Carrizo Plain occurred not earlier than A.D. 1640 and the modeled 95-percentile ranges of the three earlier earthquakes and their mean are A.D. 1540-1630 (1585), A.D. 1360-1425 (1393), and A.D. 1280-1340 (1310), indicating an average time interval of 137±44 years between large earthquakes since A.D. 1310±30. A robust earthquake recurrence model of the Carrizo section will require even more well-dated earthquakes

for thorough characterization. However, these new data imply that since A.D. 1310±30, the Carrizo section has failed more regularly and more often than previously thought.

2-037
LATE HOLOCENE SLIP ON THE IMPERIAL FAULT, MESQUITE BASIN, IMPERIAL VALLEY, CALIFORNIA *Meltzner AJ, and Rockwell TK*

We excavated a series of trenches across the Mesquite Basin section of the Imperial fault, the primary plate-boundary fault in the southern Imperial Valley, to explore its late Holocene rupture history and to document slip per event. We identified several channels that cross the fault at a high angle and are displaced in the subsurface by the fault. These channels are incised into or embedded within lacustrine strata that are associated with major filling events of Lake Cahuilla which are dated by C-14 combined with historical observations. 3D excavation of these channels has yielded information on timing and slip for the past 6 surface ruptures.

Displacement is well documented for the 1979 and 1940 events, with 15-20 cm of coseismic lateral slip occurring in each event. A small rill, which also corresponds to the feeder channel for older beheaded channels, is deflected by ~60 cm, which we attribute to the 1979 and 1940 events plus creep and afterslip. This rill, which incises the lake sediments from the ca. AD 1700 lake, appears to record slip from only these two historical earthquakes, which is consistent with earlier paleoseismic studies farther south.

Earlier events occurred in ~AD 1700 (~1.4 m RL) and ~AD 1650 (~0.2 m RL or less), with two additional large events between ~AD 1500 and 1600 (1.4 m and 1.5 m of RL slip, respectively). The lack of rounding or deflection of most paleo-channels as they approach the fault suggests that the inferred larger prehistorical displacements are not composite slips from multiple events.

These observations suggest that: (1) the 1940 and 1979 events were not "characteristic" for the northern Imperial fault, but rather, that the 1940 event sustained an incomplete rupture which was followed by the 1979 "make-up" event, perhaps due to stress loading by high slip in the border region; (2) the Imperial fault appears to be more typified by end-to-end ruptures, assuming that the larger displacements represent more complete and evenly distributed stress release; (3) the slip rate for the Imperial fault in the Mesquite Basin is ~1 cm/yr for the past five centuries; (4) slip per event ranges from about 0.15 to 1.5 m; and (5) scaling slip per event in Mesquite Basin with maximum slip near the International Border, and assuming that most end-to-end ruptures sustain 5-6 m along the central portion of the fault, suggests that the Imperial fault accommodates a slip rate of about 3-4 cm/yr, close to that estimated by GPS.

2-038
A NEW LATE HOLOCENE LACUSTRINE CHRONOLOGY FOR ANCIENT LAKE CAHUILLA, SALTON SEA, IMPERIAL COUNTY, CA: TOWARDS BASIN-WIDE CORRELATION OF EARTHQUAKE CHRONOLOGIES *Verdugo DM, and Rockwell TK*

Developing a basin-wide lake chronology is critical in understanding the temporal evolution of large seismicity in the southern San Andreas system, most strands of which cross lacustrine deposits in the Salton Depression. The Salton Sea is the latest in a series of inundations and dessications in the depression that spans back thousands of years, with prehistoric lakes collectively referred to as Lake Cahuilla. Contemporaneously to the rise and fall of Lake Cahuilla, Native American occupations, European explorations and earthquakes have occurred above and below its shoreline. Radiocarbon ages have been used to constrain the timing of these events, although the temporal resolution is poor because most of the dates are on detrital charcoal which

commonly has significant age inheritance. Furthermore, most of the archeologic dates are based on composite samples, which may have a spread of age components. While there seems to be a general consensus that there have been multiple fillings and dessications in the past 1000-1500 years, a definitive late-Holocene chronology has yet to be developed. Here we present a new chronology using the radiocarbon ages, stratigraphic lacustrine correlation and historical data from sites across the entire Cahuilla basin. We have compiled over 350 radiocarbon ages from paleoseismic trenches and archeological sites above and below the lake highstand. We have sorted and placed each date in stratigraphic context to its relationship with lacustrine and non-lacustrine periods using its sample location, elevation, depositional context (i.e., anthropogenic, geologic), type of material and source of the material dated. The stratigraphic occurrence of multiple lakes at higher elevations relative to lower elevations has provided additional constraints regarding the timing and length of individual highstands, as well as information on partial desiccations. Finally, we add historical constraints to lake levels provided by diaries and maps of European expeditions within the region. Based on these data, the most recent lake is interpreted as three sub-high stands with two partial desiccations between about AD 1600 and 1720. Lake 2 (reported as lake 3 at paleoseismic sites close to the shoreline) dates to the period of about AD 1400-1500. The third major lake inundated the basin in the 13th century, whereas a protracted generally dry period persisted between about AD 700 and 1200, with brief lakes inferred around the AD 1150 and 1000.

2-039

A GPS RESURVEY OF THE ANZA GAP REGION, CALIFORNIA: PREPARATION FOR AN EARTHQUAKE ON THE SAN JACINTO FAULT *Millar AZ, and Funning GJ*

There is a significant probability within the coming decades of rupture along the San Jacinto Fault, which has been seismically active in the past century. With this in mind, the goal of our SCEC/SURE study is to increase preparedness for several possible earthquake scenarios along the San Jacinto fault focusing specifically on the Anza, San Bernardino Valley and San Jacinto Valley segments, the region in which the Earthquake Processes group at UC Riverside would likely be first responders in the event of an earthquake.

Key components involved in the project include resurveying GPS benchmarks throughout Riverside and San Bernardino Counties and using elastic deformation models to devise post-earthquake response strategies that emphasize and prioritize particular GPS benchmarks. Initially, eighteen benchmarks were selected to be resurveyed over the course of the summer based on the year in which they were last surveyed (the most recent being in 2001) and for their locations relative to the surface fault traces and to those of continuous GPS and recent campaign sites. The original list of benchmarks has since been modified to reflect the outcome of reconnaissance work, and following the running of simple forward and inverse models. Additionally, we have created detailed site descriptions for each benchmark that will be posted on the Web at the conclusion of the project.

2-040

PALEOSEISMOLOGIC EVIDENCE FOR MULTIPLE HOLOCENE EARTHQUAKES ON THE CALICO FAULT: IMPLICATIONS FOR EARTHQUAKE CLUSTERING IN THE EASTERN CALIFORNIA SHEAR ZONE *Ganev PN, Dolan JF, Oskin ME, Owen LA, and Le KN*

New paleoseismologic data from the Calico fault reveal evidence for the occurrence of at least three, and probably four, surface ruptures during the Holocene. This new data set strongly reinforces earlier suggestions that seismic strain release across southern California may be highly clustered in time and space. Two fault-perpendicular trenches were excavated in the town of

Newberry Springs, California ~30 km east of Barstow. The trenches exposed fluvial, lacustrine, and playa sediments, consisting of pebble gravel and coarse-grained sands, silts, and clays. Although motion on two parallel fault strands that cross the site appears to be predominantly strike-slip, secondary components of vertical movement have created a down-dropped block between them. Twelve optically stimulated luminescence dates bracket surface rupture ages. The three most recent surface ruptures corroborate the pattern of earthquake clustering originally proposed in the Eastern California Shear Zone (ECSZ) by Rockwell et al. (2000). Specifically, the most recent event occurred during latest Holocene time between 0.6 to 1.1 ka and 2.0 ka. This age suggests that the Calico fault has ruptured as part of the ongoing latest Holocene cluster. The penultimate and ante-penultimate surface ruptures both occurred during a brief interval between 5-6 ka (event 2 [5.0-5.6 ka] and event 3 [5.6 to 6.1 ka or possibly 7.3ka]). Both of these ruptures fall within the penultimate seismic cluster on the ECSZ. One possible explanation for two earthquakes within the same cluster could be that the Calico fault slips ~2x faster than nearby dextral faults (Oskin et al., 2008). This higher slip rate may be accommodated via multiple ruptures during clustering time periods. Alternatively, the study site may be an overlap zone between northern and southern Calico ruptures. The 1.5m vertical separation associated with event 3 is much larger than separation in event 2. This suggests that event 3 exhibited larger displacement at the trench site. Evidence for a possible fourth event between 6.1 to 7.3ka and 8.4ka is also present in our southern trench. However, the age is not well defined. The absence of evidence for earthquakes between 2-5 ka falls within the seismic lull on the ECSZ found by Rockwell et al. (2000) – a time period when paleoseismic evidence suggests a cluster of activity in the network of faults beneath the Los Angeles region and central Transverse Ranges (Dolan et al., 2007).

2-041

RECENT OFFSET MEASUREMENTS, COACHELLA VALLEY SEGMENT, SAN ANDREAS FAULT *Williams PL, Hudnut KW, and Seitz GG*

The Coachella Valley Segment (CVS) of the southern San Andreas fault (SSAF) has not ruptured in a large or great earthquake during the past ~330 years (Sieh and Williams, 1990). Given that recurrence intervals of ~200 years have been found for the CVS (Fumal et al., 2002; Williams and Seitz, 2007; Philibosian et al., 2007), the long quiescence points to a particularly high seismic hazard (e.g. WGCEP, 2008). This paper presents detailed geomorphic slip-per-event evidence for the southern 50 km of the CVS. A sufficient sample of the fault's past behavior should indicate what to expect from future earthquakes. Detailed descriptions of channel offsets are presented for 65 independent sites, some of these preserve evidence of multiple offset events. Compilation of the survey indicates that the latest five earthquakes produced moderate, 3±1 meter offsets, with cumulative displacement of 15-17 meters. Interpreted in the context of the paleoseismic data referenced above, these data suggest a CVS slip rate of 16±1mm/yr. The data reported here were initially developed by use of aerial reconnaissance and field mapping, and were subsequently checked, refined and extended utilizing Lidar data obtained from the NCALM B4 project. Several independent features in the range of 6-25 meters were discovered during examination of the Lidar dataset, and in many cases the Lidar substantially improved assessment of fault location and confirmed the sizes of larger offsets.

2-042

AN UPDATE ON ACCESS TO GEOEARTHSCOPE LIDAR TOPOGRAPHY DATA
Crosby CJ, Nandigam V, Arrowsmith JR, Balakrishnan S, Baru C, and Phillips DA

The recently completed GeoEarthScope airborne LiDAR (Light Detection And Ranging) topography acquisition will provide unprecedented data adjacent to active faults throughout the plate boundary region of western North America. Totaling more than 5000 square kilometers, these

data offer an extremely high-resolution representation of fault zone topography and should be a revolutionary resource for researchers studying earthquake hazards, active faulting, landscape processes, and ground deformation.

GeoEarthScope LiDAR data acquisition began in spring of 2007 with the San Andreas fault system in northern California and later progressed to faults in southern California (including the Garlock and Elsinore), the Yakima Fold and Thrust Belt in Washington, Yellowstone National Park, the Tetons, the Wasatch Front, and Alaska. The complete northern California dataset was released this summer. The remaining data are currently being processed by the National Center for Airborne Laser Mapping (NCALM) and will be available this fall via the GEON LiDAR system inside the GEON portal (*http://www.geongrid.org*). The southern California data are expected to be the next release.

The GEON LiDAR system provides access to both standard digital elevation model (DEM) products derived from the LiDAR as well as LiDAR point cloud data. Users interact with a Google Map interface in the portal to select the portion of data of interest and are also provided with tools to generate custom DEM products from the LiDAR point cloud. Additional capabilities currently under development include output of DEM products in Google Earth compatible KMZ format as well as seamless Google Earth browsing of the LiDAR data for a complete fault segment.

Interest in the northern California GeoEarthScope LiDAR data has been significant, with over 10,800 one square kilometer DEMs downloaded since a subset of the data was release in late November 2007. We anticipate similar interest for each of the remaining GeoEarthScope datasets once they are released. This poster will provide an overview of the GEON-based GeoEarthScope LiDAR data distribution system as well as information on data usage and delivery status.

Southern San Andreas Fault Evaluation (SoSAFE)

2-043

AN OVERVIEW OF THE NCALM ALSM OBSERVING PROGRAM FOR THE UNAVCO SOUTHERN CALIFORNIA (SOCAL) PROJECT. *Carter W, Shrestha RL, Sartori M, Schofield S, and Slatton C*

During the period of April 2, to April 24, 2008, the National Center for Airborne Laser Mapping (NCALM) collected airborne laser swath mapping (ALSM) observations along approximately 900 kilometers of major fault lines in southern California (SoCal). Funding for the project was provided by UNAVCO, and UNAVCO and Ohio State University personnel participated in the field operations.

All of the SoCAl ALSM observations were collected with an Optech Gemini system, during 19 flights, totaling some 60 hours of flying time. The widths of the corridors covered varied from 1.2 km to 6 km, in accordance with project specifications set by UNAVCO. The nominal flying height was 750 meters above local ground level, laser pulse rates were set at 70 or 100 kHz, and the scanner was generally set at 40 Hz and a scan angle of 25 degrees (on both sides of nadir). The flying height, laser pulse rate, and swath-to-swath overlap resulted in a nominal point density of 6 points per square meter. The most challenging problem encountered during the data collection was relatively strong seasonal winds, which caused several planned flights to be delayed or canceled.

The NCALM aircraft, a Cessna an inline twin-engine aircraft, was equipped with two GPS receivers, each connected to separate antennas: a rack mounted Trimble BD950 GPS Receiver Module connected to a dual frequency high gain (35 db)Aero-antenna, and a Topcon GB 1000 receiver connected to an Aero-antenna with a 40.0 db amplifier. The Topcon receiver and associated antenna were provided by OSU. The two receivers and antennas were installed on the aircraft to evaluate their relative performance, and to minimize the loss or degradation of the final ALSM data caused by poor aircraft GPS observations. All of the aircraft trajectories used by NCALM to reduce the SoCAL ALSM observations were generated by Gerald Mader, NOAA, using the latest version of his kinematic GPS processing software. Mader typically used 4 to 6 ground base stations, from which he independently computed trajectories. The trajectories were compared and examined for any unusual differences, and then combined to form the final trajectory for each flight.

The SoCAL ALSM observations were reduced following standard NCALM computing and quality control procedures, filtered, and divided into tiles. Both the point cloud and gridded data are available and researchers wanting to obtain data for their research should contact UNAVCO.

2-044

SLIP ALONG THE SAN ANDREAS FAULT ASSOCIATED WITH THE GREAT 1857 EARTHQUAKE BETWEEN CHOLAME AND PINE MOUNTAIN, DERIVED FROM "B4" LIDAR HIGH RESOLUTION TOPOGRAPHIC DATA *Zielke O, and Arrowsmith JR*

The definition of fault segments (e.g., Cholame or Carrizo segment) along the southern San Andreas Fault (SAF) is based on the distribution of surface slip during the great 1857 earthquake. Amount and distribution of slip along the rupture are also required to estimate the magnitude of this event and are used to estimate average recurrence intervals of large earthquakes. The classic study by Sieh (1978) -examining aerial photographs and traversing most of the surface rupture- revealed offsets ranging from 3.0 to 9.5 meters along the 300 km long, central part of the 360 to 400 km long surface rupture. He found that the variation is broadly systematic, with uniform slip along

each of several long segments, but abrupt changes between the segments (e.g., ~3.5 m in Cholame segment, ~9.0 m in Carrizo segment). A similar study by Lienkaemper (2001) concentrated on the Cholame segment. Although data were too sparse and ambiguous to resolve details of the 1857 slip, the slip amount was determined to be distinctively larger (~5 m) than previously estimated. Both studies relied mainly on field observation and aerial photographs of offset landforms --mostly ephemeral channels crossing the fault trace(s) at high angles.

We use "B4" LiDAR high resolution topographic data (resolution: 0.25 m) to determine the slip distribution of the 1857 earthquake along the Cholame and Carrizo fault segments. After fault line and offset linear features (i.e., fluvial channels) are traced at a site, we determine the position of upstream and downstream profile. Then we back-slip one profile relative to the other in 0.1m increments and calculate the elevation difference between both profiles. The amount of slip where the difference between both profiles has its minimum is considered the optimal displacement estimate. We measured offsets for channels identified by previous studies and utilized the spectacular resolution of the LiDAR data to find additional geomorphic features that were offset in 1857 and prior earthquakes.

Although this work is still in progress, preliminary results show relatively uniform slip of ~4.6m for the Cholame Segment. Inspection of offset gullies not previously identified along the Carrizo Segment suggest that the ramping (increase in slip from 3 to 9m) proposed by Sieh (1978) may not occur. In the Carrizo Plain, we found a number of gullies that were offset by only 4-6m, suggesting that the observed 9m offsets may be the result of more than one earthquake.

2-045
TECTONIC GEOMORPHOLOGY OF THE SAN ANDREAS FAULT ZONE FROM HIGH RESOLUTION TOPOGRAPHY: AN EXAMPLE FROM THE CHOLAME SEGMENT *Arrowsmith JR, and Zielke O*

High resolution topographic data along fault zones are important aids in the delineation of recently active breaks. A 15 km-long portion of the south-central San Andreas Fault (SAF) along the southern Cholame segment preserves spectacular tectonic landforms such as benches, troughs, scarps, and aligned ridges that indicate recurring earthquake slip. Recently acquired LiDAR topographic data along the entire southern SAF ("B4" project) have shot densities of 3-4 m^2. Computed from the LiDAR returns, Digital Elevation Models (DEMs) of 0.25 to 0.5 m resolution using local binning with inverse distance weighting and 0.8 m or larger search radii depict the tectonic landforms at paleoseismic sites well enough to rate them confidently. Mapping of recently active breaks using a LiDAR-only based approach compares well with aerial photographic and field based methods. The fault zone varies in width from meters to nearly 1 km and is comprised of numerous en echelon meter to km-length overlapping sub parallel fault surfaces bounding differentially moving blocks elongate parallel to the SAF. The semantic variations of what constitutes "active" and the importance of secondary traces influence the breadth and complexity of the resulting fault trace maps.

2-046
THE SAN ANDREAS FAULT ZONE IN SAN GORGONIO PASS: A GEOLOGIC-FRAMEWORK PERSPECTIVE *Matti JC*

The pioneering work of C.R. Allen (1957) in San Gorgonio Pass (SGP) demonstrated three points that have stood the test of time. First, a single throughgoing trace of the modern San Andreas Fault (SAF) cannot be mapped confidently through the Pass; second, the architecture of the SAF zone in the Pass is extraordinarily complex; third, any SAF rupture is likely to be complicated. For these

reasons, SGP has come to be known as a structural knot in the SAF—a knot that plays an enigmatic role in scenario earthquakes.

From oldest to youngest, the SAF zone in SGP consists of four discrete strands, each having its own movement history period: (1) the Wilson Creek strand (~5 to ~4.0 Ma, ~40 km); (2) the Mission Creek strand, the major SAF strand in terms of right-slip (~90 km) but not the site of active faulting since ~1.0 Ma; (3) the Mill Creek strand, locus of mid to late Quaternary right-slip (~8-10 km); and (4) the San Bernardino strand (~2-3 km), the modern trace of the SAF that approaches SGP from the northwest via Burro Flats but loses its geologic expression before it reaches the core of SGP. Two young SAF strands approach SGP from the Coachella Valley (CV): (a) the Banning strand and (b) the Garnet Hill strand; both are aligned with the San Bernardino strand, but they do not meet it at the surface. Instead, the SGP Fault zone intervenes, forming a transverse contractional system that obscures any Holocene right-slip faults that once may have formed a throughgoing SAF. No tectonogeomorphic evidence exists for a throughgoing earthquake rupture on the SAF in the SGP region in the last several thousand years, despite a generally similar chronology of paleoearthquakes in the CV and the Cajon Pass region on either side of the Pass.

Ongoing fault-history and landscape studies suggest that the longer Quaternary history of right-slip in the SGP region may be comparable to the Holocene history—that is, slip throughout the SAF zone may have been considerably lower in SGP relative to the CV. Especially at the mouth of Mission Creek, slip on the combined Mill Creek and Mission Creek strands may have been quite low, with Quaternary deposits as old as 0.5 Ma displaced no more than 8-10 km. Matti and Morton (1993) used these data to propose that Quaternary slip on the SAF has largely stepped left across SGP and onto the San Jacinto Fault, beginning as recently as 1.2 Ma. Of interest to SoSAFE: is the Holocene San Gorgonio Pass knot in the SAF tying up or untying?

2-047

UNCERTAINTIES IN SLIP RATE ESTIMATES FOR THE MISSION CREEK STRAND OF THE SOUTHERN SAN ANDREAS FAULT AT BISKRA PALMS OASIS *Behr WM, Rood DH, Fletcher KE, Guzman NE, Finkel R, Hanks TC, Hudnut KW, Kendrick KJ, Platt JP, Sharp WD, Weldon RJ, and Yule JD*

This study focuses on uncertainties in geologic slip rate estimates on the southern San Andreas fault where it offsets an alluvial fan (T2) at Biskra Palms Oasis in southern California. We provide new estimates of the amount of offset of the T2 fan aided by trench excavations, and new cosmogenic 10-Be age determinations from the tops of 12 boulders on the fan surface. We present three alternative offset models: a minimum, maximum, and preferred of 660 m, 980 m, and 770 m, respectively; and we assign an age of 50 ± 5 ka from the 10-Be data, which is significantly older than previously recognized, but is consistent with ages from U-series on pedogenic carbonate from T2 described in a companion presentation by Fletcher et al. (2008). These new constraints lead to a range of slip rates of between 12 and 22 mm/yr with a preferred estimate of 15.6 mm/yr for the Mission Creek strand of the southern San Andreas fault. We also place these results in the context of discrepancies between geologic and geodetic slip rates. Previous studies suggested that the geologic and geodetic slip rates at Biskra Palms were incompatible. We find, however, that considerable uncertainty affects both the geologic and geodetic slip rate estimates, such that if a real discrepancy between these rates exists for the southern San Andreas fault at Biskra Palms, it cannot be demonstrated with available data.

2-048
STRATIGRAPHY AND OSL DATING OF THE BISKRA PALMS ALLUVIAL FAN: PRELIMINARY RESULTS *Medina Luna L, Yule D, and Rittenour T*

Biskra Palms, CA, is an area where the Banning and Mission Creek faults, two complex segments of the San Andreas Fault, offset a cement quarry-exposed alluvial fan, revealing its sedimentation history. Geochronologic research has been ongoing over the past 20 years, research crucial for constraining the slip rate of the San Andreas Fault and understanding the hazards facing Riverside County and Southern California. Previous work has focused on dating the upstream T2 surface of the fan using 10Be cosmogenic radionuclide and U-series age dating methods.

More recently, Jerome van der Woerd et al. (2006) calculated a slip rate of ~16 mm/yr using an offset estimate of ~565 meters and a T2 surface age of 35,000 yrs based on 10Be cosmogenic radionuclide age dating methods. Keller and Bonkowski (1982) calculated a slip rate of ~ 23-35 mm/yr using an offset estimate of 700 meters and T2 surface age on the order of 20-30,000 yrs, an overestimate according to van der Woerd (VDW) et al. (2006). However, VDW et al. (2006) sampled cobble-size material that may underestimate the surface age if removal-or deflation- of the uppermost part of the surface has occurred, and used piercing points along the edge of the fan now believed to be a fault, providing VDW et al. a false fan offset. To test the potential problem with the 35,000 yr age of VDW et al. (2006) other researchers have determined cosmogenic ages of large boulders (Behr et al. in prep) and U-series ages of carbonate rinds of granitic cobbles in the K soil horizon beneath T2 surface (Fletcher et al., in review); both works are indicating a T2 surface age of ~45-50,000 yrs.

My current research examines both upstream and downstream sections of the alluvial fan, focusing on the downstream section where I have described the sedimentology and stratigraphy of the 80 meter exposed alluvial fan. Preliminary age control is determined by the single aliquot optically stimulated luminescence (OSL) dating method applied on stratigraphically collected samples within both fan sections. Unlike cosmogenic and U-series surface dating, OSL provides the age of sediment deposition. Objectives of this research are to 1) use OSL dating to determine the ages of the quarry-exposed sedimentary layers to bracket the time of fan deposition and thus determine a sedimentation rate and 2) to compare the OSL ages with the cosmogenic and U-series ages, enabling for calibration between the three dating methods.

2-049
DETERMINING FAULT OFFSETS AND SLIP RATES ON THE CLAREMONT STRAND OF THE SAN JACINTO FAULT ZONE *Onderdonk NW*

Recent studies have shown that Holocene slip rates along the southernmost San Andreas Fault, south of its juncture with the San Jacinto Fault, may be slower than previously supposed (e.g., McGill et al., 2007; Fletcher et al., 2006) while the San Jacinto Fault has a larger slip rate than previously thought (Kendrick et al., 2002; Rockwell et al., 1990; Morton and Matti, 1993). In addition, geodetic studies indicate that the San Jacinto Fault may be accommodating a larger amount of the plate boundary displacement than the southernmost San Andreas Fault (e.g., Becker et al., 2005, Fialko, 2006).

The Claremont strand of the San Jacinto Fault Zone occupies a key location for studying the distribution of strain across the Southern San Andreas System. The fault provides the physical link between the San Andreas Fault and the rest of the San Jacinto Fault Zone and is in close proximity to the San Bernardino Mountains restraining bend of the San Andreas Fault. This goal of this study is to determine Quaternary slip rates for this stretch of the San Jacinto Fault Zone to compare to slip

rates elsewhere along the San Jacinto Fault Zone and along the nearby section of the San Andreas Fault.

Along the northern section of the Claremont Fault, a number of parallel and sub-parallel faults have been observed in the San Bernardino Valley sediments and bordering uplifted areas that are accommodating some strain (e.g., Morton and Matti, 1993; Schell, 2008). At the southern end, the Claremont Fault bounds the northern edge of a releasing step-over with the Casa Loma Fault, and additional slip has occurred on the Hot Springs Fault segment to the northeast. However, in the Moreno Valley area, no significant parallel faults are observed and other than sub-parallel folding in the Timoteo Badlands, the Quaternary deformation is confined to a zone no more than .5 km wide.

Analysis of B4 LIDAR data and field mapping in the Moreno Valley area reveal a number of offset features with which to determine the slip rate on the fault. The younger offsets range from 15m to 40 m with 8 streams offset approximately 20 ± 5m in one location. Older offsets range from 110 to 160 m. Quaternary mapping and preliminary soil descriptions indicate that deposits from a range of Quaternary ages are offset by the fault and thus provide the means to determine slip rates over various time intervals. The ages of these deposits are being determined using both radiocarbon and OSL dating methods.

2-050
PRELIMINARY SLIP RATES ALONG THE SAN BERNARDINO STRAND OF THE SAN ANDREAS FAULT *McGill SF, Weldon RJ, and Owen LA*

Results from three sites along the San Bernardino strand of the San Andreas fault suggest that the latest Pleistocene slip rate decreases southeastward from ~ 25 mm/yr at the confluence of Lone Pine and Cajon Creeks in Cajon Pass (Weldon and Sieh, 1985) to a rate in the mid-teens (mm/yr) at two sites along the central portion of the San Bernardino strand (Badger Canyon and Plunge Creek). At Plunge Creek, the slip rate is measured from the correlation of a truncated channel edge southwest of the fault with a terrace rise northeast of the fault. Three radiocarbon dates that constrain the age of initial incision of the riser (~ 32 ka) suggest a slip rate of 11 mm/yr (95% confidence interval of 3.6 to 17.6 mm/yr; ignoring 3 OSL dates of 14-20 ka that are viewed as being anomalously young due to bioturbation, which is likely at this site). Two OSL dates that constrain the age of abandonment of the riser (~14-15 ka) suggest a slip rate of 14.1 mm/yr (95% confidence interval of 8.1 to 21.7 mm/yr). At the Badger Canyon site, an offset alluvial fan with an age of ~13 ka (OSL) to ~ 15 ka (C-14) yields a slip rate of 12.8 mm/yr (95% CI: 7.2-19.7 mm/yr). An older fan at the same site yields a rate of 13.6 mm/yr (using the 27.5 ka C-14 age) or 17.7 mm/yr (using the OSL age of ~ 20 ka). A riser incised into this fan yields a slip rate of 13.2 mm/yr (95% CI: 11.1-16.7 mm/yr; based on C-14 dates on detrital charcoal).

We propose that slip transfers from the Mojave section of the San Andreas fault to the northern San Jacinto fault zone in the vicinity of Cajon Pass, where the two fault zones parallel each other and are only 2.5 km apart for a distance of about 16 km along strike. Within this proposed transfer zone, an offset landslide with a Be-10 age on exposed boulders yields a slip rate of 19 mm/yr (range 13-28 mm/yr). This rate is intermediate between the ~ 25 mm/yr rate a few km to the northwest at Cajon Creek and the rates in the mid-teens (mm/yr) to the southeast at Badger Canyon and Plunge Creek.

At Badger Canyon, rates measured over the the past ~30 ka and past ~14-15 ka are consistent with each other, although the uncertainties are large enough to allow for moderate changes in slip rate

over time. These latest Pleistocene rates, however, are still substantially higher than rates inferred from elastic block modeling of geodetic data.

2-051
SPATIAL AND TEMPORAL SLIP RATE VARIABILITY ON THE SAN JACINTO FAULT *Le KN, Oskin ME, Rockwell TK, and Owen LA*

The role of the San Jacinto fault in accommodating plate boundary motion is pivotal to understanding fault system behavior in southern California. We present new slip rate results from alluvial fans displaced by two parallel strands of the southern San Jacinto fault zone: the Clark fault and Coyote Creek fault. Alluvial fans were mapped in the field with aid of 'B4' LiDAR imagery and dated using cosmogenic 10Be exposure. We find that slip rates 1) varied synchronously by at least a factor of two over the past ~35 kyr and 2) change significantly along strike as slip is transferred southeastward from the Clark fault to the Coyote Creek fault. Latest Pleistocene (~35 kyr) to present dextral slip rates for the Clark fault are 4.6 ± 1.6 mm/yr at the Rockhouse Canyon and 1.5 ± 0.4 mm/yr near the southern Santa Rosa Mountains. For a comparably aged displaced alluvial fan at Ash Wash along the Coyote Creek fault, we find a slip rate of 3.1 ± 1.0 mm/yr. Combined, these yield an average rate of slip along the San Jacinto fault system of 7.7 ± 2.6 mm/yr over the past ~35 kyr. Mid-Holocene to present rates are significantly faster along both fault strands. Displaced ~5 ka alluvial fans show that the Clark fault slips at a rate of 7.7 ± 1.8 mm/yr at Rockhouse Canyon and 3.9 ± 1.4 mm/yr at the southern Santa Rosa Mountians. At Ash Wash, the Coyote Creek fault may have slipped at a rate as high as 12.4 ± 3.5 mm/yr over the past ~2 ka. Overall these Holocene rates are comparable to geodetic slip-rate estimates of 15 to 21 mm/yr for the San Jacinto fault zone, and imply that presently it may dominate plate boundary motion in southern California. The apparently synchronous variation of slip-rate along both strands of the San Jacinto fault suggests that the rate of loading across the fault zone has varied significantly over the past ~35 kyr.

2-052
OLD EARTHQUAKES, NEW DATES: AMS 14C DATES ON CHARCOAL FROM PALLETT CREEK *Scharer KM, Gerard TL, and Weldon RJ*

The Pallett Creek paleoseismic record holds a keystone position in most attempts to develop rupture histories for the southern San Andreas fault. Unlike the other long records on the fault, however, Pallett Creek radiocarbon ages were determined by decay counting methods rather than accelerator mass spectrometry (AMS) methods. The organic layers at Pallett Creek contain a heterogeneous mix of partially decomposed, in-situ plant material, charcoal and wood detritus, and invasive roots, all of which would contribute (in competing ways) to the dates of the large samples required for decay counting methods and the resulting earthquake ages.

We present 40 new AMS dates from the Pallett Creek site and compare these to the original layer ages of Sieh et al. (1989) and Sieh (1984) and earthquake ages recalculated by Biasi et al. (2002). Careful examination of samples revealed that charcoal fragments are a common component of the organic-rich layers. To take advantage of small sample sizes dateable by AMS, 22 dates are from individual charcoal pieces and 4 dates are from composite charcoal samples (when pieces were too small for separate dates). The remaining 14 dates are for bulk samples from layers where the charcoal was too finely disseminated to pick out and include analyses for both AAA and humic pretreatments.

In general, the AMS dates compare very well to the original large-sample dates. As expected, some AMS charcoal pieces are >100 cal years older than others in the same layer, indicating old source

material or longer travel times for the detrital material. The most interesting difference is for the older layers (P52-P35), where most of the AMS dates are younger than the original dates. Because the AMS dates are for individual charcoal pieces, they provide maximum age estimates for the layer, suggesting that the original dates are older than the layer age. An important consequence of the AMS dates is younger ages for earthquakes F and I, and because layer 52 is the lower bounding layer for events N and R, these earthquakes ages also become younger. As a result, the AMS-derived earthquake chronology appears less clustered than the original, although pending AMS dates including several near P52 may alter this initial conclusion. Finally, we also present a comparison of the earthquake ages in Biasi et al. (2002) with OxCal models of the original and new AMS derived dates.

2-053

SLIP RATE SITE ON THE SAN ANDREAS FAULT NEAR LITTLEROCK, CA *Weldon RJ, Scharer KM, Sickler RR, Pruitt AH, Gilleland CL, and Garroway J*

Work at the Littlerock site has focused on two offsets that have been interpreted to yield slip rates from about 2-4 cm/yr for time intervals of ~3500 and ~450 years (3 earthquakes based on the nearby Pallett Creek chronology). In response to a 2007 SoSAFE field review we addressed three key points to complete the project. For the older ~3500 year old offset, we confirmed that the offset "yellow gravel", previously only dated and exposed well on the north side of the fault, really exists on the south side and that there are no older deposits on the south side that could have been scoured from the north side (thus allowing for an older age and slower slip rate). Our second objective was to extend the younger offset channel to the fault to confirm that it was cleanly truncated (and thus did not flow along the fault and have less offset). Finally, we collected additional C-14 samples from deposits associated with both offsets.

We dug two large benched pits into the main tributary channels on the south side of the fault and found 6-8 m of an alluvial deposit that is visually identical to the "yellow gravel" (re-exposed on the north side for comparison). Seven stratigraphically consistent dates from these pits and the original T1 exposure show that the "yellow gravel" accumulated continuously between about ~3500 and ~1000 BP. We infer that the major incision event that set the geomorphology of the ~130 m offset ended just before our oldest date in the "yellow gravel", yielding a slip rate of just under 3.7 cm/yr. While it is possible that offset of the deep channel preceded onset of deposition of the "yellow gravel", we found no older deposits, and the switch from deep downcutting to aggradation is the most likely event to set the geomorphology of the ~130 m offset.

To test the younger offset we progressively excavated between Trench 16 and the fault to trace the channel to the fault. The thalweg and the western margin of the channel were traced to the Juniper Hills bedrock directly above a bedrock fault, providing clear evidence that the channel was cut by movement of the shutter ridge. Based on the outlet on the north (opposite) side of the fault, the channel is offset between 9 and 20 m, with a preferred value (exits straight out the outlet) of 17-18 m. C-14 dates above and below the channel suggest an age of 1440 to 1660 AD, consistent with offset caused by the last 3 earthquakes documented at Pallett Creek and a slip rate of ~3.6 cm/yr.

2-054

LONG-TERM SLIP RATES OF THE ELSINORE-LAGUNA SALADA FAULT, SOUTHERN CALIFORNIA BY U-SERIES DATING OF PEDOGENIC CARBONATE IN PROGRESSIVELY OFFSET ALLUVIAL FAN REMNANTS *Fletcher KE, Sharp WD, and Rockwell TK*

The Elsinore-Laguna Salada fault (ELSF) is one of the principal strands of the San Andreas fault system in southern California, however its seismic potential is often de-emphasized due to previous estimates of a low slip rate. The fault zone has produced two historic earthquakes over M6, with the 1892 event estimated at >M7; thus further investigation of the long-term slip rate on the ELSF is warranted.

On the western slopes of the Coyote Mountains (CM), southwest Imperial Valley, a series of alluvial fans are offset by the ELSF. These fans can be correlated to their source drainages by their distinctive clast assemblages, thereby defining measurable offsets. Clast proportions were determined by counting clast-types at 10 cm grid-points on a 1 m square grid. Populations of 300-600 points yielded definitive matches between displaced alluvial fans and their sources, indicating that this is a useful method for distinguishing among plausible sources with lithologically distinct clast populations. Two fan remnants and one buried soil that are dateable by U-series are offset within a 600m segment of the fault, by 78 ± 6m, 83 ± 29m and 580 ± 110m. In CM gravels 10's ka and older, carbonate forms continuous, dense, yellow coatings up to 3 mm thick on the undersides of clasts. Carefully selected samples of dense, innermost lamina weighing 7 to 104 milligrams analyzed by TIMS are geochemically suitable for precise U-series dating with U = 0.7- 3.8 ppm, and median 238U/232Th ~ 37. CM samples yield reproducible U-series ages for coatings from the same microstratigraphic horizon (e.g., 48.1 ± 1.7 and 50.0 ± 1.6 ka; 33.8 ± 2.7 and 33.4 ± 3.0 ka), indicating that U-Th systems have remained closed and that inherited coatings have been avoided. Accordingly, U-series on pedogenic carbonate provides reliable minimum ages for deposition of host landforms, thereby facilitating determination of maximum bounds on corresponding slip rates. The number of progressively offset geomorphic surfaces at CM affords the opportunity to examine the pattern of slip on the ELSF over time scales from a few thousand to a few hundred thousand years. Initial results indicate that the ELSF has slipped at a maximum mean rate of about 2 ± 0.2 mm/yr over the past 43 ka in the SE CM. The rate may be higher to the NW where slip increases in recent past ruptures. Available data are consistent with a much higher slip rate (~5.5 mm/yr) prior to 43 ka, but further work is needed to assess this possibility.

2-055

CONCEALED MARGIN OF THE BISKRA PALMS ALLUVIAL FAN, THRUST FAULT OR LANDSLIDE?: FOR THE SLIP RATE OF THE COACHELLA VALLEY SEGMENT, SAN ANDREAS FAULT *Guzman NE, and Yule D*

The Coachella Valley segment of the San Andreas fault is a principally linear feature, which consists of several splays, including the Banning and Mission Creek segments. An alluvial fan, dissected into three segments by two strands of the Mission Creek fault, is adjacent to the Biskra Palms Oasis near the city of Indio, Ca. This is one of a few limited geological features existent that can be used to obtain a sense of slip on the southern San Andreas fault. Keller et al. (1982) completed a study at Biskra Palms fan, compiling general geologic information such as stratigraphy and fault mapping; the main effort was to obtain a slip rate along this portion of the fault using soil horizon mapping to date the fan surface and fan reconstruction to get total movement offset, ultimately acquiring an estimate age of 20-30 ka. A more recent study by van der Woerd et al. (2006) uses the decay of Beryllium and Aluminum isotopes in granitic cobble and boulder tops to constrain the age of the Biskra alluvial fan, obtaining an age of 35.5 +/- 2.5 ka. However, both studies in offset reconstructions use the northwestern facing geographical limit of the lower fan segment, referred to as T2l by van der Woerd et al. (2006), and are now possibly recognized as erroneous. This study investigates the estimated stratigraphic extent of T2l by examining trenches dug at the base of hillsides across the stream channel bordering the questioned physical extent of T2l and within the upper northwestern limit of the fan. A total of four trenches

were excavated with six trench wall exposures used to characterize and define this periphery. Trenches revealed Palm Spring Formation fine sands and gravels overridden and sheared along a shallow dipping, nearly horizontal plane, with oxidized alluvial soil, gravels and colluvial material. This boundary may be the Banning fault locally thrusting Palm Spring Fm material over the northwestern edge of T2l or a landslide. Below the surface T2l is distinguished by a rust colored soil horizon; this soil horizon is similar in color and texture to horizons exposed in numerous trenches. The active stream channel bordering the edge of T2l may have eroded an artificial boundary, thus meaning the true boundary is perhaps concealed. Using an estimated location for the reevaluated geological limit of T2l may allow for a more accurate fan reconstruction and coupled with modern dating techniques, can yield a new slip rate at Biskra Palms.

2-056
EXPLORATION OF THE IMPACT OF GROUND RUPTURE SHAPE ON SELECTION OF RUPTURE SCENARIOS DEVELOPED FROM PALEOSEISMIC DATA ON THE SOUTHERN SAN ANDREAS FAULT *Biasi GP, and Weldon RJ*

Paleoseismic evidence at individual sites on a major fault must somehow be combined in order to develop a history of ground rupture along the fault. Uncertainties in dating paleoearthquakes make the association between sites even more uncertain. Recently developed methods provide an alternative approach to correlating individual events. Rather than focus on individual correlations of evidence, the new approach attempts to develop all possible correlations admitted within dating errors. Surface ruptures developed in this way may involve as few as one paleoseismic site or all the sites on the fault. If a multi-event history is available at many sites, an ensemble of possible rupture histories, or scenarios, for the fault may be constructed. Collateral information may be used to select most likely scenarios from the ensemble. Among measures used to select among scenarios, the most discriminating developed to date has been to compare the sum of displacements of ruptures with the total fault displacement predicted from the total time in the scenario and the fault slip rate at the point being considered. The methodology for developing ruptures and scenarios, and selecting among them was developed and used by the Working Group for California Earthquake Probabilities in their 2008 (WGCEP-08) report to the California Earthquake Authority.

An important assumption for ranking scenarios has been the shape of the rupture profile assigned to each rupture. Rupture length falls out more or less directly because the rupture must include the paleoseismic sites it is constructed from, but the rupture displacement has been more controversial. An analytic average shape was adopted for initial work and for the WGCEP-08 report that was derived from an early compilation by Hemphill-Haley and Weldon (BSSA, 1999). This shape has certain average properties to commend it, but few alternative shapes have been explored more than heuristically. We investigate in this poster alternative ways of assigning and scaling rupture profile shapes and their impact on selection of rupture scenarios. We consider assignment of actual rupture profiles selected at random, selection of characteristic ruptures, and resampling from actual ruptures to approximate a bootstrap uncertainty bound for each scenario. Data and applications are on data from the southern San Andreas fault.

2-057
PREVIEW OF THE NEXT BIG ONE: CREATING A PERMANENT SAN ANDREAS FAULT EARTHQUAKE AND SALTON SEA LAKE HISTORY EXHIBIT AT THE SALTON SEA STATE PARK, CALIFORNIA *Seitz GG*

Assessing the San Andreas Fault's future behavior and earthquake hazard is largely based on observations of its past behavior. In preparation for the "big one", we have an unprecedented

opportunity to preserve a spectacular San Andreas Fault exposure with a record of 6 earthquakes and 5 lake episodes. The southernmost San Andreas Fault is one of the most likely faults to generate a great earthquake in Southern California. Its high slip rate of 15-25mm/yr, long quiescence of ~325 yrs compared to the average recurrence interval of 180 yrs, and single-event displacements of greater than 3 meters for the last 3-4 events, make this portion of the fault appear ready for a large magnitude earthquake sooner than other faults in California.

The southern 40 miles of the San Andreas fault along the shrinking Salton Sea are located within the area of ancient Lake Cahuilla. The episodic filling and drying of Lake Cahuilla resulted in the deposition of sediments that provide a unique high-resolution recorder of past earthquakes. We are working at the Salt Creek South (SCS) site and the excavations offer a spectacular view of the faultzone. The SCS site is the only "deep water" site, 70 m below the high shoreline, which translates into an additional minimum of ~60 yrs of lacustrine deposition for each of 5 lake episodes, or an additional 300 years of lacustrine record in the past 1300 years compared to other paleoseismic records. Although other long record sites have been developed in the Coachella Valley, they are all located at or above the high shoreline. Now that we are completing a phase of this project, we are interested in preserving this trench exposure for educational purposes.

Why create a permanent San Andreas Fault Earthquake and Salton Sea Lake History Exhibit?

- It would be the only exhibit in the United States that enables visitors to see an earthquake fault below the surface.
- It would be the only exhibit that shows the Salton Sea's lake history.
- The exceptionally dry climate in the Salton Sea region make it feasible to preserve this site in a nearly natural state.
- With the uncertain future of the Salton Sea restoration, this exhibit may provide a rare scientific view of the regions past, that would facilitate appreciation of the natural history of the region.
- Allows field trips to show how earthquake research is accomplished.
- The exhibit can encourage visitors to be prepared for future earthquakes and support future research.

Fault Rupture and Mechanics (FARM)

2-058

CORRELATION OF FAULT SEGMENTS WITH RUPTURE SEGMENTS AS A FUNCTION OF GEOMETRICAL COMPLEXITY AND STRUCTURAL CHANGES *Zielke O, and Arrowsmith JR*

Most long active faults have historically ruptured over only a part of their total length in large earthquakes. Surface ruptures often terminate at geometric or structural discontinuities in the fault zone, leading to speculation that faults may be portioned into consistent rupture segments along which slip is restricted to the individual segment where it initiated. In this hypothesis, the maximum earthquake magnitude for each segment can be estimated (via scaling relationships; e.g., Wells and Coppersmith, 1984), even in the absence of historic large earthquakes. This approach requires definition of fault segments based on changes in physical properties along the fault. The question arises then of what scale the property change (e.g., fault orientation, fault roughness, frictional behavior, and downward extension of fault) must be to cause partial or full segmentation, and where partial segmentation allows multi-segment rupture and full segmentation does not.

Using the numerical earthquake simulator "FIMozFric", we investigate the effect of geometric and structural changes of the fault zone on rupture segmentation by systematically changing parameters that control fault segmentation (fault roughness, bends, stepovers, and gaps). The simulator creates long (~10's kyrs) seismic records including time, magnitude, rupture length, rupture width, slip distribution, and surface displacement of each earthquake. While identification of fault segments is based on fault geometry and structure, we look at the surface displacement of individual events to identify rupture segments. Then we compare fault and rupture segments for each record to determine their correlation as well as the probability of multi-segment rupture as a function of geometric and structural control. At this stage, we test methods to quantify the different geometric discontinuities based on their surface expression.

The results of this study may be applied by seismologists and paleoseismologists to define rupture segments based on structurally-defined fault segments. The definition of rupture segments allows estimating the maximum earthquake magnitude that may occur on an individual segment as well as the probability of multisegment rupture –both being important in seismic hazard assessment.

2-059

INFLUENCE OF HETEROGENEOUS COUPLING ON THE SPATIAL PATTERN AND RECURRENCE OF SEISMIC RUPTURES *Kaneko Y, Avouac J, and Lapusta N*

Inspired by the recent Sumatra subduction earthquake sequence (2004 - present) on the Sunda megathrust, we explore the behavior of a simple fault model with lateral variations of frictional properties designed to induce lateral variations of the degree of coupling (i.e., the proportion of seismic to aseismic slip). The model consists of two velocity-weakening (potentially locked) segments separated and surrounded by velocity-strengthening (potentially creeping) zones. The width of the central velocity-strengthening zone and the laboratory-derived friction parameters are adjusted so that each locked segment can be ruptured independently or the rupture can sometimes propagate across the central creeping zone, producing a larger earthquake event. Despite its simplicity, the model produces complex earthquake cycles with a variety of earthquake slip patterns. The model can be used to qualitatively explain the relation of interseismic coupling to co-seismic asperities on the Sunda Megathrust. By varying the strength and width of the velocity-strengthening region, we identify the parameter regime in which such region would act either as a "permanent" or as a "weak" barrier to the coseismic rupture over many earthquake cycles. The

results suggest that variations in the moment rate of an earthquake combined with the distribution of afterslip can be used to infer frictional properties along a subduction interface.

2-060
LENGTH SCALE DEPENDENCE OF STRENGTH IN SYSTEMS WITH SELF SUSTAINED STRESS HETEROGENEITY *Elbanna AE, and Heaton TH*

It is customary to speak about the strength of a material as a material property independent of the length scale. This can be true for materials with a homogeneous microstructure and a homogeneous internal stress distribution. But what about the case when the internal stresses are heterogeneous? Would the strength become a scale dependent property?

It is clear that shallow crustal deformation is at least partly due to multi-scale dynamic ruptures (earthquakes) that occur in a spatially heterogeneous stress field. The question of the length scale dependence of the strength in the presence of these heterogeneous stresses is not a trivial one. In particular, the dynamics of events are dependent on the detailed stress field that has evolved through the action of all past dynamic events. A better understanding for the fracture process in these cases calls for the necessity of determining how the strength of the material changes as the size of the material changes.

Since it is computationally impossible to run full 3D realistic models for the Earth crust that spatially span several order of magnitudes, we studied a simple spring-block-slider model that shows similar complexity and exhibit many qualitative features similar to the real earth. We show that strength in dynamical systems that are characterized by stress heterogeneity is a length scale dependent property; lower for longer rupture lengths, and which is characterized by a power law with exponent related to the fractal exponent of the internal stress. We demonstrate that effect for both stress-based and energy-based definitions of strength.

2-061
SHOULD WE USE SPRING-AND-SLIDERS TO MODEL POSTSEISMIC TIME-SERIES? *Johnson KM, Miyazaki S, Segall P, and Fukuda J*

Current afterslip modeling efforts in the geodetic community are moving away from a purely kinematic approach, in which slip is estimated using standard inversion methods, towards dynamic models that incorporate stress boundary conditions and fault rheology. A common approach is to model geodetic postseismic time-series data with single-degree-of-freedom spring-slider models with a friction law prescribed at the base of the slider and an imposed sudden displacement of the spring to represent an earthquake. An increasingly popular approach to modeling afterslip with a continuum fault is to impose a velocity-strengthening rheology on a fault in an elastic half-space, subject the fault to a sudden change in stress due to imposed distribution of coseismic slip, and use boundary element techniques to solve for the evolution of afterslip.

There are limitations of both of these approaches. The spring-slider models assume slip occurs at a point and neglects the effect of an expanding afterslip zone. The velocity strengthening models neglect the state evolution effect incorporated in rate-and-state friction. Both models assume initial conditions on the fault immediately after the earthquake can be determined from steady-state sliding before the earthquake. Both models assume the earthquake can be imposed instantaneously and that the instantaneous velocity after the earthquake can be determined from the instantaneous stress change.

We show that some of the assumptions are questionable in the context of a model for 1D fault with earthquake cycles controlled by rate-and-state-dependent friction. We compare results from the two afterslip models with the postseismic phase of slip in the 1D rate-state friction models. We find that effect of state evolution on the fault as the afterslip zone expands and propagates into the velocity strengthening region is a significant factor in the rate of postseismic moment release on the fault. Models that neglect state evolution during afterslip may lead to misestimates of friction parameters using real data. We also find that assuming steady-state sliding before the earthquake and imposing sudden coseismic slip leads to underestimates of the amount of postseismic slip surrounding coseismic rupture because the initial sliding velocity is too low. Models assuming velocity-strengthening friction may lead to underestimates of postseismic slip or overestimates of the amount of coseismic slip needed to drive afterslip.

2-062
MACROSCOPIC DYNAMICS OF PULSE-LIKE RUPTURES IN SPATIALLY HETEROGENEOUS STRESS FIELDS *Elbanna AE, and Heaton TH*

Earthquake ruptures are examples of multi-scale phenomena showing spatial and temporal complexity. With the current computational capabilities, we are still far from running realistic 3D numerical models that can simulate a number of earthquake cycles large enough to enable the inference of reliable statistics and scaling laws. A big challenge then is to cross the computational gap and try to find physically based reduced models that can replicate the macroscopic features of that dynamical complexity.

As an attempt to achieve that goal, we studied the 1D spring-block-slider model. This model shows many of the features of the real Earth, such as the Gutenberg-Richter scaling law and pulse-like ruptures, besides having the merit of being computationally efficient. Moreover, we show here that it also replicates some of the results obtained in full elasto-dynamic models (e.g. Shaw 2006) such as average stress drop scaling. Our focus is on studying the dynamics of slip pulses in our model and trying to deduce a dynamical system of equations that can describe sptatio-temporal evolution of the slip pulses .

Our results show that the macroscopic dynamics of moderate and large events can be replicated by studying the energy balance of the propagating pulse. By writing an evolution equation for the kinetic energy of the pulse, we can predict when the pulse can grow or diminish. The kinetic energy of the pulse is the difference between the available strain energy and the work dissipated in friction. The higher the kinetic energy of the pulse the larger the pulse will be and vice-versa. However, the energy balance equation is just one equation in more than one unknown; it connects the kinetic energy to the pulse parameters (pulse width and amplitude) or the kinetic energy to the final slip and the frictional work. Hence we have to complement it with empirical relations between those parameters. We find a strong correlation between the pulse kinetic energy and the pulse slip as well as the pulse slip and the frictional work. By substituting those findings back in the energy balance equation, we can rewrite that equation either in terms of slip or kinetic energy. By solving this equation we can produce the macroscopic features of isolated moderate and large unilateral events (e.g. final slip, rupture length....etc).

Our future work aims at extending those results to small and bi-lateral events and examining whether the repeated application of that equation would preserve the heterogeneity in the system or not.

2-063
NEW COMPUTATIONAL APPROACH TO NONPLANAR ELASTODYANIC RUPTURES *Coon ET, Shaw BE, and Spiegelman M*

We present a new approach to modeling dynamic ruptures on nonplanar faults. A fundamental challenge for modeling rupture dynamics on complicated fault networks using current techniques is dealing with the computational mesh. Generation of a mesh that is both faithful to the underlying fault structure and suitable for efficient computation is an open problem. Here, we test the possibility of using an extended finite element method, XFEM, (e.g. [Dolbow, Moes, and Belytschko, 2001]) for problems of repeated rupture.

This method is mesh-independent -- the fault need not lie on mesh edges -- drastically reducing the requirements for suitable compuational meshes. We extend the method to include elastodynamics, and demonstrate the feasibility of XFEM by modeling long-time series of ruptures on complicated, two-dimensional fault networks. While the problems and geometries we solve are feasible with existing methods, this demonstration indicates that XFEM should prove useful for the solution of problems limited by mesh generation.

Using XFEM, sequences of elastodynamic earthquake events on networks of faults, including branching, are generated. Efficient solution via XFEM enables the study of statistics of populations of events and the effects of variation of geometry. As varying geometry is handled easily by the method, we study the resulting variation in event populations. Distributions of event rupture length, magnitude, epicenter location, and other statistical measures are presented and compared as a function of geometry. Results for flat fault are shown to be consistent with previous results on flat faults using other computational approaches. New results for complicated geometries are presented, and compared with those for flat faults.

2-064
AN EFFICIENT-FEM IMPLEMENTATION OF THE SMOOTH-TSN ALGORITHM FOR NUMERICAL MODELING OF RUPTURE PROPAGATION *Moczo P, Gális M, Kristek J, and Kristeková M*

The Traction-at-Split-Node (TSN) algorithm developed independently by J. D. Andrews and S. M. Day is so far probably the most accurate way to simulate dynamic rupture propagation in the numerical-modeling methods in which the computational domain is covered by a grid of discrete points. We implemented the TSN algorithm in our efficient formulation of the finite-element method (FEM). The FEM formulation requires less computer memory because it makes use of the global restoring-force vector instead of the global stiffness matrix. The formulation reduces considerably the computational time (compared to the standard restoring-force formulation) because it uses e-invariants (Moczo et al. 2007) in calculation of the restoring force.

Despite its superior accuracy, the standard TSN algorithm is not free from high-frequency oscillations in the slip-rate time histories in the models with the linear slip-weakening friction law. The oscillations are due to discretization of the field variables in time and space, and due to the dynamic boundary condition on the fault. The artificial Kelvin-Voigt damping or perfectly matched layers have been applied to suppress the oscillations.

In our implementation we do not apply either of the two tools. Instead we apply 2D spatial moving weighted averaging separately to each of the trial traction components. The weighted averaging combines a Gaussian-filtered with unfiltered values. We performed extensive numerical simulations in order to select the best smoothing algorithm. The examined algorithms included the

unconditional uniform averaging (the averaging applied at each grid point of the fault), four single-point criterion averaging (the averaging applied at a grid point if certain criteria at that point are met), and four 9-point criterion averaging (the averaging applied at a grid point if certain criteria at that point and 8 neighboring grid points are met).

The selected best smoothing algorithm was then tested for convergence for two distinct physical rupture propagation configurations.

The improved algorithm for the numerical modeling of rupture propagation has been implemented in the 3D causal hybrid viscoelastic FD-FE method and computer code for the numerical modeling of rupture and wave propagation.

2-065
RUPTURE PROPAGATION ACROSS FAULTS WITH LINKED STEPOVERS: A GEOMETRICAL PARAMETER STUDY *Lozos JC, Oglesby DD, and Duan B*

Segmented faults with stepovers are ubiquitous, and occur at a variety of scales, ranging from small stepovers on the San Jacinto Fault to the large-scale stepover on the San Andreas Fault between Tejon Pass and San Gorgonio Pass. Because this type of fault geometry is so prevalent, understanding how earthquake rupture propagates through such systems is important for evaluating seismic hazard. In the present study, we systematically investigate how far rupture will propagate through a fault with a linked (i.e., continuous fault) stepover, based on the length of the linking fault segment and the angle that connects the linking segment to adjacent segments.

We conducted dynamic models of such systems using the two-dimensional finite element method (Duan and Oglesby 2007). The fault system in our models consists of three segments: two parallel 10km-long faults linked at a specified angle by a linking segment of 500m, 1km, 2km, or 3km. This geometry was modeled both as a extensional system and a compressional system depending on the direction of shear.

We observed several distinct rupture behaviors, with systematic differences between compressional and extensional cases. Both shear directions rupture straight through the stepover for very shallow stepover angles. In compressional systems with steeper angles, rupture may jump ahead from the linking segment onto the far segment; whether or not rupture on this segment reaches critical patch size and slips fully is also a function of angle and stepover length. In some compressional cases, if the angle is steep enough and the stepover short enough, rupture may jump over the step entirely and propagate down the far segment without touching the linking segment. In extensional systems, rupture jumps from the nucleating segment onto the linking segment at shallow angles, but at steeper angles, rupture propagates through without jumping. Rupture propagates through a wider range of angles in extensional cases. In both extensional and compressional cases, for each stepover length there exists a maximum angle through which rupture can fully propagate; this maximum angle decreases asymptotically to a minimum value as the stepover length increases.

2-066
A FINITE DIFFERENCE METHOD FOR IRREGULAR GEOMETRIES: APPLICATION TO DYNAMIC RUPTURE ON ROUGH FAULTS *Belanger D, and Dunham EM*

We have developed a finite difference method to solve dynamic rupture problems in irregular geometries. Our objective is to connect properties of high frequency radiation produced during slip on rough faults to statistical measures of fault roughness. To handle irregular geometries, we

transform the governing equations from a non-Cartesian coordinate system that conforms to the irregular boundaries of the physical domain to a Cartesian coordinate system in a rectangular computational domain, and solve the equations in the computational domain.

To accurately capture the high frequency wavefield, we use a method that produces far smaller numerical oscillations than those plaguing conventional finite difference/element methods. The governing equations (momentum conservation and Hooke's law) are written as a system of first-order equations for velocity and stress, which are defined at a common set of grid points and time steps (i.e., there is no staggering in space or time). Time stepping is done using an explicit third-order Runge-Kutta method. The equations are hyperbolic and the fields can be decomposed into a set of waves (with associated wave speeds) propagating in each coordinate direction. Spatial derivatives are computed with fifth-order WENO (weighted essentially non-oscillatory) finite differences in the upwind direction associated with each wave [Jiang and Shu, J. Comp. Phys., 126(1), 202-228, 1996]. Rather than using data from a single stencil (i.e., set of grid points) to calculate the derivative, a weighted combination of data from several candidate stencils is used. The weights are assigned based on solution smoothness within each stencil, and stencils in which the solution exhibits excessive variations are given minimal weight. Consequently, numerical oscillations are suppressed, even in the vicinity of the rupture front and at wavefronts.

Boundary conditions are implemented by again appealing to the hyperbolic nature of the governing equations. At each point on a boundary (or fault), the solution is decomposed into a set of waves propagating into and out of the boundary. The amplitudes of incoming waves are preserved, while those of outgoing waves are modified to satisfy the boundary conditions. On the fault, this amounts to solving the friction law together with an equation expressing shear stress as the sum of a load, the radiation damping response, and the stress change carried by the incoming waves.

2-067
EARTHQUAKE RUPTURES WITH THERMAL WEAKENING AND THE OPERATION OF FAULTS AT LOW OVERALL STRESS LEVELS *Dunham EM, Noda H, and Rice JR*

We have conducted rupture propagation simulations incorporating flash heating of microscopic asperity contacts and thermal pressurization of pore fluid [Noda, Dunham, and Rice, in preparation, 2007-08]. These are arguably the primary weakening mechanisms at coseismic slip rates, at least prior to large slip accumulation. Ruptures on strongly rate-weakening faults take the form of slip pulses or cracks, depending on the background stress level. Self-sustaining slip pulses exist only within a narrow range of stresses; below this range, artificially nucleated ruptures arrest, and above this range, ruptures are crack-like. Certain features of our simulations lend support to the idea that faults operate at the minimum critical level required for propagation, such that natural earthquakes take the form of slip pulses.

Using flash heating parameters measured in recent laboratory experiments, the critical range occurs when the ratio of shear to effective normal stress on the fault is 0.2-0.3 (a range that is only mildly influenced by the choice of thermal pressurization parameters, at least within a reasonable range of uncertainty around laboratory-measured values). This level is consistent with the low stress inferred to be acting on the San Andreas fault (SAF); a ratio of shear to effective normal stress of 0.24 was measured at 2.1 km depth in the SAFOD pilot hole [Hickman and Zoback, 2004], adding further support to other measurements indicating that the maximum horizontal compressive stress is nearly perpendicular to the SAF. While the overall background stress level is

quite small, stresses concentrated at the rupture front are consistent with typical static (and low velocity) friction coefficients of 0.6-0.9; this stress concentration is required to initiate slip.

Growing slip pulses have stress drops close to 3 MPa and feature slip increasing with propagation distance at a rate of about 0.14 m/km. These values are consistent with seismic inferences of stress drop and field constraints on slip-length scaling. On the other hand, cracks have stress drops of over 20 MPa, and slip at the hypocenter increases with propagation distance at a rate of about 1 m/km.

2-068

STATISTICS OF EARTHQUAKE STRESS DROPS FOR EVOLVING SEISMICITY ON A HETEROGENEOUS FAULT IN AN ELASTIC HALF-SPACE *Bailey IW, and Ben-Zion Y*

Understanding what limits the size of earthquake stress drops has important implications for estimating ground motion. Theoretical estimates based on laboratory friction data and measurements of stress in the crust are >100 MPa, yet seismological derivations are typically of order ~1-10 MPa. The discrepancy may stem from the fact that earthquake stress drops are average values over a rupture area that may have highly heterogeneous initial stress, while the theoretical estimates assume an essentially homogeneous stress. We investigate properties of stress drops in simulations of evolving seismicity and stress field on a heterogeneous fault. The model fault (Ben-Zion & Rice, 1993) consists of a set of inherently-discrete slip patches surrounded by a 3-D elastic half-space. The discrete slip patches provide a simple representation of heterogeneities associated with segmentation and other geometrical complexities. Previous studies have shown that the model produces many statistical features of seismicity compatible with observations, e.g., frequency-size and temporal event statistics, hypocenter distributions, and scaling of source-time functions. The model simulations allow us to investigate stress drops from a range of initial stress distributions that are determined by the self-organized stress evolution along the fault over time. We show that the stress drops are systematically lower than predicted for a homogeneous fault, and that this effect is stronger as larger events are considered. Events that saturate the seismogenic zone consistently have stress drops that are ~30% of the predictions based on the average fault strength, as well as showing less variation than the stress drops of smaller events. We further investigate how this variation is affected by rheological properties of the model and hypocentral depth.

2-069

CONSTANT STRESS DROP FROM SMALL TO GREAT EARTHQUAKES IN MAGNITUDE-AREA SCALING *Shaw BE*

Earthquakes span a tremendous range of scales, more than 5 orders of magnitude in length. Are earthquakes fundamentally the same across this huge range of scales, or are the great earthquakes somehow different from the small ones? We show that a robust scaling law seen in small earthquakes, with stress drops being independent of earthquake size, indeed holds for great earthquakes as well. The simplest hypothesis, that earthquake stress drops are constant from the smallest to the largest events, combined with a more thorough treatment of the geometrical effects of the finite seismogenic layer depth, gives a new magnitude area scaling which matches the data well, and better over the whole magnitude range than the currently used scaling laws which have non-constant stress drop scaling. This has significant implications for earthquake physics and for seismic hazard estimates.

2-070
TRIGGERING EFFECT OF M>4 EARTHQUAKES ON THE OBSERVED OCCURRENCE OF REPEATING EVENTS AT PARKFIELD *Chen KH*

How the stress perturbation by nearby larger earthquakes influences earthquake recurrence is of fundamental important to understanding earthquake cycle and to determining earthquake hazard. The large population of characteristically repeating earthquakes at Parkfield provides a unique opportunity to study the degree to which stress interactions between earthquakes may influence earthquake recurrence intervals. We analyze 212 M -0.4 ~ 1.7 repeating earthquake sequences from High Resolution Seismic Network, to examine the response of the repeating earthquakes to the occurrence of M > 4 earthquakes. We found that recurrences of the updated HRSN repeating sequences exhibit a strong acceleration pattern associated with 2004 M 6 Parkfield event. The accelerated recurrence patterns of repeating sequences (repeaters) appear to be similar when they are close in space. The characteristically decaying afterslip pattern is not obvious for some of the repeaters adjacent to the largest co-seismic slip area, suggesting either that the stress changes are very heterogeneous, or that the rupture erased or shut off some of the sequence source areas. The unusually short intervals are found to occur subsequent to the M 4~5 events, which likely reflects the triggering effect of the major events. The triggering effect is most evident in a short distance of 5 km and decay with distance (approximately as 1/r). A large number of repeaters nearby the 1993 M 4.5 event allow us to carefully examine the spatio-temporal recurrence variation with respect to the mainshock. Not only the immediate acceleration of recurrence following the mainshock, the repeaters also reveal coherently reduced recurrence from 1993 to 1998. This enduring recurrence acceleration over years is likely associated with the accelerated slip induced by several M > 4 events during the early 1990s and the occurrence of aseismic transient since 1993.

2-071
EFFECT OF INITIAL CONDITIONS AND LOADING PATH ON EARTHQUAKE NUCLEATION *Fang Z, Dieterich JH, and Xu G*

Rubin and Ampuero [2005] report two distinct nucleation regimes of earthquake nucleation on faults with rate-state friction that are determined in part by the rate-state parameters a and b. With the first regime the nucleation zone spontaneously evolves toward a state of accelerating slip on a patch with fixed length which scales with L_b = GD_c/b?, where G represents the generalized shear modulus and ? is the normal stress, which is consistent with the scaling reported by Dieterich [1992]. With the second regime the nucleation zone develops as an expanding crack with a length scale that asymptotically approaches L_∞ = π^-1[b/(b – a)]^2(GD_c/b?). When a/b approaches 1, L_∞ can be more than 100 times larger than Lb, which greatly increases the probability that detectable premonitory signals will be generated by the nucleation process. However, questions arise relating to how often and how large expanding nucleation zones occur in nature. Because the nucleation regimes are also controlled by evolution of the friction state variable, to answer these questions, we have explored nucleation over a very wide range of initial conditions that result in different evolution paths for the state variable. Our results suggest that even for a large value of a/b = 0.9, expanding nucleation zones that approach the maximum size L_∞ can only develop from a very narrow range of initial conditions. In addition, the initial conditions giving large nucleation dimensions appear to be difficult to access during normal cycles of stress buildup between earthquake slip events. For most initial conditions, nucleation either evolves as a patch with fixed length or only shows slight expansion. This suggests that long-term strain precursors and seismic signals generated during the transition to dynamically propagating ruptures may be difficult to detect.

2-072

SEISMICITY IN A MODEL GOVERNED BY COMPETING FRICTIONAL WEAKENING AND HEALING MECHANISMS *Hillers G, Carlson JM, and Archuleta RJ*

Observations spanning a wide range of space and time scales suggest a strain dependent progressive evolution of material properties that control the stability of earthquake faults. The associated weakening mechanisms are counterbalanced by a variety of restrengthening mechanisms. The efficiency of the healing processes depends on local crustal properties such as temperature and hydraulic conditions. We investigate the relative effects of these competing nonlinear feedbacks on seismogenesis in the context of evolving frictional properties, using a mechanical earthquake model that is governed by slip weakening friction. Weakening and strengthening mechanisms are parameterized by the evolution of the frictional control variable--the slip weakening rate R--using empirical relationships obtained from laboratory experiments. Weakening depends on the slip of a model earthquake and tends to increase R, following the behavior of real and simulated frictional interfaces. Healing causes R to decrease and depends on the time passed since the last slip. Results from models with these competing feedbacks are compared with simulations using non-evolving friction. Compared to fixed R conditions, evolving properties result in a significantly increased variability in the system dynamics. We find that for a given set of weakening parameters the resulting seismicity patterns are sensitive to details of the restrengthening process, such as the a lower cutoff time, tc, up to which no significant change in the friction parameter is observed. For relatively large and small cutoff times, the statistics are typical of fixed large and small R values, respectively. However, a wide range of intermediate values leads to significant fluctuations in the internal energy levels. The frequency-size statistics of earthquake occurrence show corresponding nonstationary characteristics on times scales over which negligible fluctuations are observed in the fixed-R case. The progressive evolution implies that--except for extreme weakening and healing rates--faults and fault networks possibly are not well characterized by steady states on typical catalog time scales, thus highlighting the essential role of memory and history dependence in seismogenesis. The results suggest that an extrapolation to future seismicity occurrence based on temporally limited data may be misleading due to variability in seismicity patterns associated with competing mechanisms that affect fault stability

2-073

DILATANCY STABILIZATION VS THERMAL PRESSURIZATION AS A MECHANISM FOR DETERMINING SLOW VS FAST SLIP *Segall P, Rubin A, Rice JR, and Schmitt SV*

We have previously discussed the possibility that rate-state friction nucleates slip under drained conditions but that as slip accelerates dilatancy-induced pore-pressure reductions quench the instability, resulting in slow slip. Accelerating slip also leads to shear heating and consequent thermal pressurization of pore-fluids which destabilize slip, suggesting that competition between thermal weakening and dilatant hardening may control whether slip is ultimately fast or slow.

We have studied isothermal friction-dilatancy interactions assuming 2D elasticity, rate-state friction and a highly simplified dilatancy law. Pore-pressure fluctuations are governed either by simplified, isothermal membrane diffusion, or by one-dimensional diffusion into the surrounding medium computed by finite difference. For the membrane diffusion model, dimensional analysis shows that dilatant strengthening scales with the dilatancy coefficient, and inversely with effective stress. Linearized stability analysis suggests a boundary between slow and fast slip, which is supported by numerical simulations. Theory predicts that stable slip is favored by low effective stress, consistent with some seismic observations.

Model calculations with isothermal pore-pressure diffusion in a homogeneous medium are explored in the limit of vanishingly thin shearing zone. We have developed finite difference codes to couple pore-pressure diffusion with elasticity and friction. In the homogeneous diffusion case, dilatancy does not separate from the transport properties and there is no threshold for fast slip, as exists in the membrane diffusion case. Slow slip is favored by low effective stress and hydraulic diffusivity, as expected.

Dimensional analysis of the thermal-dilatancy-friction problem in the limit of vanishing shear zone thickness shows that the ratio of dilatancy to shear heating efficiency scales with the dilatancy parameter, and inversely with nominal friction, effective stress squared, and pore-compressibility. This supports the idea that slow slip is favored by low effective stress. Increasing hydraulic diffusivity decreases the dilatancy efficiency, but also diminishes the coupling of temperature changes to pore-pressure.

2-074

LABORATORY EXPERIMENTS TO UNDERSTAND DYNAMIC SLIP WEAKENING IN ROCKS AND ANALOG MATERIALS AT CO-SEISMIC SLIP RATES *Yuan F, and Prakash V*

In the present study plate-impact pressure-shear friction and the modified torsional Kolsky bar friction experiments are employed to investigate the frictional slip resistance in fine-grained Arkansas Novaculite rock, quartz and soda lime glass, at relevant normal stresses and co-seismic slip rates. The motivation of these experimental studies is to gain a better understanding of dynamic fault weakening due to flash heating of asperity contacts, so as to further delineate the conditions for which this mechanism is expected to control fault strength. The results of the plate impact experiments on soda-lime glass indicate that a wide range of frictional slip conditions exist at the frictional interface. These range from initially no-slip, followed by slip-weakening, slip-strengthening, and eventually seizure, all during a single slip event. The initial slip-weakening is most likely due to thermally-induced flash-heating and incipient melting at asperity junctions, and requires only a fraction of a mm of slip to be effective; the slip strengthening is understood to be aided by the coalescence and solidification of local softened/melt patches, which leads to continuous healing and eventual seizure of the slip interface. The maximum bulk temperature rise is attained at the frictional interface, and occurs during the slip strengthening phase (prior to the seizure of the interface). It is to be noted that during the slip-weakening phase, even though the bulk temperature rise is small, the flash temperatures at the asperity contacts are expected to approach near-melt temperatures of soda-lime glass. As slip precedes these soft near-melt asperity junctions continuously increase in size by local plastic flow leading to an increase in effective area of contact, leading to healing and eventual seizure of the slip interface. Seizure of the interface is also aided by the increase in shear-strength of the flattened asperity junctions as they are rapidly quenched by the surrounding lower temperature material. Re-initiation of slip occurs with the drop in normal stress, leading to considerable frictional heat generation. It is interesting to note that the "healed-state" is much stronger than the initial state, with the coefficient of friction being in excess of 0.8 after the re-initiation of slip. The Kolsky bar experiments show similar slip characteristics as those observed in the case of the plate impact friction experiments. The coefficient of kinetic friction during the early part of slip shows slip weakening and then decreases from an average value of 0.31 to 0.15; following this initial slip weakening the friction coefficient increases to 0.26 with an increasing slip distance -- indicating slip strengthening.

2-075
SHEAR STRAIN LOCALIZATION IN DYNAMIC RUPTURE AND STICK-SLIP MODELS *Daub EG, Manning ME, and Carlson JM*

We study the impact of shear strain localization in models of earthquake faults, investigating the dynamics of interface-scale elastic sliders and fault-scale ruptures. We account for strain localization using Shear Transformation Zone (STZ) Theory, a continuum approximation for plastic deformation in amorphous materials. STZ Theory ties fault weakening to an effective disorder temperature. While the effective temperature is distinct from thermal temperature, it will evolve in a similar manner and we include shear heating, diffusion, and relaxation terms in its governing partial differential equation. Strain localization is incorporated into faulting studies by resolving the effective temperature dynamics on a spatial grid spanning the width of the fault zone. This approach differs from the common practice of modeling fault dynamics with a slip-weakening or rate and state friction law, as the STZ law dynamically chooses how to distribute shear strain in the gouge. In a model of an interface-scale slider, localized slip increases the spring stiffness for which a stick-slip instability occurs. At low driving rates, localization can also lead to period doubling, irregular recurrence times, and varying stress drops. Localization of slip also alters the spontaneous propagation of elastodynamic ruptures. Ruptures where strain localizes exhibit larger peak slip rates and stress drops, decreased shear stress at which supershear rupture can occur, and ruptures can propagate with lower initial shear stresses as self-healing pulses.

2-076
SUPERSHEAR RUPTURES IN 3D SIMULATIONS OF EARTHQUAKE SEQUENCES AND ASEISMIC SLIP: THE EFFECT OF RHEOLOGICAL BOUNDARIES AND WEAKER PATCHES *Liu Y, and Lapusta N*

We study supershear transition and propagation of dynamic rupture through simulations of earthquake sequences and aseismic slip in a 3D fault model. The model of a planar strike-slip fault governed by Dieterich-Ruina rate and state friction contains a potentially seismogenic velocity-weakening region surrounded by velocity-strengthening regions.

We find that the rheological boundary between the velocity-weakening and velocity-strengthening regions promotes supershear transition. During interseismic periods, velocity-strengthening regions move with slip velocity comparable to the plate loading rate, while the velocity-weakening region is essentially locked. This disparity in slip concentrates shear stress next to the rheological boundary. Once earthquake rupture nucleates, it propagates faster over these areas of higher prestress than over the rest of the seismogenic region, transitioning to supershear speeds in some cases. Since the presence of such rheological boundaries on natural faults can be inferred from laboratory studies and fault observations, this factor may significantly contribute to supershear transition on natural faults. The occurrence of supershear transition in our 3D model depends on friction properties and fault stress that develops in the model before large earthquakes and can be explained by the distribution of the effective seismic ratio (Andrews, 1976) on the fault before large events.

The phenomenon of supershear transition due to rheological boundaries could not be established in prior studies, as it can only be observed in simulations that include all of the following factors: (i) inertial effects to enable supershear transition; (ii) a 3D model to include the rheological boundary in the direction of rupture propagation; and (iii) long-term slip history to establish the corresponding stress distribution on the fault before large events.

We also find that supershear transition in 3D models of long-term slip can be further promoted by favorable compact fault heterogeneity, as suggested by the 2D single-event study of Liu and Lapusta (2008). Our simulations show that adding a fault patch of lower effective peak frictional resistance can qualitatively modify the behavior of the simulated fault, resulting in occasional supershear earthquakes in a model that has no supershear events without the patch. Supershear transition occurs at the location of the heterogeneity, as advocated by Liu and Lapusta (2008).

2-077
KINEMATIC INVERSION OF PHYSICALLY PLAUSIBLE EARTHQUAKE SOURCE MODELS OBTAINED FROM DYNAMIC RUPTURE SIMULATIONS *Konca AO, Kaneko Y, Lapusta N, and Avouac J*

A common approach to investigate earthquake physics consists of producing kinematic source models from the inversion of seismic records jointly with geodetic data. The regularization of the inversion requires some assumptions to restrict the range of possible models. Here, we evaluate to what extent physically plausible models are reliably restituted in spite these restrictions. More precisely we study which characteristics of ruptures, such as rupture velocity, slip distribution, and rise time can be reliably determined from the inversion of near-field data. We use a standard inversion scheme which assumes a rupture front propagating away from the hypocenter with a simple cosine slip-time function, and searches for solutions with minimum roughness (Ji et al, 2002). To provide inversions with physically plausible sources, we generate several earthquake scenarios using 3D spectral-element simulations of dynamic rupture (Kaneko et al., 2008). The assumed model contains a planar fault in an elastic half-space. The fault is governed by rate and state friction, with a velocity-weakening region surrounded by slip-inhibiting velocity-strengthening regions. The fault properties are varied to obtain scenarios with different slip distributions and local slip durations, leading to pulse and crack-like ruptures. For the inversion, strike, dip, average rake, velocity model and the hypocenter are given, and we search for slip evolution that best fits strong-motion and GPS data at simulated stations, without a priori knowledge of moment, smoothness, rupture velocity, or slip distribution. The comparison with the input model is done only after the best-fit model is chosen among various constraint inversions. Our preliminary results show that, overall, rupture velocity and slip distribution are well-determined. Since we assume a single cosine for the slip-time function, both crack-like and pulse-like ruptures appear as pulses in the inverted models, but crack-like ruptures have larger spatial extent at each moment. The difference between the two kinds of ruptures is thus still observable. However, the slip history at a specific point on the fault cannot be obtained accurately due to the assumed shape of the slip time function. This is probably the major drawback of these inversion procedures. Our current work is therefore directed towards implementing different slip-time functions to allow a wider range of possible behavior without adding complexity to the inversion.

2-078
INTERACTION BETWEEN DYNAMIC RUPTURE AND OFF-FAULT DAMAGE *Xu S, Ampuero J, Ben-Zion Y, and Lyakhovsky V*

The high stress concentration at the front of a dynamic rupture is expected to produce rock damage (reduction of elastic moduli) in the material surrounding the main fault plane. Off-fault yielding and energy absorption in the damage process should reduce the amplitude of the ground motion. However, the reduced elastic moduli in the damaged zone can amplify locally the motion and create a waveguide that may allow the motion to propagate with little geometric attenuation. In addition, the asymmetric damage generated in the in-plane rupture mode may produce bimaterial interfaces that can reduce the frictional dissipation and increase the radiation efficiency.

Previous studies incorporated plastic yielding in simulations of dynamic rupture (Andrews, 1975, 2005; Ben-Zion and Shi, 2005; Templeton et al., 2008) while keeping the elastic moduli unchanged. In this work we examine the dynamics of earthquake ruptures and generated motion in a model consisting of a frictional fault in a medium governed by a continuum damage rheology for the evolution of elastic moduli (e.g. Lyakhovsky and Ben-Zion, 2008). We perform numerical simulations based on the Spectral Element Method to study how the parameters of the friction law, damage rheology and background stress control the rate of growth of the off-fault damage zone, the steady-state rupture speed, the energy balance, and the maximum slip rate and ground motion.

We find that, the maximum slip velocity, steady-state rupture speed and peak ground motion with increasing values of the constitutive parameters Cd (the inverse of a damage timescale) and Cv (the intensity of damage related plasticity). The relation between Cv, Cd and the rate of off-fault damage growth with rupture distance is less trivial: the damage-induced bimaterial contrast grows faster with increasing Cd, and the sign of the contrast changes at low Cv. We also compare peak ground motion in our damage model to analogous simulations using Coulomb plastic yielding.

2-079
RUPTURE PROPAGATION AND SLIP PARTITIONING ON AN OBLIQUE UPWARD-BRANCHING FAULT SYSTEM *Oglesby DD, Bowman D, and Nunley ME*

We use dynamic 3-D finite element analysis to investigate slip partitioning and rupture propagation on an oblique left-lateral/normal fault system that branches near the surface into vertical and non-vertical branches. The model consists of a 70° dipping oblique-slip fault that extends from a depth of 15km to 5km depth and then branches upwards into a vertical segment and a segment dipping 45° The use of a simple regional stress field resolved onto all fault segments results in rupture propagation only on the base and vertical faults. However, the addition of a 2km by 3km barrier onto the bottom portion of the vertical fault causes enough of a stress perturbation on the upper dipping fault to nucleate rupture on this segment, resulting in a strongly partitioned slip distribution in the system. In all cases, strike-slip motion is concentrated on the vertical fault, and dip-slip motion is concentrated on the dipping fault. These results are not sensitive to the size and along-strike location of the barrier. Other observations in our models show that as the dipping fault slips, it induces a small amount of backwards slip on the vertical fault due to the high stress drop in our models, and the close proximity of the two branch segments. Our results may have important implications for the dynamics of branched faults and geometrically complex fault systems in general.

2-080
LABORATORY INVESTIGATIONS OF THE ORIGIN OF PULVERIZED ROCKS *Yuan F, and Prakash V*

Zones of pulverized rock have been observed in surface outcrops adjacent to the fault cores of the San Andreas and other major faults in Southern California. These pulverized rocks consists of highly fractured fragments that still fit together and essentially preserve the original rock texture. The origin of these pulverized rocks is not clear, but their structural context indicates that they are clearly associated with faulting; an understanding of their origin might allow inferences to be drawn about the nature of dynamic slip on faults, including inferences concerning the coseismic resistance to slip, energy balance of earthquakes, and implications for ground motions and radiation patterns near faults. In the present study, a series of laboratory experiments are conducted on Westerly granite rock samples to investigate whether pulverized rocks can be produced under stress-wave loading conditions in the laboratory and whether they are diagnostic of any particular process of formation. In the first series of experiments a Split Hopkinson pressure

bar (SHPB) is utilized to subject cylindrical rock specimens to well defined uniaxial compressive stress-wave loading. In these experiments the amplitude as well as the duration of the compressive loading pulse is systematically varied to study the initiation and progression of fragmentation in both confined and unconfined granite samples. Well characterized lateral confinement can be generated in the cylindrical specimens during SHPB testing by utilizing metal sleeves/jackets (of known yield and flow strengths) around the specimens during the dynamic loading process. In the second series of experiments, plate-impact experiments are conducted to obtain the stress threshold for inelasticity in Westerly granite by estimating its Hugoniot Elastic Limit (HEL) under shock-induced compression. These experiments are designed to also provide spall (tensile) strength following shock-induced compression in the granite samples. The results of the SHPB experiments indicate that the peak stress for Westerly granite under uniaxial compression is ~ 210 MPa (with a strain to failure of about 0.7%) in the unconfined state; the peak stress increases to 1 GPa with a confinement pressure of 60 MPa. The HEL for the granite is estimated to be between 4.2 to 5.0 GPa. The spall strength following the shock-compression is measured to be small (~ 50 MPa), and nearly independent of the applied compression level in the range 1.2 to 5.0 GPa. The post-impact samples show a well defined spall plane with no apparent fragmentation at a shock compression level of 1.2 GPa. At higher impact velocities, fragmentation is observed up-to 1.8 GPa, and the rock samples are reduced to a powder when the impact stress level is above 2.6 GPa.

2-081
PORE FLUID PRESSURIZATION WITHIN A LOW-PERMEABILITY FAULT CORE
Vredevoogd MA, Oglesby DD, and Park SK

We investigate the impact of pore fluid pressurization on earthquake faulting when the fault occurs within a narrow zone of low permeability (the fault core). In particular, we explore the effect of placing the slip plane at different positions within the fault core, and how the proximity to the surrounding higher permeability material affects the maximum pressurization.

We also look at fault cores of various widths, to see how the distance from the slip surface to the edge of the fault core changes the timing of the pressurization effect. We also discuss how the highest pressurization can occur off the slip surface, due to the permeability contrast (Vredevoogd et. al., 2007).

2-082
FRICTIONAL EXPERIMENTS AT INTERMEDIATE SLIP RATES WITH CONTROLLING TEMPERATURE *Noda H, Kanagawa K, and Senda T*

One of the most renovative discoveries over the last decade in the fault-related science is the extreme velocity-weakening frictional behavior observed in laboratory experiments for variety of rocks [e.g. Tsutsumi and Shimamoto, 1997; Tullis and Goldsby, 2003; Prakash 2004]. These observations are explained by several mechanisms such as melt-lubrication [e.g. Shirono et al., 2006; Nielsen et al., 2008], silica-gel formation [Di Toro et al., 2004], build-up of pore pressure due to decomposition or desorption of water [O'hara et al., 2006, Rice 2007], phase transformation and generation of weak material [e.g. Han et al., 2007], and flash heating of microscopic asperities [Rice 1999, 2006; Tullis and Goldsby 2003; Beeler et al., 2007; Noda 2008].

Some of these mechanisms are sensitive to the temperature on the sliding surface while most of the existing experiments are at room temperature and the fault surface is heated by the friction. In order to investigate the physical processes operating on the fault surface, it is essentially important to conduct frictional experiments with controlling the temperature and the slip rates independently. For this purpose we set up a rotary shear apparatus at Chiba University which was

first developed for the friction of ceramics, and has already be reported by e.g. Senda et al., [1999]. This apparatus can slide a simulated fault at 1-500 mm/s for an annular sliding surface with 25 mm and 15 mm outer and inner diameters. There is an induction coil around the sample assembly which heats sample holders on which about 5 mm thick rock samples are fixed. A thermocouple is attached to one of the sample holders about 7 mm from the sliding surface, and the measured temperature can be controlled up to 1000 degreeC within 1 degreeC in accuracy.

Our preliminary result with the same gabbro as in Tsutsumi and Shimamoto [1997] indicates that at 0.5 MPa normal stress and 20 mm/s slip rate, the friction coefficient is from 0.7 to 0.8 at room temperature, decreases with increasing temperature down to 0.55-0.6 at 800 degreeC, and increases to around 0.8 at 900 degreeC. The range of the friction coefficient agrees with Tsutsumi and Shimamoto [1997] although the experimental condition is different; they changed the slip rate without controlling the temperature accurately, and we fix the slip rate and control the temperature. Our results illuminates the importance of the temperature during seismically rapid fault sliding.

2-083
ON THE HIGH VELOCITY WEAKENING OF FAULT GOUGES *Brown KM, and Fialko Y*

We present new experimental data and theory that describe the thermal weakening of fine-grained gouges during earthquake slip. We postulate that the particles in fine-grained gouges thermally soften due to an intrinsic decrease in the elastic shear modulus in response to rapid heating of the gouge layer described by a modified Watchman's equation. In our initial thermally based model, after slip has initiated and attained a critical velocity the velocity dependence of the effective coefficient of friction results from the temperature dependence of the theoretical yield strength of the contact asperities, rather than sudden loss of the asperity strength at some critical temperature. Eventual contact melting can occur depending on the effective normal stress and displacement. Our preliminary results indicate that there is a systematic evolution of the friction coefficient from ~0.6 to as low as 0.2 as velocities increase from 0.1 m/s to 2.5 M/s. The inferred power-law exponent of the velocity dependence is ~ -0.4 depending on the normal stress, considerably smaller than the exponent of -1 predicted by the flash weakening hypothesis (Rice, 2006). Our model successfully explains a significant portion of the observed velocity-weakening relationship in terms of the temperature dependence of the shear modulus (and, thus, contact shear strength). The model accounts for the fact that the evolution of contact strength during slip depends on increases in both the average shear zone temperature and transient contact temperatures. Inspection of the experimentally produced gouge using SEM images indicates that grain sizes are likely to be power law distributed the majority less than 1-5 μm in diameter. Thermal weakening is less robust than predicted from the flash weakening because (1) the observed gouge are be too small to allow adiabatic heating during transient contact, and (2) the asperity strength, and thus the efficiency of frictional heating, decrease with increasing temperature. We also note some early evolutionary weakening also occurs at rates that are too low for significant thermally activated weakening processes probably due to fabric and other mechanical effects.

2-084
EFFECT OF PRESTRESS AND NUCLEATION PROCEDURE ON RUPTURE MODES IN LABORATORY EARTHQUAKES *Lu X, Rosakis AJ, and Lapusta N*

We present experimental observations of pulse-like and crack-like rupture modes, and a systematic variation between them, on Homalite interfaces prestressed both in compression and in shear, similarly to faults in the Earth's crust. A number of explanations for the existence of slip pulses have been proposed, including velocity-weakening friction, bimaterial effect, and local

heterogeneity. We find systematic variation of rupture modes in our experiments with the ratio of shear to normal prestress and with the absolute stress level. The experiments also show that both pulse-like and crack-like rupture modes can transition to supershear speeds, which are smaller for pulse-like ruptures than for crack-like ruptures. The results are qualitatively consistent with theoretical studies of interfaces governed by velocity-weakening friction.

Our experiments indicate that pulse-like ruptures can exist in the absence of a bimaterial effect or local heterogeneity and suggest, based on comparison with theoretical studies, that the behavior of the experimental interface is controlled by velocity-weakening friction. Numerical studies show that rupture modes can also be affected by the nucleation procedure. In the experiments, ruptures initiate due to an explosion of a thin wire, which creates local reduction in compressive normal stress and hence in the interface resistance. To establish whether this reduction drives the rupture propagation outside of the nucleation region, we conduct fault-normal particle velocity measurements at the location where we measure fault-parallel sliding velocity to determine the rupture mode. The measurements indicate no reduction in compressive normal stress but rather point to slight increase in compression, indicating that the decrease in normal stress is indeed local. The rupture initiation could also affect rupture propagation through the wave-mediated memory of sliding in the nucleation region. To partially quantify that effect, we have conducted simulations with different explosion strengths. We find that the explosion strength affects the peak velocity of the rupture front but it does not change rupture duration and hence our conclusions about rupture modes. Our current work is directed towards quantifying nucleation and friction parameters of the experiments and modeling the experiments numerically.

2-085

ANALYSIS OF SUPERSHEAR TRANSITION REGIMES IN RUPTURE EXPERIMENTS: THE EFFECT OF NUCLEATION CONDITIONS AND FRICTION PARAMETERS *Lu X, Lapusta N, and Rosakis AJ*

We consider the effect of rupture initiation and friction parameters on transition of spontaneous ruptures from sub-Rayleigh to supershear speeds on interfaces governed by linear slip-weakening friction. Our study is motivated by recent experiments of supershear transition that were previously analyzed using the Burridge-Andrews (BA) model, in which a supershear daughter crack nucleates in front of the main mother rupture. The experimentally determined transition distances were compared with the ones from the BA model. It was concluded that the critical slip of the linear slip-weakening formulation needs to be pressure-dependent for a good match with experiments; the pressure dependence was derived from a micromechanical analysis. However, the rupture initiation mechanism in the experiments was conceptually different from the one adopted in the numerical work used for comparison.

Our numerical model of the experiments includes a rupture initiation procedure that captures the dynamic nature of the wire explosion used in the experiments to start rupture. The goal is to find parameter regimes that would match the experimentally observed transition distances for the entire range of experimental conditions. Our simulations show that the dynamic rupture initiation procedure significantly affects the resulting transition distances, shortening them by about 30%-50% compared to transition distances predicted by models with a smooth rupture initiation process. Moreover, for some cases, the dynamic initiation procedure changes the very mode of transition, causing a direct supershear transition at the tip of the main rupture instead of the mother-daughter mechanism. We find reasonable parameter regimes that match experimentally determined transition distances with both direct supershear transition at the rupture tip and the BA (mother-daughter) mechanism, using both pressure-independent and pressure-dependent

critical slip of the linear slip-weakening formulation. The results show that there are trade-offs between the parameters of the rupture initiation procedure and the properties of interface friction, underscore the need to quantify experimental parameters for proper interpretation of the experiments, and highlight the importance of rupture initiation in simulations of both experiments and real-life earthquake events.

2-086
SHEAR HEATING-INDUCED THERMAL PRESSURIZATION DURING EARTHQUAKE NUCLEATION *Schmitt SV, Segall P, and Matsuzawa T*

Shear heating-induced thermal pressurization has long been posited as a weakening mechanism during earthquakes. It is often assumed that thermal pressurization does not become important until earthquakes become moderate to large in magnitude. Segall & Rice [2006, JGR], however, suggested that thermal effects may become dominant during the quasi-static nucleation phase, well before the onset of seismic radiation. Using the slip evolution given by rate- and state-dependent friction--along with reasonable estimates of heat and pore pressure transport parameters--they estimated that thermal pressurization dominates weakening at slip rates in excess of 10^{-5} to 10^{-3} m/s.

We further explore this problem numerically, assuming a fault in a 2D elastic medium and accounting for full thermomechanical coupling. The fault is governed by rate and state friction with the radiation damping approximation to simulate inertial effects. Thermal diffusion is computed via finite differences on a grid that adaptively remeshes to minimize computational expense while maintaining accuracy. To start, we neglect fault zone thickness and model the fault as a plane. This approximation is valid for times much greater than the diffusion time across the fault zone. With uniform transport properties, it leads to a direct relationship between pore pressure on the fault and temperature [Rice, 2006, JGR], thus requiring only one finite difference grid.

Our results thus far indicate that thermal pressurization does in fact dominate at modest slip speeds that are slightly lower than those estimated by Segall & Rice [2006]. Interestingly, the thermal pressurization process leads to a contraction of the nucleation zone, rather than the growing crack (aging law) or unidirectional slip pulse (slip law) associated with drained rate- and state-dependent frictional nucleation.

If allowed to proceed to higher--yet still quasi-static--slip speeds, our modeled nucleation zone continues to shrink nearly to zero width. We believe this is a consequence of treating the fault as a planar surface rather than a finite-width shear zone. Such an approximation overestimates the fault temperature at higher slip speeds, when time steps are no longer much greater than the diffusion time across the width of the shear zone. Our current work is to include the finite fault thickness, so that we may conduct simulations up to speeds at which seismic radiation becomes significant.

2-087
A COMPARISON OF DAMAGE ZONE DECAY AROUND SMALL AND LARGE FAULTS *Savage HM, Brodsky EE, and Johns M*

The increase in fracture density around faults is a useful proxy for assessing the stress field when the damage formed. However, the damage surrounding large faults will inevitably be a function of the superposition of several main fault strands, in addition to farther-flung secondary faults, that form over many episodes of slip. To investigate the decay of fracture density away from a single fault with presumably few episodes of slip, we are measuring damage around small displacement faults at Four Mile Beach, Santa Cruz, CA, that are isolated or have few discrete strands. We

compare the fracture decay from our small faults with fault profiles compiled from the literature, as well as fracture profiles we are collecting along a section of the San Andreas Fault.

We are measuring linear fracture density at Four Mile Beach along several faults with displacements ranging from less than one meter to several meters. The faults experienced normal displacement and are hosted within a thinly bedded mudstone. On the opposite end of the displacement spectrum, we are collecting fracture data at Logan Quarry, a granodiorite quarry located on the western side of the San Andreas Fault in Aromas, CA. Because of the size of the field site, we developed a new fracture counting technique using ground-based LiDAR. We use an RMS roughness parameter to define the existence of a fracture and count the number of fractures along a linear transect, creating a dataset comparable to the Four Mile Beach dataset.

Preliminary results imply that damage decay around faults is well described using a power law. However, the rapidity of the decay may be a function of fault displacement. For small faults that are relatively isolated, the slope of the power law curve is approximately one. As fault displacement increases, the slope of the decay decreases. We suggest that this change is due to the superposition of decay profiles at secondary faults, which can form in increasing numbers and at increasing distances as the fault matures. In addition to looking at the decay of damage away from the fault, we also look at the width of the fault zone. Again, we compare our datasets with published studies and find that damage zone width grows approximately linearly with displacement at small offsets, but grows more slowly at offsets larger than 10-100m. This suggests that most new strands form early in the displacement history of a fault.

2-088

SPATIO-TEMPORAL DOCUMENTATION OF DAMAGE ZONE ON THE SAN ANDREAS FAULT BY FAULT-ZONE TRAPPED WAVES AT PARKFIELD SAFOD SITE *Li Y, Cochran ES, Chen P, Malin PE, and Vidale JE*

Highly damaged rocks within the San Andreas fault zone at Parkfield form a low-velocity waveguide for seismic waves, giving rise to fault-guided (trapped) waves. Prominent fault-guided waves have been observed at the San Andreas Fault Observatory at Depth (SAFOD) site, including a surface array across the fault-zone and a borehole seismograph placed in the SAFOD well at a depth of ~3 km below ground. The resulting observations are modeled here using 3-D finite-difference methods. To fit the amplitude, frequency, and travel-time characteristics of the data, the models require a downward tapering, 30-40-m wide fault-core embedded in a 100-200-m wide jacket. Compared with the intact wall rocks, the core velocities are reduced by ~40% and jacket velocities by ~25%. Based on the depths of earthquakes generating guided-waves, we estimate that the low-velocity waveguide along the fault at SAFOD extends at least to depths of ~7-8 km along the ~25-km-long rupture zone of the 2004 M6 Parkfield earthquake, with larger velocity reduction from the wall-rock velocities at the shallower depth and beneath the Middle Mountain where the larger slips occurred in the 2004 M6 event. Repeated seismic experiments conducted at the San Andreas fault at Parkfield before and after the 2004 M6 Parkfield earthquake indicate that the Parkfield low-velocity zone weakened co-seismically, and then healed back toward its pre-earthquake state over a period of several months to several years. Waveform cross-correlation measurements from repeated explosions and microearthquakes suggest that a peak decrease of ~2.5% in velocity occurred coseismically within the fault zone at seismogenic depths. Measurements from repeating aftershocks show that a ~1.2% velocity increase occurred within the fault zone in the first 3 months after the mainshock. The data recorded at the SAFOD borehole seismographs for repeated aftershocks conformed that seismic velocities within the damage zone were changed by ~0.3% in a month. The healing rate appears to be approximately logarithmic, with

the largest rate in the earliest stage of post-mainshock period. The magnitude of fault damage and healing varies along the rupture zone, but it is most prominent above ~7 km.

2-089
WAFEVORM COMPLEXITIES CAUSED BY FAULT ZONE DAMAGE: 2003 BIG BEAR EARTHQUAKE SEQUENCE *Pitarka A, Helmberger DV, Ni S, and Yin T*

Analyses of broad-band wave-form data and rupture directivity using Relative Source Time Functions from the 2003 Big Bear earthquake sequence show a clear relationship between the relative location of small earthquakes with respect to mainshock, and their rupture velocity (Vr) and characteristic fault length (L). Small events (NF) located near the main event have relatively low stress drop and relatively large Vr and L compared to more distant cross-fault events (DF) to the north. This implies that there is a difference in strain energy drop and rupture dynamics between the two types of events. The NF events display more complexity between the P-wave-train and S-wave-train. Many of these events have relatively complex S-waves compared to the DF events. The P-waves seem relatively stable since we were able predict their differences based on directivity estimates and fault-parameters. However, many of the S-waves are observationally more complex when we apply waveform inter-correlation. This suggests that such complexities are caused by wave propagation scattering. We argue that this feature is caused by fault-zone damage where energy is locally trapped in the slow leaky waveguide and then re-radiated from the lateral edges of the fault zone. The fault-zone trapped waves could also cause the complexities observed in P coda waves for the NF events.

In order to investigate the implication of fault zone damage on observed waveforms we performed high frequency (8Hz) waveform modeling using a staggered grid finite difference anelastic method and velocity models representing different fault zone geometries. The fault zone is 400 m wide and has a shear wave velocity reduction of 30%. We focused our investigation on the effects of source location relative to the fault zone, and combinations of two fault-zones crossing at depth to explain the following observations:

1. Difference in P and S wave spectra due to rupture directivity for small events rupturing inside and adjacent to a vertical fault zone.

2. Difference in P coda wave scattering as a function of azimuth between NF and DF events

3. Difference in wave-form complexity and P arrival time between the main event and small events of the Big Bear earthquake sequence as a function of azimuth

Our analyzes of recorded and simulated broad-band waveforms suggest that fault zone effects can cause waveform complexities similar to the ones observed during the 2003 Big Bear earthquake sequence.

2-090
THE EFFECT OF ASYMMETRIC DAMAGE ON DYNAMIC SHEAR RUPTURE PROPAGATION I: *Sammis CG, Biegel RL, Bhat HS, and Rosakis AJ*

High-speed digital photography was used to study rupture propagation on the interface between transparent damaged and undamaged photoelastic plates. Bilateral ruptures were nucleated on saw-cut faults at an angle α to the uniaxial loading axis. Stress concentration at the crack tips produced fringes in polarized laser light that allowed their positions to be measured in successive photos. We found that fracture damage introduces a strong asymmetry in propagation speed

different from that expected due to the lower elastic stiffness in the damaged material alone. When the tensile lobe of a rupture tip propagated through the damaged material the velocity of that rupture was reduced or stopped. By contrast, when the compressive lobe of a rupture tip passed through the damage, the velocity of that rupture was unaffected by the damage. A physical interpretation is that passage of a tensile lobe through the damage expends energy by lowering the normal stress on pre-existing cracks thus allowing frictional sliding along the crack surfaces. When the compressive lobe of the rupture passes through the damage, compressive stresses prevent sliding, only minor energy is dissipated, and the damage has almost no effect on the velocity. This effect can produce asymmetric propagation for earthquake ruptures on slip surfaces near the edge of the highly damaged fault zone.

2-091
THE EFFECT OF ASYMMETRIC DAMAGE ON DYNAMIC SHEAR RUPTURE PROPAGATION II: WITH MISMATCH IN BULK ELASTICITY *Bhat HS, Biegel RL, Sammis CG, and Rosakis AJ*

We investigate the asymmetry of ruputure velocity on an inteface that combines a bulk elastic mismatch with a contrast in off-fault damage. dynamic ruptures on the interface. Dynamic ruptures were propagated on the interface between thermally shocked (Damaged) Homalite and polycarbonate plates. The anelastic asymmetry introduced by damage is defined by 'T' and 'C' directions depending on whether the tensile or compressive lobe of the rupture tip stress concentration lies on the damaged side of the fault. The elastic asymmetry is commonly defined by '+' and '-' directions where '+' is the direction of slip of the softer material. Since damaged Homalite is stiffer than polycarbonate our directions are 'T+' and 'C-'. Theoretical and numerical studies predict that shear rupture on elastic bimaterial interfaces propagates in the '+' direction at the generalized Rayleigh wave speed or in some numerical cases at the P-wave speed of the harder material, Pfast, while in the '-' direction the rupture propagates at sub-shear speed or at the P-wave speed of the softer material, Pslow, depending on the loading conditions. We observe that the off-fault damage effect overcomes the elastic bimaterial effect in dynamic rupture propagation. In the 'C-' direction the rupture propagates at sub-shear to supershear speeds, as in undamaged bimaterial systems, reaching a maximum speed of Pslow. In the 'T+' direction however the rupture propagates at sub-shear speeds or comes to a complete stop due to increased damaged activation (slip and opening along micro-cracks) which results in the reduction of stored elastic potential energy and energy dissipation along the micro-cracks. Biegel et al. [2008] found similar results for propagation on the interface between Homalite and damaged Homalite where rupture speeds were slowed or even stopped in the 'T-' direction but were almost unaffected in the 'C+' direction.

2-092
EXPERIMENTAL INVESTIGATION OF A TRANSITION BETWEEN STICK-SLIP AND CREEP AS A FUNCTION OF TEMPERATURE, SLIP RATE, AND NORMAL STRESS *Mitchell EK, Brown KM, and Fialko Y*

We investigate frictional properties of crystalline rocks to map the transition between stick-slip (velocity-weakening) and stable creep (velocity-strengthening) behavior as a function of: slip velocity, temperature and normal stress. We performed a series of direct shear tests on diabase and novaculite for velocities of 10-5 - 3x10-2 mm/s, temperatures of 25-500°C and normal stresses of 1-15MPa. Analysis of data reveals four basic types of frictional behavior: stick-slip, episodic slow-slip events, quasi-sinusoidal accelerated creep and stable sliding. Episodic acceleration and peak slip velocities progressively decrease through these phases in the above order. As temperature increases and forcing velocity decreases, the sample progresses from stable sliding, to sinusoidal accelerated creep, to stick creep, and then to stick-slip. The transition seems to occur around 200°C

for dry diabase and dry novaculite. Another trend in the onset of stick slip occurs due to normal stress. Seen best at higher temperatures, a transition from stable sliding to stick slip occurs with increasing normal stress. Our observations are broadly consistent with predictions of the rate and state friction theory, indicating that lower slip rates and higher normal stresses result in enhanced interlocking of contacts on a frictional interface. Our data show that elevated temperatures give rise to the same effect, suggesting a thermally-activated nature of the asperity contacts. Surprisingly, we did not observe a high-temperature transition from stick-slip back to stable sliding in novaculite (purely silicic lithology), even at temperatures as high as 500°C. Such a transition is widely believed to be responsible for the brittle-ductile boundary defining the bottom of the seismogenic layer. Our observations may highlight the role of water on the brittle-ductile transition and suggest that the velocity weakening behavior can extend considerably deeper than typically thought, at least in the dry middle-to-lower crust. We also point out potential similarities between the periodic accelerated creep observed in our experiments at the boundary between the stick-sip and stable sliding regimes, and episodic slow-slip events reported near the velocity-neutral transition in a number of subduction zones. The slip rates observed during slow-slip events in our experiments have the same order of magnitude (10-8 m/s) as the slow-slip events in the Cascadia subduction zone.

2-093
HETEROGENEITY OF FOCAL MECHANISM ORIENTATIONS IN DIFFERENT PARTS OF THE SAN JACINTO FAULT ZONE *Bailey IW, Ben-Zion Y, Becker TW, and Holschneider M*

We investigate earthquake heterogeneity associated with different parts of the San Jacinto fault zone in terms of the statistical variation of focal mechanism orientations. Our analysis is based on a catalog of ~12,000 focal mechanisms for earthquakes with magnitude between zero and five recorded between January, 1984 and July, 2003. The focal mechanisms are double-couple solutions computed from first-motion data using the program HASH (Hardebeck & Shearer, 2002). Individual focal mechanisms are associated with one of seven sections of the San Jacinto fault, based on their horizontal distance from the fault trace according the USGS quaternary fault map. We assess the deformation properties of fault sections by summation of their potency tensors. We investigate the earthquake heterogeneity for each fault section based on the orientation statistics of the double-couples, which are described by distributions of rotation angles and rotation axes for the minimum rotation between all pairs within each population. We relate the heterogeneity of earthquakes to fault heterogeneity by numerical simulations that consider slip along a set of fault planes with varied orientations. The slip direction of each fault is computed from the maximum shear stress produced by a specified regional stress tensor. Our inferences from the simulations are compared to measures of fault complexity inferred from the patterns of fault traces.

2-094
TRANSITIONS TO CHAOS IN DIETERICH-RUINA FRICTION *Erickson BA, Birnir B, and Lavallee D*

We began investigations into the Dieterich-Ruina (D-R) friction law in previous work by studying the behavior of a single slider-block under this law. We found transitions to chaos in the numerical solution to this system when a specific parameter was increased. This parameter, ? = (B-A)/A is the ratio of the stress parameters (B-A) and A in D-R friction. The parameter A = d(?)/d(log(v)), where ? is the frictional stress and v is the velocity of the slider, is a measure of the direct velocity dependence (sometimes called the "direct effect") while (A-B) = d(?_{ss})/d(log(v_{ss})), is a measure of the steady-state velocity (v_{ss}) dependence. When compared to the slip weakening friction law, the parameter (B-A) plays a role of a stress drop while A corresponds to the strength

excess. We found that transitions to chaos for a single block occur for ? ≈ 9. We also studied the behavior of a system of three blocks under D-R friction, finding that transitions to chaos occurred for smaller values of this parameter ?. Taking this study a step further, we derive the elastic wave equation in 1-d under Dieterich-Ruina friction to obtain the position u(x, t), the slip relative to the driver plate. Using uniformly distributed initial conditions and periodic boundary conditions, we find that numerical solutions to this PDE bifurcate under critical values of the same parameter ?. For ? ≈ 4.7, transitions to chaotic solutions occur. For this range of parameter values, the chaotic behavior occurs only in time; the spatial structure is preserved. We compute the structure function, S_1(x,t), to explore statistically stationary states of the solution. In these cases, the structure function will have the property of being only a function of the lag variable t. We also compute the average of the spectra computed for many runs with different initial conditions in order to view the distribution of frequency.

2-095

FORCE CHAINS IN SEISMOGENIC FAULTS VISUALIZED WITH PHOTOELASTIC GRANULAR SHEAR EXPERIMENTS *Hayman NW, and Daniels KE*

Natural faults have many granular characteristics, including granular fault rocks and spatiotemporal patterns of slip behaviors akin to granular systems. We present experimental results which provide insight into granular behavior in natural faults. The experiments allow us to directly image force chains within a deforming granular media through the use of photoelastic particles. The apparatus consists of a spring-pulled slider block which deforms a photoelastic granular aggregate at a constant velocity. Particles that carry more of the load appear brighter when viewed through crossed polarizers, making the internal stresses optically accessible. The resulting pattern is a branched, anisotropic force chain network inclined to the shear zone boundaries. Under both constant-volume and dilational boundary conditions, deformation occurs predominantly through stick-slip displacements and corresponding force drops. The particle motion and force chain changes associated with the deformation can either be localized to the central slip zone or span the system. The sizes of the experimental slip events are observed to have power-law (Gutenberg-Richter-like) distributions; a particle scale controls the lower limits of the power-law distributions. For large drops in pulling force with slip, the power-law tail of the size distributions is strongly affected by the choice of boundary condition. For small force drops the probability distributions are approximately independent of boundary condition. These size-dependent variations in stick-slip behavior correspond to changes in the force chain network: on average, small events correspond to local force chain or particle rearrangements, whereas large events correspond to system-spanning force chain changes and/or particle-slip. Such force chain behavior may be responsible for similar size-dependent behaviors of natural faults.

2-096

PORE PRESSURE OSCILLATIONS ENHANCE PERMEABILITY IN THE LABORATORY *Elkhoury JE, Niemeijer AR, Brodsky EE, and Marone CJ*

Shaking produced by earthquakes triggers other distant and not so distant earthquakes [Hill et a., l1993,Felzer and Brodsky 2006]. It also increases stream flows and spring discharges and even enhances oil production [Rojstaczer and Wolf 1992, Manga et al., 2003, Beresnev and Johnson 1994]. These observations have been explained by an increase in permeability. If this effect is harnessed and engineered, it would have major impacts on oil recovery and environmental engineering [Beresnev and Johnson 1994]. Recent observations show that indeed seismic waves from earthquakes can triple the effective permeability in natural systems [Elkhoury et al., 2006]. Here we present the first experimental evidence of permeability increases in fractured rock samples subject to dynamic stresses. We oscillate the pore pressure through a rock with a fracture and measure the

resulting permeability change. We use Berea sandstone samples under triaxial stresses with confining pressure of 9MPa and 20 MPa of normal stress. We start with DI water flowing through an intact rock sample at constant pore pressures. Then, we shear the sample in-situ developing a through going fracture. Once the flow rate stabilizes, we oscillate the pore pressure for 120 sec at a 20 sec period with amplitudes of 0.02 to 0.3 MPa. We observe a clear transient increase in permeability induced by the oscillatory pore pressures akin to shaking from earthquakes. Permeability increases with increasing amplitude of the oscillatory pore pressure by up to 50\%. The maximum value of the permeability increases is 5x$10^{-16}\,m^2$. After the oscillations are over, the permeability recovers as the inverse square root of time to the pre-oscillations level over 10's of minutes. The recovery indicates a reversible mechanism like unclogging and clogging of fractures, as opposed to an irreversible one, like micro-fracturing, as responsible for the transient permeability enhancement. Our result has clear consequences. It points at the feasibility of dynamically controlling permeability of fractured systems. Its application ranges from hydrology and oil reservoir engineering to geophysics and earthquakes triggering mediated by permeability enhancement in fault zones due to shaking from other earthquakes.

2-097
A PHYSICAL MODEL FOR WIDESPREAD NEAR-SURFACE AND FAULT ZONE DAMAGE INDUCED BY EARTHQUAKES *Ma S*

Seismic observations indicate that material velocities at shallow depths decrease over a large area after large earthquakes. The reductions are widespread, and occur at distances of up to several source dimensions. A persistent low-velocity fault zone has also been documented extensively from seismic and geodetic observations, in which the velocity drops further after large earthquakes. Dynamic stresses carried by seismic waves in the near surface or accompanying rupture at depth in the fault zone, are thought to create these velocity reductions by causing material damage. However, a rigorous physical interpretation as to why modest dynamic stresses can cause widespread near-surface damage, and why fault damage zones form, is lacking. By using a Drucker-Prager yielding criterion to simulate dynamic rupture propagation on a strike-slip fault, I show that the widespread near-surface damage is caused by material yielding induced by seismic waves under the low confining pressure. Because the confining pressure increases with depth, materials yield more easily near the surface. The yielding zone at depth is narrowly confined near the fault, but its thickness broadens dramatically near the surface, forming a 'flower-like' damage zone, which is commonly observed in the geologic record. The fault zone damage at depth is induced by the large dynamic stress associated with the rupture front, and can be induced by strong seismic waves ahead of the rupture front near the Earth's surface. These results have important implications for the formation and evolution of fault zones, and possibly for the dynamic triggering of earthquakes as well.

2-098
DAMAGE ASYMMETRY IN FAULT STRUCTURE OBSERVED GEOLOGICALLY CAN BE GENERATED BY BILATERAL RUPTURES ALONG A BIMATERIAL INTERFACE *Duan B*

Damage asymmetry in fault structure has been observed along some strike-slip faults recently (e.g., Dor et al., 2006a,b, 2008). These geological observations are very useful constraints for fault and rupture mechanics. The previous theoretical study by Ben-Zion and Shi (2005) has shown that unilateral ruptures along a bimaterial interface can produce asymmetric off-fault damage. In this study, we find that asymmetric off-fault damage can also be generated by bilateral ruptures along a bimaterial interface. We perform elastoplastic calculations on 2D plane strain models, with slip-weakening friction laws on faults to govern dynamic rupture propagation and Mohr-Coulomb

plastic yielding criterion to characterize off-fault elastoplastic response in the medium. With a variety of model parameters, we find that ruptures along a bimaterial interface are bilateral, with strong asymmetry in slip velocity on the fault and off-fault plastic strain distribution between the two rupture directions. Many such bilateral ruptures along the material interface can generate the damage pattern similar to that observed in the field, with significantly more damage on the stiffer side of the fault. Thus, observed damage asymmetry in the field is a general part of bimaterial effects and is not necessarily indicative of unilateral ruptures on the faults as proposed previously. As a community, we are still unable to predict rupture propagation direction, even in the case where a major fault separates dissimilar rocks.

2-099

DIRECT MEASUREMENT OF ASPERITY CONTACT GROWTH IN QUARTZ AT HYDROTHERMAL CONDITIONS *Beeler N, and Hickman SH*

Room-temperature friction and indentation experiments suggest fault strengthening during the interseismic period results from increases in asperity contact area due to solid-state deformation. However, field observations on exhumed fault zones indicate solution-transport processes, pressure solution, crack healing and contact overgrowth, influence fault zone rheology at hypocentral conditions. Contact overgrowths result from gradients in surface curvature, where material is dissolved from the pore walls, diffuses through the fluid and precipitates at the contact, cementing the asperities together. To measure the overgrowth rate we use a contact between convex and flat lenses prepared from quartz single crystals. The loaded contact is viewed continuously within a heated pressure vessel through a window using a long-working-distance microscope and convergence is monitored using reflected-light interferometry. Contact normal force is constant with an initial normal stress of 1.7 MPa.

Four single-phase experiments were conducted at temperatures between 350 and 530C at 150 MPa water pressure, along with two controls: one single phase, dry at 425C and one bimaterial at 425C and 150 MPa water pressure. No contact growth or convergence was observed in the controls. For wet single-phase contacts, growth was initially rapid and then decreased with time following an inverse squared dependence of contact radius on aperture. No convergence was observed over the duration of these experiments, suggesting that neither significant pressure solution nor crystal plasticity occurred at these stresses and temperatures. The formation of fluid inclusions indicate that the contact is not uniformly wetted. The contact is bounded by small regions of high aperture, reflecting local free-face dissolution as the source for the overgrowth, a definitive indication of diffusion-limited growth. Diffusion-limited growth is also consistent with the inverse squared aperture dependence. However, the apparent activation energy is ~125 kJ/mol, much higher than expected for silica diffusion in bulk water. When our lab-measured overgrowth rates are extrapolated to the 5 to 30 micron radius contacts inferred from recordings of M-2 sized earthquakes at SAFOD and NELSAM, we find rates of contact area increase that are orders of magnitude faster than in dry, room temperature friction tests. This suggests that natural strength recovery should be dominated by fluid-assisted processes.

2-100

GROUND PENETRATING RADAR IMAGES COMPARED WITH A TRENCH LOG AND A RADON PROFILE FOR FIELD LOCATION OF THE IMPERIAL FAULT TRACES IN THE COLONIA CASTRO, MEXICALI, BAJA CALIFORNIA, MÉXICO.
Lázaro-Mancilla O, López D, Reyes-López J, Carreón-Diazconti C, and Ramírez -Hernández J

The need to know the exact location in the field of the trace of the Imperial Fault in Mexicali has been an important affair due that the topography in this valley is almost flat and fault traces are

hidden by plow zone. For this reason is important appeal to geophysical studies for the location of these geological features. In this study, two 100 MHz Ground Penetrating Radar (GPR) profiles were carried out for comparison, first, with a trench log and, second, with a radon concentration profile. For locate the study site we turn to a previous study carried out by Andrew Peter Thomas in 1965. The first GPR profile was carried out near the trench reported by Thomas and serve us to calibrate the GPR image. Afterward the radon (222Rn) concentration was measured in 9 stations along a traverse profile to the Imperial Fault in the Colonia Castro of Mexicali, Baja California, with the purpose of locate additional traces of the Imperial fault with the support of the second GPR profile. The Radon results allow us to identify three stations where the values exceed 40 picocuries per liter (pCi/L), these stations can be associated to fault traces, and two places where the peak values are at the level of 20 (pCi/L). Although the station 5 are not a peak, the observed value of 13.80 (pCi/L) allow us to explain the results of second GPR profile. The average of the detected radon concentration, that was of the order of 22.11 (pCi/L), is considered high in relation to those measured for studies of effects in the health in a indoor radon study in the city of Mexicali. The results of this study allow us to think in the possibility that exist places in Mexicali city and their valley that have the same values or perhaps higher, mainly near areas to the geologic faults and specially near to the Imperial Fault. Due to the apparent goodness of this study and to the lack of outdoor radon studies we will continue with this kind of surveys in Mexicali city and its valley.

2-101

SPECTRAL ANALYSIS OF THE SURFACE SLIP PROFILES AND SLIP INVERSIONS FOR THE 2001 KOKOXILI (TIBET) EARTHQUAKE *Lavallee D*

The 2001 Kokoxili (Tibet) earthquake provides a unique opportunity to study surface slip profiles. The surface slip profiles have been measured along the fault for a distance of the order of 270 km without any significant change in the strike direction. Measurements include the displacement parallel and perpendicular to the fault, however, the recorded earthquake slip profiles are irregularly sampled. Traditional algorithms used to compute the discrete Fourier transform are developed for data sampled at regular spaced intervals. It should be noted that interpolating the slip profile over a regular grid is not appropriate when investigating the spectrum functional behavior or when computing the discrete Fourier transform. Interpolation introduces bias in the estimation of the Fourier transform that adds artificial correlation to the original data. To avoid this problem, we developed an algorithm to compute the Fourier transform of irregularly sampled data. It consists essentially in determining the coefficients that best fit the data to the Sine and Cosine functions at a given wave number.

The algorithm is tested by computing the power spectrum of the slip profiles of the Kokoxili earthquakes. In addition, we also compute the power spectrum for the slip inversions computed for the Kokoxili earthquakes. For all the slip models, we found that the power spectrum curves are attenuated according to a power law behavior. However the power laws characterizing the slip inversions decrease at a faster pace when compared to the power law computed for the slip profiles recorded at the surface. This result suggests that the correlation embedded in the slip models is larger than the correlation computed for the slip profile recorded at the surface.

A similar comparison between the slip profile recorded at the surface on the Arifiye segment of the North Anatolian Fault zone and a kinematic source inversion for the 1999 Izmit (Turkey) earthquake lead to a similar conclusion.

2-102

INVERSION OF STRONG MOTION DATA FOR THE 2004 CHUETSU NIIGATA EARTHQUAKE *Masson J, and Archuleta RJ*

The October 23, 2004, M 6.8 Chuetsu mid Niigata thrust earthquake occurred on a reactivated normal fault. The hypocenter is at 37.307N, 138.839E and at a depth of 10.6 km. The fault strikes 212 degrees with a dip of 47 degrees. This earthquake was widely recorded by KiK-net, KNET and JMA stations. Using the method of Liu and Archuleta (2004), we inverted 3-component band-passed (0.1–1.0 Hz) velocity time series from 20 stations that were well distributed in azimuth. Because of known velocity changes, we used two different anelastic velocity structures for stations to the northwest and southeast. We computed a suite of inversions. In general, we find that the maximum slip (~2 m) occurs updip from the hypocenter with relatively small slip near the hypocenter. The rupture velocity is between 2.5 km/s and 3.0 km/s. We also did a number of different tests to examine the spatial resolution of the stations we were using. The results indicate that the misfit in the data can grossly underestimate the resolution of the model. In our simple models we checked for how well slip in the hypocentral region might be resolved. If slip were concentrated at the hypocenter, the stations apparently would partly resolve the slip. However, there are cases where the slip is more distributed in space that indicate the stations have relatively poor resolution of the slip near the hypocenter. There are more stations that can be added that might improve the resolution.

Seismology

2-103

GEOTECHNICAL SITE CHARACTERIZATION IN CALIFORNIA *Yong A, Hough SE, Schwarz S, Yu E, Louie JN, and Wills CJ*

The recent 29 July 2008 Mw5.4 Chino Hills earthquake generated moderate shaking intensities and provided a reminder that we live in earthquake country. In support of scientific efforts to better understand and predict ground motions, we continue efforts to improve geotechnical site characterizations in California. First, we report updates to our MySQL-based site characterization repository introduced two years ago at the 2006 SCEC Annual Meeting. The PHP-based web-accessible table (*http://sitechar.gps.caltech.edu/table.php*) has been updated to a version (*http://sitechar.gps.caltech.edu/table2.php*) that includes site information for 17 seismograph networks, for a total of 782 individual seismic stations. The table now includes the predicted Vs30, or average shear wave velocities in the upper 30 m (Wills et al., 2000; Wills and Clahan, 2006), along with the reported elevation of the station sites. In addition, a total of 69 observed Vs30 measurements were acquired through the SeisOpt®ReMi™ (refraction microtremor; ©2007 Optim Inc.) surface wave dispersion analysis method. These measurements, located at SCSN (Southern California Seismographic Network) station sites, are now included in the database. Although available and preserved in the previous version (*http://sitechar.gps.caltech.edu/table.php*), the updated table no longer provides geologic descriptions of each site. Finally, users can also retrieve site information through a link on the Southern California Earthquake Data Center Research Tool website (*http://www.data.scec.org/research.html*). To explore the reliability of estimated Vs30 values, we regress the observed (SeisOpt®ReMi™) values against the predicted values from both the Wills et al. (2000) and the Wills and Clahan (2006) data sets. We find correlation coefficients of just under 0.6 for both models. Significant imprecision in predicted Vs30 values is expected and can be attributed to the natural variability of Vs within geologic units and to the lack of precision in the small-scale statewide maps. It is clear that, while state-wide maps indicate reasonable Vs30 trends across a region, additional Vs30 measurements, more detailed maps and more detailed site categories are needed for detailed microzonation. Further studies to determine the predictive performance of other site characterization proxies (topographic slope and distance from hard rock) and a combination of proxies (geology with topographic slope as terrain units) are under way.

2-104

PRODUCTS AND SERVICES AVAILABLE FROM THE SOUTHERN CALIFORNIA EARTHQUAKE DATA CENTER (SCEDC) AND THE SOUTHERN CALIFORNIA SEISMIC NETWORK (SCSN) *Yu E, Chen S, Chowdhury F, Hutton K, Given D, Hauksson E, and Clayton RW*

Currently the SCEDC archives continuous and triggered data from nearly 3000 data channels from 375 SCSN recorded stations. The SCSN and SCEDC process and archive an average of 12,000 earthquakes each year. The SCEDC provides public access to these earthquake parametric and waveform data through its website *http://www.data.scec.org* and through client applications such as STP and DHI. This poster will describe the most significant developments at the SCEDC in the past year.

Increased data holdings:

• Beginning Jan 1, 2008 the SCEDC began continuously archiving high sample rate channels of 80 sps or 100 sps.

• Station response updates in the field are now available to the community within 24 hours through our web site or STP. In addition to our broadband stations, dataless SEED volumes for all online telemetered short period stations in the SCSN are also now available.

Updated hardware and improved performance:

• Recent upgrades in database servers and waveform file storage have resulted in improved performance in both event catalog and waveform archive searches. Tests show an improvement of 55% in response time for triggered searches and 129% improvement for continuous waveform searches in STP.

Data Center performance during the 2008 M5.4 Chino Hills Earthquake Sequence:

• The SCEDC obtained and made accessible parametric information for this event 71 seconds after the event occurred. The first waveforms became accessible within 8 minutes of the event origin time.

• Statistics from the SCEDC website and applications STP and DHI show a large spike in data requests after the event, with the largest demand being in the hour afterwards. This usage pattern shows the growing expectation of real time or near real time event and waveform data availability by the research community and public. Our approach to distributing this data is well suited to meet this trend.

2-105
QUAKEML: CURRENT STATUS AND RECENT DEVELOPMENTS *Euchner F, Schorlemmer D, Kästli P, and the QuakeML Working Group*

QuakeML is an XML exchange format for seismological data, mainly earthquake catalogs. The current QuakeML release (Version 1.0.1) covers basic event descriptions, including picks, arrivals, amplitudes, magnitudes, origins, focal mechanisms, and moment tensors. It is currently in Proposed Recommendation status and is undergoing a public Request for Comments (RFC) process which is documented online at *http://quakeml.org/RFC_BED_1.0*.

QuakeML has recently been adopted as a distribution format for earthquake catalogs by GNS Science, New Zealand and the European-Mediterranean Seismological Centre (EMSC). These institutions offer prototype QuakeML web services. Furthermore, integration in the CSEP (Collaboratory for the Study of Earthquake Predictability) testing center software developed by the Southern California Earthquake Center has started, replacing legacy Matlab code (*http://www.cseptesting.org*).

ETH Zurich and USC are developing QuakePy, a Python-based seismicity analysis toolkit which uses the QuakeML data model. The current release covers the full QuakeML 1.0.1 standard, including imports/exports of the NDK moment tensor data format. The first large-scale application in QuakePy is the PMC method for calculating network recording completeness (Schorlemmer & Woessner 2008, in press). Completeness results for the SCSN (Southern California Seismic Network) can be retrieved through the CompletenessWeb (*http://completeness.usc.edu*, see CompletenessWeb poster).

Future QuakeML development will include an extension for macroseismic information. Furthermore, development on seismic inventory information, resource identifiers, and resource metadata is under way.

Online resources: *http://www.quakeml.org*, *http://www.quakepy.org*

2-106
TIME-FREQUENCY MISFIT AND GOODNESS-OF-FIT CRITERIA FOR QUANTITATIVE COMPARISON OF TIME SIGNALS *Kristek J, Kristeková M, and Moczo P*

The time-frequency (TF) representation of a signal provides unique and complete information on the signal and is a very good basis for signal analysis and thus also for quantitative comparison of signals. This is especially true about the TF representation defined using the continuous wavelet transform and progressive analyzing wavelet. The TF representation enables us to define unambiguous TF envelope and phase of the signal at each (t,f) point, and, consequently, envelope and phase differences at each (t,f) point. Having these it is possible to define a variety of the TF misfit and goodness-of-fit criteria depending on the goal of the comparison. The misfit criteria quantify the level of disagreement and are more suitable for relatively close signals. The goodness-of-fit criteria allow looking for the level of agreement rather than details of disagreement between the compared signals and are more suitable in case of larger differences between the signals.

Kristekova et al. (BSSA 2006) developed TF misfit criteria for quantitative comparison of one component signals assuming one of them to be a reference. Here we develop a systematic theory of the TF misfit and TF goodness-of-fit criteria for three-component time signals. We include the locally and globally normalized criteria. We also include criteria in case when one of the two compared signals can be considered a reference, and criteria in case when the comparison does not allow viewing one signal as a reference.

We numerically illustrate applications of the misfit and goodness-of-fit criteria to practically important cases.

The software package TF_MISFITS_GOF_CRITERIA developed by Kristekova et al. (2008) for numerical computation of the TF misfit and goodness-of-fit criteria is available at *http://www.nuquake.eu/Computer_Codes/index.html*.

2-107
DEPTH LOCALIZATION OF SEISMICITY ON STRIKE-SLIP FAULTS IN CALIFORNIA *Boutwell C, Powers PM, and Jordan TH*

We investigate the distribution of earthquake ruptures in three separate dimensions along California strike-slip faults. Previous work by Powers and Jordan (in prep.) shows that the average rate of small earthquakes along California strike-slip faults obeys a power-law of the form R~(x^2 + d^2)^(- ? /2), where the rate R is in events/km^2, x is the distance from a fault, ? is the decay rate of seismicity, and d is the near-fault inner scale. However, they do not consider the depth variability of earthquake hypocenters. We therefore perform a reconnaissance of their fault-referenced data set to determine if there is significant on-fault versus off-fault variability in earthquake depths. For each fault segment, we compute the depth variance in 4d km wide fault-normal bins, centered on the fault. For particularly long fault segments, we take the average variance over several shorter fault-parallel sub-segments. Results show interesting regional variations. In southern California, on-fault earthquake hypocenters are strongly localized in depth,

but become more distributed with distance from a fault. In contrast, variance of hypocenter depths in northern California is similar both on and off of faults. Similar regional variations are observed for ? and d, so depth variance likely correlates with fault properties such as seismic productivity, creep rate, and cumulative offset. These results have important implications for fault-based models of seismicity, which can be used to improve current earthquake forecasting methods such as ETAS.

2-108
CORRELATIONS BETWEEN FAULT-PROPERTIES AND NEAR-FAULT SEISMICITY DISTRIBUTIONS *Powers PM, and Jordan TH*

The decay of seismicity with distance from strike-slip faults in California is well described by a power-law of the form R~(x^2 + d^2)^(-?/2), where x is distance from a fault, ? is the decay rate of seismicity, and d is a near-fault inner scale. The scaling parameters, d and ?, vary regionally: seismicity is more localized on faults in northern California (small d; large ?) than in southern California (large d; small ?). To determine if d and ? vary systematically with properties such as fault-width, on-fault earthquake density, cumulative offset, and aseismic slip-rate, we compute d and ? for sets of related strike-slip fault segments. We compute fault width and earthquake density using fault-segment catalogs from our previous work; for cumulative offset and aseismic slip rate we rely on published observations. Despite several outliers, both d and ? exhibit correlations with fault properties. In particular, ? is strongly correlated with fault width, earthquake density, and cumulative offset implying an evolution towards increased localization of seismicity over time. These results contribute to a better understanding of fault zones at seismogenic depths and help understand the significance of d and ? in the context of damage zone and rate-and-state models of near-fault seismicity.

2-109
SEISMIC SIGNATURES OF FAULT-OPENING MOTION *Shi Z, and Ben-Zion Y*

Earthquakes are typically assumed to be caused by shear faulting. While this assumption is made explicitly or implicitly in almost all earthquake-related studies, it is recognized that earthquake ruptures may also include tensile component of faulting. Tensile faulting could be generated by failures in geothermal, volcanic and other extensive regimes, collision of rough surfaces involved in rupture process, and changes of normal stress induced by rupture propagation along a bimaterial interface. One set of signals that may reflect tensile faulting are non-double-couple earthquake mechanisms. However, non-double-couple mechanisms may also be produced by shear faulting in an anisotropic medium and a combination of several different double-couples. To find other potential seismic signatures of fault-opening motion, we perform a theoretical parameter-space study involving analysis of synthetic seismograms generated by sources with fault-opening components. By using a numerical implementation of the 3D analytical solution of Ben-Zion (1990, 1999), we compute synthetic seismograms produced by seismic sources with a tensile component using several different receiver configurations. We systematically examine the arrival time, polarity and amplitude information of different seismic phases in order to find robust seismic signatures indicative of fault-opening motions during earthquake ruptures. Our initial investigation reveals a seismic phase between the P and S arrivals produced uniquely by the tensile motion. Another candidate signal is the fault-parallel-component seismogram recorded close to the fault. In theory, the fault-parallel component of the radiation from a shear dislocation source approaches zero as the receiver location approaches the fault plane. However, this is not the case for the tensile dislocation source. Therefore, the contribution from the tensile dislocation source is more pronounced in this type of seismograms.

2-110

PRECISE RELATIVE LOCATION OF SAN ANDREAS FAULT TREMORS NEAR CHOLAME, CA USING SEISMOMETER CLUSTERS *Shelly DR, Ellsworth WL, Nadeau RM, Burgmann R, Ryberg T, Haberland C, Murphy JM, and Fuis GS*

Non-volcanic tremor, similar in character to that generated at some subduction zones, was recently identified beneath the strike-slip San Andreas Fault (SAF) in central California. Using a matched filter method, we closely examine a 24-hour period of active SAF tremor and show that, like tremor in the Nankai Trough subduction zone, this tremor is composed of repeated similar events. We take advantage of this similarity to locate detected similar events relative to several chosen events. While low signal-to-noise makes location challenging, we compensate for this by estimating event-pair differential times at "clusters" of nearby temporary and permanent stations rather than at single stations. We find that the relative locations consistently form a near-linear structure in map view, striking parallel to the surface trace of the SAF. Therefore, we suggest that at least a portion of the tremor occurs on the deep extension of the fault, similar to the situation for subduction zone tremor. Also notable is the small depth range (a few hundred meters or less) of many of the located tremors, a feature possibly analogous to earthquake streaks observed on the shallower portion of the fault. The close alignment of the tremor with the SAF slip orientation suggests a shear slip mechanism, as has been argued for subduction tremor. At times, we observe a clear migration of the tremor source along the fault, at rates of ~20 km/hr.

2-111

ESTIMATING THE RUPTURE VELOCITY OF SMALL EARTHQUAKES *McGuire JJ, Ide S, Kim M, Iidaka T, and Hirata N*

Studies of earthquake scaling are extremely common but have been inconclusive in determining the existence of any fundamental differences in the mechanical processes controlling small and large earthquakes. While many studies have found a deficit of radiated energy per unit moment release in small earthquakes, work by Ide and Beroza (2001) called these interpretations into question. Much of the uncertainty in whether there are major differences between small and large earthquakes results directly from the difficulty in measuring the energy radiated by small earthquakes. Kanamori and Rivera (2004) pointed out that if the observed deficiency in radiated energy for small earthquakes is real, then either the rupture velocity and/or the static stress drop must decrease for small earthquakes. A surprising result since some studies have suggested that small earthquakes have higher stress drops. If this difference was reflected primarily in rupture velocity, the velocity of magnitude 3 earthquakes would be at most half (for e=0.5) of that in magnitude 7 earthquakes.

We estimated the rupture velocity of earthquakes between M3 and M5 for faults in California and Japan using an Empirical Green's Function (EGF) deconvolution technique. The time functions resulting from the EGF deconvolution show clear variation in their durations as a function of azimuth for a given earthquake. This signal is inverted for the second moments of the earthquake's space-time moment-release distribution which provide a lower bound on rupture velocity (McGuire 2004). The EGF approach leads to relatively tight constraints on earthquake scaling because the azimuthal variation in time function duration is more clearly resolved than the azimuthal variation in corner frequency. We find no evidence for a decrease in rupture velocity with earthquake size. Magnitude 3 events within the rupture zones of the 2000 M6.5 Tottori and 2004 M6 Parkfield earthquakes have rupture velocities that are indistinguishable from those of the mainshocks on the same faults and error analysis demonstrated that rupture velocities faster than 2.0 km/s are required with best fit values closer to 3 km/s. These general patterns hold true for crustal earthquakes in many regions of Japan recorded by the HINET array. We find that the value

of the Kanamori and Rivera scaling parameter e is between 0 and 0.3 indicating no resolvable dynamical differences between magnitude 3 and magnitude 7 crustal earthquakes

2-112
FINITE FAULT MODELING FOR MODERATE-SIZED EARTHQUAKES (M ~ 5) IN SOUTHERN CALIFORNIA *Shao G, Ji C, and Hauksson E*

We develop a finite fault inverse system to routinely study the rupture process of moderate-sized earthquakes within the southern California. The slip model is constrained by matching the body waves recorded at local stations. We calculate the earth response with the 1D smoothing SoCal model but correct the 3D structure effects on the body waves by adding time shifts and frequency dependent amplitude corrections [Tan and Helmberger, 2007]. We have constructed a table of the 3D time-correction for each stations based on Hauksson's update 3D Southern California model, using a 3D finite difference algorithm [Vidale, 1990]. We construct the amplitude corrections based on the analysis of a magnitude ~ 4 aftershock with known source mechanism. We test the method using recent Mw 5.4 Chino Hills earthquake.

2-113
EARTHQUAKE STRESS DROPS AND INFERRED FAULT STRENGTH ON THE HAYWARD FAULT *Hardebeck JL, and Aron A*

The Hayward Fault and other faults of the East Bay provide an opportunity to study variations in earthquake stress drop with depth, faulting regime, creeping versus locked behavior, and the strength of the wall rocks on either side of the fault. We use the displacement spectra from borehole seismic recordings of 529 M1.0-4.2 earthquakes in the East Bay to estimate stress drop using an empirical Green's function method (Shearer et al., 2006). The median stress drop is 8.7 MPa, and 50% of stress drops are between 3.2 MPa and 25 MPa. Several lines of evidence indicate that stress drop is controlled by the applied shear stress, even though the median stress drop values are significantly less than the theoretical shear stress assuming strong faults (Byerlee's law) and hydrostatic pore pressure. There is a trend of increasing stress drop with depth, with median stress drop of about 5 MPa for 1-7 km depth, about 10 MPa for 7-13 km depth, and about 50 MPa deeper than 13 km. Higher stress drops are observed for a deep cluster of thrust-faulting earthquakes near Livermore than for a deep cluster of strike-slip events on the Calaveras Fault. The changes in stress drops with depth and faulting regime imply that stress drop is related to the applied shear stress. We compare the spatial distribution of stress drops on the Hayward Fault to models of creeping versus locked behavior of the fault, and find that high stress drops are concentrated around the major locked patch near Oakland. This also suggests a connection between stress drop and applied shear stress, because the locked patch might be expected to experience higher shear stress as a result of either the difference in cumulative slip or the presence of higher-strength material. Comparison of stress drops with the wall-rock geology at depth does not show a correlation between stress drop and rock strength, suggesting that the fault strength is not directly related to the strength of the wall rock.

2-114
OVER TWO ORDERS OF MAGNITUDE VARIATION ARE DETERMINED SOLELY BY SLIP FOR A GROUP OF SMALL EARTHQUAKES ON THE SAN ANDREAS FAULT NEAR PARKFIELD, CA *Harrington RM, and Brodsky EE*

Ordinarily, earthquake magnitude is controlled by both rupture length and slip variation. Here we show that a special population of earthquakes has a constant rupture length, but varying slip. We compare the source time function pulse widths of 25 earthquakes on the San Andreas Fault, and 11

earthquakes on surrounding secondary faults to show that the earthquakes on the San Andreas Fault near Parkfield have a constant duration in this group with magnitudes ranging from 1.4 to 3.7. In contrast, earthquakes on secondary faults indicate the more usual source parameter scaling suggestive of a constant stress drop, i.e. they have an increase in duration with magnitude. The earthquakes on the San Andreas Fault are located approximately 20 km to the northeast of the 1966 mainshock epicenter, along the fault, to approximately 5 km south of the 2004 epicenter. Unlike previously studied repeating sequences, the magnitudes are not constant, nor is the repeat time regular. The secondary faults are located at distances of 5 km or greater from the trace of the San Andreas Fault, and are almost certainly not part of the active or historically active plate boundary fault system. The constant source duration observation for the earthquakes on the San Andreas Fault suggests that fault area stays constant over the magnitude range of our data set.

A repetitive rupture of a small, locked asperity in a creeping fault can explain the constant duration. The dimension of the asperity could pre-determine the fault area. Therefore the observation directly measures the scale of the heterogeneities on the fault. We observe heterogeneities of 120, and 160 m in diameter.

Calculated stress drop values of the earthquake population on the San Andreas Fault range from 0.18 MPa to 63 MPa, and values on secondary faults range from 0.31 MPa to 14 MPa. The differences in duration between the events on the San Andreas Fault and on secondary faults suggest that earthquakes on the San Andreas Fault are inherently different. Cumulative slip values on the secondary faults are negligible in comparison to cumulative slip values on the San Andreas Fault. We speculate that faults with more cumulative displacement have earthquakes which may rupture differently. Furthermore, the differences in source properties between the two populations might be explained by differences in fault surface roughness.

2-116
SELF-SIMILARITY AND ITS BREAKDOWN OF RUPTURE GROWTH OF EARTHQUAKES IN PARKFIELD REGION *Uchide T, and Ide S*

It is one of fundamental problems in earthquake seismology to understand the natures of rupture growth of earthquakes. The scaling of earthquakes source parameters provides clues to this problem. The similarities of eventual source parameters, such as fault length, width, displacement, stress drop, and rupture duration, are basically accepted [e.g., Kanamori and Anderson, 1975]. However it is not confirmed whether the dynamic rupture of each earthquake grows self-similarly.

In this study, we examine the self-similarity of the rupture growth by comparing the moment and moment rate functions of Mw 2.2 – 6.0 earthquakes in Parkfield region by slip inversion analyses using seismic data of GEOS operated by USGS and HRSN by the Berkeley Seismological Laboratory. Only the 2004 Parkfield earthquake (hereafter referred to as the Mw 6.0 event) is analyzed using the multiscale slip inversion method [Uchide and Ide, 2007].

We discuss on normalized moment rate functions, where time and moment rate are normalized by a reference rupture time expected from an empirical self-similar scaling, To = 10^(– 5.43) Mo^(1/3), where Mo is the eventual seismic moment, and the average moment rate determined by Mo/To, respectively. Except the Mw 6.0 event, the normalized moment rate functions are similar; each has a peak around the half of rupture time, and the peak value is 2.0 – 3.5 times of the average moment rate. However the rupture growth process of the Mw 6.0 event is different from the others: the rupture time is more than twice of the reference one, and the normalized moment rate function has a gentler peak.

Next we discuss on the moment functions in a log-log graph. Seismic moment of each event increases along with the common growth curve, Mo(t) = 2 × 10^17 t^3, decelerates, and stops growing. The moment function of Mw 6.0 event also grows along with the same growth curve until 1 s after the onset, but gentler after 1 s . That is because the thickness of seismogenic layer limits the width of earthquakes. According to the relocated hypocenter distribution [Thurber et al., 2006], the thickness of the seismogenic layer around the hypocenter of Mw 6.0 event is ~ 5 km. In our slip model the rupture front reach at the edge of the seismogenic layer in 1 s.

The fundamental image of earthquake growth processes suggested by this study is a limited self-similarity as followings. Each earthquake grows self-similarly, along the common growth curve, Mo(t) = 2 × 10^17 t^3, independent on its eventual magnitude. The growth curve can be suppressed by the thickness of a seismogenic layer. The earthquake rupture growth decelerates by some chance, its moment function runs off the common growth curve, and the rupture terminates.

2-117
VARIATIONS OF VELOCITY CONTRASTS AND FAULT ZONE DAMAGE ALONG THE PARKFIELD SECTION OF THE SAN ANDREAS FAULT USING FAULT ZONE TRAPPED WAVES *Lewis MA, Ben-Zion Y, Peng Z, Shi Z, and Zhao P*

We investigate variations of velocity contrasts and damage zones in the Parkfield region of the San Andreas fault (SAF), using fault zone trapped waves generated by the total internal reflection of waves within a low velocity fault zone layer. The trapped waves follow the S or P wave arrival, are dispersive, characterized by high amplitudes and lower frequencies, and are particularly apparent in the vertical or fault parallel components of motion. The specific features of these waves are highly dependent on the fault zone structure within which they are generated and hence they can be used to obtain high resolution fault zone images. This study is part of a larger project on imaging material interfaces and damage zones in the Parkfield region using data from multiple seismic networks. Much of the previous work has concentrated on using fault zone head waves. These observations have established the strength and variations of the contrast in velocity across the SAF. Direct wave travel time inversion and head wave moveout studies indicate that the northeast side of the fault is generally slow and the southwest side is generally fast with a ~5-10% difference in velocity. However, towards the southeast, near both the seismic station at Gold Hill and the hypocenter of the 2004 Parkfield earthquake, the velocity contrast is reduced to ~0-2%.

Here we expand and develop upon the results from the head waves studies with observations of fault zone trapped waves. We make observations of trapped waves in near fault stations of the high resolution seismic network and other networks in the Parkfield region. Synthetic waveforms generated using a model of two quarter spaces with differing velocities separated by a low velocity layer, show a separation between the direct body (S or P) wave and trapped wave onset in a fault zone station. In contrast, when the velocities in the quarter spaces are the same, the trapped and body waves are continuous. We find strong variation in the strength and character of trapped waves at the different stations and events along the fault and will attempt to correlate the variations with changes of the velocity contrast indicated by the head wave analysis.

2-118
HIGH-FREQUENCY BURSTS DURING STRONG MOTION – TRIGGERED OR "DRIVEN"? *Fischer AD, and Sammis CG*

High-pass filtering (>20Hz) of acceleration records from the 1999 Chi-Chi Taiwan and 2004 Parkfield, California earthquakes reveal a series of bursts that occur only during strong shaking. Initially interpreted as originating from asperity failure on the Chelungpu fault [Chen et. al,

B.S.S.A., 2005], bursts observed during the Chi-Chi earthquake were subsequently determined to be a local effect within about 1 km of the seismic stations [Fischer et. al, B.S.S.A., 2008a]. The same bursts were observed at the UPSAR array during the Parkfield earthquake and constrained to originate less than 20m from the instruments [Fischer et. al, G.R.L., 2008b]. It is tempting to assume the high-frequency bursts are small versions of the larger triggered events documented during the passage of surface waves. However, rate-and-state friction rules out dynamic triggering on such small, shallow slip patches. An alternative hypothesis is that the bursts are not triggered but are driven by simultaneous shear and tensile stresses near the surface during the strong motion. At 2 Hz, Sv to P wave mode conversion at the free surface produces tensile stresses to depths of 70m. Where standard triggering releases stored elastic energy and adds to the incident wavefield, this new driving mechanism takes shear stress out of the 2Hz strong motion and reradiates it at high frequencies. This process may play an important role in the attenuation of strong ground motion by converting low frequency to high frequency energy at an estimated efficiency between about 0.2 and 15%.

2-119
SOURCE PROPERTIES AND EARLY AFTERSHOCKS OF THE JULY 29 2008, MW 5.4, CHINO EARTQUAKE *Ruiz Paredes JA, and Ampuero J*

On July 29 2008 a Mw 5.4 earthquake shook Southern California. Its epicenter, near Chino Hills, lies in an area of dense seismological instrumentation, and creates a special opportunity to further understand the rupture complexity and general source properties of moderate sizes earthquakes. We present an analysis of strong motion records of the Chino earthquake. Using empirical Green's functions, we estimate the apparent source time function (ASFT) from P- and SH-waves recorded within 30 km epicentral distance by the Southern California Seismic Network, with waveform data available through the Southern California Earthquake Data Center. ASTFs are obtained by applying a regularized time-domain deconvolution between mainshock and aftershocks records, with positivity constraints. We are investigating the second-order spatio-temporal moments of the source, following the method proposed by McGuire (2004). Our preliminary analysis reveals a source duration significantly shorter than 1 second, in the short end of the usual value range observed for earthquakes of this magnitude. Owing to the particularly complete azimuthal coverage of the available recordings, the method can potentially yield insights on rupture directivity and help resolve the fault plane ambiguity. Indeed the aftershock locations lie on a deep sub-horizontal plane, and do not help differentiating which of two possible dipping fault planes was activated during the mainshock. Moreover, we are identifying and relocating early aftershocks buried in the first 5 minutes of the mainshock coda. Time-frequency analysis, high-pass filter and matched filter techniques are applied to identify these aftershocks and to determine relative time picks. We are investigating whether these early aftershocks delineate better the mainshock fault plane.

2-120
INTEGRATED THREE-DIMENSIONAL SEISMIC VELOCITY MODEL OF THE LA BASIN *Lin G, Thurber CH, and Zhang H*

We are developing an integrated Vp and Vs tomographic model of the greater Los Angeles Basin region. The fundamental scientific motivations for this study are to address the need for a significantly improved three dimensional model that can be used as a starting point for waveform tomography studies and to provide self-consistent earthquake locations (and focal mechanisms) with high accuracy and precision that can be used to improve the SCEC Community Fault Model.

Our starting model incorporates (spatially decimated) velocity values from the latest Harvard SCEC Community Velocity Model (CVM-H), which is imbedded within our existing Vp and Vp/Vs southern California model. This approach allows for the resolution of deeper crustal structure while retaining a high-resolution representation of the shallow structure in a unified, self-consistent model. The model is currently represented by a uniform 2 km horizontal grid in the high-resolution area of the CVM-H model and the seismically active Northridge region and 4 km elsewhere. The vertical nodes are positioned at 1, 3, 6, 9, 12, 15, 20, 25 and 35 km (relative to mean sea level). Available active-source data (primarily LARSE 1 and 2) are included in the inversion, along with data from about 4,000 earthquakes consisting of catalog phase picks and cross-correlation data. A key point is that double-difference tomography with waveform cross-correlation differential times has not previously been applied to the LA Basin region. Our preliminary results for the LA Basin show generally higher velocities from the surface to about 6 km depth, except for the Palos Verdes area, which has mostly lower velocities. In the surrounding region, we find higher velocities beneath the San Fernando Valley to about 12 km depth and lower velocities beneath the Transverse Ranges from about 6 to 12 km depth. Our model reduces the data misfit by about 50%.

2-121

USING MAGNETIC INCLINATION AND RELATIVE PALEOINTENSITY AS A MEANS OF CORRELATING AND DATING STRATIGRAPHY IN THE LA BASIN

Thomas TW, Martinez AU, Lund S, Dolan JF, Leon LA, and Shaw JH

Paleomagnetic data gathered from boreholes drilled across the locus of most recent folding above the Compton blind-thrust fault have proven useful in correlating stratigraphy between boreholes and in determining chronostratigraphy. We drilled 13 continuously cored boreholes, each with better than 95% recovery along a 1.4-km-long, north-south transect across the locus of back limb folding above the southern segment of the Compton thrust fault in Lakewood, CA. Our cores unearthed alternating intervals of course-grained sands, gravels, fine-grained silts, clays, and organic-rich clays down to a depth of ~40m. The main source of these sediments was most likely the San Gabriel river ~2 km East of the study site, with material possibly also coming from the Los Angeles river, ~7 km to the West. Correlations based on visual core descriptions provide one method of determining the timing and rate of uplift along the Compton blind-thrust, but in some structurally key locations, these correlations remain uncertain. Paleomagnetic inclination and relative paleointensity data are being tested as an alternative means of correlating and dating selected boreholes. Initially, we took ~70 samples every 125 cm along the entire downhole length of holes 10 and 11. Subsequently, we took ~230 samples spaced every 2.5 cm over an 8-m-thick clay interval near the base of holes 10, 11, and 12. Our initial results indicate that inclination and relative paleointensity can be correlated among holes. We may have also found evidence for the Mono Lake excursion at ~33ka, which would be consistent with 14C dates recovered from the cores. Recognition of this excursion and related paleomagnetic field variability, if confirmed by our ongoing work, will provide a useful means of stratigraphic correlation for late Pleistocene growth strata.

2-122

USING MAGNETIC SUSCEPTIBILITY AS A MEANS OF CORRELATING STRATIGRAPHY IN THE LOS ANGELES BASIN.

Martinez AU, Thomas TW, Dooling PR, Lund S, Dolan JF, Leon LA, and Shaw JH

We drilled thirteen continuously cored boreholes to depths of 30 to 40 m along a 1.4-km-long, north-south transect across the locus of back limb folding above the Compton blind thrust fault. Core recovery was excellent, averaging greater than 95% for the section. The cores consist of

alternating intervals of course-grained sands, gravels, and cohesive, fine-grained silts, clays and organic-rich clays. The main source of these sediments was most likely the San Gabriel River, which is located ~2 km East of the study site, with material possibly coming from the Los Angeles River, ~7 km to the West. In order to corroborate our cross-borehole correlations, which were based on visual comparison, we are using high-resolution records of magnetic susceptibility (Chi) to correlate stratigraphy between four boreholes that appear to span the steepest part of the young fold. Specifically, we are focusing on cores 7, 10, 11 and 13, which are 30 to 100 m apart from one another. We measured the magnetic susceptibility every 2.5cm in all boreholes using a Bartington probe sensor. We have attempted to correlate between pairs of boreholes under a working assumption that the Chi records should be correlatable. Our initial results suggest that this hypothesis is largely correct, but we have also encountered segments of the cores in which the Chi data do not correlate between cores. These results demonstrate that magnetic susceptibility is a useful tool in correlating stratigraphic horizons that might otherwise be difficult to correlate with other methods.

2-123
A BRIEF HISTORY OF LUMINESCENCE GEOCHRONOLOGY AS IT HAS BEEN APPLIED TO USGS PALEOSEISMOLOGY ASSESSMENTS AND MAPPING PROJECTS *Mahan SA*

The aim of paleoseismology is to assess the probability and severity of future earthquakes using the geologic record of past earthquakes. To this end, geology and geomorphology provide a context for the location and amount of past fault ruptures; geochronology provides the critical temporal context for the occurrence and sequencing of earthquakes prior to the historic record. Traditionally, carbon-14 dating has been employed for geochronologic purposes; however, materials containing carbon are not always associated with earthquake-related deposits, and the technique's dating range is limited to around 40,000 years. Because it is not subject to these restrictions, luminescence dating (Thermoluminescence [TL] and optically stimulated luminescence [OSL]), has been used to directly date the last time sediment associated with fault movement was re-deposited and thus exposed to sunlight. Prescott and Robertson (1997) review comparisons between luminescence dating methods as well as other Quaternary geochronological methods, and this discussion is included in the poster presentation. A paper by M. Fattahi ("Dating Past Earthquakes and Related Sediment by Thermoluminescence Methods; a Review"; in press, QI) provides an excellent history of early luminescence work.

The U.S. Geological Survey (USGS) has used luminescence dating techniques since 1996, in order to more fully elucidate past fault movements as identified in trenches. Luminescence data and research pertaining to paleoseimology has been published for such locations as southern California, Nevada, Utah, Indiana, and Colorado in USGS publications, National Earthquake Hazards Reduction Program reports or refereed journal publications. In this poster three luminescence dating studies will be presented in detail: (1) Paleoliquifaction sites within the New Madrid Seismic Zone, located along the Wabash River of Indiana; (2) A 95-mile long lineament in northeastern Colorado near the town of Anton, CO, where a trench was excavated to determine whether the lineament formed due to Pleistocene faulting; and (3) fine-grained layers within alluvial-fan deposits from southern Death Valley that were dated, and the resulting implications of those ages for climate-driven sedimentation along a tectonically active mountain front.

2-124
PALEOCLIMATE CONSTRAINTS ON CHANNEL INCISION AND EARTHQUAKE SLIP AT THE BIDART FAN SITE, SAN ANDREAS FAULT, CALIFORNIA *Noriega GR, Grant Ludwig LB, Akciz SO, and Arrowsmith JR*

Laterally offset channels are one of the main geomorphological features that are commonly used to infer slip rates, estimate the magnitude of these paleoearthquakes and their recurrence intervals. Difficulty in constraining the age of channel incision, however, generally introduces large uncertainties into the calculations. We combine paleoclimate data from southern California with paleoseismologic data from the Carrizo section of the San Andreas Fault (SAF) to better interpret the age of some of the ephemeral stream channels that are offset by paleoearthquakes that ruptured this section of the SAF. In this study, we assume that runoff from precipitation is the main driving force of channel incision in the Carrizo Plain, and by identifying the extreme wet and dry periods based on the readily available climate data, particularly precipitation data, we narrow down the timing of initiation of channel incision. This allows us to examine the rate of channel incision across the San Andreas fault and compare it with the rate of seismic events. We identified several extreme climate events (wet years) as likely dates of channel incision events in the Carrizo Plain. The findings reveal new constraints on incision of two channels in the Bidart Fan site. We propose that a channel (NW channel) that has been offset 14.6 to 18.4 m, could have been incised during an extreme wet year in either A.D. 1366 or A.D. 1418. A second channel (SE channel) that is offset 7 or 8 m probably incised in A.D 1642. Grant and Sieh (1994) indicated the 14.6 to 18.4 m offset of the NW channel is due to the 1857 and one or two previous earthquake(s). Grant and Sieh (1994) inferred 7 or 8 m offset of the SE channel is due to the 1857 earthquake alone. The new climate inferred dates of channel incision, along with earthquake dates from Akciz et al. (submitted) suggest the NE channel may have been offset by three or four earthquake events, and the SE channel has been offset by the 1857 and possibly by a previous earthquake.

2-125
CRUSTAL ANISOTROPY MEASURED NEAR THE CALICO FAULT IN THE EASTERN CALIFORNIA SHEAR ZONE *Colella H, and Cochran ES*

We present preliminary results from a study of crustal anisotropy near the Calico Fault located in the Eastern California Shear zone. Shear wave splitting is used to approximate the in situ stress field and/or shear fabric near the fault and examine whether proximity to the main slip plane affects the observed anisotropy. Between June and November 2006, approximately 65 seismic stations were deployed in a grid spanning 4 km across and 1.5 km along the Calico fault to explore seismic properties of a fault that has not experienced a major earthquake in hundreds to thousands of years. Here we examine shallow crustal anisotropy determined using the 37 earthquakes that occur within the shear wave window, with an angle of incidence less than 45 degrees, during the experiment period. Splitting parameters are determined using an automated cross-correlation method that determines the fast direction and delay time for each station-event pair. Preliminary results show significant scatter in fast directions and delay times, but suggest a fast direction between N15°W and N15°E. Future work will examine the relationship between observed shear wave splitting and event-station path.

2-128
EVOLVING AFTERSHOCK SEISMICITY USING RATE-STATE EQUATIONS IN A 3D HETEROGENEOUS STRESS FIELD *Smith DE, and Dieterich JH*

We combine 3D models of stress heterogeneity [Smith, 2006; Smith and Heaton, 2008] with a formulation for seismicity based on rate-state friction [Dieterich, 1994; Dieterich, et al, 2003] to

examine aspects of aftershock seismicity: 1) Spatial patterns as a function of time, 2) seismicity rates and, 3) and changes of focal mechanisms in aftershock sequences. Key features we observe for the simulated aftershock period are: 1) Approximately 1/t, Omori Law behavior, 2) initial clustering of aftershocks in regions of greatest Coulomb stress then transitioning to a more even spatial distribution with time, and 3) some seismicity in stress shadow areas due to the pre-existing heterogeneous stress. In addition, we find that stress inversions of aftershock focal mechanisms in the models indicate large apparent rotations of stress that are far in excess of the true stress rotations. For example, for simulations with spatial mean deviatoric stress 50 MPa subjected to stress perturbation of 2 MPa at the onset of the mainshock, the focal mechanism inversions give apparent" stress rotations of 3°-34° although the actual rotations are less than 2°. Also, the focal mechanism inversions produce transient increases in the mean misfit angle, ?, (generally though to correlate with stress heterogeneity) although the stress heterogeneity in the model remains constant. Both the apparent changes in stress orientation and misfit angles decay during the aftershock period. These results agree with previous conclusions [Smith, 2006; Smith and Heaton, 2008] that failures in a heterogeneous stress field are biased toward the stressing rate or stress perturbation. In our model the biasing arises because failure surfaces that are well oriented with respect to stress perturbations experience larger transient seismicity rate changes than surfaces that are misaligned. An important conclusion is that significant rotations of focal mechanism inversions can occur in a moderately strong crust (mean stress 50 MPa) if stress is heterogeneous. Consequently, one cannot conclusively demonstrate low crustal strength (≤ 10 MPa) from observations of focal mechanisms solutions following stress perturbations. Another significant conclusion is if one tries to measure stress heterogeneity changes using ?, some fraction of an increase in ?, could be due to the interaction of stress heterogeneity with changing seismicity rates.

2-129

NUMERICAL STUDIES OF SMALL REPEATING EARTHQUAKES AND THEIR SOURCE PARAMETERS USING RATE AND STATE FRICTION LAWS *Chen T, and Lapusta N*

Small repeating earthquakes have short recurrence times and known locations, and hence they present a rare predictable opportunity for detailed observation and insights into earthquake physics. We simulate repeating earthquakes in a 3D model based on the Dieterich-Ruina rate and state friction law. In the model, a small circular patch with steady-state velocity-weakening friction is surrounded by a much larger velocity-strengthening region. Our simulations use the 3D methodology of Liu and Lapusta (AGU, 2006) that fully resolves all aspects of seismic and aseismic behavior of the fault, including inertial effects during repeating earthquakes. When the patch size is smaller than the nucleation size implied by the underlying rate and state formulation, all slip on the patch is aseismic. For larger patch sizes, small repeating events occur, with slip rates of order of 1 m/s and sharp stress drops; however, the patch also experiences significant aseismic slip. By varying the patch radius, we are able to produce repeating earthquakes between moment magnitudes 0.3 and 3.7, and the corresponding fraction of aseismic slip on the patch varies from 0.999 to 0.2. The events in our model (i) reproduce the observed scaling $T\propto M_0^{1/6}$ of the repeat time {\it T} and seismic moment M_0 and (ii) have source dimensions and stress drops typical for earthquakes of comparable sizes and similar to recent inversions for Parkfield repeaters. Remarkably, the scaling $T\propto M_0^{1/6}$ is independent of the variation of rate and state parameters a and b within a factor of 4. The scaling is also reproduced (i) in a model with a rectangular velocity-weakening patch, with events of different sizes obtained by keeping the width of the patch fixed and the length of the patch varied, (ii) with quasi-dynamic approach, and (iii) in 2D fault models with an adjusted moment computation that reinterprets slip in terms of a

3D model. Our current studies are directed towards determining the scaling for larger events using 2D simulations and considering other forms of rate and state friction.

2-130
USING 3D FRÉCHET KERNELS TO INVESTIGATE WAVE EXCITATION AND PROPAGATION IN SOUTHERN CALIFORNIA *Allam AA, Jordan TH, and Chen P*

In this study we use 3D Fréchet kernels to gain insight into wave propagation in Southern California. Structural complexity in Southern California gives rise to three-dimensional waveforms which are unaccounted for by simple 1D models. Fréchet kernels, or sensitivity kernels, are a useful tool which can be used to analyze these phases because kernels can be calculated for any waveform from any part of the seismogram; a priori knowledge of phase type is unnecessary. Based on the 3D SCEC Community Velocity Model version 4.0 (CVM-S4), we compute Fréchet kernels by a scattering-integral method, which involves convolving point-source generated earthquake wavefields with the receiver Green tensors (RGTs), produced by three orthogonal unit point forces acting at the receiver locations. In this presentation we provide examples of sensitivity kernels for waveforms from magnitude 3.5-5.5 earthquakes and discuss the insight they provide into the complexities of 3D wave propagation in Southern California.

2-131
SOUTHERN CALIFORNIA ADJOINT MOMENT-TENSOR INVERSIONS *Kim Y, Liu Q, and Tromp J*

Southern California Moment Tensor solutions for 9 source parameters (6 moment tensor elements, latitude, longitude, and depth) are sought to minimize a misfit function computed from waveform differences. The gradient of a misfit function is obtained based upon two numerical simulations for each earthquake: one forward calculation for the southern California model, and an "adjoint" calculation that uses time-reversed signals at the receivers. A nonlinear conjugate gradient algorithm is used to iteratively improve the earthquake source model while reducing the misfit function. We test the inversion code by perturbing each component of the CMT solution, and see how the perturbed value converges. Next, we demonstrate full inversion capabilities using the 9 September 2001, ML 4.2 Hollywood event. We compare our result with that obtained by performing a Hessian-based spectral-element moment-tensor inversion introduced by Liu et al. (2004). Finally, we provide a table containing map view figures of the vertical-component adjoint wavefield near the original source for all of the basic "beachball" earthquake mechanisms, thereby illustrating the relationship between the mechanism and the adjoint wavefield.

2-132
ASYMMETRIC ALONG-STRIKE EARTHQUAKE DIRECTIVITIES ON THE NORTHERN SAN ANDREAS FAULT *Schorlemmer D, and Ben-Zion Y*

Analytical and numerical studies indicate that ruptures on bimaterial faults that separate different rocks propagate predominately in the direction of slip on the compliant side of the fault (referred to as the preferred direction). Observational studies revealed strong asymmetry of rock damage in the structures of the San Andreas, San Jacinto and North Anatolian faults, consistent with the theoretical prediction for ruptures on bimaterial faults. However, more direct tests reflecting properties of many earthquake ruptures on natural bimaterial faults are lacking. Here we examine earthquake directivities on the northern San Andreas fault by analyzing stacked dynamic triggering patterns of approx. 16,500 earthquakes at different spatio-time scales. The results show strongly enhanced dynamic triggering to the south-east, consistent with the theoretical prediction

for the velocity contrast across the San Andreas fault in the area. The findings have considerable implications for earthquake physics and analysis of seismic hazard associated with large faults.

2-133
CORNER FREQUENCIES AND STRAIN-DROPS FROM S-WAVES GENERATED BY EARTHQUAKES ALONG THE KARADERE-DÜZCE BRANCH OF THE NORTH ANATOLIAN FAULT *Yang W, Ben-Zion Y, and Peng Z*

We estimate the strain-drops of aftershocks of the 1999 ?zmit and Düzce earthquakes using S-waves recorded by a local seismic array along the Karadere-Düzce branch of the North Anatolian fault in the 6 months following the Izmit mainshock. The method is associated with separation of source, travel-time and station spectral terms and stacking results at several stages to enhance the signal-to-noise ratio. The strain-drops are obtained by fitting iteratively the separated source spectra of 201 nearest neighboring events in different amplitude bins to the ?2 source spectral model. The strain-drops obtained from S-waves generally match those derived in an earlier study from P-waves (Yang et al., 2008). We find that the P-wave corner frequencies are systematically higher than the S-wave corner frequencies, which is consistent with the source model of Madariaga (1976), and those measured by Abercrombie (1995) and Prieto et al. (2004). Since the S-wave window includes various converted and scattered waves, this may increase the fitting error to the derived strain-drops of S-waves and produces scatter in the ratio of P/S corner frequencies. The next step is to apply a waveform cross-correlation technique to identify clusters of similar events in the data set. In each cluster, we stack similar waveforms and measure the pulse widths of P- and S-arrivals. This provides a direct way to quantify the corner frequency shift and an independent method to obtain source parameters. Updated results will be presented in the meeting.

2-134
EXAMINATION OF SCALING BETWEEN EARTHQUAKE MAGNITUDE AND PROPOSED EARLY SIGNALS IN P WAVEFORMS FROM VERY NEAR SOURCE STATIONS IN A SOUTH AFRICAN GOLD MINE *Lewis MA, and Ben-Zion Y*

We analyze near-source seismograms, recorded in a deep South African mine for scaling between signals early in P waveforms and the magnitude M of the events. The data consist of recordings at 26 stations of 122 events with -1.5 < M < 2.5 and hypocentral distances as low as ~100 m. We examine four signals, belonging to two classes. Signals in the first class include Ellsworth-Beroza and Iio measurements assumed to reflect signatures of seismic nucleation phases. Signals in the second class consist of Nakamura type predominant period and Wu-Zhao corrected peak displacement in the early waveforms, related to measures of the stress drop and local magnitude. Candidates for the Ellsworth-Beroza signals, involving a weak arrival before the main P phase, exist for only 20-30% of the waveforms. These phases do not appear to be associated with a general component of the rupture initiation process. The Iio signal increases with increasing M but may be attributed, at least partially, to statistical effects. The predominant period and peak displacement have significant correlations with M, which remain robust when the analysis time window is reduced from 3 sec or before the S wave arrival to 0.01 sec. The latter is shorter than the estimated rupture duration for events with M > ~0, implying that the earthquake size is affected statistically by the initial rupture strength. If these correlations hold for larger earthquakes, as suggested by other studies, the early predominant period and peak displacement are useful for early warning systems.

2-135
EARTHQUAKE SOURCE ESTIMATION AND 3D CRUSTAL MODELS *Helmberger DV, Wei S, Zhan Z, Tan Y, and*

Several new methods have been developed to retrieve local Green's functions based on the cross-correlation of ambient noise (station-to-station) and conventional (source-to-station) inversions. The latter methods provide the most broadband results but require accurate source parameters for phase-delay recovery which depends on the starting model. We can avoid this trade-off by applying the cut-and-paste technique which allows adjustable timing shifts to correct paths. We use a tomographic model based on these delays from a large population of events to predict those derived from the recent Chino Hills event and perform a test against direct inversion results. Delays derived from ambient-noise relative to the nearest stations are generally compatible but indicate multi-pathing issues along some paths. It appears that these two methods can be combined to achieve more accurate results.

2-136
COMMUNITY VELOCITY MODEL FOR THE NEW MADRID REGION, CENTRAL U.S. *Boyd OS, Soble J, and Verbanaz R*

In 1811-1812, a series of three major earthquakes struck the Central United States in the New Madrid Seismic Zone. Having magnitudes near 7.5 and being located within the relatively stable interior of the North American Continent, these events produced widespread strong shaking. If these events were to occur today, there would be substantial devastation to people, buildings and transportation and communication infrastructure. To better understand this threat and in preparation for the upcoming bicentennial, the US Geological Survey is planning to produce and support sophisticated numerical simulations of earthquake rupture and seismic wave propagation due to a repeat of these events. To kick off this effort, the USGS began the development and construction of a community seismic velocity model for use in these numerical simulations. We have collected existing research regarding the p- and s-wave velocities, impedance contrasts and densities of the lithosphere in the New Madrid region and synthesized these results into a single model that can be used in earthquake simulations. We have identified areas of missing or incomplete information for further study. The region covers an area of approximately 600,000 square km from Little Rock, Arkansas across to Nashville Tennessee, up to St Louis, Missouri. The model has currently been gridded at 3 km lateral resolution and from 5-m resolution near the surface to 10-km resolution at 100 km depth. Less but still substantial uncertainty exists for the Mississippi Embayment where a majority of the research has been done. Newer regional models such as those by van der Lee and others and Liang and Langston have improved regional resolution beyond a 1-dimensional model, but for ground motion simulations, greater resolution outside the Embayment is desired.

2-137
SURFACE WAVE CONSTRAINTS ON CRUSTAL S-WAVE VELOCITY STRUCTURE *Yano TE, Tanimoto T, and Alvizuri CR*

S-wave velocity structure at shallow depths is crucial for accurate ground motion prediction and seismic hazard. In order to improve crustal S-wave velocity structure, we have developed a new procedure for joint inversion of Rayleigh wave short period data (about 0.1-0.4 Hz) using particle motion (ZH ratio or equivalent to H/V) and phase velocity data.

Our particle motion data are the ratios between vertical and horizontal amplitudes of Rayleigh waves (hereafter ZH ratios), measured from ambient noise. The most sensitive depth range is in the upper 5 km, thus this data set will be crucial to constrain S-wave velocity in very shallow structure. The most attractive aspect of this data set is that it is free from contamination from deep structure. Basic procedures to obtain fundamental Rayleigh wave signals were described in Tanimoto and Alvizuri (2006). Data were measured from continuous records typically for two years, for

broadband stations in California Integrated Seismic Network (CISN). Data were selected between 0.13-0.37 Hz for which S/N is high. In our analysis, ZH ratios show characteristic regional behaviors, in particular for basins where ZH ratios show a minimum around 0.15-0.20 Hz. In fact, this behavior of ZH ratio data helps discern whether a station is in a basin structure.

Phase velocity data were obtained from Green's functions, generated by cross-correlations of seismograms (hereafter correlograms). This data set in the frequency range, 0.13 to 0.20 Hz, is sensitive to the upper 10-20 km, thus provides constraints on average S-wave velocity in the upper crust. We used at least one-year to at most four-year length of CISN data. From pairs of about 140 stations, we selected about 1500 good S/N correlograms, which Rayleigh wave records, obtained from vertical-vertical cross-correlations. Frequency range of 0.13 to 0.20 Hz was chosen where S/N is high. This range could be extended slightly further but noise is high between 0.1 and 0.2 Hz for Southern California. Thus, correlograms are analyzed within 0.13 to 0.20 Hz.

As the depth sensitivities of ZH ratios and phase velocity are complimentary, they can be inverted simultaneously to resolve the entire upper crust. Our ultimate goal is to improve our predictive capability of ground motions, in particular for urban areas which are typically in basin structures.

Meeting Participants

AAGAARD Brad, *USGS*
AGNEW Duncan, *UCSD*
AGUILAR Victor, *ELAC*
ALLAM Amir, *USC*
ALVAREZ Melva, *PCC*
AMPUERO Jean Paul, *Caltech*
ANDERSON John, *UNR*
ANDREWS Dudley Joe, *USGS*
APPLEGATE David, *USGS*
ARGUS Donald, *JPL*
ASANO Kimiyuki, *Kyoto University*
ASSATOURIANS Karen, *UWO*
BAILEY Iain, *USC*
BALTAY Annemarie, *Stanford*
BARBOT Sylvain, *UCSD*
BAUSTERT Jeff, *Image Work Communications*
BEELER N. M., *USGS*
BEN-ZION Yehuda, *USC*
BENTHIEN Mark, *SCEC / USC*
BERTI Ryan, *USC*
BIASI Glenn, *UNR*
BIRD Peter, *UCLA*
BLANPIED Michael, *USGS*
BOESE Maren, *Caltech*
BOORE David, *USGS*
BOUTWELL Christiann, *University of South Carolina*
BOYD Oliver, *USGS*
BROCHER Tom, *USGS*
BROWN Kevin, *UCSD*
BUDNITZ Robert, *LBNL*
CADENA Ana, *CWU*
CAMPBELL Kenneth, *EQECAT, Inc.*
CANORA-CATALAN Carolina, *Universidad Complutense de Madrid*
CATCHINGS Rufus, *USGS*
CHEN Kate, *Berkeley*
CHEN Rui, *CGS*
CHEN Ting, *Caltech*
CHOURASIA Amit, *SDSC*
CHU Annie, *UCLA*
CLAYTON Robert, *Caltech*
COLELLA Harmony, *UCR*
COON Ethan, *Columbia University*
COX Dale, *USGS Multi-Hazards*
CROWELL Brendan, *UCSD*
CUI Yifeng, *SDSC*
DALGUER Luis, *ETH-Zürich*
DAVIS Paul, *UCLA*
DE GROOT Robert, *SCEC / USC*
DEVECCHIO Duane, *UCSB*
DEWEY James, *USGS*
DISCHLER Jennifer, *ASU*
DOLAN James, *USC*
DUAN Benchun, *Texas A&M University*
ELBANNA Ahmed, *Caltech*
ELLIOTT Austin, *UC Davis*
ELY Geoffrey, *USC*
FANG Zijun, *UCR*
FELZER Karen, *USGS*
FIELD Edward, *USGS*
FISCHER Adam, *USC*
FLOWERS Rosie, *Rust College*
FROMENT Bérénice, *University of Joseph Fourier*
FUKUDA Junichi, *Indiana University*
FUNNING Gareth, *University of California, Riverside*
GAO Haiying, *University of Oregon*
GILCHRIST Jacqui, *UCSC*
GOEBEL Thomas, *USC*
GOULET Christine, *UCLA*
GRAVES Robert, *URS*
HADDAD David, *ASU*
HAGER Bradford, *MIT*
HAIRSTON Jennifer, *USC*
HANKS Tom, *USGS*
HARDEBECK Jeanne, *USGS*
HARRINGTON Rebecca, *UCLA*
HASELTON Curt, *California State University, Chico*
HAUKSSON Sven, *UCI*
HEARN Elizabeth, *UBC*
HEERMANCE Richard, *USGS*
HERRING Thomas, *MIT*
HOLBROOK Chris, *CA Office of Homeland Security*
HOUGH Susan, *USGS*
HUBBARD Judith, *Harvard*
HUMPHREYS Eugene, *Oregon*
HUYNH Tran, *SCEC*
JACKSON David, *UCLA*
JANECKE Susanne, *Utah State*
JOHNS Matthew, *UCSC*
JOHNSON Leonard, *NSF*
JONES Lucile, *USGS*
JORDAN, JR. Franklin, *John R. Byerly, Inc.*
KANE Deborah, *UCSD*
KELLER Edward, *UCSB*
KENT Graham, *UCSD*
KING Nancy, *United States Geological Survey*
KOHLER Monica, *UCLA*
KONCA Ali Ozgun, *Caltech*
KREEMER Corné, *UNR*
KRISTEK Jozef, *Comenius University Bratislava*
LANGBEIN John, *USGS*
LAPUSTA Nadia, *Caltech*
LAVALLEE Daniel, *UCSB*
LAWRENCE John, *Image Work*
LE Kimberly, *UC Davis*
LEE Kwangyoon, *UCSD*
LEGG Mark, *Legg Geophysical*
LEON Lorraine, *USC*
LI Yong-Gang, *USC*
LIU Pengcheng, *USBR*
LIU-ZENG Jing, *Institute of Tibetan Plateau Research, Chinese Academy of Sciences*
LLENOS Andrea, *MIT/WHOI*
LOHMAN Rowena, *Cornell University*
LOZOS Julian, *UCR*
LU Xiao, *Caltech*
LYNCH David, *USGS*

MADARIAGA Raul, *ENS/ Paris*
MAHAN Shannon, *USGS*
MARQUIS John, *SCEC*
MARTIN Geoffrey, *USC*
MATTI Jonathan, *USGS*
MCAULIFFE Lee, *USC*
MCGUIRE Jeff, *WHOI*
MCRANEY John, *USC*
MEDINA LUNA Lorena, *CSUN*
MENGES Christopher, *USGS*
MILETI Dennis,
MILLER Brittney, *USC*
MILNER Kevin, *USC*
MINSON Sarah, *Caltech*
MITCHELL Erica, *UCSD*
MURPHY Janice, *USGS*
MUTO Matthew, *Caltech*
NEE Philip, *UCR*
NODA Hiroyuki, *Caltech*
NUNLEY Melissa, *CSU Fullerton*
OGLESBY David, *UCR*
OKI Satoko, *ERI, University of Tokyo*
OLSEN Kim, *SDSU*
ONDERDONK Nate, *CSU Long Beach*
ORTEGA Gustavo, *CALTRANS-LA*
PACE Alan,
PANCHA Aasha, *UNR*
PERRY Suzanne, *USGS*
PHILIBOSIAN Belle, *Caltech*
PIERCE Brandee, *USC*
PLATT John, *USC*
PONTI Daniel, *USGS*
POWELL Robert, *USGS*
PRAKASH Vikas, *CWRU*
PRIETO German, *Stanford*
PURASINGHE Ruwanka, *UC Davis*
QUITTMEYER Richard, *Integrated Science Solutions, Inc.*
REDVALE Jolene, *San Bernardino County Museum*
REITER Leon, *Consultant NWTRB*
RICE James, *Harvard*
RIVERA Armando, *ELAC*
ROCKWELL Thomas, *SDSU*
ROSA Javier, *Rutgers University*
ROUSSEAU Nick, *Cal State University, Northridge*
RUBINSTEIN Justin, *USGS*
RUIZ PAREDES Javier, *Caltech*
RYU Hyeuk, *Stanford*
SAMMIS Charles, *USC*
SAVAGE Heather, *UCSC*
SCHARER Katherine, *Appalachian State*
SCHLOM Tyanna, *CSUF*
SCHMEDES Jan, *UCSB*
SCHOENBERG Frederic, *UCLA*
SCHORLEMMER Danijel, *USC*
SEGALL Paul, *Stanford*
SEKIGUCHI Haruko, *Kyoto University*
SHAFER Luke, *CSULB*
SHAO Guangfu, *UCSB*
SHAW Bruce, *LDEO*
SHEARER Peter, *UCSD*
SHEEHAN Anne, *Colorado*
SHI Zheqiang, *USC*
SHRESTHA Ramesh,
SLADEN Anthony, *Caltech*
SMITH Deborah, *UCR*
SOLIS Teira, *University of Texas at El Paso*
SONG Seok Goo, *URS*
SPINLER Joshua, *University of Arizona*
SPUDICH Paul, *USGS*
STEIDL Jamison, *UCSB*
STEVENS Jennifer, *UCR*
STOCK Joann, *Caltech*
TABORDA Ricardo, *CMU*
TANNER Felicia,
TEMPLETON Elizabeth, *Harvard*
THATCHER Wayne, *USGS*
THURBER Clifford, *Wisconsin*
TINSLEY John, *USGS*
TOKE Nathan, *ASU*
TREIMAN Jerry, *CGS*
TSURUOKA Hiroshi, *University of Tokyo*
TUNG Jack, *CSULA*
UCHIDE Takahiko, *Univ. Tokyo*
VAN AALSBURG Jordan, *UC Davis*
VELASQUEZ Christina, *CSU San Bernardino*
VERDUGO Danielle, *SDSU*
WALLACE John, *UCLA*
WANG Feng, *USC*
WANG Tien-Huei, *UCR*
WATERHOUSE Hannah, *USC*
WECHSLER Neta, *USC*
WEI Meng, *SIO / IGPP*
WEISER Debbie, *USGS*
WELDON Ray, *Oregon*
WESNOUSKY Steven, *University of Nevada, Reno*
WHITCOMB James, *NSF*
WHITNEY John, *USGS*
WILLIAMS Charles, *RPI*
WILLIAMS Patrick, *SDSU*
WILSON Rick, *CGS*
WONG Ka, *UCLA*
WYATT Frank, *UCSD*
XU Shiqing, *USC*
YANG Jing, *Caltech*
YANO Tomoko, *UCSB*
YONG Alan, *USGS*
YU Ellen, *Caltech*
YUAN Fuping, *CWRU*
ZANDT George, *University of Arizona*
ZAREIAN Farzin, *University of California - Irvine*
ZENG Yuehua, *USGS*
ZHAO John, *GNS Science*
ZOBACK Mary Lou, *RMS*

Group 1 Poster Layout

Group 1 posters are available for viewing at the following times:

SUNDAY, SEPTEMBER 7, 2008
20:00 – 22:30 Poster Session I

MONDAY, SEPTEMBER 8, 2008
14:00 – 15:30 Poster Session II
20:00 – 22:30 Poster Session III

NOTE: Poster numbers are given above the title of each abstract. The first digit indicates the Poster Group, and the last three digits indicate the poster board assignment, as shown in the layout to the right.

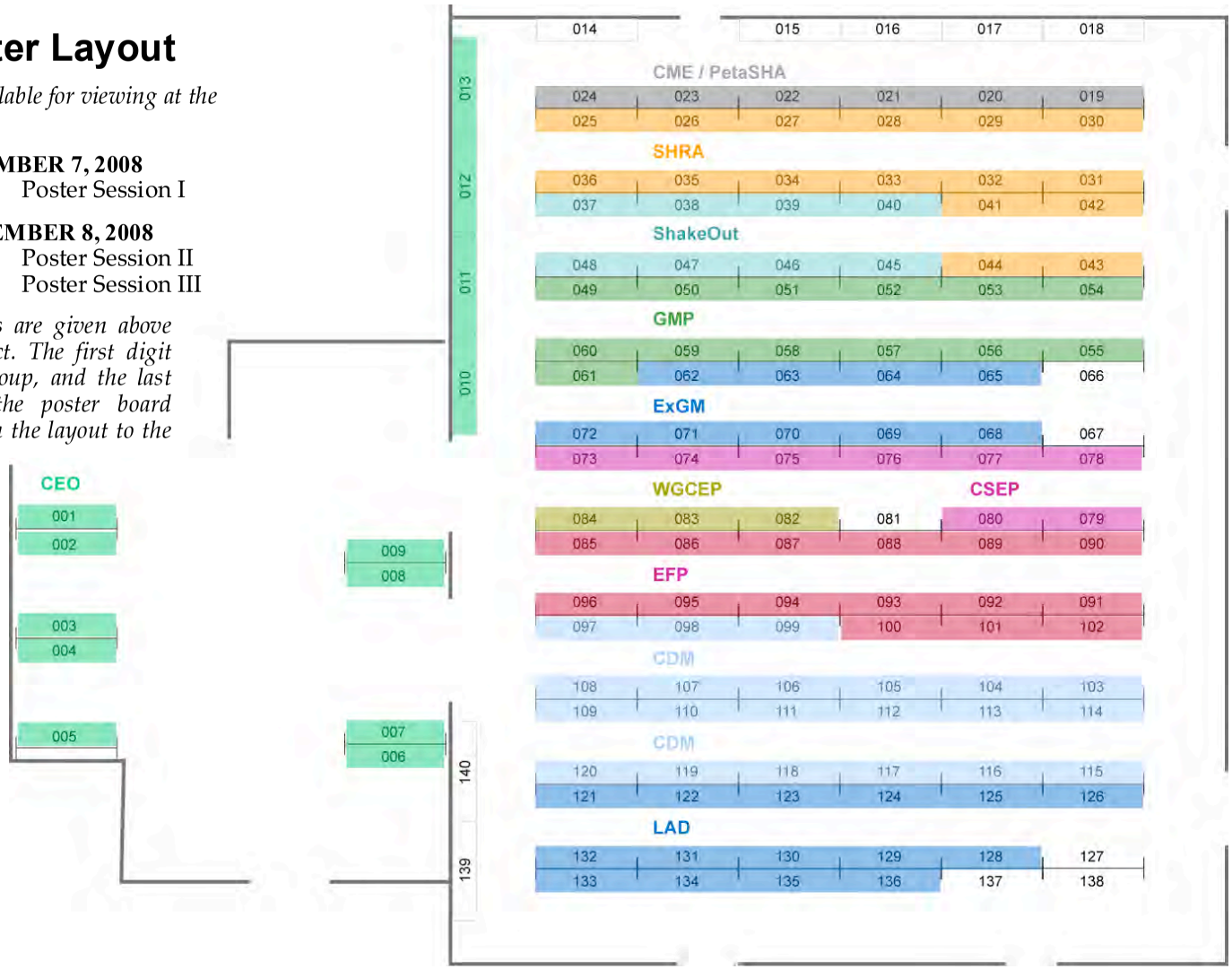

Group 2 Poster Layout

Group 2 posters are available for viewing at the following times:

TUESDAY, SEPTEMBER 9, 2008

13:30 – 15:00 Poster Session IV
20:00 – 22:30 Poster Session V
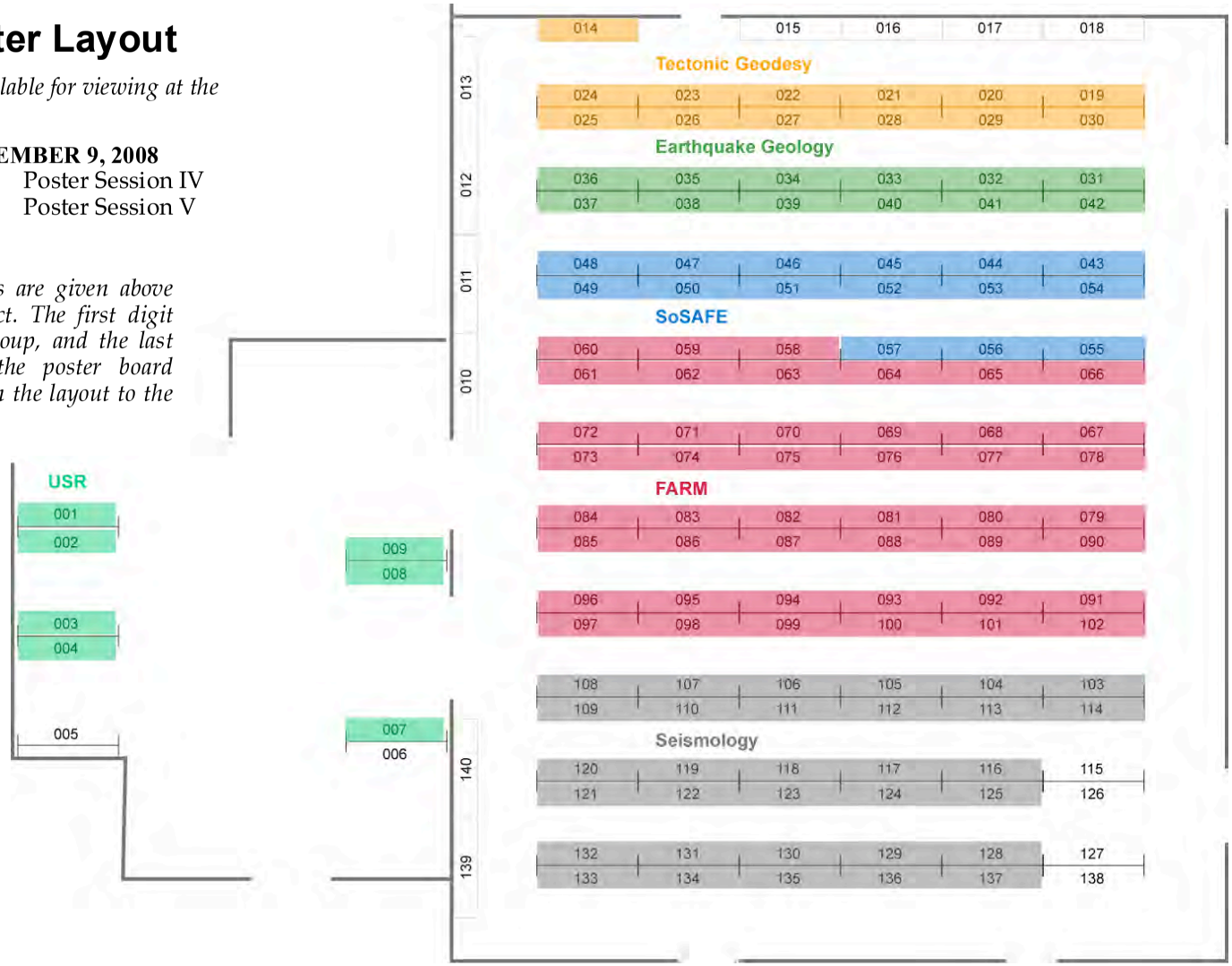
NOTE: Poster numbers are given above the title of each abstract. The first digit indicates the Poster Group, and the last three digits indicate the poster board assignment, as shown in the layout to the right.